Receptor for Advanced Glycation End Products Mediates NADPH Oxidase Signaling in Human Skeletal Muscle

BY

Brian K. Blackburn

B.A., DePaul University 2005

M.S., California University, 2010

THESIS

Submitted as partial fulfillment of the requirements for the degree of Doctor of Philosophy in

Kinesiology, Nutrition and Rehabilitation Science

In the Graduate College of the

University of Illinois at Chicago, 2019

Chicago, Illinois

Dissertation Committee:

Dr. Jacob M. Haus PhD., Chair and Advisor, Department of Kinesiology

Dr. Tracy Baynard, Ph.D., Department of Kinesiology and Nutrition

Dr. Giamila Fantuzzi, Ph.D., Department of Kinesiology and Nutrition

Dr. Shane Phillips, Ph.D., Department of Kinesiology and Nutrition

Dr. Zhenyuan Song, Ph.D., Department of Physical Therapy

DEDICATION PAGE

To my wife Susan, and my beautiful children Cole, Bella and baby pending (Noah),
without whom this work would have been completed two years earlier and far fewer of my youthful, black hairs would have been butchered by the surmounting grays. In the vastness of space and immensity of time, it has been my absolute joy and to share one heart between us all.

Susan, "the root of my roots, the buds of my bud and the sky of my skies." One picturesque October afternoon, alongside the Hudson River adorned in fall's leaves, I vowed to "carry your heart in my heart." That day, those few words seemed like the most important verse of our story. Now, however, I can't help but focus on something we may have missed in the newness of our young love. Perhaps this oversight was just a matter of youthful disregard, but as we have grown, standing side-by-side amongst tides of opposition, I realize our poem, like our love, has evolved. Through all of the lonely nights I have made you suffer, through all of the lone parenting you embraced while I studied, and through the financial hardships this pursuit has caused, we have finally reached the end. On this day, I want to direct your attention to a new verse of our love. Although I will always and forever carry your heart in my heart, I want you to know "whatever is done by only me is your doing, my darling."

To my children, thank you for your unwavering love while I was not my best. All of this was for you. Every tear I have shed, every defeat I endured over the past 7 years was to give you the best life I am capable of. More importantly, the completion of this program is a testament to the Blackburn resilience and determination. Your very DNA is woven with an indomitable spirit. Someday, it will define you. I promise Most importantly, I want you to know that life swings hard, and it does not offer any free lunches. But we swing harder. No matter what the adversity, we never sink.

To my family: Mom, Dad and The Dancing Bear, thank you for raising me strong, for forging a rock that effortlessly opposes the angriest of crashing waves. Thank you for teaching me to flourish in a fight and to find serenity in circumstances that most people would recognize as utter chaos. The foundations you instilled gave me the courage to accept this overwhelming challenge in the first place. Look how far I have come. Tenacity course though Blackburn veins. To Apa, Ama and Emo, thank you for being the father and husband to my family in my absents. To Apa, some very special thanks. Thank for showing the depths one man is willing go for the love of his daughter and his family. Thank you for giving up everything to help see me through this experience. Thank you for showing me that love and family are mightier than money and success. Amah, thank you for being my shoulder to cry upon. Emo, thank you for being my cheerleader and caretaker during the writing of this paper

Dr. Haus, thank you for practicing the ways of alchemy, for you have transformed a student with a very basic education into something so much more. You never let me quit myself, thank you for always giving me "just enough rope to hang myself", but stepping in to save me when those frequent hangings occurred.

To my incredible lab members, to you I say, at dawn of light, all darkness disappears. Thank you for being my dawn, day after day, month after month and year after year. All of you are my family, you will be a piece of me until I take my last, dying breath. To my beloved brothers, Rattle Snake Jake, Edwin, Ale(X), and Bloodshed, my foot would not be upon this finish line without each and every one of you. To my sisters, Abeer, Tori and Kelly, you brought balance and joy to a lab filled with meatheads. Any time any of you need an older bother to beat someone up for you, I am your man.

To all my friends, Ray, Louis/Jen, Puto (show me the pathway) and Shanty Jen, you all believed I was crazy for pursuing this, and you were right. Thank you for loving me and standing by my side through this bout of insanity. Now of sound mind, I can confidently say that I love you guys.

ACKNOWLEGMENTS

TABLE OF CONTENTS

TABLE OF CONTENTS: CONTINUED

LIST OF TABLES

ABBREVIATIONS

4-HNE	4- Hydroxynonenal
AGER1	Advanced Glycation End Product Receptor 1
AGEs	Advanced Glycation End products
Akt/PKB	Protein Kinase-B
ALB	Native Albumin
AP-1	Activator Protein 1
CAT	Catalase
CML	Carboxymethyllysine
cRAGE	Cleaved RAGE
dAGEs	Dietary AGEs
DPI	Diphenyliodonium
EDRAD	Endoplasmic-reticulum-associated Protein Degradation Pathway
EDRF	Endothelium-Derived Relaxing Factor
ER	Endoplasmic Reticulum
ERK1	Extracellular Signal–regulated Kinases
esRAGE	Endogenous Secretory RAGE
FAs	Fatty Acids
FOXO	Forehead box O
G6Pase	Glucose-6 phosphatase
GLUT4	Glucose Transporters 4
GLY-ALB	Glycated Albumin
GPX	Glutathione Peroxidase
GSK-3	Glycogen Synthase Kinase-3
H_2O_2	Hydrogen Peroxide
HAS	Human Serum Albumin
HGA	Human Glycated Albumin
HGP	Hepatic Glucose Production
HMGB1	High Mobility Group Box1
HPAECs	Human Pulmonary Artery Endothelial Cells
HSkMCs	Human Skeletal Muscle Cells
$^{\cdot}$OH	Hydroxyl Radicals
Ig	Immune Globulin
IGT	Impaired Glucose Tolerance
IL-1	Interleukin 1
IL-6	Interleukin 6
IMB	Inclusion Body Myositis
IRS1	Insulin Receptor Substrate
JNK	c-Jun N-terminal kinases
LCFAs	Long Chain Fatty Acids
LHC	Lean Healthy Control
MAP	Mean Arterial Pressure
MAPK	Mitogen-Activated Protein Kinase
MC	Mesangial Cell
mDia1	Mammalian Diaphanous-1
mTOR	Mammalian Target of Rapamycin

NADPH Oxidase	Nicotinamide Adenine Dinucleotide Phosphate-Oxidase
NF-κB	Nuclear Factor-Kappa Beta
NGT	Normal Glucose Tolerance
NHT2D	Natural History of Type 2 Diabetes
NO	Nitric Oxide
Nox 2	$gp91^{phox}$
NRROS/ LRRC33	Negative Regulator of Reactive Oxygen Species,
O_2^-	Super Oxide
OS	Oxidative Stress
$p22^{phox}$/ CYBA	Human Neutrophil Cytochrome b-Light Chain
p38	p38 Mitogen-activated Protein Kinases
$p40^{phox}$/ NCF4	Neutrophil Cytosolic Factor 4
$p47^{phox}$/ NCF1	Neutrophil Cytosolic Factor 1
$p67^{phox}$/ NCF2	Neutrophil Cytosolic Factor 2
PDBu	Phorbol 12,13-dibutyrate
PDK1	Pyruvate Dehydrogenase Kinase
PEC	Pulmonary Endothelial Cells
PEPCK	Phosphoenolpyruvate Carboxykinase
PIP 2	Phosphatidylinositol Diphosphate
PIP 3	Phosphatidylinositol Triphosphate
PI3-K	Phosphatidylinositol-3-kinase
PKB	Protein Kinase B
PKC	Protein Kinase C
PKCα	Protein kinase Cα
PTEN	Phosphatase and Tensin Homolog
PTP	Protein Tyrosine Phosphatases
Rac 1	Ras-related C3 botulinum toxin substrate 1
RAGE	Receptor for Advanced Glycation Endproducts
RAGEct	RAGE Cytoplasmic Tail
RAS	p21/Ras protein
ROS	Reactive Oxygen Species
Rho	Rho-GTPases
SH2	Src Homology 2 Domain
SOD	Superoxide Dismutase
SR	Sarcoplasmic Reticulum
sRAGE	Soluble RAGE
Src	Src Protein Tyrosine *Kinases*
T2DM	Type 2 Diabetes Mellitus
Tks5	Tyrosine Kinase Substrates with 5 SH3 Domains)
TBARS	Thiobarbituric Acid Substances
TG	Triglycerides
TLR	Toll Like Receptor
TNF-α	Tumor Necrosis Factor
TT	Transvers Tubule

Chapter I. Introduction

I.A. Introduction to the Problem

The critical health impact the incidences of Type 2 Diabetes Mellitus (T2DM) has imposes on public over the past decade is emerging as the a foremost cause of death in the United States [1]. The natural history of T2DM, also described as the glucose tolerance continuum is a multifactorial condition that results in chronic hyperglycemia superimposed with insulin resistance and glucose intolerance [2, 3]. While no tissue is immune to the damaging effects of chronic hyperglycemia, its impact on skeletal muscle may be most critical for whole body metabolism as skeletal muscle composition makes up nearly half of total body mass and more than 80% glucose uptake via healthy insulin signaling [4]. Human skeletal muscle responds to unfavorably to chronic hyperglycemia by increased generation of reactive oxygen species (ROS), which in turn, activates of pro-inflammatory signaling pathways and potentiating a pro-oxidant and pro-inflammatory environment [5, 6]. The precise mechanisms that underlie these metabolic abnormalities are still poorly defined [7]. Elucidation of the molecular events implicit in hyperglycemia-induced ROS production is essential for the treatment and prevention of T2DM and the subsequent development of complications such as nephropathy, neuropathy, and retinopathy. Of the many pathological events associated with T2DM, the most deleterious may be the increased expression of the receptor of advanced glycation end products (RAGE). RAGE is a multi-ligand receptor that has been identified as a potent activator NF-κB (nuclear factor-kappa beta) and subsequent production of inflammatory cytokines. The mechanisms by which RAGE induces NF-κB have been shown to be strongly associated with ROS production, particularly in skeletal muscle tissue [8-10]. Further, RAGE induced NF-κB signaling also initiates the self-transcription of RAGE, thus producing a futile cycle that generates greater RAGE protein expression at the cell membrane. These molecular events propagate RAGE signaling, promote ROS production and exacerbate inflammation [11, 12]. Thus, RAGE-

expressing cells are susceptible to multiple cellular insults, which induce future complications associated with diabetes.

Although the exact mechanisms by which these events occur are unclear, RAGE induced ROS generation may be dependent upon the assembly and activation pattern of the NADPH oxidase enzymatic system, a multi-subunit enzyme complex that produces superoxide (O_2^-) by one electron reduction of molecular oxygen through the Nox 2 subunit [13, 14]. Under homeostatic conditions, the NADPH oxidase enzyme complex assembles, and disassembles to produce episodic bursts of O_2^-. This process is tightly regulated by the phosphorylation of p47[phox], a principle subunit that initiates enzyme complex assembly through the colocalization of additional cytosolic factors, including p67[phox], p40[phox] and Rac 1/2 (**Figure 2**), [15-17]. Under homeostatic conditions, Nox 2 induced O_2^- is a transient event, and disassociation of p47[phox] from the complex terminates Nox 2 action. Under pathological conditions, such as T2DM, p47[phox] phosphorylation is upregulated, provoking heightened NADPH oxidase complex assembly and increased O_2^- production [18, 19]. One potential kinase that may be modulating increased p47[phox] phosphorylation is non-tyrosine kinase (Src). Src is recruited by ligand bound transmembrane receptors that are absent of intrinsic tyrosine kinase activity [20]. When phosphorylated at tyrosine 419, Src undergoes a conformational change, which exposes the SH1 domain's kinase site [21, 22]. Once active, Src signals cell stress responses by phosphorylating downstream targets associated with oxidative stress and inflammation [23].

Interestingly, RAGE activation has been shown to initiate Src kinase phosphorylation and subsequent NADPH oxidase complex assembly [24, 25]. RAGE is absent of intrinsic tyrosine kinase activity and once ligand bound, the RAGE cytoplasmic domain associates with mammalian diaphanous-1 (mDia-1) the FH1 domain, which has been shown to transmit RAGE signaling to downstream targets [26]. Active mDia-1 has been implicated in associating with Src kinase's SH3 domain, converting Src from inactive

to an active state [27, 28]. In various tissue types, active Src phosphorylates and initiates the translocation of both p47^{phox} and p67^{phox} for NADPH oxidase complex assembly. Likewise, increased Src activity has reported to be a principal mechanism associated in the development of insulin resistance and diabetic nephropathy [29, 30]. Thus, it appears likely that a RAGE/ NADPH oxidase complex signaling axis may be linked by mDia-1 dependent Src kinase activation (**Figure 1**).

RAGE signal transduction and concomitant Nox 2 O_2^- production disrupts the balance between ROS generation and scavenging. Thus, maintaining the integrity of antioxidant defense is critical for optimal cellular function and prevention of a pro-oxidative environment. Several decades of dietary and nutraceutical research efforts suggest that antioxidant supplementation may be advantageous in preventing oxidative stress and the development of many chronic diseases [31, 32]. However, results from randomized control trials have been unconvincing in the setting of preventative therapy. Thus, an alternative strategy may be to enhance the expression of endogenous defenses, or to reveal new mechanisms of intrinsic antioxidant defenses [33]. Intriguingly, a study conducted by Noubade *et al.* (2014), demonstrated that Nox 2 enzyme activity is regulated by a novel, leucine-rich protein, dubbed negative regulator of reactive oxidative species (NRROS, also known as LRRC33). NRROS directly competes with the p22^{phox} subunit for Nox 2 co-localization. NRROS-bound Nox 2 is then flagged for degradation by intracellular proteases, thereby promoting a favorable balance between ROS production and removal.

Paradoxically, NRROS protein is predisposed to degradation through pro-inflammatory signaling responses, suggesting that ROS and subsequent inflammation reduce NRROS defense [34]. Further, NRROS limits toll like receptor (TLR) inflammation, and tags TLRs for degradation in a similar manner

as Nox 2. TLRs and RAGE share analogous mechanistic properties, mutual binding ligands and signaling events. Further, accumulating evidence indicates that RAGE and TLR collaborate in immune response initiation and host defense [35, 36]. Thus, NRROS may be a fundamental scavenger of transmembrane proteins that augment the oxidative and inflammatory milieu.

Figure 1.
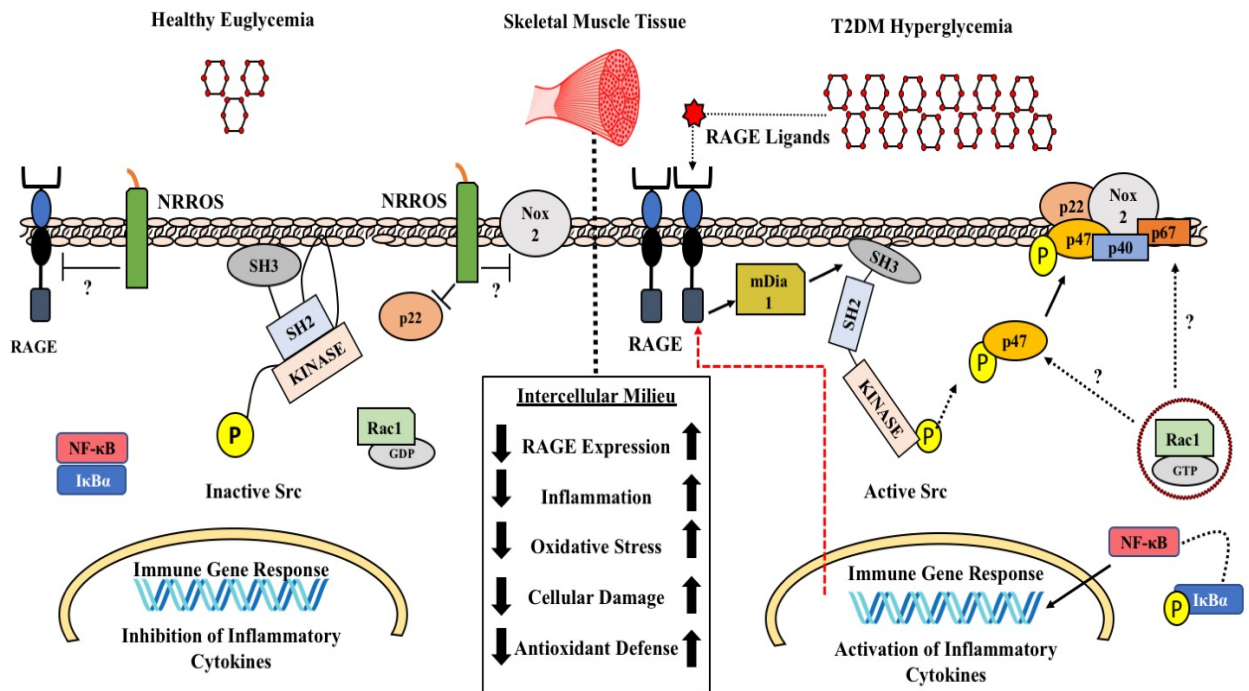
Figure 1. Working model for the investigation of the RAGE/Nox 2 Axis.
RAGE, Receptor for Advanced Glycation Endproducts; mDia 1, Mammalian Diaphanous-1; Src (inactive/ Active), non-tyrosine kinase Src; p47, p47phox; Rac 1, Rac 1; Nox 2, pg91phox ; p22, p22phox, p67, p67phox; 02.-, superoxide; NF-κB, nuclear factor kappa-light-chain-enhancer of activated B cells; IκBα, I kappa B alpha; NRROS, Negative Regulator of Reactive Oxidative Species.

I.B Purpose of This Study

It appears evident that a RAGE/NADPH oxidase axis (here after referred to as RAGE/Nox 2 axis) fundamentally augments ROS production, and the loss of counter-regulatory NRROS indicate a principle alteration that drives development of diabetic complications. While a RAGE/Nox 2 axis has been proposed, and studied in vascular and kidney tissues, its role in skeletal muscle has not been elucidated. Likewise, tissue specific expression and temporal regulation of NRROS has not previously been characterized. Skeletal muscle is a vast, highly metabolic and plastic organ, making it an innovative platform to investigate diabetes [37]. Further, skeletal muscle expresses RAGE several fold greater than vascular and neuronal tissues. To investigate these mechanisms in human skeletal muscle, we aim to determine the mediators of RAGE signaling on NADPH oxidase activity and the potential protective role of NRROS. Of great metabolic importance, is identifying the role of insulin in the proposed paradigm given skeletal muscle is the chief location for greater than 80% of insulin-mediated glucose disposal, and we have previously shown that insulin has direct effects in mediating NADPH oxidase complex assembly [38-40]. Therefore, the collection of both basal and insulin stimulated skeletal muscle samples, obtained during the hyperinsulinemic-euglycemic clamp procedure, may exhibit independent regulation of the RAGE-Nox 2 signaling axis.

1.C Specific Questions & Aims

Based upon the weight of the existing literature, coupled with the above preliminary data, we propose the following questions, aims and hypotheses:

Question 1: *How does the manifestation of T2DM impact expression patterns of RAGE and NADPH oxidase signaling intermediates in human skeletal muscle?*

Specific Aim 1: In basal and insulin-stimulated human skeletal muscle samples obtained during the hyperinsulinemic-euglycemic clamp procedure, we intend to distinguish the RAGE/Nox 2 axis signaling intermediates in a cohort of lean healthy individuals and T2DM subjects.

Hypothesis 1: The working hypothesis is that the presence of insulin and T2DM will increases RAGE-mediated NADPH oxidase intermediate protein expression, while negatively influencing inflammatory mediators compared to lean healthy control subjects.

Question 2: *Is RAGE dependent Nox 2 activation mediated by Src kinase?*

Specific Aim 2: Elucidate the mechanism of RAGE-mediated signal transduction in the activation of Nox 2 in primary human skeletal muscle cells treated with the RAGE ligand, glycated albumin.

Hypothesis 2: The working hypothesis is that RAGE-dependent mDia-1 activation mediates Src kinase phosphorylation and subsequent NADPH oxidase complex assembly via phosphorylation of p47^{phox}.

Question 3: *What cellular factors and/or physiological stimuli augment RAGE signaling events and subsequent ROS generation?*

Specific Aim 3: Explore the putative role of NRROS within a narrow scope. First, we intend to characterize NRROS protein expression among LHC and T2DM in basal and insulin-stimulated skeletal muscle obtained during the hyperinsulinemic-euglycemic clamp. Next, we aim to elucidate how AGE stimulation impacts NRROS expression in primary human skeletal muscle cells.

Hypothesis 3: The working hypotheses is that NRROS protein will demonstrate the greatest expression in LHC adults and decrease in obese and T2DM cohorts. Further, RAGE activation will decrease NRROS expression in primary human skeletal muscle cells.

Chapter II. Literature Review

II. A. The Natural History of Type 2 Diabetes: An Overview

Type 2 Diabetes Mellitus (T2DM) is a chronic metabolic syndrome that is the major cause of mortality in both developed and underdeveloped nations [41]. It is projected that approximately 400 million individuals international are currently diagnosed with T2DM. By the year 2030, some 240 million more individuals will be living with this progressively debilitating disease [42]. Presently, the incidence of T2DM in the U.S. are rapidly increasing among the world's population [43]. With growing diabetes diagnoses among children, young adults, and an estimated 30 million adults, T2DM is a serious health concern placing a considerable economic burden on U.S. healthcare system, with over $332 billion in annual costs [44]. Understandably, investigating the etiology and pathogenesis of T2DM is of considerable importance.

T2DM is a progressive disease that initiates chronic complications strongly associated with excess morbidity and mortality. Further, the manifestation of diabetes triggers succession of long-term metabolic abnormalities involving multiple systems that challenges the body's capability to control and uphold systemic glucose homeostasis (**Figure 2**). Maintaining normal glucose tolerance (NGT) within narrow physiological limits (NGT) depends on a delicate equilibrium between insulin secretion and insulin sensitivity at highly metabolic organs [45]. In human metabolism, glucose disposal is regulated chiefly by insulin-mediated glucose uptake on target tissue including the liver, skeletal muscle and to some degree adipose tissue [46]. Disturbances in normal insulin kinetics provokes deviant glucose homeostasis and prompt a departure from NGT to impaired glucose tolerance (IGT) and finally overt T2DM [47]. While countless factors have been associated with the pathogenesis of diabetes, insulin resistance appears to be the earliest pathogenic injury to develop in the natural history of T2DM [48]. Insulin resistance is term

best explained by a decreased physiological response to circulating insulin, thereby negatively impacting the ability to promote glucose uptake [49]. Although the precise mechanism surrounding the regression to insulin sensitivity is not fully elucidated, the onset of insulin resistance has been significantly correlated with chronological aging, excess weight gain, poor dietary habits and sedentary lifestyle [50-52]. Evidence now indicates that in most populations, the progression from IGT to overt T2DM is driven by changes in degrees of insulin resistance in insulin-sensitive tissues, and these events represents the primary injury that disrupts NGT and initiates glucose disequilibrium [53-55].

Figure 2.

Pathogenies of T2DM

| Sedentary Lifestyle | Poor Dietary Habits | Chronological Aging | Obesity |

Mild Insulin Resistance

↓

Compensatory Hyperinsulinemia ← **Increased Beta Cell Activity**

↓

Compensated Insulin Resistance at Insulin Sensitive Tissue

↓

Impaired Glucose Tolerance

↓

- **Over T2DM**
- **Insulin Resistance**
- **Chronic Hyperglycemia**

← **Beta Cell Failure**

Developing long –term diabetic complications
Advanced Glycation End Products (AGEs)
Chronic Inflammation
Reactive Oxidative Species (ROS)
Loss of Antioxidant Defenses
Increased Receptor for Advanced Glycation End Products (RAGE) Expression

Long –term diabetic complications
Retinopathy
Cardiovascular Disease
Neuropathy
Nephropathy

Figure 2. An overview representation of the pathogenies of T2DM and development of long-term diabetic complications.

II. A. I The Natural History of Type II Diabetes: The pathogenesis of the diabetic syndrome

Several metabolic amoralities arise in tissue resistant to insulin action. (1) Pancreatic β-cells intensify the production of insulin and secretion patterns in an effort counterbalance defects in insulin action at the liver, adipose and skeletal muscle. (2) During fasting conditions, hepatic glucose production (HGP) is elevated and fails to be suppressed by circulating insulin (3) Glucose disposal at skeletal muscle becomes

compromised and diminished glucose uptake further exacerbates rising plasma glucose levels. Jointly, these events produce a compendium of pathophysiological changes that further reduce insulin sensitivity, minimize glucose disposal and foster the development of chronic hyperglycemia **(Figure 3)** [3, 56].

II. A. II Pancreas Impairments Across the Natural History of T2DM

The primary function of islet cells is to manufacture and emit insulin in response to a glucose challenge [57]. When circulating glucose levels begin to rise, beta cells quickly respond by secreting insulin while at the same time increasing insulin hormone production [58]. Beta cells tend to alter their functionality during the early stages of T2DM [59]. Over the course of the natural history of T2DM, beta cells will intensify their activity and secrete super-physiological concentrations of insulin (also known as compensatory hyperinsulinemia) to regulate to impaired glucose tolerance (**IGT**), this compensation will maintain glucose homeostasis for a period of time [60-62]. Beta cell compensation will occur for variable lengths of time. However, as an individual further progresses along the continuum, beta cells become exhausted in their compensatory efforts to maintain euglycemia. Through this process, beta cells begin to falter, and systemic insulin levels begin to decline. When this goal cannot be achieved, gross decompensation of glucose homeostasis occurs, and hyperglycemia [63-66]. Underlining these adverse changes in beta cell action, glucagon, (a catabolic hormone that is released to break down glycogen and promote glucose secretion) increases it secretory activity further inducing a hyperglycemic condition [67].

Figure 3.
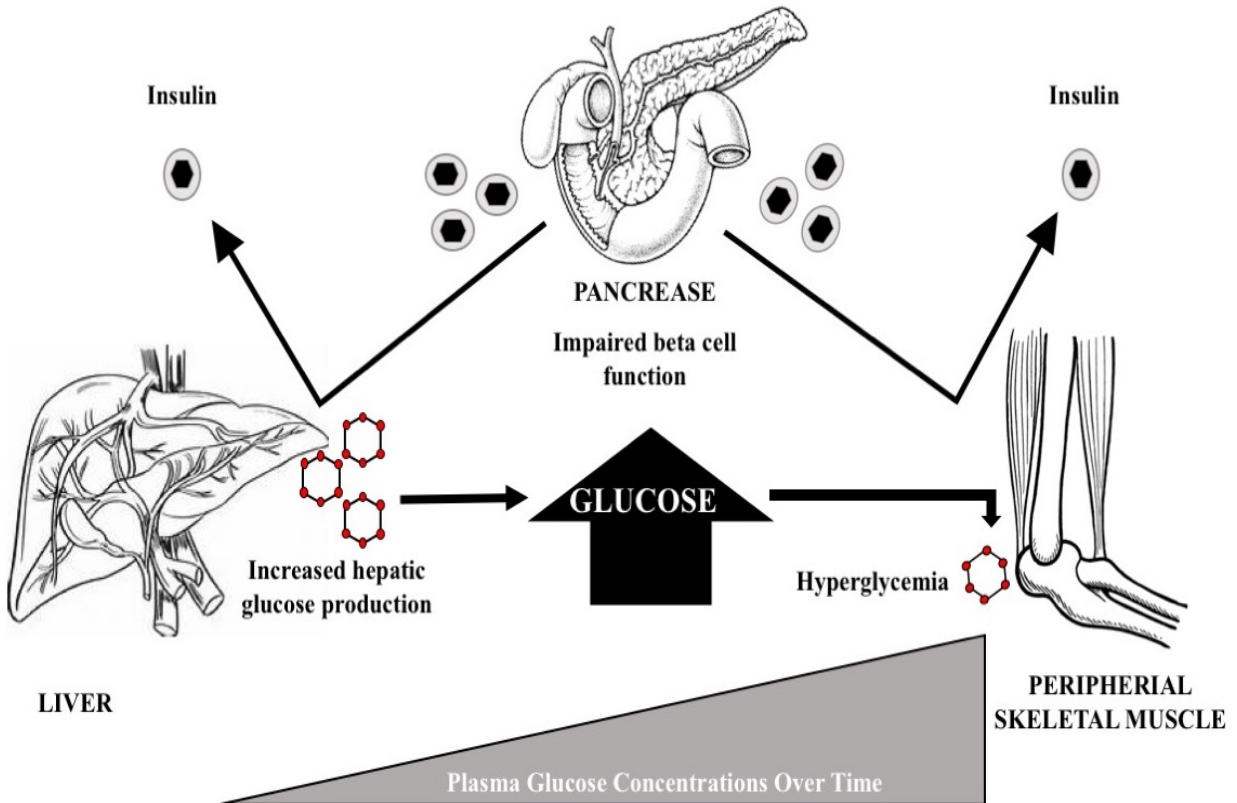
Figure 3. Phenotypic Manifestation of T2DM.
Representation of the three converging metabolic anomalies across the Natural History of T2DM leading to the development of hyperglycemia. Insulin resistance, impaired beta cell function and increased hepatic glucose production all intersect to generate chronic hyperglycemic conditions.

II. A. III Liver Impairments across the Natural History of T2DM

The liver plays a central role in establishing whole-body glucose homeostasis [68]. The various functions

of the liver are carried out by hepatocytes, where most hepatic functions are tightly regulated by circulating

insulin levels [69]. According to current dogma, an increase in hepatic glucose production is considered a pivotal event in insulin resistance development and further progression through the T2DM continuum [70]. Therefore, insulin resistance at hepatocytes represents a key injury in the pathogenesis of diabetes, resulting in the appearance of fasting hyperglycemia.

During fasted states, hepatic glucose production **(HGP)** accounts for 80 - 90 % of the necessary blood glucose to maintain global physiological activities [71]. Glucose concentrations released by the liver appear in the blood at levels that range between 1.9 to 2.2 mg/kg/min in healthy individuals, but these values are elevated in diabetic phenotype [72, 73]. A series of studies show that the two-primary mechanism that control fasting HGP, glycogenolysis and gluconeogenesis, is augmented in individuals with T2DM [74-76]. Studies propose that these mechanisms become uninhibited in the progression to overt T2DM and therefor have been labeled as contiguous factors on increased HGP and augmenting gluconeogenic flux. [77]

In postprandial states, conversely, HGP must be repressed to avert large surges in blood glucose consternations. This event is largely coordinated by insulin action and counter regulatory system of hormones (namely glucagon) working cooperatively to uphold normal blood glucose levels [78]. Insulin acts on the suppression of HGP by decreasing glycogenolysis and gluconeogenesis processes [79, 80]. Two mechanisms by which insulin directly regulates these events are through suppression of glucose-6 phosphatase (G6Pase) and two phosphoenolpyruvate carboxykinase (PEPCK), [81, 82]. PEPCK is a vital enzyme that initiates the preliminary step in the conversion of CREB cycle intermediates into serviceable glucose, thereby being a primary component responsible for glyconeogenic glucose production [83, 84] Under insulin sensitive conditions, circulating insulin inhibits the gluconeogenesis pathway by

suppressing PEPCK activity, protein expression and gene transcription [85]. Conversely, as demonstrated in numerous animal studies, the onset of obesity and mild insulin resistances increases PEPCK activity and mRNA levels 3-fold over lean, healthy animals, thereby increasing gluconeogenic processes and contributing substantially to hyperglycemic conditions [86]. G6Pase is the mandatory enzyme of hepatic glucose production responsible for catalyzing the final reaction preceding glucose release in blood [87]. Insulin reduces G6Pase activity and hepatic glucose output in healthy subjects. This response is initiated by decreasing glycogenolysis and enhancing glycogen accumulation [88]. Thus, gluconeogenic mechanisms becomes unrestrained in diabetic conditions due deficient insulin action. [89]. This adverse modification in hepatocyte function contributes to impaired gluconeogenesis suppression and increase circulating glucose in both fasted and fed conditions [90].

During the onset of obesity and further progression through the T2DM continuum, the reduction of insulin sensitivity at the liver diminishes insulin-mediated inhibition of HGP. Thus, the rate of HGP in T2DM individuals increases substantially compared to health counterparts [91].

II. A. IV. Skeletal Muscle Impairments across the Natural History of T2DM

Skeletal muscle is a distinctively vital tissue in maintaining normal glucose levels, and defects in skeletal muscle's ability to metabolize glucose profoundly corrupts glucose tolerance [92]. Skeletal muscle is the archetypal target tissue for insulin action, and it is reported that the vast majority of all glucose disposal occurs at the skeletal muscle, in an insulin-stimulated state [93]. These observations are supported by research conducted utilizing leg catheterization studies, where insulin -mediated glucose disposal accounted for $80 - 90$ %-fold increase in postprandial, glucose uptake. Conversely, in a T2DM phonotype, insulin mediated glucose uptake has been shown to be markedly decrease [94, 95]. Therefore, it is no

surprise skeletal muscle represents the foremost site for insulin resistance, impacting a significance percentage of overall glucose disposal [96].

While the mechanism surrounding insulin resistance in human skeletal muscle are immense, causal abnormalities responsible for impaired glucose dispose range from defects in insulin receptors, impaired enzyme activity, loss of Glucose Transporters 4 (**GLUT4**) translocation capacity and defective intracellular signaling [97-99]. Glucose disposal at skeletal muscle is dependent upon an intracellular] response, where by insulin indirectly activates the translocation of GLUT4 (Glucose Transporters 4) to the sarcolemma to receive and uptake circulating glucose [100]. Insulin signaling initiates a cascade of cellular events and during the transition from NGT to IGT, defects begin to occur along the signaling cascade [101]. Before considering some of the potential defects that impair insulin signaling, it will be advantageous to review the common concepts surrounding normal insulin action. The activation of the insulin receptor initiates once insulin binds to the receptor's extracellular hub. This interaction induces a structural change within the receptor, resulting in phosphitylation of β subunits upon the tyrosine kinase domain [102]. Once the activation of tyrosine residues has become active, tyrosine catalytic activity becomes markedly enhanced and the phosphorylation of several downstream targets can commence [103].

Following insulin receptor activation, a signal is propagated downstream to diverse insulin regulated targets. Various enzymes, protein-transporters and insulin-sensitive genes activate and mediate a myogenic effect or recruit glucose transport vesicles [104]. Several cytosolic intermediates are needed to propagate these cellular responses to insulin. Initially, Insulin Receptor Substrate (**IRS 1**) becomes activated by interacting with the insulin receptor's tyrosine residues. Once phosphorylated, IRS 1 preferentially binds to Src Homology 2 **(SH2)** homology domains. Specially, IRS 1 will associate with

regulatory subunits p110 and p85 to form a docking site for other intermediate interactions. This dimer will then recruit phosphatidylinositol-3-kinase (**PI3-K**) to form an enzyme complex [105]. Once formed, this enzyme complex activates PI3-K, promoting the transformation of phosphatidylinositol diphosphate (**PIP2**) to phosphatidylinositol triphosphate (**PIP3**) [106]. PIP3 phosphorylate **PDK1** (phosphoinositide-dependent protein kinase1) which directly activates PKB (protein kinase B), also identified as Akt and protein kinase C (**PKC**) [107]. Succeeding its recruitment, active Akt induces the phosphorylation of many downstream substrates. Active Akt induces cellular proliferation growth, and survival responses by further stimulating downstream targets including, mammalian target of rapamycin (**mTOR),** Forehead box O (**FOXO**) and Glycogen Synthase Kinase-3 (**GSK-3**) [108-110]. In skeletal muscle, these kinases collaboratively stimulate translocation of GLUT4 to the plasma membrane, facilitating the entry of glucose into the intracellular space [111]. Clearly, skeletal muscle insulin sensitivity encompasses a cascade intracellular signaling events, and defects in the signals anywhere along the previously mentioned sequences result in the development of progressive insulin resistance and other diabetic associated complications.

II. B. Conventional Mechanism Underlining Insulin Resistance in Skeletal Muscle

Much attention has been dedicated to the mechanics involved in transmitting information from the insulin receptor to the cytosolic effectors. However, in the case of T2DM, the question remains whether pre or post-binding abnormalities is the primary lesion associated with decreased insulin sensitivity in peripheral tissue. Early work in this field investigated how receptor quantity and binding traits could be negatively altered in the development of T2DM. In one study, obese mice demonstrated a significant reduction in insulin binding in contrast to their healthy counterparts [112]. Conversely, later rodent model works disproved these earlier studies by demonstrating that insulin resistant rodents matched their healthy

counterparts in insulin binding efficiency, and insulin signaling [113]. The results obtained from this work suggest that receptor abnormalities may not be the origin of insulin resistance. In more recent studies Kono et. al. set out to determine if receptor habitation impacts signaling potential, several groups have investigated how receptor characteristics could led to the increase probability of developing insulin resistance. This group recognized that maximal glucose disposal is mediated by only a fraction of insulin receptor occupancy. Therefore, GLUT 4 translocation and glucose uptake is elicited by 10 – 20% of receptor occupancy [114-116]. Collectively, these findings suggest that insulins affinity for the insulin receptor, insulin binding capacity and receptor occupancy may be secondary defects that could occur after the development of overt T2DM. Further, fluctuations in circulating insulin may not impose any adverse biological responses that could result in the development of insulin resistance. Thus, It would appear that insulin action is mediated through a minor portion of receptor occupancy, thereby suggesting decreased responses to insulin signaling is a result of post binding defects.

The autophosphorylation events that occur at the insulin receptor's C-terminus are located within the cytosolic region of the cell. In T2DM subjects, tyrosine- autophosphorylation kinase activity is blunted, resulting in submaximal transmission of the insulin signal [117, 118]. While the implications of reduced autophosphorylation of tyrosine residues will have a global impact on cellular transmission, the implications on IRS recruitment may be most impactful. While IRS1 protein concentrations appear to be unaffected across the natural history of T2DM, its activity has been shown to be repressed in T2DM subjects [119]. In order to become active and further propagate the insulin signal, IRS1 activation is contingent upon the phosphorylation of a serine or threonine residue. This event is initiated by active tyrosine residues upon the beta subunits of the insulin receptor [120]. Two hypotheses surrounding IRS 1 activation and propagation defects are currently being debated. The first mechanism may involve the

recruitment of proteasomal machinery to degraded IRS proteins upon activation of insulin receptors [121]. A second mechanism underlining this phenomenon results from over activating insulin receptors during a hyperinsulinemia condition. Paz et.al. demonstrated insulin resistance increases insulin receptor activation and consequently increases serene/threonine phosphorylation upon the IRS active site. These series of events resulted in obstruction of IRS docking to other insulin dependent intermediates and failure to transmit insulin signaling[122].

In a majority insulin resistance research, immunoprecipitation studies and in vivo assays demonstrate that PI3K alterations are strongly associated with IRS protein dysfunction and impaired downstream propagation [123, 124]. While the exact mechanisms surrounding PI3K's contribution to degraded insulin signaling are still uncertain, recent studies indicates that complications could exist in PI3K recruitment by IRS1 at tyrosine phosphorylated by IRS1, unfavorably modulation of PI3K action through interaction with RAS, or increased regulator action of PTEN, which impacts PIP_3 activity and further diminish downstream targets [125, 126] PI3K at mediates glucose disposal via insulin signaling cascade. In skeletal muscle, insulin-induced PI3K recruitment and activity is diminished across the Natural history of T2DM [127]. These adverse alterations to PI3K have been associated with significant decreases in whole-body glucose disposal and the development of hyperglycemia [128]. Most importantly, perhaps, PI3 K activation regulates the intracellular PIP_3, resulting in the phosphorylation of Pyruvate Dehydrogenase Kinase (PDK1), and PDK/Akt. Both of these latter enzymes reside upstream from GLUT4 transporters [129]. Thus, upstream complications in insulin propagation will certainly impact downstream targets that are essential for GLUT4 translocation and glucose disposal into the cell.

Perhaps the most important insulin mediated target within the cascade is Akt. This serine/threonine kinase mediates key insulin – induced metabolic actions [130, 131] . Akt activation occurs via phosphorylation of Ser473 and Thr308 residues, and in skeletal muscle, this action is dependent on PDK, respectively [132, 133]. The mechanism underlining impaired insulin-induced activation of Akt in the Natural History of T2DM is still a much-debated matter. Some studies reveal that T2DM skeletal muscle demonstrates substantial reductions in Akt phosphorylation at the enzymes activation sites, Ser473 and Thr308 [134, 135]. Krook et al. reinforced these findings by examining Akt activation characteristics at different time points along the Natural History of T2DM. Having surveyed isolated muscle fibers among obese T2DM and BMI matched, non-diabetics subjects, Krook and colleagues observed that insulin-mediate Akt activation was significantly reduced in diabetics compared to their non-diabetic counterparts [136].

The aforementioned signaling mediators correspondingly contribute to downstream insulin signaling from the activation of the insulin receptor to various insulin-responsive targets. If the propagation of this signal is uninterrupted, GLUT4 will translocate to the cellular membrane to uptake circulating glucose and deliver it for cellular metabolism [137]. GLUT4 translocation is a significant event in orchestrating systemic glucose homeostasis. Reports indicate that suppressed GLUT4 action exemplifies one of the initial defects, which substantially contribute to insulin resistance in skeletal muscle [138, 139]. Studies conducted in T2DM adipose tissue and skeletal muscle reveal GLUT4, translocation, irrespective of circulating insulin, becomes compromised across the Natural History of T2DM [140]. While diminished glucose uptake in diabetic adipose tissue is linked with marked decrease in GLUT4 protein expressions, skeletal muscle GLUT4 protein and mRNA levels remain unaffected compared to non-diabetic samples [141, 142]. However, concentrations of insulin-induced GLUT4 translocation diabetic skeletal muscle are reduced by 90% [142]. Since skeletal muscle upholds GLUT4 protein expression across the Natural

History of T2DM, it seems evident that impairments within the insulin signaling cascade is accountable for quelling vesical translocation and glucose uptake. The decisive goal of insulin signaling is to recruit GLUT4 vesical for glucose disposal, thereby upholding global glucose homeostasis. GLUT4 trafficking is dependent on a complex series of phosphorylative events across an arranges of insulin sensitive proteins involved in regulating GLUT4 trafficking. It is evident that defective trafficking is not an isolated event, but rather amalgamation of deficiencies across the insulin signaling pathway.

The Natural History of T2DM denotes a sequence of metabolic abnormalities transgressing cooperatively over a continuum, inevitably resulting in frank T2DM. While this review surveys the disease through a narrow scope of core defects in beta cell function, hepatic glucose physiology and reduced insulin sensitivity at key organs, our understanding of T2DM continuum has broadened considerably. It is now evident that the progression of T2DM is multisystem disease driven by defects in other tissues types including alpha cells, adipose tissues, the brain, and the gastrointestinal tract [3]. In varying degrees, these metabolic aberrations exacerbate the mounting core defects, integrating on a common pathway of hyperglycemia.

II. B. I. Unconventional Mechanism Underlining Insulin Resistance in Skeletal Muscle

While the aforementioned mediators underlying the development of insulin resistance and subsequent impaired glucose disposal have been meticulously studied, secondary mechanisms also arise concurrently with hyperglycemia, which further attenuates insulin action in skeletal muscle. Synchronically, these multiple insults result in further progression across the natural history of T2DM.

The development of chronic hyperglycemia independently accelerates non-enzymatic glycation reactions between protein-reactive amino groups, and glucose [143] . These unregulated and spontaneous protein modifications result in the production of Amadori products, which can further undergo additional modifications thereby producing the irreversible **Advanced Glycation End Products** (AGEs) [144]. It is well documented that elevated concentrations of AGEs preferentially bind to ligand specific receptors and induce a variety of diabetic complications including insulin resistance, inflammation and ROS [10, 145-147].

Thus, the development of AGE-related complications in the human body is a secondary mechanism that compromises insulin-mediated glucose uptake on two distinct fronts. On the one hand, direct protein glycation and readily in hyperglycemic conditions [148]. The second consequence of AGE formation is the activation of the proinflammatory RAGE receptor. AGE/RAGE binding activates a variety of cellular responses that achieve chronic inflammation and impaired glucose sensitivity [149].

Critical investigations into glycated proteins, whether as early-stage glycation products or irreversible AGEs, have demonstrated that elevated blood glucose concentrations promote the adverse modifications of various proteins, specifically in the context of T2DM [150]. However, one such target that is highly receptive to non-enzymatic glycation modification is human serum albumin (**HSA**) [151, 152]. These transport proteins are one of the most widely expressed proteins in human serum, accounting for nearly 50% of the total serum protein concentration [153]. Studies indicate that human glycated albumin (**HGA**) concentrations are elevated in individuals living with T2DM [154, 155]. Further, HGA is an influential RAGE activator. Upon binding, HGA-mediated RAGE activation initiates downstream signaling cascades that are strongly associated with insulin resistance, inflammation, and ROS generation [156, 157].

In 2003, Miele and colleagues demonstrate that AGE-effectuated RAGE activation induces insulin resistance. Having stimulated L6 cells with HGA for 24 hours Miele and colleagues showed that AGE treatment induced a 3-fold increase in protein kinase Cα (**PKCα**) activation compared to control cells, designating PKCα as likely mediator responsible for blunting insulin action. In a follow-up, 2008 study, Miele's team further established that L6 cells stimulated with HGA treatment also resulted in phosphorylated Src kinase at tyrosine 416, which once active, colocalized to form a complex with RAGE and PKCα. This complex was further shown to cooperate with IRS-1(insulin receptor substrate-1) and prevent downstream insulin signaling cascades (**Figure 4**). Treatment of L6 cells with Src inhibitors abolished these events and maintained insulin sensitivity [158].

These results indicate that AGEs possess the ability to collaborate with the traditional mechanism accountable for developing insulin resistance. AGE/RAGE interaction is then a secondary mechanism by which insulin action is further blunted in L6 cell lines. It would then seem that an investigation into how AGEs induce the interplay between RAGE, Src and other mediators of insulin resistance in human skeletal muscle and HSkMCs is a necessary next step.

Figure 4
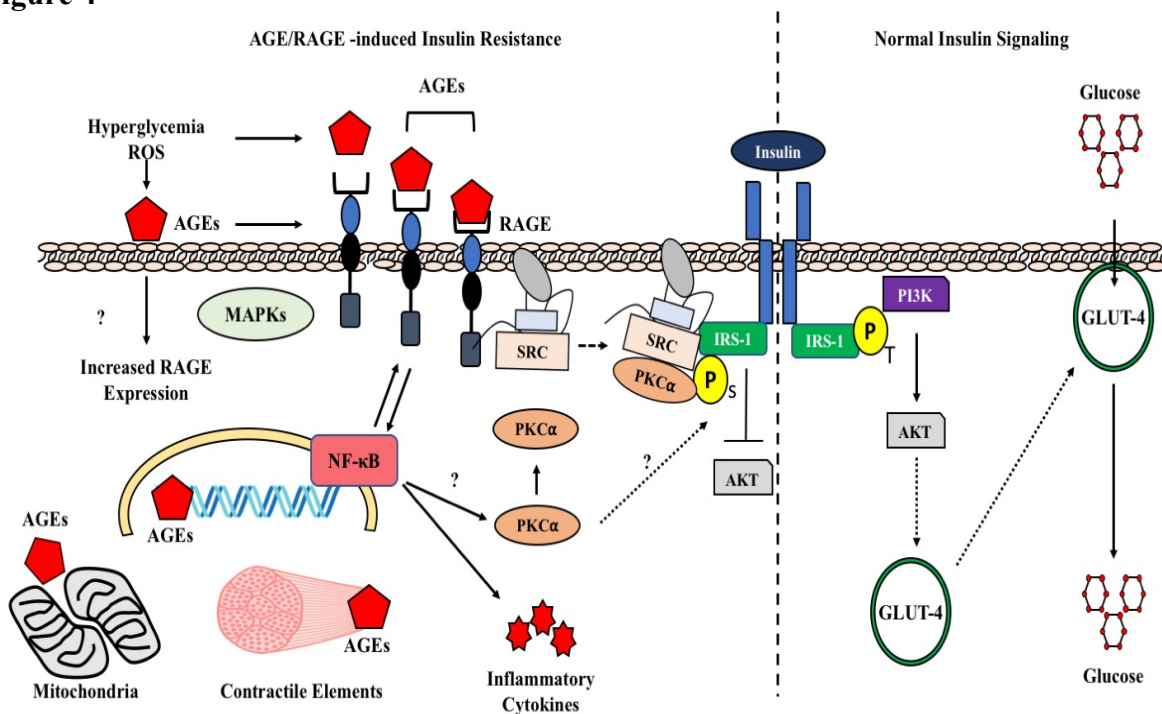
Figure . Working model for the potential mechanisms involved in AGE/RAGE induced insulin resistance in human skeletal muscle. AGEs, Advanced Glycation End Products, RAGE, Receptor for Advanced Glycation Endproducts; Src, Tyrosine Src Kinase, IRS-1, Insulin Receptor Substrate 1, PKCα, Protein kinase C alpha, Akt, Protein Kinase B, NF-κB, Nuclear Factor Kappa-light-chain-enhancer of Activated B Cells, AMPKs, Mitogen-activated Protein Kinase, PI3K, Phosphatidylinositol-4,5-bisphosphate 3-kinase, GLUT4, Glucose Transporter Type 4

II. B. II. Whole body metabolism: The Impact of Skeletal Muscle Health

Human skeletal muscle is one of the most significant metabolic tissues throughout the human body. It is a vast organ comprising of approximately half of total body mass in adults and accounts for one quarter

of the resting metabolic rate, designating skeletal muscle as a major determinate in resting metabolic expenditure [159]. Often the metabolic importance of skeletal muscle is discounted, yet this tissue must manage with a variety of divergent activates and metabolic profiles.

Skeletal muscle has a dynamic ability to metabolize both glucose and fatty acids in an effort to convert chemical energy to mechanical energy. In postprandial states, skeletal muscle is critical in maintaining metabolic homeostasis, as it is a major location for insulin-induced glucose uptake [94]. This event converts glucose into useable energy via aerobic and anaerobic glycolysis, thereby directly contributing to whole body glycemic control. Further, skeletal muscle is a central organ for storing glycogen, possessing a substantial capacity over hepatocytes [160]. Commonly, skeletal muscle is partitioned into two unique fiber types, which are distinguished as slow and fast twitch fibers. Slow twitch fibers, designated as type I fibers, are rich in mitochondria, rendering them as highly oxidative fiber that are optimal for low intensity activities that are longer in duration [161]. Conversely, fast twitch fibers, identified as type IIa & IIb, express an abundance of glycolytic enzymes, which are high necessary for high- energy consuming activities that occur through anaerobic and aerobic glycolysis[162, 163]. Jointly, these multifactorial mechanisms are driven by intercellular processes, which furnish skeletal muscle with the machinery to govern fuel selection and maintain metabolic flexibility during energy shifts [164, 165]. Alterations in skeletal muscles' ability to respond according to conditional changes in metabolic demand is hypothesized to be a key causative factor in insulin resistance and the advancement of T2DM [166, 167].

Importantly, Skeletal muscle also embodies a vital location for large influxes of fatty acids (**FA**) to be used in energy production and storage [168]. Under healthy conditions, FA undergo oxidation, a process

that produces a necessary fuel source for muscle metabolism. Furthermore, studies conducted in more recent years suggest that the role of FA extend beyond simply fuel production, as they also exemplify intracellular messengers, and gene regulators directly involved in regulating lipid metabolism. While the maintenance of FFA balance locally at the skeletal muscle is imperative for systemic metabolism, dysregulation of FFA uptake and oxidation in skeletal muscle is associated irreversible impairments of cellular functions by inducing inflammation, apoptosis, proteolysis and subsequently autophagy.

The succession of obesity, insulin resistance, and frank diabetes compromises FFAs metabolism, both locally at the skeletal muscle, and globally [169, 170]. At a local level, studies indicate that skeletal muscle insulin sensitivity and intramuscular triglycerides (**TG**) are negatively correlated, suggesting that TG accumulation in muscle strongly predicts a degree of insulin resistance [171, 172].

Additionally, studies conducted in insulin resistant animals and humans, show that FA uptake at both oxidative and glycolic muscle fibers is markedly increase with the onset of obesity, and further become exacerbated across the T2DM continuum [173-175] Further evidence also indicates that throughout the natural history of T2DM, a reduction in insulin sensitivity at the muscle result in intermuscular accumulation of long chain fatty acids (**LCFAs**) and ceramides, also identified as lipotoxicity. [176]. These alterations in FFAs depositing contribute greatly to the development of diabetes and correlate strongly with defects in TG syntheses, TG breakdown, FFA uptake, and most importantly lipid induced NF-κB activation [177-180].

Collectively, these adverse alterations in FFAs metabolism may upregulate RAGE expression in skeletal muscle via two sperate pathways. First, increased skeletal muscle FFAs uptake has been shown to

stimulate NF-κB activation, inducing its nuclear translocation and subsequent gene transcription. Not only does this event contribute to insulin resistance autonomously, but it may also stimulate the upregulation of RAGE protein expression. While research focusing on lipid-induced overexpression NF-κB and RAGE upregulation in skeletal muscle is limited, numerous studies have identified NF-κB as a potent stimulator of RAGE expression. Hence, loss of FFAs regulation & lipid-induced overexpression of NF-κB may be two critical events that may alter RAGE expression, inflammation and ROS production.

In a global context, the onset of obesity also provokes elevated levels of FFA circulating in the plasma. Adipose tissue excretion of FFA through unregulated lipolysis is hypothesized as the principal result of insulin resistance at adipocytes and remains the one most widely accepted mechanistic links to heightened plasma FFA. New research focusing on intensified expression of plasma fatty acids indicate this event may also impact skeletal muscle RAGE expression. Studying the function of RAGE receptor in high-fat feeding, Song and colleagues identified that mice with heightened levels of circulating FFA revealed significant expression of potent RAGE ligands consisting of Carboxymethyllysine (**CML**) and high mobility group box1 (**HMGB1)**. Furthermore, rodents that showed intensification in RAGE ligand appearance also demonstrated elevated peripheral inflammation that was not identified in control groups. To emphasize the finding presented by Song et. al., Ann Marie Schmidt conceived a "two-hit" model for metabolic agitations provoked by ligand -bound RAGE. The second hit encompasses various forms of cell stress that are induced by RAGE ligand interaction, resulting in chronic inflammation and adverse cellular function. Fathered, increased appearance of RAGE ligands has been shown to increase RAGE expression[181-183]

II. C. Hyperglycemia Promotes the Generation of Advanced Glycation End Products

Indeed hyperglycemia, superimposed by skeletal muscle insulin resistance, is the prevailing accelerator behind the diabetes associated complications [184]. Currently, links between chronic hyperglycemia and the complex metabolic events associated with skeletal muscle insult are not fully elucidated. However, the chemical modifications between proteins and reducing sugars, also known as Advanced Glycation End Products (AGEs), may represent a degree of clarification [185].

AGEs are comprised of a group of heterogeneous molecules that develop endogenously when glucose non-enzymatically forms covalent adducts with, lipids, nucleic acids and proteins through the Maillard reaction [186-188]. This post- translation modification is a culmination of chemical rearrangements occurring slowly over 3 distinct stages: initial, midway and late. In the initial phase, protein glycation is instigated by the nucleophilic incorporation of a carbonyl group from reducing glucose to free amino group on protein. This reaction occurs rapidly and forms a highly unstable and reversible Schiff bases [189]. The initial stages of this reaction are deeply contingent on the circulatory concentrations of plasma glucoses. Thus, in the T2DM phenotype, excessive quantities of glucose readily impact the early reactions in AGE formation [190]. Over several weeks, Schiff base compounds undergo further alterations, thereby progression them into more stable Amadori products in the midway phase [191]. By way of oxidative and dehydration reactions, Amadori products reduce into an assortment of dicarbonyl compounds, thus, oxidizing conditions resulting from ROS are necessary mechanisms in the formation of prevailing AGEs such as CML, a principal and extensively researched AGE product implicated in numerous diabetes-associated complications [192]. Finally, in the late stages of glycation, dicarbonyl compounds develop crosslinks among neighboring proteins, resulting in protein aggregation and irreversible formation of AGEs [193]. At the completion of the Maillard reaction, bio-active AGEs possess the capability to insult

a multitude of structural components such as myelin, basement membranes, bone and lipid derived constituents [194-196]. Collagen, another prime target for AGE cross-linking events, suffers enhanced rigidity and increased resistance to collegian renewal one modifies by AGEs [197]. Independent of AGE mediated structural modifications, recent studies indicate that AGEs may suppress insulin signaling [158]. While these mechanisms are not fully understood, AGEs are implicated in obstructing intracellular propagation events that induce GLUT4 translocation and glucose uptake [198]. Thus, deleterious chemistry of AGE formation is implicated in a vast range of pathologies. Thus, AGE modified proteins disrupt the native molecular form and function of macromolecular structures, underline the complications such as neurological disorders, connective tissue complications, vascular damage and insulin resistance, all of which are observed in T2DM [199-201].

II. C. I. Advanced Glycation End Products: Accumulation and Balance

Generally, AGE formation is an endogenous event, which occurs continuously as a natural byproduct of normal metabolism [202]. However, additional dietary AGEs **(dAGEs)** can be derived exogenously when ingested with food [203]. The application of intense heat in food preparation induces non-enzymatic crosslinking characterized by the Maillard reaction [204]. Although dAGEs are naturally present in uncooked animal sourced foods, applying heat based, low moisture cooking methodologies (i.e. grilling, sautéing, baking) will significantly accelerate dAGEs formation prior to ingestion [205]. While accurately quantifying food derived dAGEs is a difficult task, reports indicate that 10% of ingested dAGEs are absorbed into the circulation, while less than half of circulating dAGEs get absorbed into tissue [206]. Although marginal amounts of dAGEs absorption have been reported, the incorporation of dAGEs critically alters the internal milieu by initiating cytokine generation, inflicting glomerular injury and provoking ROS generation [207-209]. In animal studies, Cia et al. demonstrated that the consumption of

AGE fortified mouse chow significantly increased AGEs serum levels and oxidative stress concurrently, compared to their controlled counterparts [210]. This work suggests that dAGEs initiate an immediate response that not only rapidly increase serum AGEs levels, but also negativity impacts the redox state of the internal milieu. Furthermore, in a studied designed to investigate the impact on daily ingestion of dAGEs, Kochinski et. al. showed that frequent dAGEs consumption by 38 diabetics further exacerbates the diabetic phenotype by increasing the risk renal and vascular injury. This group's findings attributed these injuries to the development of AGE induced renal and vascular lesions [211]. Taken together, both exogenous and endogenous AGEs jointly increase plasma AGE concentrations and AGE pooling in the tissue. Thus, the degree of total AGEs with in the human body may exert significant reactivity with essential tissue structures and biochemical processes.

II. C. II. Regulating AGE Formation

Regardless of their origins, exogenous vs. endogenous, the global circulating AGE pool must be regulated and removed from the body to prevent future deleterious modifications associated with diabetes [212, 213]. AGE catabolism and elimination is complex process, which is dependent on the alliance of many factors spanning form protein turnover regularity and anti-oxidant defenses to receptor-mediated AGE degradation and renal elimination [214, 215]. AGE-dependent complications arise when any or all of these mechanism waver, amounting to reduction in clearance of serum AGEs and further tissue accumulation [216]. Among the mentioned mechanisms, diminished protein turnover appears to be centric stimulus in serum and tissue AGEs accumulation [217-219]. It has been reported that the pathological crosslinking between AGEs and proteins with long half-lives renders the AGE-modified protein relatively stable. Importantly, this chemical rearrangement produces protein that is resistant to protein turnover and proteolysis, ending in the accumulation of cross-linked products both intra and extracellularly [220].

Decreased protein turnover capacity is a phenomenon that is significantly accelerated in diabetes, where augmented serum AGEs concentrations are believed to be a reflection of diabetic complication severity [221]. The kidneys activity participates in the degradation and removal of AGEs, and studies show that there are significant inverse correlations between kidney function and serum AGEs. AGE- proteins are incapable of filtering across the glomerular membrane until they are degraded into AGE-peptides by proteolytic machinery [222, 223]. In both human and animal studies, the diabetic phenotype demonstrates that various degrees of renal dysfunction are strongly associated with increased AGEs concentrations and markedly reduces AGEs extraction [211, 224, 225]. Augmented AGE formation and reduced renal clearance are accountable for the emergence of carbonyl stress, ROS, chronic inflammation and the upregulation of pathogenic cellular signaling cascades, all occurrences observed in T2DM. Thus, a general decline in any or all of the defensive mechanisms ends in significant imbalance between the production and detoxification of reactive AGEs adducts. In diabetes, AGE disequilibrium result from chronic hyperglycemia promoting greater glycation events, which contribute significantly to oxidative stress (**OS**) and inflammation in diabetes and diabetic complication.

AGEs possess the capacity to bind to multiple receptors [226-228]. While most initiate deleterious signaling cascade, others act as scavenger receptors and aid in degrading AGEs [201]. In part, regulation of AGE-induced complications is therefore carried out by the counteroffensive, transmembrane receptor advanced glycation end product receptor 1 (**AGER1**), or advanced glycation end product receptor 1 [229]. AGER1 is a compensatory mechanism that is a known suppressor AGE accumulation and AGE- medicate tissue damage [230]. In a healthy system, AGER1 is upregulated when high levels of circulating AGEs are detected. Therefore, the protective AGER1 maintain AGE equilibrium [228]. However, in diabetic conditions, this defensive mechanism is inhibited, and AGER1 expression is significantly reduced while

circulating AGEs cumulate [231, 232]. The loss of AGER1 expression is associated with an increased expression of injurious AGEs receptors such as RAGE. Thus, it would seem that AGER1 and RAGE share an inverse relationship (**Figure 5**).

Figure 5.
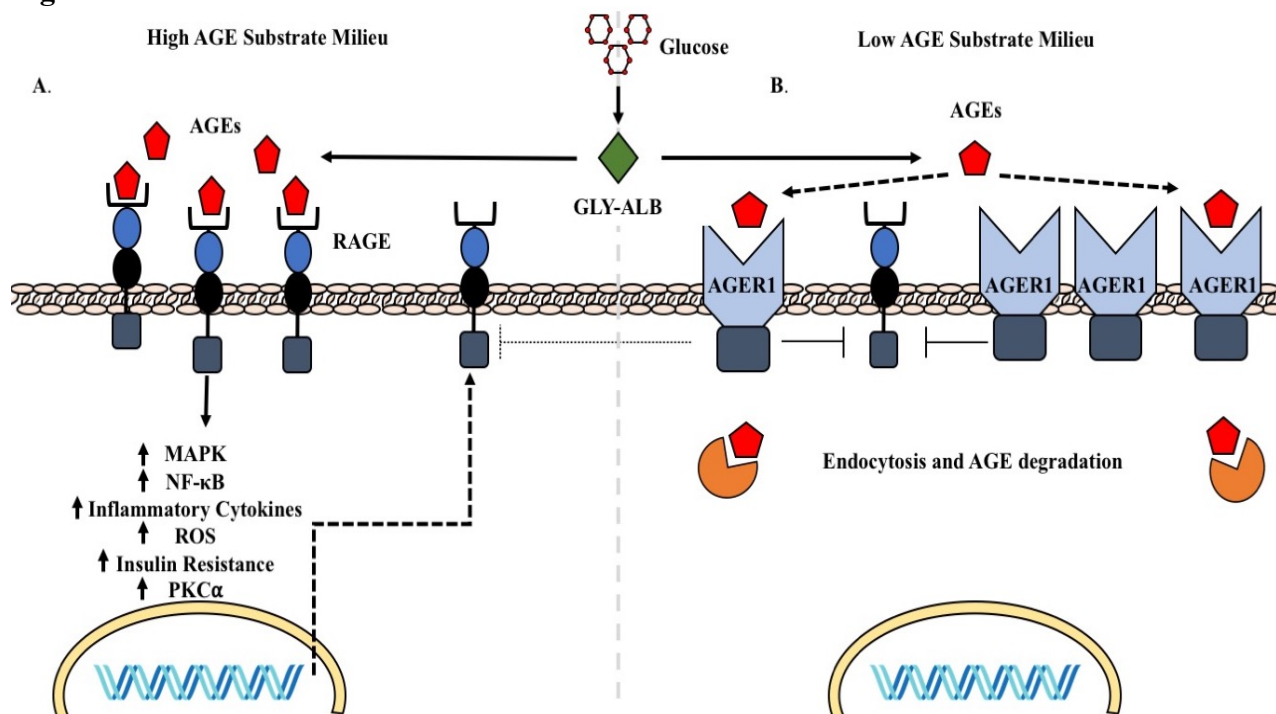
Figure 5. Hyperglycemic-induced albumin glycation results in the generation of Amadori products. These early glycation articles can then progress to irreversible, advanced glycation end products. Receptor-dependent pathways are activated by AGEs. Excessive AGE substrates result in RAGE activation, receptor overexpression and the upregulation of deleterious RAGE-mediated pathways (A). Conversely, low AGEs substrate availability initiates Advanced Glycated End Product Receptor 1 scavenger receptors. Consequently, AGEs endocytosis and undergo intercellular degradation (B). AGEs, advanced glycation end products, GLY-ALB, Glycated Albumin, RAGE, Receptor for Advanced Glycation End Products, AGER1, Receptor for Advanced Glycation End Products Receptor.

Early reports associated AGE turnover and clearance as the primary task of AGER1, but recent reports indicate that AGER1 also represses RAGE signaling, NF-KB activation, and downgrades oxidative - mediate damage pathways, designating AGER1 as a master suppressor of adverse signaling networks associated with AGE/RAGE binding [233]. To demonstrate how AGER1 suppresses RAGE and oxidative signaling, Torreggiani et al. revealed that preserving of AGER1 levels counterbalance AGE- mediated inflammation and subsequent free radical production. This group employed founder mice that were genetically modified to overexpress AGER1. Both AGER1 modified, and wild-type rodents were exposed to a diet with increased fat macronutrient content for eight weeks to induce endogenous AGE formation and unfavorably modify the inflammatory and oxidative milieu. At the conclusion of the study, AGER1 transgenic mice exhibited normal glucose control, lower inflammation and oxidative stress. On the other hand, wild-type mice exhibited severe hyperglycemia, augmented inflammation and oxidative stress [234]. Thus, this work demonstrated that AGER1 degrades AGEs accumulation, thereby stifling AGE accumulation by endogenous and exogenous origins.

In another in-vitro study, Changyong and colleagues set out to determine if AGER1 mediates AGE turnover and reduces proinflammatory signaling in the mesangial cell (**MC**). Changyong et al. utilizing murine MC that were overexpressed with human AGER1 and RAGE. 20 g/ml of AGE-BSA and native BSA were incubated with MC for 4 hours. Radioisotope labeling demonstrated that AGER1 expressing cells showed a substantial increase in AGE uptake and degradation compared to MC cells lacking AGER1 expression. Further, this work also revealed that MAPK activation was substantially higher in cell lines devoid of AGER1. Conversely, MC expression of AGER1 showed no significant alteration in MAPK activation [235].

Perhaps the most important work currently centering around AGER1 is a study conducted by Uribarri colleagues in 2011. In an effort to examine the potential relationship between high carbohydrate feeding and the generation of glycoxidants *in vivo*, Uribarri et al. assessed how dietary AGEs impacted RAGE-mediated pathway activation in healthy and T2DM subjects. This study randomly assigned either a standard diet (> 20 AGE Eq/day) or an AGE-restricted diet (< 10 AGE Eq/day) among 18 healthy subjects and 18 T2DM subjects over the course of 4 months. Upon the conclusion of the study, Individuals with T2DM assigned to the AGE restricted diet exhibited significant reductions in circulating metabolic and inflammatory markers compared to Individuals with T2DM designated to the standard AGE diet. Notably, AGE scavenger receptor AGER1 gene expression and protein levels were prominently increased, whereas T2DM consuming the standard AGE diet revealed no protective alterations. Interestingly, this work also established that restricted AGE feeding significantly reduce AGE/RAGE axis mediators designated to T2DM subjects. Serum AGEs, proinflammatory cytokines, p47^{phox} mRNA and indicators of ROS-mediated lipid peroxidation (8-isoprostanes) were also significantly reduced as a result of restricted AGE feeding. Collectively, these data ultimately resulted in a normalization of serum insulin levels and improved glucose uptake in subjects that restricted dietary AGE consumption [231].

In summary, the buildup of AGEs, whether by endogenous or exogenous origins, are substantially linked to insulin resistance development, impaired glucose deposal, ROS generation and diabetic associated complications. Therefore, the consequences of AGE generation, accumulation and receptor binding induce a variety of deleterious signaling cascades that produce a pro-oxidant and pro-inflammatory cellular milieu. Conversely, a restriction of AGEs, in tandem with conserving native AGER1 defense systems, result in favorable reductions in oxidative stress, inflammation and restoration of insulin sensitivity and normal glucose disposal. (**Figure 6**).

Figure 6.
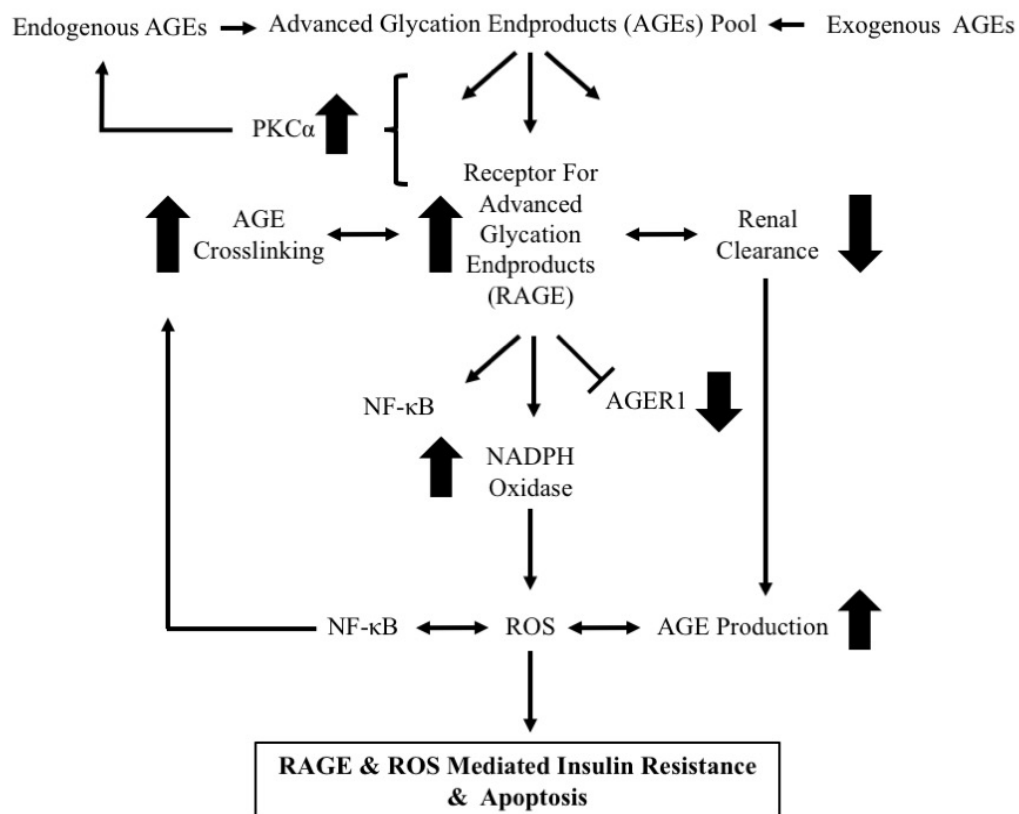
Figure 6. Outline of AGE/RAGE Binding Implications on the Generation of ROS in the Cellular Milieu. AGE-medicated RAGE activation stimulates pro-oxidant and pro-inflammatory responses. These events result in insulin resistance and ROS-mediated cell dysfunction/apoptosis. AGEs, Advanced Glycation End Products, RAGE, Receptor for Advanced Glycation Endproducts, AGER1, Advanced Glycation End Products Receptor 1, NF-κB, Nuclear Factor Kappa-light-chain-enhancer of Activated B Cells, ROS, Reactive oxygen Species, PKCα, Protein kinase C alpha.

II.D. The Receptor for Advanced Glycation End products

Bio active AGEs impose deleterious effects via the **RAGE (**Receptor for Advanced Glycation End products**)** with proven pathogenic implications, as they upregulate pro-inflammatory and oxidative cellular pathways [236]. RAGE is a affiliate of the immune globulin (**Ig**) superfamily of transmembrane receptors and its biological impact in development of chronic diseases is dependent on location, and chronicity of activation [237] (**Table 1**). Although RAGE research in human skeletal muscle is still a developing area of investigation, animal studies have confirmed that RAGE protein and gene expression in skeletal muscle is more abundant than any other tissue, appropriating skeletal muscle an attractive platform to further unravel RAGE signaling biology [238].

TABLE 1. RAGE IS IMPLICATED IN MECHANISMS THAT DRIVE THE PATHOGENESIS OF DIABETIC COMPLICATIONS

Mechanism of Action	Ligand	Target Tissue	Biological Effect	Ref #
RAGE-mediated Vascular Complications	AGEs/S100 AGE-BSA	Endothelial Cells Smooth Muscle Cells	↑ Vascular permeability ↑ Inflammation ↑ Remodeling ↑ Atherogenesis ↑ Atherosclerosis ↑ LDL oxidation	[239-243]
RAGE-mediated Nephropathy	AGEs β2-integrin Mac-1	Glomerular epithelial cells	↑ Glomerular filtration rate ↑ Glomerular sclerosis ↑ Podocyte effacement	[244-247]

RAGE-mediated Arthritis	AGEs/S100 AGE-BSA	Synovial tissue Bone Cartilage	↑ Osteoarthritis ↑ Rheumatoid arthritis	[240, 248-251]
RAGE-mediated Cancer	AGEs/S100 AGE-BSA	Beta Cells Bladder Hepatocytes	↑ Activate cancer cells ↑ Stimulate proliferation ↑ Invasion ↑ Metastasis	[252-255]
RAGE-mediated Neurodegeneration	AGEs/S100	Microglia Neurons Endothelial cells	↑ Neurofibrillary tangles ↑ Plaque development ↑ Beta amyloid peptide	[256-258]

II. D. I. Physiological & Pathophysiology Implications of RAGE Signaling

RAGE functions in both physiological and pathological contexts throughout human chronologic aging. During pre-and postnatal developmental stages, RAGE is highly expressed and reports indicate that it plays a vital role in signaling cellular proliferation events, migration and upholding a degree of cellular homeostasis in specific cell types [259]. During the progressions towards adulthood, however, RAGE becomes significantly repressed and maintained at lower levels, where RAGE signaling may be implicated in the attenuation of acute inflammation, tissue remolding and host defense [260, 261].

In the pathological context of chronic diseases, such as T2DM, RAGE expression becomes sharply augmented by the appearance of signaling molecules including AGEs, S100s, and HMGB1 [262-264]. The presence and accumulation of these chemical moieties dictate RAGE activity to propagate sustained cellular dysfunction, resulting in tissue injury[265]. Upon ligand interaction, a wide array of RAGE-mediated cellular pathway cascades become active including MAP kinases, p38, SAPK/JNK, rho-GTPases, phosphoinositol-3-kinase, ERK1/2 (p44/p42), JAK/STAT, and different PKC isoforms [26,

265-267]. Importantly, the human RAGE gene contains promoter regions for interferon-γ response element, IL6 and Nuclear Factor Kappa B (**NF-κB**), thus, the deposition of these common motif ligands robustly stimulate pro-inflammatory activity [268-270]. Multiples studies indicate that active RAGE incites NF-κB activation, initiating translocation to the cell nucleus, where it intensifies transcription and release of NF-κB regulated TNFα, IL6 and IL1 [271]. This event is important because NF-κB is capable augmenting RAGE transcription by binding to the RAGE promoter regions, thereby increasing RAGE protein expression and initiating a self-perpetuating inflammatory cascade [259, 272]. Chronic RAGE activation therefore results in a perpetuating self-signaling cascade that has been identified in endothelial cells, smooth muscle cells, molecular phagocytes and diabetic vasculature [237, 273, 274]. Employing anti –RAGE IgG antibodies quells RAGE signaling and represses NF-κB activity, impeding adverse intracellular signaling [275].

II. D. II. RAGE Expression in Human Skeletal Muscle

RAGE signaling in skeletal muscle is a multifaceted issue as research indicates that active RAGE induces not only pathological events but also acts as a primary mediator in muscle repair and growth responses [158, 276] **(Table 2)**. It is hypothesized that these distinct functions are contingent on the accumulation or scarcity of RAGE amassing on skeletal muscle fibers. Immunostaining of human muscle reveals AGEs and pro-inflammatory RAGE are positively correlated with weight gain and chronological aging [277]. In a pathogenic phenotype, the skeletal muscle would exhibit elevated a RAGE intensity, whereas, in a health phenotype, RAGE intensity would be reduced, respectively [278, 279]. While limited evidence exists on RAGE expression specifically in skeletal muscle, literature centering on the relationship between skeletal muscle and RAGE indicate that ligand-bound RAGE is capable of imposing global disturbances on

skeletal muscle properties that span beyond proinflammatory/oxidative injury to biochemical, architectural and contractile modifications [265, 280, 281].

Ligand -bound RAGE stimulates biochemical irregularities that disturb glucose disposal in skeletal muscle cells. n a 2008 study conducted by Cassesse and colleagues, AGE/RAGE interaction promoted insulin resistance in L6 cells that were treated with glycated albumin (GLY-ALB) for 48 hours. This treatment resulted in RAGE-mediated upregulation of protein kinase C alpha (PKCα). Further, active PKCα was detected co-associating with IRS1 and Src Kinase proteins, forming a complex cytosolic that obstructed further downstream insulin signaling. Additionally, in-vivo experiments were also conducted in tandem with cell culture work. Extracted tibialis muscle from C57/BL6 mice fed diets high levels in AGEs exhibited impaired insulin action which resulted in a significant reduction in glucose uptake compared to mice fed low AGEs. Both in-vitro and in-vivo efforts associated with this study demonstrated significant increase in skeletal muscle PKCα activity [158] . Conversely, utilization of MK-I-81, a novel AGE inhibitor, in C2C12 cells resulted in the termination of AGE-induced PKC activation and RAGE-mediated insulin resistance [282].

TABLE 2. RAGE SIGNALING IN SKELETAL MUSCLES

Mechanism of Action	Ligand	Target Tissue	Biological Effect	Ref #
RAGE-mediated Insulin Resistance/ Metabolic Derangement	AGEs/S100 AGE-BSA	L6 Skeletal Muscle Bx	↑ AMPK ↑ Phospho-PKCα ↑ Src Kinase	[158, 282, 283]
RAGE-mediated Inflammation	HMGB1 AGEs	Skeletal Muscle Bx	↑ Neurodegeneration/ ↑ IBM ↑ Phospho-Erk	[284, 285]
RAGE-mediated Structural Alterations	AGEs	Skeletal Muscle Bx	↑ Compromised non-contractile proteins ↑ Myopathy ↑ Atrogin-1 ↑ Myogenesis	[283, 286]
RAGE-mediated Reparation	S100B	C2C12 TA Muscle	↑ Macrophage infiltration ↑ Pro-regenerative activity ↑ MMP Activity	[287-289]
sRAGE-mediated Defense	AGEs	Skeletal Muscle Bx	↑ Muscle mass health ↑ Normal Glucose Tolerance	[290, 291]

TABLE 2. AGEs, Advanced Glycation End Products, RAGE, Receptor for Advanced Glycation End Products, AGE-BSA, Advanced Glycation End Product-modified Bovine Serum Albumin, AMPK, AMP-activated Protein Kinase, HMGB1, High Mobility Group Box 1 Protein, Phospho-PKCα, Phosphorylated Protein Kinase C Alpha, IBM, Inclusion Body Myositis, Phospho-Erk, Extracellular Signal-regulated Kinase-1, sRAGE, Soluble RAGE, S100B, S100 calcium-binding protein B, TA Muscle, Tibialis Anterior Muscle.

Skeletal muscle RAGE expression also provokes degenerative and inflammatory mechanisms that adversely alters muscle architecture and functional properties. After conducted skeletal muscle biopsies in subjects diagnosed with inclusion body myositis (**IBM**), Muth et al. demonstrated upregulated RAGE expression, circulating ligands were upregulated and mediators of muscle fiber degeneration and inflammation associated with IBM. In this study, the HMGB1/RAGE axis medicated extracellular signal-regulated kinase (Erk) phosphorylation, which demonstrates that RAGE-mediated Erk activation contributes to chronic inflammatory cell stress in human skeletal muscle [284].

In skeletal muscle, elevated RAGE expression is also linked with muscular atrophy in addition to contractile dysfunction. In a study conducted by Chiu et al. RAGE signaling was identified as a primary component in the development and exacerbation of diabetic myopathy. Chiu observed that diabetic patients exhibit significantly higher levels of muscle atrophy marker, Atrogin-1, than lean, healthy counterparts. To determine if RAGE signaling played a role in compromised muscle structure and heightened Atrogin 1 expression, C2C12 and HSMPC myotubes were stimulated with various concentrations of AGEs or BSA. Experimental cells revealed that AGE/RAGE interaction induced significant elevations in Atrogin 1 while considerably reducing myotube circumference in a dose-dependent manner. Importantly, treating cells with RAGE neutralized antibodies inhibited AGE/RAGE signaling, thereby maintaining myotube integrity [283]. RAGE signaling events also impaired noncontractile tissue associated with skeletal muscle structure. Serrao et al. employed muscular biopsies to determine if AGE/RAGE interaction impacted knee mobility in the development of osteoarthritis. While this work revealed no notable differences in RAGE expression among healthy and individuals with early-stage knee osteoarthritis, others have indicated that AGE/RAGE signaling compromises

noncontractile components of skeletal muscle by intensifying cross-bridging maturation, resulting in tissue rigidity and mobility impairments [286, 292, 293].

Nonenzymatically regulated AGE cross-linking, and RAGE coupling may not be an entirely unregulated event in human skeletal muscle. Current scientific reviews have confirmed that a soluble RAGE isoform (sRAGE) is detectable in serum and may signify a novel marker indicating RAGE activity in-vivo. sRAGE is theorized to be both an AGE scavenger as well as a rival target for ligands predestined for RAGE binding [294-296]. Thus, sRAGE maintains beneficial qualities that may neutralize the injurious AGE/RAGE Axis. In a cross-sectional study, comprised of 390, non-diabetic participants, Kim et al. reported that circulating sRAGE concentrations were positively correlated with muscle mass subjects that are 40 years of age with no pre-existing conditions [290]. This report signifies that adverse modifications in skeletal muscle mass or structure may be interrelated to regressions in circulating sRAGE capacity to scavenge AGEs. Discernibly, these relationships necessitate more comprehensive research efforts.

 Intrinsically, when skeletal muscle becomes compromised in mass or function, sRAGE defenses appear to be reduced. Further, Miranda et al. revealed that circulating levels of sRAGE, **cRAGE** (Cleaved RAGE) and **esRAGE** (endogenous secretory RAGE) were all reduced in subjects with IGT and T2DM. While the mechanisms responsible for declines in protective sRAGE concentrations are currently unknown, decreased circulating sRAGE levels are linked to the development of metabolic complications such as altered in glucose tolerance and the development of diabetes. Likewise, in a study investigating the relationship between circulating sRAGE and risk factors related with atherosclerosis, Moriya et al. established that individuals with low- sRAGE levels demonstrated greater atherosclerotic risk factors than individuals with more robust sRAGE levels [291]. These findings suggest that sRAGE levels diminish in

correlation with the development of metabolic complications and inflammation, thereby decreasing AGE scavenging potential. sRAGE regulates RAGE signaling faculty through targeting circulating AGEs. The more robust sRAGE levels are in the circulation, the more efficiently tissues can protect themselves from AGE/RAGE signaling events.

Paradoxically, skeletal muscle RAGE expression also plays a pivotal role in muscle health. Recent improvements in our understanding of RAGE biology confirms that active RAGE is not limited to pathological signaling, but rather, RAGE has also been recognized for its role in maintaining tissue homeostasis and mediating repair processes following muscle injury [297, 298]. AGE/RAGE binding promotes inflammation resolution in several tissues types [299]. It has been hypothesized the RAGE-mediated promotion of phagocyte infiltration is an essential step in the attenuation of chronic inflammation. Sorci et al. suggest that S100B/RAGE interplay may represent a necessary repair switch, signaling the activation and deactivation proinflammatory activity in the early phases of muscle repair. In myofibrils, robust levels of RAGE ligand S100B are released upon tissue injury. These events are reported to initiate myoblast proliferation and differentiation processes that are required for skeletal muscle repair [287]. Likewise, a study conducted by Riuzzi et al. revealed that RAGE knockout model suppresses the regenerative process in muscle injury, delaying the expansion and of myotube populations. Importantly, S100B/RAGE interplay appears to be advantageous to muscle health when S100B regulated and released in moderation [288]. Tubaro et al. observed that an overexpression of S100B in myoblasts, abolishes reparative processes, but rather induces the RAGE-mediated ROS production, NF-KB activation, and apoptosis [300].

II. D. III. RAGE and Reactive Oxidative Species Production

RAGE is rapidly becoming recognized as ROS signaling cofactor. Active RAGE is believed to be a dominant constituent in the generation, propagation and unrelenting nature of ROS generation, which directly contributes the diabetic complications [301]. While the literature concerning RAGE induce ROS in skeletal muscle is limited, numerous studies in a variety of cell types demonstrate a distinct relationship between RAGE activation and consequential increase of intracellular of ROS. Yan et.al. produced early evidence in RAGE induced ROS production by examining the redox state of endothelia cells treated with various AGEs. This group immunoprecipitated AGEs from diabetic plasma and delivered them to endothelial cells, where the interaction higher concentrations of thiobarbituric acid substances (**TBARS**), which is a common indicator of oxidative stress and cell damage [302]. The production of TBARS rapidly decreased in the presents of RAGE-blocking antibodies and antioxidants. In animal, *in vivo* models, the infusion and ingestion of AGEs developed a robust TBAR expression and increased the activation of redox sensitive NF-κB, significantly. These adverse reactions, were also reduced in the presents of RAGE-blocking antibodies and antioxidants[303, 304]. Subsequent studies indicated RAGE as a key mechanism in ROS production and the development of free radicals in macrophages, where by RAGE induces ROS and the activation of NF-κB [305]. Moreover, Li and colleagues demonstrated that AGE-RAGE interaction-initiated ROS generation in mesangial cells. This group demonstrates that RAGE activation induces elevations in ROS as early as 60 minutes, and these levels were maintained for several hours [14, 306].

 II. D. III. RAGE May Promote ROS Generation in Human Skeletal Muscle

In diabetes, a unifying theme has been widely accepted, suggesting that excessive generation of mitochondrial superoxide is the underling event that incites the development of oxidative stress [307].

RAGE signaling has been implicated in these events [308]. Based upon theses earlier findings, a key question that still remains is by what mechanism does active-RAGE generate ROS in human skeletal muscle? Skeletal muscle ROS production is both complex and paradoxical biology, as free radicals are produced as necessary secondary messengers and pathological mediators [309, 310]. Under normal physiological conditions, skeletal muscle produced ROS is reported to play a principal role in modulating muscular force generation, controlling gene expression and regulating insulin signaling events [311, 312]. Skeletal muscle fibers are rich with ROS generation machinery and it has been shown that several cellular locations including the mitochondria, Sarcoplasmic Reticulum **(SR),** Transvers Tubules **(TT)** and the Sarcolemma all contribute to ambient ROS levels[313, 314]. Of these sites, the mitochondria have received the greatest consideration in ROS generation, specifically during basal respiration [315]. However, significant oscillation of mitochondrial ROS occurs as a result of many common muscular actions such as cytokine response, and intense muscle contraction, where by the increased ROS generation occurs [316]. During oxidative phosphorylation, mitochondrial ROS production and emission is a minimal occurrence [317]. However, this is an flawed procedure, and a small degree of electrons seep from the respiratory chain and into the mitochondria. [318]. Explicitly, complexes 1 and 3 of the mitochondria's electron transport chain has received the greatest amount of attention concerning the generation of superoxide, where early reports estimated some 3-5% of consumed oxygen endured electron reduction ending in the free radical generation comprising superoxide ($\cdot O_2^-$) and non-radical production of hydrogen peroxide (H_2O_2) [319, 320]. Under basal conditions, free radicals are immediately scavenged by antioxidant enzymes and redox balance is maintained [321].

In a diseased state, however, a chronic overproduction of mitochondria ROS is believed to generate excessive superoxide, promoting redox imbalance and oxidative implicated in pathogenesis of T2DM[322]. In diabetes, a common hypothesis remains the forefront of redox biology: That the

generation of aberrant mitochondrial superoxide is the primary event that activates secondary pathological mediators and tissue injury [323]. However, a lack of comprehensive data exists on the mechanistic relationship between RAGE signaling and mitochondrial ROS production in the diabetic skeletal muscle. Most studies merely conclude that RAGE-dependent ROS production results in mitochondrial permeability, and this injury intensified ROS ambient levels [324-326] This would suggest then that the mitochondria may not be the prevalent source of ROS under pathological conditions, rather it may be a victim of oxidative damage generated from cytosolic origins. Interestingly, Coughlan and colleagues offer a novel perspective on RAGE signaling in aberrant ROS generation as it relates to the mitochondria. By introducing AGEs to healthy rodents overexpressing RAGE, researchers found significant intensifications in cytosolic ROS production. AGE-medicated ROS production accelerated mitochondrial permeability and induced oxidative stress. In diabetic rodents, exposure to AGEs significantly accelerated the development of oxidative stress compared to their healthy counterparts [324]. These data propose that AGE/RAGE engagement initiates a series of events, which generation of cytosolic ROS, independently of the mitochondria. Further, RAGE activation of NADPH oxidase may induce downstream intensification of ROS through the initiation of mitochondrial sourced superoxide [14].

In recent years, cytosolic ROS production has overshadowed the prevalence of mitochondrial stimulated reactive oxidative intermediates, emerging as the leading (or preliminary) source of free radical generation in skeletal muscle cells. One source of RAGE-induced ROS production within the cytosol of muscle cells may be Nicotinamide Adenine Dinucleotide Phosphate (NADPH) oxidases **(Nox's)** located in the sarcolemma [327, 328]. Many recent studies detail the role of RAGE provoked NADPH oxidase activation. Wautier and colleges demonstrated that carboxy methyl lysine **(CML)** treated endothelial cells promoted intracellular hydrogen peroxide, by way of NADPH Oxidase. Further treatment of these cells

in cultuere with diphenyliodonium **(DPI),** an inhibitor of NADPH Oxidase, abolished ROS production and suppressed RAGE signaling effects [14]. Moreover, Thallas-Bonke et al. demonstrated RAGE activation induced NADPH oxidase derived ROS in mesangial and renal tubulointerstitial cells. By employing a Nox inhibitor, apocynin, this group observed decrease in NADPH Oxidase activity, inflammation and fibrogenic reactions in diabetic kidney [329]. Finally, Zang et al. revealed that a 48-hour incubation of Glycated Bovine Serum Albumin **(GLY-ALB)** stimulated cultured rat cardiomyocyte ROS. Zang reported that after 24 hours of incubation, NADPH oxidase activity was elevated 160% for control cells, subsequently activating NF-κB and quickening the development of diabetic-mediated heart disease [330]. Collectively, these findings show a direct and potent relationship among the AGE-RAGE axis and NADPH Oxidase activation (**Figure 5**). Thus, a definitive characteristic is in place to demonstrate the presence of a RAGE/Nox 2 signaling axis. Clearly, as shown by numerous studies in various tissues, this axis is implicating in an array of diabetic complications. While inadequately charted in human skeletal muscle, RAGE/Nox 2 axis is an attractive target to investigate as its presence may directly contribute to chronic inflammation, oxidative stress and insulin resistance. Interestingly, such adverse alterations in the REDOX balance could hasten the conversion of Schiff base products to more stable Amadori rearramaments, generation more endogenous AGEs [331]. These actions would provoke a deleterious cycle of chronic RAGE activation, RAGE upregulation, ROS formation and the development of oxidative stress [332, 333].

II. E. The RAGE/ NADPH Oxidase Axis

RAGE signaling is a unique event, as the receptor's cytoplasmic tail is without endogenous tyrosine kinase activity [334]. The absents of kinase activation suggests that RAGE propagation may heavily dependent on cytosolic docking associates, which might be implicated in the activation of multiple downstream

signaling pathways, specifically in the pathogenesis of T2DM [335]. Regrettably, the scope surrounding RAGE-mediated NAPDH oxidase activation in skeletal muscle is indeed narrow. Furthermore, supporting evidence concerning probable RAGE-dependent signaling intermediates responsible for NADPH oxidase assembly is even more constricted. The RAGE cytoplasmic tail (**RAGEct)** is responsible for RAGE-mediated signal propagation and alterations of cellular properties [336]. It has been reported that RAGE signaling is dependent on RAGEct interaction with the intracellular effectors such as mammalian diaphanous 1, or **mDia1** [337, 338]. RAGE can incite unfavorable cellular processes by associating with mDia1's formin homology, **(FH1)** domain. The interaction between these proteins is dependent on active RAGE recruiting mDia1 to its cytosolic tail where mDia1 will dock with Arg-5 and Gln-6 of RAGEct. To further demonstrate the importance of ofmDia1 in RAGE medicate signaling, RAGE mutation studies reveal that alterations to Arg-5 and Gln-6 result in a distribution of binding potential between RAGE and mDia1 and reduces RAGE-mediated downstream signaling events [336].

Ubiquitously expressed, formins and responsible for variety of fundamental cellular processes, including cell adhesion, cytokinesis, and the activation of GTP-bound Rho proteins. Once release from autoinhibition, active mDia1 induces cytosolic nucleation and elongation of actin chain assembly in support of cell division and migration (**Figure 7)**

Figure 7.
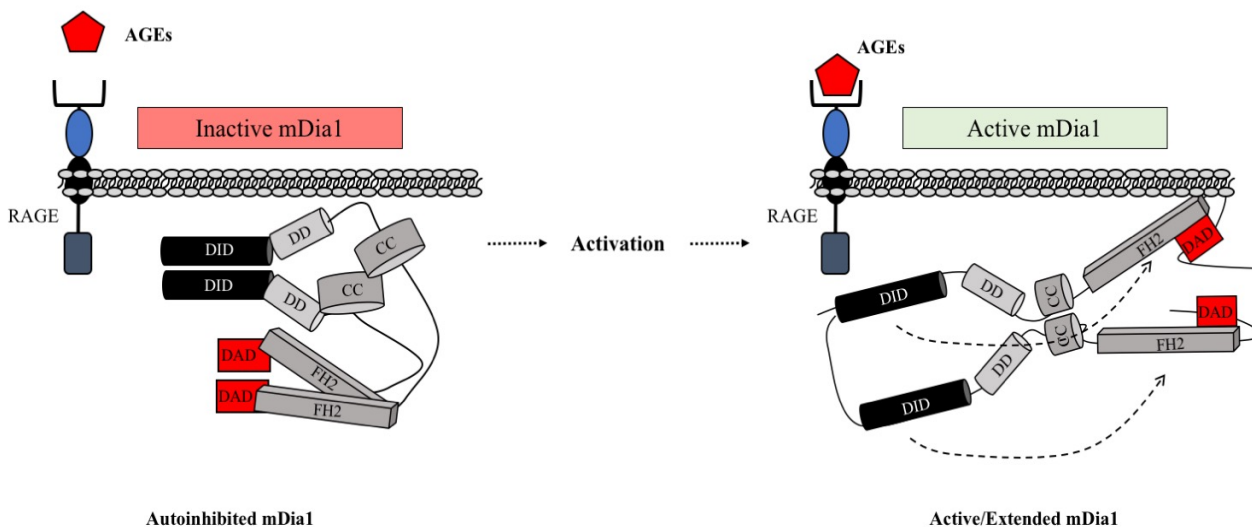
Figure 7. mDia1 Activation Sequence.
mDia 1 is reported in governing microtubule and microfilament dynamics. Reports indicate that mDia1 is necessary for RAGE signaling. The RAGE cytoplasmic domain recruits mDia1, converting mDia 1 from an autoinhibited to active state. AGEs, Advanced Glycation End Products, RAGE, Receptor for Advanced Glycation End Products, mDia 1, The Diaphanous-related Formin 1

While mDia1's role in cytoskeleton dynamics is well understood, its connection to the pathogenesis of T2DM is less defined [339, 340]. Hudson et al. further solidified these early findings by examining more of the molecular interactions between RAGE and mDia1. Employing both *in vitro* and *in vivo* work, Hudson demonstrated that RAGE cytosolic tail networks with the mDia1 via its proline rich formin homology-1 **(FH1)** domain [341, 342]. Further investigations into RAGE-mDia1 docking revealed more

details regarding the interaction. Both *in vitro* & *in vivo* work identified two amino acid primarily responsible for RAGE-mDia1 interface. Rai et al. demonstrate the RAGE cytosolic tail contains Arg-5 and Gln-6, and these residues are responsible for mDia1 docking upon RAGE activation. In vascular smooth muscle cells, site-directed mutagenesis of these residues ended in loss of mDia1 binding and downstream signaling capacity, however, these experiments have not yet been conducted in human skeletal muscle [336]. These studies suggest roles of RAGE and mDia1 may be a fundamental mechanism governing pathogenic singling within the RAGE paradigm. Although no studies have identified RAGE-mDia1 association in human skeletal muscle, it appears that upon activation, RAGEct recruits mDia1 to activation and to stimulate a RAGE -dependent signaling networks.

II. E. I. SRC Tyrosine Kinase

Src tyrosine kinase is recognized as a RAGE signaling mediator implicated in RAGE-mediated NF-κB activation, inflammation, and ROS development in diabetic complications [23]. Growing scientific evidence indicates that the Src family of kinases engage non-tyrosine kinase receptor, such as RAGE, and propagate their signals to other cytoplasmic mediators [343, 344]. While its role in both physiological and pathological settings are well defined in diverse tissues, the target of Src in skeletal muscle remains unclear, as it is implicated in multiple, unassociated cellular events.

Src kinase has been identified in many cells including skeletal muscle, where it regulates an array of intramolecular interactions by tyrosine phosphorylation of targets involved in cellular transformation, cell growth, differentiation and survival [345-347]. Src interacts with substrates via three Src homology domains (SH 1- 3). SH2 and SH3 participate in protein to protein interface, while the SH1 domain contains the active kinase site [348]. A physical analysis of Src reveals that the kinase is highly regulated through

two major phosphorylation sites consisting of Try416/419 and Try530 [349, 350]. Multiple reports identify Try530 as the most critical residue involved in Src autoinhibition [351]. Specifically, when phosphorylated, p-Tyr527 links to the SH2 domain, which effectively renders Src inaccessibly closed, suppressing catalytic kinase activity [352]. Dephosphorylation of Tyr527 interrupts the link with SH2 domain and molecule unfolds to reveal its active state [353]. Interestingly, Src kinase can be activated by mechanical forces [354]. Proteins that target Src's SH2 domains can disrupt blocked Src and activate the kinase. Importantly mDia1 has been reported to target Src's SH2 domain and activate it by mechanically unfolding the protein [355]. A second critical phosphorylation site is Tyr (416/419), located in the in the SH1 domain's activation loop [356]. After dephosphorylation of Tyr530, Tyr416 autophosphorylates, giving downstream mediators access to substrates to the kinase site [357], (**Figure 8**).

Figure 8.
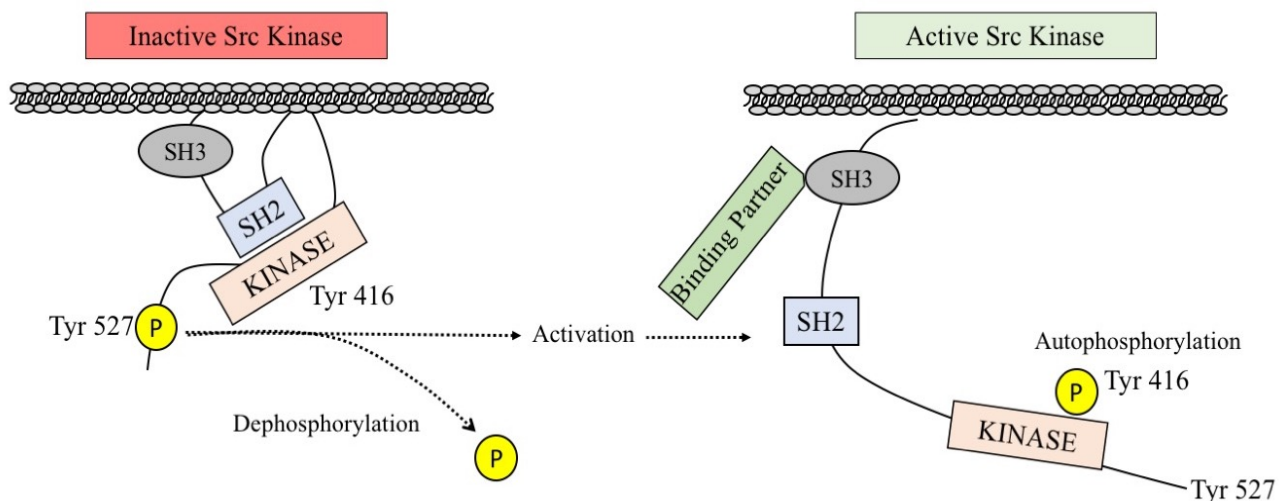
Figure 8. Src kinase regulation by phosphorylation and dephosphorylation
Phosphorylation sites of Src include an activating phosphotyrosine 416 (Tyr 416) that results from autophosphorylation, and an inhibiting phosphotyrosine 527 that results from phosphorylation by C-terminal Src kinase. Dephosphorylation of phosphotyrosine 527 increases Src kinase activity. Src, non-tyrosine kinase Src, SH3, SRC Homology 3 Domain, SH2, SRC Homology 2 Domain, Tyr 527, Tyrosine Residue 527, Tyr 416, Tyrosine Residue 416.

In skeletal muscle, Src is depicted both as a myogenic agent as well as a regulator of metabolic events. Under normal circumstances, Src is predominantly inactive in cells, being switched on only at specific times. However, if the delicate balance between phosphorylation and dephosphorylation status becomes disrupted, adverse changes can occur in Src activity with drastic consequences. The nominal publications focusing on skeletal muscle tissue represents Src as a fundamental component of basal insulin signaling and acute ROS producing. In a study conducted by Rosenzweig et al. fully differentiated myotubes recruited Src kinase activity in insulin signaling and glucose uptake. Rosenzweig established that insulin binding prompted a rapid rise in Src activation, which directly catalyzed the phosphorylation of tyrosine

residues of Protein Kinase C (PKC) and GLUT4 transporters. This study further reported that the application of PP2, a known Src inhibitor, decreased the Src-PKC interaction and decreased phosphorylation of PKC [30]. In another study investigating Src activity in skeletal muscle, Ristow et al. determined Src to be a necessary cofactor in ROS production. During an extensive analysis of kinases regulated by exercise, Src kinase family members identified as a critical node directly involved in the generation of oxidative and intracellular stress. Ristow et al. revealed that Src was one of 15 kinases activated during exercise-induced reactive oxygen [358].

While an abundance of publications identifying RAGE as a Src activator exists in scientific literature, limited evidence is found regarding the association in human skeletal muscle. Notably, active Src has been detected in pathological ROS production, insulin resistance, and inflammation in diverse tissues. Yang and colleagues confirmed this association by treating 3T3-L1 cells with various concentrations of AGEs. This application promoted RAGE medicated Src activation that resulted in the development of ROS via NADPH oxidase. Importantly, this group also indicated that Src is ROS sensitive protein, and the production of radicals induces cyclic Src over activity [359]. In a study investigating RAGE activation and endothelial permeability, Warboys et al. discovered that active RAGE induced a complex formation consisting of ctRAGE, Src, and PKCα. This event induced a rapid surge in free radical production by NADPH oxidase and increased endothelial cell permeability [360]. Similar Src associations were also discovered in smooth muscle cells by, where AGE-mediated RAGE activation in L6 cell lines increased Src phosphorylation, resulting in the significant production of ROS, increased interleukin 6 (IL6), and activation of the NF-κB [23, 361].

In skeletal muscle, these associations are not well studied. A search of the scientific literature exhibits that a single publication exists, which examines the potential presence of a RAGE/Nox 2 axis. Cassese et al. showed that AGEs signaling in L6 myotubes impaired insulin action by activation protein kinase C (PKC). This event was mediated by a pathogenic complex formation consisting of RAGE/IRS-1/ and Src kinase [158]. Src's role in ROS production, independent of RAGE activity, has also been implicated in muscle wasting conditions. Gervasio and colleagues reported that Src kinase activation underlies the pathogenesis of ROS production in the development of muscular dystrophy [362]. Similarly, two other groups revealed that the underlying mechanism responsible for the acceleration Duchenne muscular dystrophy in mouse muscle was Src-induced NADPH oxidase ROS production [363, 364]. These studies further demonstrated that pharmacological and genetic inhibition of Src kinase reduce oxidative stress and improve pathophysiological abnormalities in mouse muscles.

II. E. II. NADPH Oxidase

Evidence now indicates that Src kinase may pivotal element in the activation of NADPH oxidase and studies have shown that RAGE-mediated NADPH oxidase activation is contingent on Src kinase [365]. The only known function of NADPH oxidase is to produce free radicals [366]. Skeletal muscle biology depends on ROS generation for it has been shown to play an influential role in healthy physiology [367]. Since the mitochondria have always been deemed the chief ROS producer in human skeletal muscle, additional ROS producing machinery has been extensively overlooked. After the discovery of human skeletal muscle free radical production, researchers began to examine for cytosolic origins of ROS generation. Through these efforts, NAD(P)H oxidases emerged as primary ROS producing agent in skeletal muscle redox biology and pathology [368].

NADPH Oxidase is a multi-subunit enzyme that serves the singular functional purpose of producing intracellular superoxide ($O2^{.-}$) by catalyzing the reduction of O2 to $O2^{.-}$ [369]. NADPH oxidase is currently verified as a significant source of free radical production, and over the past 20 years, NADPH oxidase-induced radical generation has emerged as a central element in the development and acceleration of diseases concerning reactive oxygen species and oxidative stress [370]. Conversely, NADPH oxidase is also a key mechanism in signaling activity in normal cellular biology [371, 372]. The dual nature of this oxidase, superimposed by the discovery of seven NADPH oxidase isoforms, limits a comprehensive understanding of its part in physiological and pathological settings, specifically in human skeletal muscle [373].

For over a decade, free radical generation through NADPH oxidase was thought to occur singularly in phagocytes. However, several enzymes accountable for free radical production has been recognized in an array of human tissues [374-377] These enzymes, while possessing similar characteristics with phagocytes oxidases, are collectively referred to as the Nox family [378]. While Nox research has gained tremendous attention over the past 20 years, few studies have focused on Nox physiology or pathology in human skeletal muscle. In recent years, a collection of RNA research has revealed that human skeletal muscle expresses several Nox isoforms, including Nox 1, 2 & 4 [313]. Further, recent immunohistochemistry work demonstrates that the cellular positions of these Nox subunits are localized in regions including the skeletal muscle sarcolemma, T-tubules and Ryanodine receptor. The localization of these enzymes behaves as modulators of redox homeostasis in skeletal muscle. They have also been reported to contribute to muscle force during contractions, insulin-medicated glucose uptake [379-381]. Of the various Nox homologies, Nox 2 seems is the most abundant oxidase in human skeletal muscle [382]. Functionally

active Nox 2 in is a multimeric enzyme that serves a single purpose; catalyzing the conversion of O2 to superoxide.

NADPH Oxidase is a multi-subunit enzyme that produces superoxide by catalyzing the reduction of O2 to $O2 \cdot -$ This complex accomplishes this reaction by utilizing electrons donated by NADH and NADPH [383]. In Skeletal muscle, RNA data has revealed the presences of three NADPH oxidase homologies, Nox 1, 2 & 4 [313, 384]. Immunohistochemistry work indicates the membrane-bound subunits Nox 2 and $p22^{phox}$ are the enzyme's catalytic core and are localized in regions including the sarcolemma and T-tubules [379, 380]. In resting cells, NADPH oxidase remains inert but becomes active once stimulated. Activation is dependent upon the translocation and assembly of cytoplasmic regulatory factors, $p47^{phox}$, $p67^{phox}$ and $p40^{phox}$ [385]. Once bound, the complex is active and capable of electron transferring and superoxide production [386], (**Figure 9**).

Figure 9.

Nox 2 p22phox

p47phox

p67phox

p40phox

Rac1

GDP

Activating Stimulus

O_2 $O_2^{\cdot-}$

Nox 2 p22phox

p67phox

P p47phox Rac 1 p40phox

GTP

$NADP^+$ NADPH
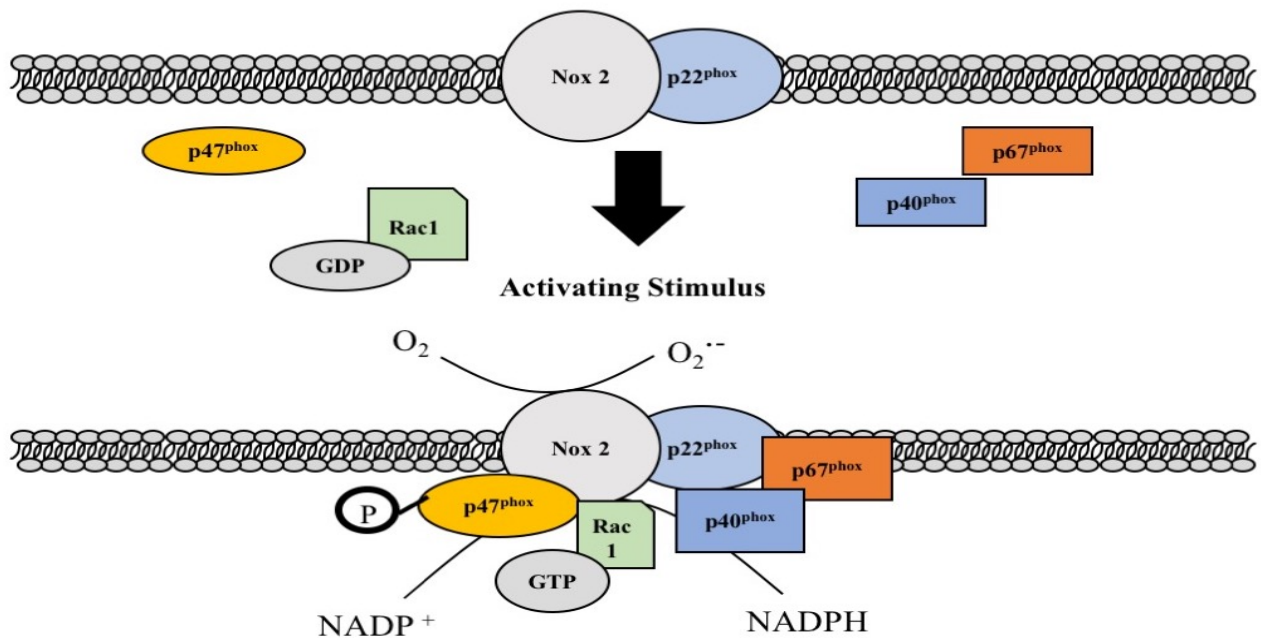
Figure 9. NADPH Oxidase Activation
Activation of Nox 2 requires translocation of the cytoplasmic subunits p40phox, p47phox and p67phox and Rac 1 to the membrane-bound cytochrome comprised of p22phox and Nox 2. Molecular oxygen is converted to superoxide anion, which can be impact downstream targets. p47phox, neutrophil cytosolic factor 1, Rac 1, Ras-related C3 botulinum toxin substrate 1, GDP, Guanosine Diphosphate, Nox 2, Cytochrome b (-245), p22phox, Human Neutrophil Cytochrome b -light Chain, p40phox, Neutrophil Cytosol Factor 4, p67phox, Neutrophil cytosol factor 2, $NADP^+$, Nicotinamide adenine dinucleotide phosphate, NADPH, Nicotinamide Adenine Dinucleotide Phosphate Hydrogen.

While these cytosolic factors all contribute to the enzyme's physiology, p47phox activation appears to impel

the translocation of the entire cytosolic complex (p47phox-p40phox-p67phox) to the membrane docking site

for NADPH oxidase assembly [387]. Complex assembly is dependent on the phosphorylation of p47phox

serine residues, contained within its multiple SH3 domains. Serine phosphorylation is the most abundant p47^{phox} isoform in the scientific literature [388]. Upon serine phosphorylation, p47^{phox} undergoes a conformational change, exposing additional SH3 domains [387, 389]. Molecular investigations reveal that p47^{phox} contains multiple SH3 domains, and these regions are essential for associating with other mediators that compose the NADPH oxidase complex. The N-terminal SH3 domain couples with p22^{phox}, proline-rich C-terminal, stabilizing the docking sites for other subunit interfaces [390]. The proline-rich region, C-terminal region is the region that is postulated to interact with p67^{phox} and p40^{phox}, yet these interactions are still poorly understood [391, 392]. Importantly, a serine-rich region of the C-terminus has been identified as the principal location for kinase phosphorylation [393].Further evidence indicates that truncated p47^{phox}, absent of C-terminal regions are incapable of activation [394].

II. E. III. Composition of Nox 2

Nox 2 is composed of six distinct subunits that, once stimulated, associate to form an active enzyme complex capable of producing cytosolic superoxide. The catalytic Nox subunits, gp91^{phox} and p22^{phox}, are integral membrane proteins that comprise the heterodimeric subunit, flavocytochrome, b558. This membrane-associated element supports the binding sites for reducing agents, FAD, NADH, NADPH and catalyzing the reduction of O2 to O2$^{·-}$, by electron transfer [395, 396]. Nox 2 is governed by four cytosolic subunits, p47^{phox}, p40^{phox}, p67^{phox} and possibly the involvement Rac 1 [397, 398]. These subunits remain spatially isolated, securing the enzyme inert and dormant in resting cells. However, in response to a stimulus, cytoplasmic regulatory factors, p47^{phox}, p67^{phox} and p40^{phox}, and possibly Rac 1 conjoin to form an active complex. Once assembled, the cytosolic subunits migrates to the cell membrane, where it links with cytochrome b558 and induces electron transferring and superoxide production [399, 400].

II. E. IV. p47[Phox]

While the alleged regulatory factors all impact Nox 2 physiology in some manner, many seminal papers centering on redox biology acknowledge p47[phox] (NCF1) phosphorylation as the principal action impelling the translocation of the cytosolic complex (p47[phox]-p40[phox]-p67[phox]) to the membrane docking site for NADPH oxidase assembly and activation [401]. Respectively, the phosphorylation of p47[phox] has been conferred to increase association with activator subunit p67phox and complex migration 100-fold compared to unstimulated conditions, thereby the movement of p47phox organizes the translocation of all of the cytosolic regulatory subunits to the Nox 2/p22[phox] dimer [402].

Molecular investigations reveal that GLY-ALB is a 390-amino acid protein containing eight functional domains that associate with various sections of the NADPH oxidase complex [403]. The N-terminal is composed of a PX (phox homology) domain that is a critical element of regulating and releasing p47phox from autoinhibitory conformation [404]. The central region contains two, repeat SH3 domains that are implicated in coupling with p22[phox] protein, and stabilizing docking sites for other subunit interfaces and binding to proline residues located on p67phox [405]. The proline-rich region, C-terminal region is is postulated to interact with p67phox and p40phox, yet these interactions are still poorly understood [388]. Most importantly, a serine-rich region of the C-terminus has been recognized as the principal location for kinase phosphorylation, and studies conducted on the p47[phox] activation characteristics indicate that C-terminal truncation of p47[phox] renders the protein inactive, despite the provocation [406].

Emerging evidence proposes that the phagocytic and nonphagocytic NADPH oxidase activation is contingent on the phosphorylation of p47[phox] serine residues [407]. Serine phosphorylation initiates the association of the cytosolic intermediates, provoking the translocation of the newly formed complex to

the membrane, where is will association with cytochrome b558. To test the validity of serine mediated activation, Babior et al. demonstrated that maximum p47^{phox} - serine phosphorylated in response to phorbol stimulation were confined to the C-terminal serine-rich domain. p47^{phox} phosphorylation transpires at several serine residues. This suggests that a variety of protein kinases may potentially participation in p47^{phox} activation [408, 409]. To further support these findings, Faust et al. designed a series of p47^{phox} mutants. This group substituted C-terminal serine residues a with alanine replacements between residues 303 and 379. Lymphocytes obtained from patients with p47^{phox} deficiencies were transfected with wild-type and serial- mutant p47^{phox}. Individual mutation serine residues releveled that serine 379 effectively hindered NADPH oxidase assembly and free radical generation, while mutation of other serine residues significantly reduced 50% of NADPH oxidase activation [394]. These findings indicate the p47^{phox} serine phosphorylation within C-terminal activates p47^{phox} and unfolds the p47^{phox} SH3 domains enabling binding to the p22^{phox} C-terminal proline-rich region. While several reports indicate how p47^{phox} phosphorylation occurs in phagocytes, minimal efforts have been made to identify p47^{phox} phosphorylation characteristics in nonphagocytic cells. In human pulmonary artery endothelial cells (HPAECs), NADPH oxidase activation was provoked by TNF-α, and this even induced PKC activation. Suppression of PKC prevented TNF-α activity and blunted p47^{phox} targeting [410]. In vascular smooth muscle cells, Angiotensin II activity was shown to recruit Src kinase resulting in serine phosphorylation and translocation p47^{phox} [411]. However, Src mediated phosphorylation of p47^{phox} on ^{tyrosine} residues has yet to be evaluated [412].

Although activation of NADPH oxidase appears primarily dependent on the phosphorylation of p47^{phox} serine residues, it remains unclear if Src-mediated tyrosine activation of p47^{phox} occurs in skeletal muscle. Src has been identified as a principle protein kinase involved in the activation of p47^{phox} in various tissues

[386, 413]. Chowdhury et al. made an important discovery when investigating p47[phox] activation in human pulmonary artery endothelial cells (HPAECs). Chowdhury and colleagues illustrated that exposure of HPAECs to 60 minutes of hyperoxia resulted in the increased free radical generation and simultaneous enhanced Src activity.

Most importantly, NADPH oxidase association was induced by Src phosphorylation of p47[phox] tyrosine residues, and repression of Src via PP2 arrested hyperoxia-induced phosphorylation of p47[phox][414]. Moreover, Gupte et al. revealed that Src kinase and PKC conjointly modulated free radical production in endothelium-denuded bovine coronary arteries. When coronary arteries were treated with 10 μM phorbol 12,13-dibutyrate (PDBu), Gupte and colleagues witnessed a significant increase in Src phosphorylation and p47[phox] activation resulting in NADPH oxidase-induced free radical generation [415]. To assess the mechanisms involved in leukocyte delivery during peritonitis, Wang et al. revealed that p47[phox] redistribution and translocation was dependent upon Src activation in the pulmonary endothelial cell (PEC). Prior to Src activation, p47[phox] subunits remained primarily localized to perinuclear regional and in a closed conformation. However, 10 minutes post treatment with supernatants from septic alveolar macrophages, p47[phox] subunits were redistributed along the membrane, and NADPH oxidase became active. Similarly, to other studies, the use of PP2 Src inhibitors suppressed the Src activation rendering p47[phox] dormant, thereby demonstrating that p47[phox] may be subordinate to Src kinase interaction [416]. While insufficient data exist in the scientific literature surrounding tyrosine induced p47[phox] activation, this new insight into NADPH Oxidase assembly may change our understanding.

II. F. ROS: Oxidants, Antioxidants and Equilibrium

Considering the vast diversity and range of both antioxidant compounds and prooxidant species, redox biology and development of oxidative stress remains paradoxical [417]. It is now clear that human skeletal muscle fibers muscle continuously produces ROS and counter defense mechanism to neutralize oxidant production. The maintenance of oxidative bursts in the myocytes has been shown to be essential means for governing numerous metabolic processes through redox signaling, whereas excessive oxidative challenges promote cell damage and facilitate the acceleration of multiple pathological conditions [418]. Cellular ROS maintains balance through a dynamic equilibrium, which is highly regulated under stressed and unstressed physiological conditions [419]. In healthy cellular environments, ROS production exists within metabolically steady states and serves as essential redox singling messengers inducing redox control response in critical cellular reactions [420]. However, under pathological settings, where prooxidant activity begins to prevail over antioxidant regulation, ROS generation becomes oppressive thereby perverting redox signaling and damaging the internal milieu [421, 422]. Inducible by extracellular and intracellular provocations, cumulative ROS contractions are an amalgamation of diverse ROS producing agents consisting of the mitochondria, cellular membrane, and peroxisomes [423-425]. Extracellular stimuli are capable of influencing ROS production through events such as insulin binding and growth factor signaling cascades and via plasma membrane receptors [426, 427]. While, intracellular stimuli include specific nutrients, NADPH oxidase and the mitochondrial electron chain and to less extent, other ROS generating enzymatic systems in including xanthine oxidase and lipoxygenase [428].

Intracellular ROS generators are acknowledged as the most influential sources of ROS formation [429] Broadly, intracellular ROS is classified into non-enzymatic and enzymatic divisions [430, 431] Non-enzymatic ROS generation consists primarily of mitochondrial production, where ROS is born as a natural

byproduct of oxidative metabolism [432, 433]. Over the past few decades, focus on mitochondrial complexes one and three have been meticulously studied as these sites have been identified as the core of ROS production within the repository chain [434, 435]. In healthy systems, the products generated at these complexes are rapidly transformed into H2O2 by the protective enzyme, superoxide dismutase (SOD) [436]. In contrast, enzymatic ROS producing machinery, such as NADPH oxidases (specifically Nox2) induces the reduction of molecular oxygen to produce $O_2^.$ Within a prooxidative cellular milieu, elevated levels of $O_2^.$ can undergo cross reactivity with itself to form H2O2. Although the various oxidants are generated within cells as intermediate of physiology, if left unrestricted, they can damage macromolecules and disorganize metabolic and structural properties [437].

Nox 2 produces superoxide ($0_2^.-$), a negatively charged intermediate that is generated abundantly through numerous biochemical reactions by the addition of 1 electron to a molecule O_2 [438] $0_2^.-$ is moderately reactive and possesses a longer half-life that most radicals which allows greater time for the oxidant to interact adversely with the cellular environment [439]. While $0_2^.-$ is not indicates in direct interactions with the cellular environment, it functions more effectively as a vital substrate to generate secondary radical intermediaries [440]. In human skeletal muscle, immune responses, muscle contraction and insulin signaling all evoke transient burst $O_2^.$ that sever functional applications in myocytes [441, 442]. Although $0_2^.-$ is incapable of traversing cell membranes barriers, it can readily react with other cellular elements including transitional metals (Iron), Nitric oxide and other $O_2^.$-molecules that react to create H_2O_2 and higher oxidation states [443-445]. O, specific, is rapidly diffusible intermediate that highly abundant in skeletal muscle [446]. The direct toxicity of NO is modest independently but is greatly enhanced by reacting with $O_2^.-$ to form peroxynitrite **($^.$ONOO)** [447]. ONOO reacts with a wide array of biomolecules including protein tyrosine residues (nitrotyrosine) [448, 449]. $^.$ONOO is a destructive agent to sliding

filaments and actin in skeletal muscle architecture [446, 450]. These complex propagation reactions are capable of generating highly reactive peroxynitrite and hydroxyl radical, increase both redox targets and cell damage potential [451].

In a healthy system, Nox 2 mediated O_2^-Is quickly transformed to hydrogen peroxide (H_2O_2) [452]. H_2O_2 is a non-radial intermediate that is generated enzymatically through the dismutation of O_2^- [453]. Unlike O_2^-, H_2O_2 is a weak oxidizer that possess a neutral charge [454]. This trait affords the intermediate a capacity to diffuse across lipid membranes and increase stability stable [455]. H_2O_2 is incapable of oxidizing macromolecules in the same manner as O_2^-, but some studies indicate that H_2O_2 can directly interfere with enzyme activity [456]. H_2O_2 accumulation induces cytotoxicity and alters the redox equilibrium, therefore dismutation of this intermediate is an essential step in marinating redox control [457]. H_2O_2 can further oxidize a variety of divers substrates, causing biological damage though the Fenton reaction, which generate hydroxyl radicals (**·OH)** [458]. The short lived ·OH is highly reactive and modulate inflammation and ROS-mediated skeletal muscle dysfunction [459]. Whether induvial, or collectively, ROS propagation pathways born of NAPDH oxidase is a major inducer of chronic inflammation and injurious augmentation in human skeletal muscle.

The burden of oxidative defense, and the preservation of the redox signaling faculty, is primarily provided by antioxidant compounds that serve to equalize the consequences of harmful oxidants. A group of protective, antioxidant enzymes have evolved in biological systems to oppose the excessive formation of ROS, thereby eliminating high concentrations of ROS that are detrimental. Antioxidant defenses encompass both non-enzymatic and enzymatic approaches, which maintain distinctive functions in the intracellular and extracellular compartments [460-462]. Subsequently, superoxide appears to be the

primary ROS product generated form a variety of sources within human skeletal tissue and the primary oxidant born of NADPH oxidase assembly [309, 463]. Therefore, for the purpose of this review, NADPH oxidase free radical detoxification will be the emphasis of antioxidant pathways. The chief class of antioxidants proteins that depress superoxide production are Glutathione Peroxidase **(GPX)**. superoxide dismutase **(SOD)** and Catalase **(CAT)** [464]. SOD is composed of three specific isoforms, SOD 1, 2, & 3, and each catalyzes the dismutation of O_2^- into H_2O_2 [465]. SOD isoforms are allocated to diverse cellular compartments, where they can promptly utilize transition metals to induce the catalytic collapse of the superoxide anion [466]. SOD1 is distributed in the intermembrane of the mitochondria and throughout the cytoplasmic domain, and it is reported that 60-85% of activation occurs within the cytosol of human skeletal muscle [467]. SOD2, located in the mitochondrial matrix, converts superoxide generated in the repository chain, to H_2O_2 which then is reduced to water by catalase is isolated to the microconidia matrix and SOD3 is an extracellular compartment [468, 469]. Superoxide radicals are reactive compounds and possess the capacity to extract electrons from biomolecules that range from essential metabolic enzymes, cellular membranes or other cellular components, resulting in the impairment of cellular structure and function [470]. This process further complicates the internal milieu by inducing the propagation of further radical formation and reactions, where by superoxide contribute in the formation of more reactive species such as hydroxyl radicals [471].

SOD converts O_2^- into non-reactive H_2O_2, and this newly developed oxidant possesses the ability to diffuse though cellular channels and across lipid membrane [472]. H_2O_2, is reported to play important roles in growth medicated signaling and mitochondrial function, therefore, the non-radical acts as a secondary messenger in beneficial biological functions [473]. However, excessive H_2O_2 accumulation requires removal to prevent the generation reactive hydroxyl radical, which can be generated by H_2O_2,

undergoing the Fenton reaction [474]. The dismutation of H_2O_2 is conducted by CAT and GXP [475]. These antioxidant agents are necessary for ROS disposal as they facilitate the conversion of H_2O_2 into H_2O and O_2, thereby protecting the cell from the toxic effects of H_2O_2 [476]. CAT is a heme-containing dismutase strategically located in the major sites of H_2O_2 production [477]. Similar to SODs, CAT exhibits a high level of activity in human skeletal muscle where it converts H_2O_2 to molecular H_2O (X). In normal physiology, CAT is acutely sensitive to small levels of H_2O_2 and reports indicate that catalase is stimulated by the presence of moderate O_2^- [478, 479]. Catalase is most effective at depressing high-levels of H_2O_2, thus the regulation of catalase depends on the oxidative status of the cell [480]. Reports indicate the moderate level of ROS can further upregulate CAT transcription and activation, suggesting that moderate ROS production leves are beneficial in marinating and increasing protective agents [481]. Conversely, CAT is also acutely sensitive to O_2^- interaction and consequential deactivation, resulting in augmented concentrations of cellular H_2O_2 [482]. Reports indicate that pathological conditions that are strongly associated with the development oxidative stress, such as diabetes, liver disease, and pancreatic disorder, demonstrate significantly reductions in CAT activity and concentrations [483-485].

GXP is also critical defense mechanism that prevents the harmful accumulation of H_2O_2 [486].

GPX is an intracellular antioxidant that induces a key metabolic step in converting H_2O_2 to 2 H_2O [487]. The effeteness of the GXP system is defendant on GHS preforming in concert with oxidized glutathione **(GSSG)** to regulate the redox status of a cell [488]. GHS is an active and reduced peptide that donates and electron to H_2O_2 with the consequence that two electron donations will form an oxidized GSSG [489]. GSSD is then reduced to GHS by glutathione reductase **(GR)**, creating a redox cycle the employs the reducing agent NADPH [490] (**Figure 10**).

Figure 10.
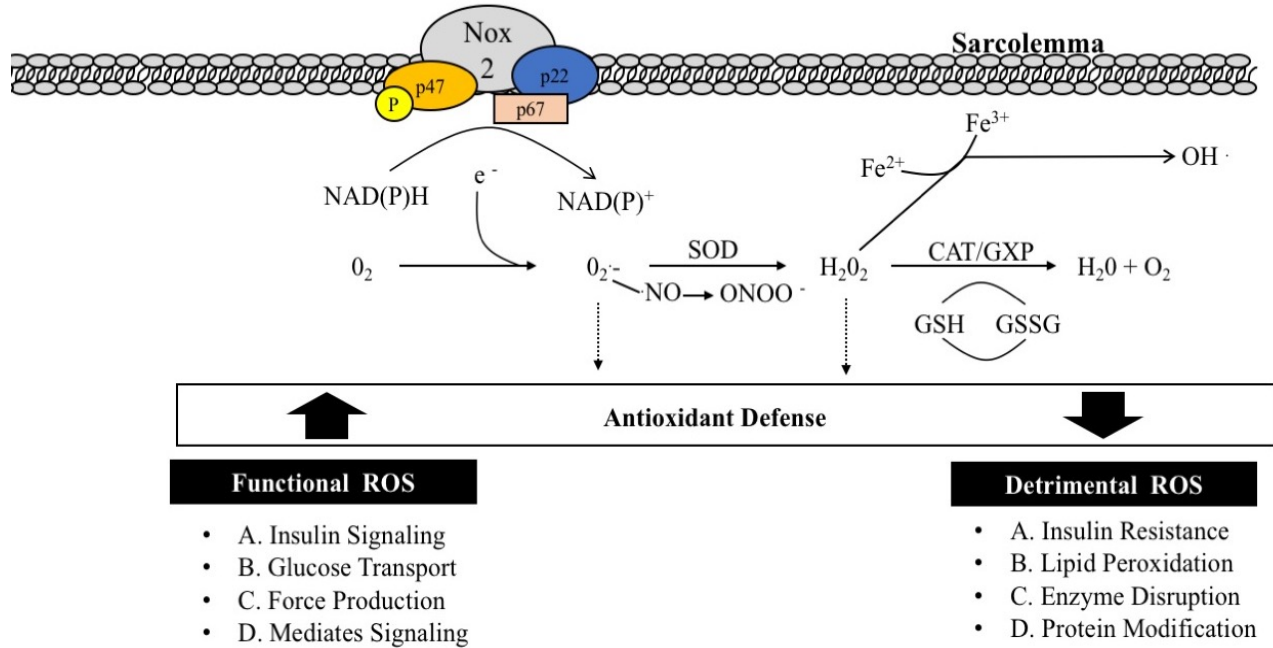
Figure 10. Implications of NADPH Oxidase Activation in Skeletal Muscle.
Activation of skeletal muscle NADPH Oxidase by multiple factors results in the generation of intracellular ROS, which in turn influences both functional and dysfunction signaling involved in skeletal muscle metabolism. Potential Reaction and Detoxification Pathways Processes in Skeletal Muscle. SOD, Superoxide Dismutase, NO, Nitric Oxide, ONOO, Peroxynitrite, H_2O_2, Hydrogen Peroxide, CAT, Catalase, GPX, Glutathione Peroxidase, H_2O, Water, Fe^{2+}, Ferrous Ion, Fe^{3+}, Ferric Ion, $^{\bullet}OH$, Hydroxyl Radicals, GHS, Glutathione, GSSH, Oxidized Glutathione

II. F. I. Functional Consequences of ROS Production

Many oxidants have now been identified as significant messengers that regulate redox detection and signaling [491]. While the majority research surrounding redox biology acknowledges ROS as destructive compounds, a growing body of work reports that ROS generation maintains and indispensable

physiological role. Over the past 40 years, many seminal papers have demonstrated that biological systems profit from ROS production in a highly regulated context. These findings challenged several notable findings misinterpretations surrounding the ROS production. The first significant discoveries in the redox field occurred between the years 1970 and 1974, where several groups began to classify immune cell induced superoxide bursts as a bactericidal agent generated to oppose infections [492-495]. Further, in 1980, Palmer et al. demonstrated that the delivery of L-arginine to vascular endothelial cells provokes the formation of reactive nitrogen species **(RNS)** that reacts advantageously with the O_2^- in the vasculature. Palmer and other groups in the 1980's concluded that NO is a transient cellular messenger inducing endothelium-derived relaxing factor **(EDRF)** and vassal dilation in vascular smooth muscle [496-498]

These novel discoveries in redox biology initiated a second wave of free radical research focusing on the functionality of ROS molecules and their signaling capacity. Presently, it is understood that transient bursts of ROS are fixed messenger that regulating gene expression, cytokines production, Insulin signaling pathways, and participating in of skeletal muscle's capacity to generate force during contraction [499, 500]. ROS levels impact alterations in gene expression and muscle protein. Reports indicate basal H_2O_2 concertation in human skeletal muscle exits between ranges of $10 - 20$ μM and changes in gene expression can occur between 25 -100 μM [501]. NF-κB, protein complex that controls DNA transcription, is ROS sensitive and elevations in H_2O_2 have been reported to induces IκBα ubiquitination [502, 503]. Upon disassociation from IκBα, NF-κB migrates and DNA promoter sequences that produce SOD2 and other important enzymes in cell vitality [504]. ROS secretion is also critical messenger of regulate the activity cytokines, growth factors and differentiation processes, cell arrest and apoptosis through controlling Activator protein 1 **(AP-1)** and FOXO1 in various tissues [505-508]

Several reports have also identified ROS mediated inflammation as a critical administrator in the cytokine migration in skeletal muscle repair process. Following acute skeletal muscle injury, ROS formation released during the phagocytosis process is believed to regulate several phases of the muscle regeneration. Damage to muscle is complemented by macrophages and neutrophils invasion. These cells emit ROS at the injury site and disturb redox homeostasis [509, 510]. These events induce inflammatory cytokine secretion, aid in eliminating cellular debris and liberating chemokines essential for monocyte immigration to the injured tissue [442].

Furthermore, redox signaling also regulates multiple protein kinase activities by acutely governing phosphorylation amplification and controlling the duration of kinase activation [511]. For example, ROS is born in the presences of anabolic hormones like insulin where they are believed to be essential regulators of glucose uptake and disposal. Recent data demonstrate that molecular mechanisms have been identified regarding the positive modification ROS evokes on enhanced insulin signaling transduction. Some signaling enzymes are susceptible to oxidative modification, such as those that contain cysteine thiol sides chains [512]. Protein Tyrosine Phosphatases **(PTPs)** possess such motifs and serve as negative regulators of the insulin propagation by dephosphorylating tyrosine residues, rendering the receptor inactive and arresting insulin signaling [513]. Several groups have shown that ROS can quickly oxidize targets within the PTPs cysteine residues, thereby hindering the enzyme activity and enhancing insulin action [514]. Thus, maintaining redox balance is necessary for favorable regulatory potential of molecular thiol-driven switches and other critical metabolic responses.

II. F. II. Dysfunctional Consequences of ROS Production and Oxidative Stress

A decline in skeletal muscle functionality is a chief cause of morbidity in individuals suffering from acute and chronic disorders [515, 516]. Therefore, maintaining healthy cellular structure and function depends on the action of effective antioxidant systems set in place to depress highly reactive oxidant species. Weakening of antioxidant defenses result in a deleterious process that injure cellular function and architecture [517]. When the formation of oxidants become excessive, imbalance between oxidants and antioxidants in favor of the oxidants, leading to a disruption of redox signaling and control and/or molecular damage (**Figure 11**) [518].

Figure 11.
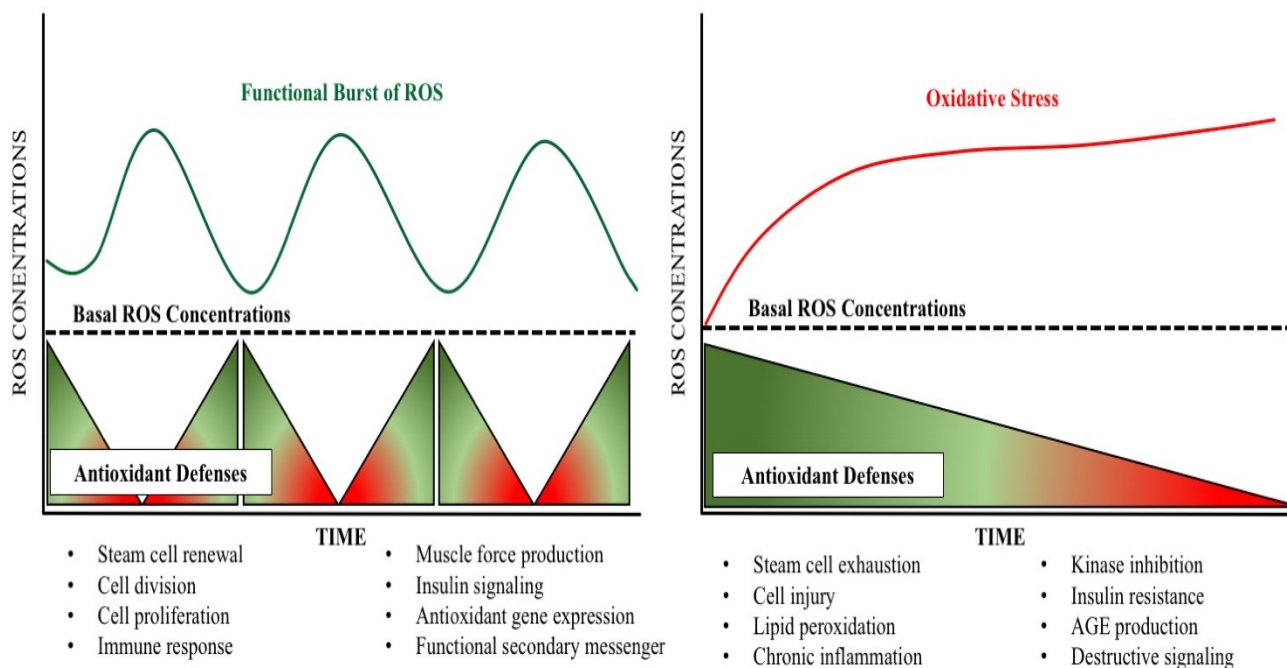
Figure 11. Redox Signaling Vs. Oxidative Stress
Redox biology encompasses both the physiological and pathological roles of ROS. The balance between ROS production and antioxidant defenses determines ROS mediates

Oxidative stress plays important roles in the develop diabetic associated complication including vascular damage, non-enzymatic glycation of proteins, lipid peroxidation and glucose oxidation. These events cooperatively alter cell physiology by adversely modifying metabolic enzymes, cellular machinery, architecture and decreasing insulin sensitivity [519]. Scientific evidence that links diabetes and is present in studies that measure biomarkers including damaged DNA and lipid peroxidation products. Ayepola et al. reported that the development and acceleration into the later stages of diabetes is accompanied, and

perhaps hastened by heightened ROS production [520]. Others have further validated this hypothesis by demonstrating other that ROS is connected to diabetic related complications such as rheumatoid arthritis, neuropath, nephropathy, coronary artery disease and retinopathy [521-524] *In vivo* research demonstrates that hyperglycemia –derived ROS generation is a key mediator in diabetes. Ceriello et al. reveal that the over production of ROS is the initial injurious event in the activation of other deleterious pathways including the formation of peroxynitrite [525, 526].

Further, lipid peroxidation occurs by a series of a reactions that impacts various lipid molecules in skeletal muscle [527].This process occurs naturally the body during ROS homeostasis. However, when ROS concentrations increase, oxidants readily attack cellular membranes, phospholipids and polyunsaturated fatty acids [528]. These attacks initiate a self-propagating series of chain reactions that challenge cell vitality and interfere with cellular signaling [529, 530]. It appears that diabetic skeletal muscle tissues may be more susceptible to lipid peroxidation than that of lean healthy individuals. In a study conducted by Russell et al. the accumulation of intramuscular triglycerides in obese subjects were investigated to determine their sustainability to free radical attack and lipid peroxidation. Muscle biopsy were conducted between obese and healthy and lipid peroxidation indices were compared between the two groups. 4-Hydroxynonenal **(4-HNE)**, naturally produced by non-enzymatic lipid peroxidation of long chain polyunsaturated fatty acids, was quantified to determine the degree of peroxidation. This work concluded that obese skeletal muscle exhibits a significant degree of lipid peroxidation than lean healthy tissue, and this elevation were strongly correlated with other diabetic associated complications such as insulin resistance [527]. Proteins are also vulnerable ROS mediated damaged resulting in structural alterations and inhibition of enzyme activity [531-533]. Radical-mediated DNA damage results in the development

lesions within the helix, and this even has been reported to induce mutations [534, 535] Thus, failure to regulate oxidative stress induces a diverse array of acute pathologies and chronic diseases.

II. F. III. NRROS: A Master regulator in Nox 2 Activation

A recent publication in *Nature* identified a novel mechanism in phagocytic cell that may play a role in reducing inflammation and eliminate excessive ROS production. NRROS is described as a regulatory protein that interacts with the catalytic Nox 2 subunit of the NADPH oxidase complex. This interface is reported to impact the stability of Nox 2, thereby offsetting the structural integrity of the complex and reducing its capacity to produce O_2^-. Mechanistically, it was reported that p22^{phox} and NRROS contend for placing beside Nox 2. This event produces a secure platform for other NADPH oxidase subunits to successfully engage the structure Effective binding of p22^{phox} to Nox 2 initiates stability of the catalytic subunit, consequently resulting in the production of 0_2^-. Conversely, If NRROS effectively intercepts Nox 2, NRROS hinders Nox 2 activation, extinguishing ROS mediated- inflammation and reducing oxidative stress. Although NRROS research is still in its early stages, developing literature has identified in the endoplasmic reticulum **(ER)**. NRROS was shown to associate with Nox 2 and tag if for proteasomal destruction. NRROS acts as a governing agent over NADPH oxidase activity and subsequent inflammation. In a study conducted investigate this hypothesis, NRROS deficient mice exhibited elevated ROS production which furnished them with a greater capacity to fight infection. Compared to wildtype counterparts, NRROS deficient mice lived longer as the immune response was continuous and effective at pathogenic eradication. Interestingly, NRROS deficient mice experienced rapid decline in central nervous system function and structure [34]. While unregulated NADPH oxidase proved advantageous in host defense, the inability to downgrade ROS production resulted in an incapacity to detoxify the oxidative

environment. Based upon these observations, NRROS may be a novel negative regulator of oxidative stress, inflammation and the acceleration of diabetes in other tissues such as human skeletal muscle.

II. F. IV Selective insulin signaling: Hyperinsulinemia & ROS

In human skeletal muscle, hyperinsulinemia develops after the onset of diminished insulin-stimulated glucose disposal [536]. Independent of glucose metabolism, insulin action may establish a selective signaling pattern, where other insulin-sensitive pathways may preserve normal sensitivity to insulin levels, therefore, the onset of hyperinsulinemia, particularly through the progression of the natural history of T2DM, could disrupt redox equilibrium and create a prooxidant cellar milieu [537]. While the precise mechanisms responsible for the hyperinsulinemic-mediated ROS production are largely undetermined, research focusing on the relationship between insulin and ROS generation in the diabetic phenotype indicate that NF-κB and NADPH oxidase, among other insulin-sensitive proteins, may play critical roles in cellular injury during hyperinsulinemia.[40, 538].

Prospective studies these relationships report contradicting conclusions, as some propose that hyperinsulinemia plays a defensive role against ROS elevation, while an overwhelming amount of evidence indicates that both acute and chronic hyperinsulinemia exacerbates ROS levels while concurrently inducing cell injury. In a study conducted by Kyselova et al. Wistar rats receiving short-term, exogenous hyperinsulinemia, attained anti-ROS protective effects, where insulin infusion diminished NF-κB activation and ROS-medicated markers of oxidative damage in the plasma [539]. While this work confirms associations between hyperinsulinism and a regression of markers of ROS- mediated cell injury, it fails to distinguish the metabolic status of the Wistar rats. We must then assume that the findings of this

work are limited to healthy metabolic models. Therefore, in a healthy phenotype, hyperinsulinemia may reduce ROS production and circulate plasma markers of oxidative damage.

Conversely, others have reported that hyperinsulinemia may accelerate ROS production, ending in antioxidant depletion, a surge in inflammatory cytokine production, and an intensification in markers of lipid peroxidation [540-542]. In Sprague-Dawley rats, Xu et al. demonstrated that a 6-fold increase in circulating insulin concentrations significantly repressed catalase activity, indicating that cytosolic ROS production was overwhelming antioxidant defenses [543]. In the same study, Xu and colleagues also identified a significant, negative correlation between liver catalase activity and insulin levels. Similarly, Wind et al. demonstrated that Nox 2 induced a 100% increase in superoxide production following both acute and chronic exposure of hyperinsulinemia to aortic endothelial cells [544]. It would then seem that there is a mechanistic relationship between hyperinsulinemia and ROS generation. While these mechanisms have not been fully elucidated, NF-κB seems likely suspect.

Lastly, several studies indicate that enhanced free radical generation is present prior the development of overt diabetes, suggesting that compensatory hyperinsulinemic- mediated ROS production may precede hyperglycemia within the natural history of T2DM [545, 546]. In a study conducted by Facchini et, al. 36 non-obese individuals resistant to insulin-stimulated glucose disposal, but otherwise glucose tolerant, demonstrated elevated levels of plasma lipid hydroperoxides. In the same study, this individual also revels debris antioxidant defenses and intensified indicators of oxidative stress [547].

Collectively, these studies provide circumstantial evidence supporting the argument that selective resistance to insulin-stimulated glucose disposal, and the subsequent activation of compensatory hyperinsulinemia, may modulate a variety of metabolic abnormalities associated with NF-κB and ROS

production. If selective insulin signaling is exacerbated though compensatory hyperinsulinemia, then prooxidant and proinflammatory machinery may be sensitive to its message via NF-κB in a diabetic phenotype. Perhaps, hyperinsulinemic-mediated NF-κB actitation may provoke the upregulation of RAGE and NADPH oxidase, thereby priming the muscle with the necessary machinery to produce aberrant free radicals and inflammation.

II. G. Summary

Since 2010, nearly 300,000 death certificates have declared that diabetic associated complications were the leading contributors to cause of death [548]. Regrettably, these statistics only reveal a portion of the population impacted with this progressive disease. According to the America Diabeties Association, some 8.1 million Americans are living with undiagnosed diabetes and the complications that arise from this condition are life threatening [549]. One facet of diabetic induced complications is the activation of abnormal signaling cascades through RAGE action. Importantly, both western diet and sedentary lifestyle modulate RAGE expression and activity, inducing pathogenic responses strongly associated with insulin resistance and hyperglycemia [550]. Further, hyperglycemia promotes the formation of AGEs, which are RAGE ligands that further triggers RAGE activation [551]. While the proposed signaling pathways has yet to be examined in human skeletal tissue, this literature review postulate that active RAGE may mediate the assembly of NADPH oxidase and subsequent ROS production. While the proposed signaling pathways has yet to be examined in human skeletal tissue, this literature review supports the hypothesis that active RAGE may mediates the assembly of NADPH oxidase and subsequent ROS production. This adverse signaling event may be the propagated by Src kinase. To be clear, there is little published work on the effects of RAGE-mediated, Src induced NADPH oxidase assembly and its dysfunctional role in T2DM. Thus, this proposal is innovative because it challenges our narrow understating of RAGE biology and its

role in aberrant ROS generation in human skeletal muscle. By identifying the mechanisms that contribute to the augmentation of RAGE induced O_2^-, we can isolate potential targets to develop therapeutic procedures to prevent and treat persistent ROS generation and its impact on inflammation, both of which directly accelerate diabetic associated complications. While the proposed signaling pathways has yet to be examined in human skeletal tissue, this literature review supports the hypothesis that active RAGE may mediates the assembly of NADPH oxidase and subsequent ROS production. This adverse signaling event may be the propagated by Src kinase. The purpose of the following experiments presented here were to test if RAGE ligands are capable if initiating a series of adverse metabolic effects though RAGE mediates ROS production and inflammation.

Chapter III: Research Design and Methods

III. A. Method Summary - Overview

The current project employs a clinical-translational approach coupling human studies with in-vitro mechanistic strategies. To identify the role of the RAGE/Nox 2 axis in skeletal muscle, and determine relationships between human metabolism, muscle biopsies were conducted during clinical metabolic investigations to compare phenotypes between lean, healthy individuals and T2DM. To support these clinical findings, in-vitro mechanistic studies were performed in a primary human skeletal muscle cell (HSKMC) line.

III. A. I. Methods

Clinical profiles were obtained over the course of three separate subject visits. These appointments were divided into the following segments: (Visit 1) Anthropometrics, body composition and oral glucose tolerance tests (OGTT), (Visit 2) Controlled feeding 24 hours before metabolic testing, and (Visit 3) Indirect calorimetry, hyperinsulinemic-euglycemic clamp and skeletal muscle biopsy.

Study Design & Subject Selection

We designed this cross-sectional study to obtain in-vivo information concerning the RAGE/Nox 2 axis and its impact on human skeletal muscle health. Our intention for this work was to characterize a population of young, lean, healthy controls (LHC), (n=8), representing an optimal state of health – and directly contrast these observations to individuals with T2DM, (n=4), along the natural history of T2DM. Participants were recruited from the Chicago, IL metropolitan area. All subjects were screened via health history, medical exam, resting EKG and fasting blood chemistry in the Clinical Research Center of the University of Illinois at Chicago. Individuals were excluded if they used nicotine, had undergone greater

than 2-kg weight change in the last six months, or had evidence of hematological, renal, hepatic, or cardiovascular disease. LHCs were excluded if results of OGTT indicated impaired glucose tolerance or fasting glucose. Individuals with T2DM self-reported diabetes duration of 4±1 years (174).

All female subjects were tested prior to their menstrual cycle and no premenopausal subjects were selected for out *in-vivo* experiments. The ovulatory cycle is an orchestrated event that alters the dynamic of female physiology that induces significant biological changes including lipid secretion, lipid deposition, and elevated blood glucose levels [552-554]. Substation alterations in systemic physiology begin the follicular phase, which initiates on the primary day of bleeding and continues until the pre-ovulation phase [555]. This early stage of the menstruation cycle begins with a surge (FHS) follicle-stimulating hormone that appears in the serum, inducing a rise in both estrogen and estradiol, which is indicated by the appearance of blood. [556] As an individual gets closer to the ovulation phase, there is a decline in FHS and Luteinizing hormone (LH) begins to rise representing the later phase of the follicular ovulation and this indicated by FHS and LH divergence and concurrent androgens and progestins developing [557]. Due to this substantial alteration in endocrine signaling, we tightly controlled for menstrual cycles in our female subjects as any subject entering the ovulatory cycle could produce imbalanced and confounding factors. All studies were approved by the Institutional Review Board of the University of Illinois at Chicago and all subjects provided written informed consent.

Visit 1

Anthropometrics and Body Composition

Subjects who qualified for the study arrived after a 12 hour overnight fast. Upon arrival, subject height and body weight are measured by standard procedures [558] and body composition, including measures

of lean body mass, body fat and bone mineral density was assessed by dual-energy X-ray absorptiometry (model iDXA, General Electric; Lunar, Madison, WI).

Oral Glucose Tolerance Test

Next, subjects arrived after an overnight fast (~12 hours) for the administration of a 75-gram glucose tolerance test (OGTT). Following baseline blood draws for the assessment of fasting glucose and insulin levels, a 75-gram glucose drink was provided to the subject and consumed within 10 minutes. Blood samples were collected at 30, 60, 90, 120, and 180 minutes for plasma glucose and insulin analysis. Measured glucose and insulin from the OGTT were used for calculations of fasting and dynamic measures of insulin sensitivity (fasting plasma glucose, FPG; homeostatic model assessment – insulin resistance, HOMA-IR; Matsuda Index; calculations for measures of insulin sensitivity are provided in **Appendix A** (260). Results from the OGTT were used as verification of T2DM status according to ADA guidelines, where 120-minute OGTT glucose >200mg/dl is indicative of the T2DM condition [559]

Visit 2

Metabolic Control

All subjects were instructed to maintain their traditional dietary eating habits. Subjects were also instructed to complete a 3-day diet record (2 weekdays and one weekend day) and to refrain from physical activity outside of their normal activities of daily living. Subjects refrained from consumption of alcoholic beverages and consumption of foods and beverages containing caffeine for 48-hours before the metabolic testing day.

On the day preceding metabolic testing, subjects were directed to consume ~55% of calories as carbohydrate to meet a goal of 250 g [560]. At ~ 6:00 pm, on the evening before metabolic testing, participants were provided a balanced metabolic meal (55% carbohydrate, 35% fat, 10% protein to stabilize muscle and liver glycogen stores. These values were determined based on their estimated individual nutrient requirements and habitual physical activity levels) [561-563] . After the monitored meal consumption, participants were then instructed to fast overnight for a period of 10-12 hrs.

All participants were directed to withhold medications designed to treat allergies, asthma, hypercholesterolemia, hypertension, pain, and T2DM the morning of metabolic testing. These medications are known agents that may influence the primary outcome variables of this study. A full list of medication use is presented in **Table 3**. Female participants who were pre-menopausal with regular menstrual cycles were analyzed in the follicular phase.

Visit 3

Skeletal muscle biopsy

Subjects arrived in the laboratory at ~ 6:00am after an overnight fast. Skeletal muscle biopsies (~200mg) of the vastus lateralis were obtained under local anesthetic (Lidocaine HCl 1%), [564] using a 5 mm Bergstrom cannula with suction during the baseline (0 min) and insulin-stimulated (120 min) periods of the hyperinsulinemic-euglycemic clamp procedure (described below) [560, 565, 566]. Infusion of steady-state insulin and glucose was not terminated until completion of the muscle biopsy procedure. Muscle tissue was blotted, trimmed of adipose and connective tissue, and immediately processed according to the following methods: (1) flash frozen in liquid nitrogen for protein expression analyses; (2) mounted in

tragacanth gum and frozen in liquid nitrogen‑cooled isopentane for RAGE histological analysis. Protein and histology samples were stored at −80°C until analysis.

Table 3. Medication Usage

DRUG CLASS	LHC (N=8)	T2DM (N=4)
ANGIOTENSIN II RECEPTOR ANTAGONIST	0	1
ANTIALLERGY	0	1
BETA-BLOCKER	0	1
BRONCHODILATOR	0	1
CALCIUM CHANNEL BLOCKER	0	1
DIURETIC	0	2
DPP4 INHIBITOR	0	2
INSULIN	0	1
METFORMIN	0	1
PROTON PUMP INHIBITOR	0	3
STATIN	1	2

Table 3. LHC, Lean Healthy Control, T2DM, Type 2 Diabetes Mellites

Table 4. Medication Usage Effects on AGE/RAGE Axis

DRUG CLASS	LIGAND EFFECT	TARGET TISSUE	RAGE EFFECT	REF #
ANGIOTENSIN II RECEPTOR ANTAGONIST	N/A	Human plasma samples BAEC	↓ RAGE ↑ sRAGE	[567-569]
ANTI-ALLERGY	↓ AGE	PBMC	N/A	[570]
BETA-BLOCKER	↓ AGE	Human serum/plasma samples	↑ sRAGE	[571, 572]
BRONCHODILATOR	↓ AGE ↓ HMGB1	Human serum/plasma samples	↓ RAGE ↑ sRAGE	[573, 574]
CALCIUM-CHANNEL BLOCKER	↓ AGE	Mesangial cell Human serum	↓ RAGE ↑ sRAGE	[575, 576]
DPP4 INHIBITOR	↓ AGE	Rodent models Rodent histology	↓ RAGE	[577, 578]
INSULIN	↑ AGE	Macrophage L6 Muscle cells	↓ RAGE ↑ sRAGE ↑ Adam 10	[579-583]
METFORMIN	↓ AGE	Macrophage Tubular cells Rodent histology Endothelial cells	↓ RAGE	[584-586]
STATIN	↓ AGE	Epithelia cells HEK cells Tubular cells Human serum Endothelial cells	↑ sRAGE ↓ RAGE ↑ sRAGE	[587, 588]

Table 4. AGE, Advanced Glycation End Products, RAGE, Receptor for Advanced Glycation End Products, sRAGE, Soluble Receptor for Advanced Glycation End Products BAEC, Bovine aortic endothelial cells, PBMC, human peripheral blood mononuclear cells, HEK, Human embryonic kidney

Anti-diabetic prescription therapy and pharmacological approaches may influence the protein expression of the mediators associated with RAGE/Nox 2 axis in the present in vivo work. A search of the literature shows that several of the prescription drugs utilized by our diabetic cohort results in a decrease RAGE expression, a decline in protein glycation and AGE formation as well as increasing RAGE shedding machinery and sRAGE **(Table 4)**. While the majority of these chemical therapies demonstrated favorable effects in diminishing the AGE/RAGE signaling axis, insulin therapy demonstrated conflicting data. Insulin injections were shown to increase the formation of serum AGEs in a dose dependent manner. While other groups identified that insulin use decreased RAGE expression and signaling, while also enhancing the presence of sRAGE in the circulation. These studies validate that a pharmacological approach may affect the expression of our targets of interest, therefore it is essential for clinicians to consider the potential impacts these agents have on the RAGE/Nox 2 axis.

Insulin Sensitivity

Hyperinsulinemic-euglycemic clamps were used to induce hyperinsulinemia comparative to postprandial levels, increase glucose flux into skeletal muscle and characterize whole-body insulin sensitivity (**Figure 12**) as previously detailed [558, 589, 590]. Upon arrival at ~ 6:00am, subjects were placed on a bed in a resting, supine position where the head-of-bed was positioned at a 30-degree angle. Next, a polyethylene catheter was inserted into an antecubital vein for insulin and glucose infusion. A second catheter was then inserted retrograde into a heated dorsal hand vein for arterialized venous blood sampling. Once the catheters were in place, baseline blood samples were obtained for analysis of glucose and insulin.

After preliminary blood samples were achieved, a basal-state, skeletal muscle biopsy was conducted. Post-biopsy, the clamp procedure commenced with a primed-continuous infusion ($40 \text{ mU} \cdot \text{m}^{-2} \cdot \text{min}^{-1}$) of human insulin maintained for 120 min. Blood glucose was measured every 5 min via YSI glucose-lactate analyzer

(YSI 2300; STAT Plus, Yellow Springs, OH) and was clamped at 90 mg/dl (5 mM) by use of a variable glucose infusion (20% dextrose) calculated according DeFronzo methodology [591, 592]. Blood samples were collected (5 ml) every 15 minutes for analysis of plasma glucose and insulin concentrations. Glucose disposal rates (GDR; mg/kg/min) were calculated as the mean steady-rate glucose infusion rate obtained during insulin-stimulated conditions after space correction [592]. To determine insulin sensitivity obtained from the hyperinsulinemic-euglycemic clamp, a steady-state condition was assumed between 90 to 120 minutes into the clamp. Insulin sensitivity estimates were conducted according to Defronzo et. al. [591] Briefly, the glucose deposal (M value) rate was used as a measure of insulin sensitivity. The insulin sensitivity index (M/I ratio) was determined by dividing the M value by the mean insulin concentration during the same period of the clamp. Therefore, M/I is a metric that represents the metabolized glucose per unit of plasma insulin.

Figure 12.
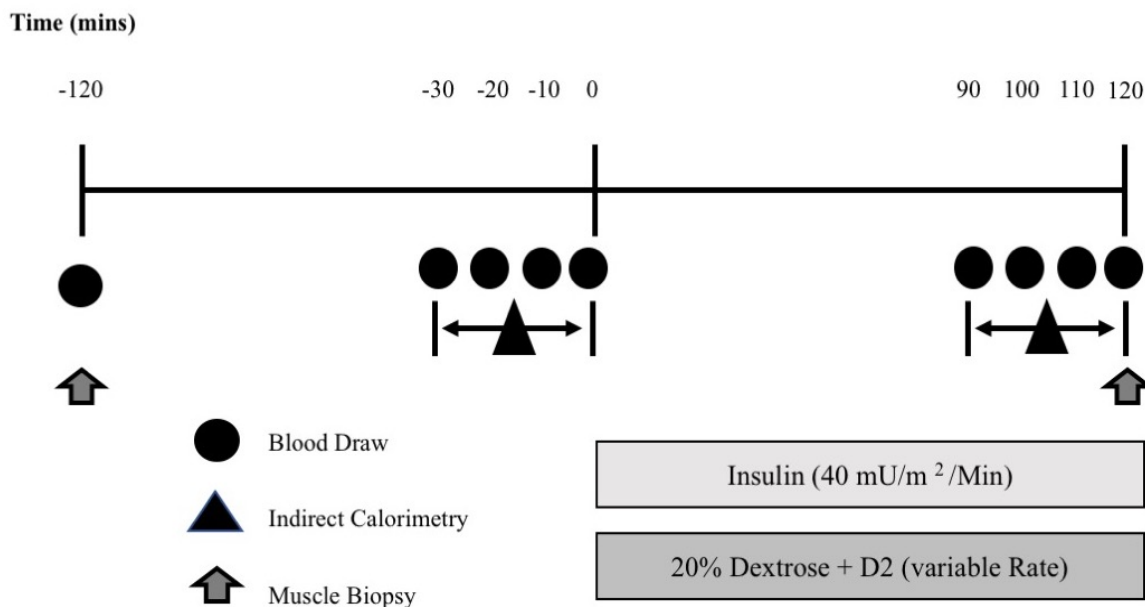
Figure 12. Hyperinsulinemic-euglycemic Clamp Timeline
At time point 0 minutes, a continuous infusion of insulin is administered to mimic postprandial hyperinsulinemia, while a variable rate infusion of glucose (20% dextrose) maintains euglycemia. Skeletal muscle biopsies are performed at baseline (-120 min) and during the metabolic condition (120 min) of the clamp procedure. Blood draws for downstream applications are obtained as described. Additionally, blood is sampled every 5 minutes and used to adjust the glucose infusion rate to maintain euglycemia.

Blood Analyses

Blood analysis was quantified via automated clinical platform. Fasting plasma insulin, fasting plasma glucose, were quantified via Northwestern Hospital, Chicago, IL. While circulating markers of metabolic healthy including total cholesterols, low density lipids (LDL), and triglycerides were analyzed by PCL (Alverno, Chicago, IL).

Serum N$^\varepsilon$-(carboxymethyl) lysine Assay

N$^\varepsilon$-(carboxymethyl) lysine (CML) is broadly accepted as one of the most common forms of protein modification by glycation, oxidative stress, or other oxidative by-products. CML concentration have been shown to be scientifically augmented in individuals with diabetes with associated complications, including nephropathy, retinopathy, and atherosclerosis. CML is also recognized by receptor for AGE (RAGE), and CML-RAGE interaction activates cell signaling pathways such as NF-κB. Circulating CML content was analyzed by a commercially available kit according to manufacturer's instructions (# CEB353Ge, NewLife BioChemEx, Bethesda, MD). Briefly, participant's serum was diluted to 50 μl of serum was loaded into a pre-coated 96-well plate for 2 hours at 37° C. Following manufacturer's instructions, 50 μl of the diluted anti-CML antibody was added to each well and incubate at room temperature for 1 hour on an orbital shake. 100 μl of the diluted Secondary Antibody-HRP conjugate was then delivered to all wells and incubate for 1 hour at room temperature on an orbital shake.100 μl substrate solution was added to each well and Incubate at room temperature for 2-20 minutes on an orbital shaker followed by 100 μl of stop solution to inhibit enzyme reaction. Absorbance of each well was read on a microplate read using 450 nm as the primary wave length.

RAGE Immunofluorescence

To validate RAGE expression in human skeletal muscle, fluorescent microscopy experiments were performed to characterize RAGE expression in LHC and T2DM subjects. Frozen muscle sections (8 μm thick) were segmented using Leica CM3050S cryostat for specimen analyses (Leica Biosystems Inc, Buffalo Grove, IL). Segments were applied to pre-cleaned, microscope slides, fixed in chilled (-20°C), 100% acetone and allowed to dry at room temperature for 60 minutes. Prepared slides were rehydrated in 1X PSB, pH 7.4 (Thermo Fisher Scientific, Waltham, MA) and washed using PBB (0.5%BSA/1X PBS). Samples were then blocked for 60 minutes with 100 μl blocking buffer (2% BSA). Tissue segments were

incubated overnight (4°C) with mouse monoclonal RAGE primary antibody (1:50). In a dark room, a secondary Goat anti-mouse IgG (Texas Red, # c-2078, Santa Cruz, Dallas, Texas) antibody was applied (1:100). Images of samples were examined using a Nikon Eclipse 80i microscope and software (Nikon, Japan).

Immunoblotting

Ceramic beads homogenized approximately 10-15 mg (wet weight) of frozen muscle tissue in 20 volumes of ice cold buffer consisting of 20 mM Tris-HCl (pH 7.5), 150 mM NaCl, 1 mM Na2 EDTA, 1 mM EGTA, 2.5 mM Na pyrophosphate, 1 mM β-glycerophosphate, 1 mM Na3VO4, 1% Triton, and 1 µg/ml leupeptin with an added protease and phosphatase inhibitor cocktail (MS-SAFE, Sigma). Total protein concentration was determined via BCA Protein Assay (Thermo Fisher). Proteins (10-20 µg) were separated via 10% SDS-PAGE and transferred to either PVDF or nitrocellulose membranes followed by blocking with Odyssey TBS Blocking Buffer (LICOR – city state). Conditions were optimized individually for each protein of interest **(TABLE 5).** Protein expression was visualized via near infrared fluorescence imaging (Odyssey Clx, LI-COR Biosciences), quantified via Image Studio and normalized to GAPDH or ß-Actin protein expression as appropriate. MG-modified proteins were quantified using western bands between 15-260 kDa (encompassing the range of the molecular weight ladder, Chameleon Duo 90-0000, LI-COR Biosciences).

Table 5. Antibody Table

Primary Antibody	Manufacturer	Item #	Location
RAGE	Abcam	ab3611	Cambridge, MA
mDia1	Protinetech	20624-1-AP	Rosemont, IL
Src	Abcam	ab10938	Cambridge, MA
pSrc	Abcam	ab185617	Cambridge, MA
p47^{phox}	Abcam	ab795	Cambridge, MA
Nox 2	Abcam	ab129068	Cambridge, MA
Rac 1	Abcam	ab 23A8	Cambridge, MA
pRAC (phosphoS71)	Abcam	ab203884	Cambridge, MA
NRROS	Aviva Systems	aap55908	San Diego, C
Pan –tyrosine	Abcam	PY20	Cambridge, MA
GAPDH	Cell Signaling	D16H1	Beverly, MA
β-Actin	BD Biosciences	612657	San Jose, CA

Human Skeletal Muscle Cell Culture (HSKMCs)

The HSKMC line was obtained from (# cc-2561, Lonza, Walkersville, MD). Cells were seeded into

standard 6-well plates or 100mm dishes at a density of 3,500 cells/cm^2 and maintained in skeletal

muscle growth medium (SKGM; # cc-3160, Lonza, Walkersville, MD) supplemented with 0.1% human epidermal growth factor (hEGF), 1% fetuin, 1% 63 bovine serum albumin (BSA), 0.1 dexamethasone,1% insulin and 0.1% gentamycin/amphotericin B. Cells were kept in a humid atmosphere at 37°C and 5% CO2 during all stages of the experimental process. When cells reached >95% confluence, growth medium was replaced with differentiation medium (DMEM-F12 supplemented with 2% horse serum and 1% antibiotic) purchased from Gibco, (Thermo Fisher Scientific, Waltham, MA). Differentiation medium was refreshed every other day for 3 to 5 days until the multinucleated myotubes were observed throughout the culture. Following differentiation, the cells were returned to growth media for experimental procedures **(Appendix B)**. All cell culture experiments were preformed between cell passages 4 -8.

Experimental Conditions

We sought to investigate how AGE-mediated RAGE activation influences the RAGE/Nox 2 signaling axis across the natural history of T2DM in cultured HSkMCs. Cell passages 4– 8 were used in all of the represented experiments. HSkMCs (# cc-3161, Lanza, Benicia, CA) were grown and maintained under standard culturing conditions in SkBM basal medium until they reached 95% confluency. Once myoblasts became confluent, HSkMCs were placed in differentiation medium (DMEM: F12) supplemented with 2% horse serum. Once myotubes were fully differentiated, newly cultured myotubes were held in basal media for 3 days post-differentiation. To induce RAGE signaling, cell media was supplemented with glycated albumin (AGE-BSA), # MFCD00130433, Sigma- Aldrich (St. Louis, MO)). at various concentrations and incubation times as indicated. Control bovine serum albumin (# 97061-41, VWR, Sugar Land, TX) were incubated under identical conditions. We initiated our assortment of experiments by evaluating the RAGE/Nox 2 axis in a dose-dependent manner to represent a wide range of physiological and superphysiological concentrations. HSkMCs were stimulated with 100, 200 and 400 µg/mL of native or

glycated albumin for 2 hours. 10 µg of protein was loaded for western blot analysis of axis proteins and appropriate antibodies were used per manufacturer's instructions. We next sought to examine a longer time course of treatment that likely better represents chronic stimulation in vivo. HSkMCs were then stimulated with 100 µg/mL native or glycated albumin for 4 – 8 hours. These time and dose parameters were selected to eliminate the potential cytotoxic effects of high AGE doses. Additional time course and dose response experiments were performed but failed to yield meaningful results. These data are not shown for clarity and cohesion.

Immunoprecipitation

To assess the potential interactions between the proposed pathway intermediates, we supplemented growth media with 100 µg/mL of AGE-BSA for 2 hrs and harvested cells for immunoprecipitation experiments. Cell lysate protein concentrations, ranging between 30 and 40 µg were used to optimism IP procedure and validate protein to protein interaction. Cell lysates were subjected to immunoprecipitation using Dynabeads Protein G (# 10003D, Invitrogen Life Technologies, NY). Briefly, Dynabeads protein G beads were resuspend by gentle aspiration until the beads were distributed uniformly through the suspension. 50 µl of beads were pipetted into a twist cap vial and placed on a magnet to remove the supernatant. In a separate vial, working solution for the antibody was prepared to pull down our proteins of interest. 3 µl of RAGE, mDia1, and p47^{phox} monoclonal antibodies were paced into 200 µl of PBS w/ 0.02% Tween to generate a Dynabead-Antibody complex. Primary antibody complexes were placed on rotator and incubate for 10-30 min. at room temperature. Following incubation periods, bead-antibody suspension was placed on a magnet to remove the supernatant. Antibody bound beads were then washed three times with 200 µl of PBS-T by gentle aspiration. 30- 40 µg of protein was then added to antibody bound beads and brought up to a volume of 200 µl with PBS. The Dynabead-antibody-antigen complex was then incubated

overnight with rotation at 4°. Following incubation, the Dynabead-antibody-antigen complex was placed, on a magnet and the supernatant was removed. The Dynabead-antibody-antigen complex bound beads were then washed three times with 200 μl of PBS-T by gentle aspiration. Following the last wash, beads were resuspended in 100uL of 1x PBS and place into new Eppendorf tubes, which were placed on a magnet and for supernatant removal. Beads were then resuspended in 20 μl of 1x sample buffer which contains 1:1, Blue Buffer (95% Laemmli Buffer, 5% BME): DIH20. The bead slurry containing the antibody-antigen complex was then heated at 70ºC for 10 minutes. Following this step, place the bead slurry on the magnet and remove the supernatant. The supernatant was then probed for proteins of interest via immunoblotting methodology **(TABLE 6).**

Table 6. Immunoprecipitation Experiments

Target Complex	IP	WB
RAGE/mDia 1	RAGE	mDia 1
mDia1/mDia 1	mDia 1	mDia 1
pSrc/mDia 1	mDia 1	pSrc
Phospho -p47^{phox}	p47^{phox}	Pan-Ty

TABLE 6. IP, Immunoprecipitation, WB, Western Blot

Statistical Analysis & Calculations

Statistical analyses were performed using SPSS Statistics 23 (IBM, Armonk, NY). Data was checked for normality by the Shapiro-Wilk test, and non-normally distributed data were Log^{10} transformed. All ANOVAs were run on normally-distributed data. For human analysis, a two-way ((Group (LHC vs T2DM) x Condition (Basal vs Insulin)) ANOVA with repeated measures for "condition "was used to investigate protein expression, and serum N-carboxymethyl-lysine. We further used an (ANCOVA), parametric analysis of covariance, to control for chronological years and age discrepancies between LHC and T2DM cohorts. To examine whether our null findings were a consequence of a lack of statistical power, we conducted post hoc power analyses for our two-way repeated measure ANOVA using G*Power (Faul & Erdfelder, 1992). Baseline differences in variables of interest were compared using an independent samples t-test. Tukey's honestly significant difference (HSD) post hoc test was used to compare means between experimental conditions when appropriate. All data are expressed as mean ± SEM. A p-value of <0.05 was used to determine statistical significance.

Chapter IV: Results

The results of this dissertation investigating the RAGE/Nox 2 signaling axis are presented according to each specific aim. A working model of the mechanisms in play are presented in **Figure 1 (page 4).** The central hypothesis of our research is that active RAGE initiates NADPH oxidase assembly and subsequent ROS through Src kinase recruitment and activation, which may be attenuated by NRROS degradation of Nox 2. We sought to investigate this central hypothesis by investigating the following specific aims:

Results Pertaining to Specific Aim 1:

Subject Characteristics: *Baseline Characteristics & Metabolic Data*

Baseline characteristics of the study population are presented in **Table 7**. A young, lean healthy control group (LHC) was selected to represent a model of optimal health. Of particular interest, individuals with T2DM were older, maintained a higher BMI and had higher percentage of body fat than LHC (all $P < 0.0001$). Additionally, Individuals with T2DM were more insulin resistant according to fasting (HOMA-IR), glucose-stimulated (2hr-OGTT glucose) and experimental hyperinsulinemia (GDR) measures compared to LHC ($P < 0.0001$).

Table 7. Subject Characteristics

Subject Characteristics	LHC	T2DM
n (M, F)	8 (4,4)	4 (1,3)
Age, years	26.3 $\pm$ 1	59 $\pm$ 6*
Weight, kg	64.3 $\pm$ 14.2	105.1 $\pm$ 5.6*
BMI, kg/m^2	22.3 $\pm$ 2	36.5 $\pm$ 3 *
Body fat, %	24 $\pm$ 1.9	45 $\pm$ 2.6*
MAP	85 $\pm$ 3	98 $\pm$ 7
FFM, kg	49 $\pm$ 3.8	57$\pm$ 4.5
Total Cholesterol, mg/dL	154 $\pm$ 9	147 $\pm$ 6
LDL Cholesterol, mg/dL	86 $\pm$ 12	80 $\pm$ 8
TG, mg/dL	74 $\pm$ 9	78 $\pm$ 15
FPG mg/dL	85 $\pm$ 2	151 $\pm$ 23*
FPI, µU/mL	5.8 $\pm$ 0.7	8.2 $\pm$ 1.6
HOMA-IR, AU	1 $\pm$ 0.3	2 $\pm$ 0.3
HbA1c, %	5.2 $\pm$ 0.1	8.2 $\pm$ 1.2*
2-hr OGTT Glucose, mg/dL	78 $\pm$ 4	268 $\pm$ 66*
OGTT glucose iAUC, mg/dL/2hr	3178 $\pm$ 309	5344 $\pm$ 1658*
OGTT insulin AUC, µU/ml/2hr	3949 $\pm$ 326	2606 $\pm$ 1220
Matsuda Index, AU	8.1 $\pm$ 1.8	4.6 $\pm$ 0.7*
GDR, mg/kg/min	9.1 $\pm$ 0.6	4.1 $\pm$ 0.5*
Clamp insulin, µU/mL	71.8 $\pm$ 7.25	96.3 $\pm$ 7.22*
M/I, mg/kg/min/µU.ml	0.14 $\pm$ 0.01	0.04 $\pm$ 0.02*

TABLE 7. Data represent mean ± SEM; BMI, body mass index; fat%, percentage of body fat; MAP, mean arterial pressure; FFM, fat free mass; TG, triglycerides; FPG, fasting plasma glucose; FPI, fasting plasma insulin; GDR; hyperinsulinemic-euglycemic clamp-derived glucose disposal rate; clamp insulin, steady-state plasma insulin concentrations at end of clamp; HbA1c, hemoglobin A1c; LHC, lean healthy control; OGTT, oral glucose tolerance test. * Significant difference between LHC and T2DM ($P < 0.05$).

The Effects of Whole-Body Insulin Stimulation on Serum N-carboxymethyl-lysine

To determine if serum levels of carboxymethyl -lysine **(CML)** were significantly increased in subjects with type 2 diabetes, and if circulating levels of AGEs are modulated under hyperinsulinemic conditions, we measured serum CML at basal and under insulin-stimulated conditions of the clamp procedure. Under balsa conditions, serum levels between LHC and T2DM groups were similar (LHC 15.8 ± 4.6 vs. T2DM 24.7 ± 6.3 pg/mL). Following 120 minutes of insulin infusion, CML levels remained unaffected (LHC 10.3 ± 2.2 vs. T2DM 21.25 ± 8.8 pg/mL).

Figure 13.
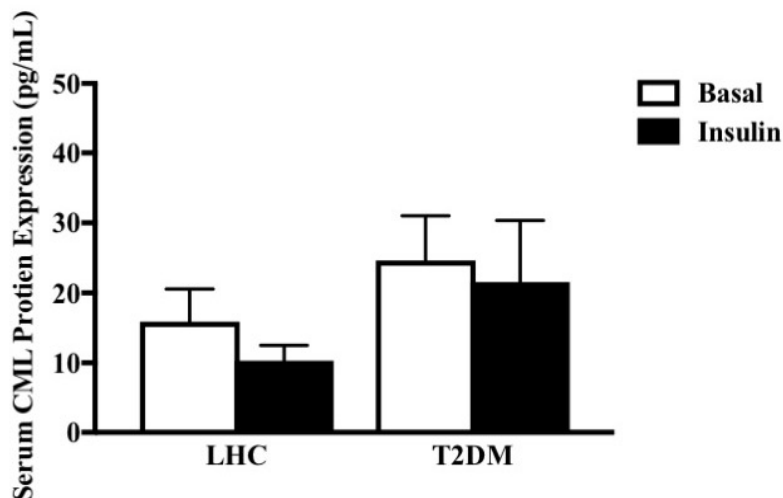
Figure 13. Comparison of serum carboxymethyl-lysine levels between lean healthy controls and individuals with type 2 diabetes during basal and hyperinsulinemic conditions. CML concentrations in LHC (n = 8) and T2DM (n = 4) during basal and insulin stimulated states of the hyperinsulinemic- euglycemic clamp. P < 0.05 was considered significant and data are presented as mean ± SEM.

RAGE Immunofluorescence in LHC and Individuals with T2DM

Immunofluorescence staining in human skeletal muscle revealed the distribution of RAGE in LHC and T2DM skeletal muscle phenotypes. In **Figure 14,** individual myofibers are represented in an axial cross-section of a muscle fiber bundle. Samples obtained from T2DM skeletal muscle exhibit considerably more intense immunofluorescence-mediated signals to lean health counterparts. This cross-sectional data confirms that RAGE is not only present and elevated in diabetic phonotype, but it also localized to

the sarcolemma, where AGE-RAGE interaction can activate important signal transduction pathways and subsequently induces the transcription of mediators for inflammation.

Figure 14.
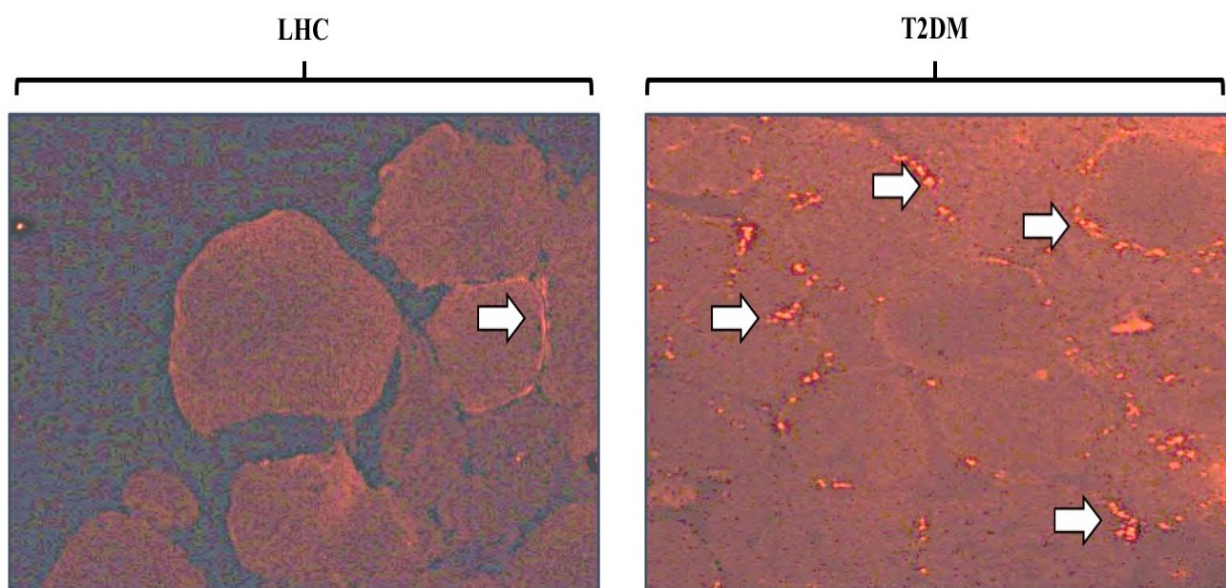
Figure 14. Immunofluorescent staining for cells expressing RAGE in human skeletal muscle. Skeletal muscle punch biopsies were performed this on single subjects used for qualitative validation of RAGE protein expression in lean, healthy controls and individuals with type 2 diabetes. Tissues were obtained from the vastus lateralis muscle during baseline periods of the hyperinsulinemic-euglycemic clamp procedure previously described above. Samples were analyzed by immunofluorescence using anti-RAGE antibodies (Texas Red).

The Effects of Whole-Body Insulin Stimulation on Phospho-IκBα.

At various stages of insulin resistance, NF-κB pathways are increasingly activated in a variety of cell types [562]. Therefore, we next set out to determine if hyperinsulinemia significantly increased NF-κB expression in subjects with type 2 diabetes compared to lean healthy individuals under both basal and insulin-stimulated conditions. Activation of NF-κB pathway transpires when IκBα, a potent inhibitor of NF-κB is degraded by either proteasomal degradation or ubiquitination allowing NF-κB to enter the nucleus and exerts its transcriptional activation on growth factors [562, 563]. It has been reported that upon departure, phosphorylation of IκBα at Ser32 and Ser36 site for it be a target of ubiquitination and degradation [564]. We utilized phospho-IκBα as a surrogate marker for NF-κB activity, for we hypothesize that increases in of NF-κB may have a critical impact on RAGE/Nox 2 mediator upregulation in skeletal muscle. **Figure 15** demonstrates that at baseline, phosphorylation of IκBα levels between LHC and T2DM groups are similar (LHC 0.061 + 0.7800 vs. T2DM 0.049 + 0.0015 AU; P = 0.790). After 120 minutes of insulin infusion, a 62% in phospho-IκBα expression occurred in lean heavy control subjects (*P* = 0.036). Conversely, individuals with T2DM showed a non-significant increase in phospho-IκBα between basal and insulin-stimulated conditions.

The Effects of Whole-Body Insulin Stimulation on RAGE/Nox 2 Mediators

Our next step was to quantify the signaling constituents of the RAGE/Nox 2 axis in human skeletal muscle using an immunoblotting approach. Baseline RAGE protein expression between LHC and T2DM phenotypes were similar. Under clamp conditions, LHC exhibited no deviation form baseline RAGE levels, while hyperinsulinemic conditions increased RAGE expression by 44% in the T2DM group (*P* = 0.197**).** Since increased RAGE expression has been shown to further induce inflammation and oxidative stress in both *in vivo* and *in vitro* studies, we investigated RAGE in available muscle tissue. The negative result of protein

expression discrepancy for this experiment seemed particularly important to the overall interpretation of the results. We, therefore, carried out a post hoc power analysis using G*Power analysis software to determine if whether our experimental design had enough power to detect a significant between our two cohorts. In a subset of LHC (n=8) and T2DM (n=4), total RAGE protein expression was not different between groups at baseline (p>0.05). Given our limited sample size, we performed a post-hoc power calculation (continuous endpoint, two independent samples) with α=0.05 that revealed our data had a 95% power. To inform us about potential future studies we performed a sample size calculation (continuous endpoint, two independent samples) where α=0.05 and ß=0.2 which revealed 322 subjects (161 per group) would be sufficient to detect a significant difference if our sample means remained the same. Likewise, if we conducted the same post-hoc power calculation with insulin stimulated samples, our calculations reveal data only a 95 % power again. In future studies, future studies a sample size of 142 subjects (71 per group) we would be needed to achieve statistical significance **(Figure 16)**.

Likewise, mDia1 protein expression was similar between groups under basal conditions ($P = 0.429$). Following 120 minutes of insulin infusion, mDia1 concentrations between either group remained unchanged. mDia1 protein expression is associated with RAGE activation and signal propagation. We also investigated mDia1 in limited muscle tissue. In a subset of LHC (n=8) and T2DM (n=4), total mDia1 protein expression was not different between groups at baseline (p>0.05). To determine if our insignificant results were a result of being underpowered in sample size, we conducted another post hoc power analyses. Given our limited sample size, we performed another post-hoc power calculation (continuous endpoint, two independent samples) with α=0.05 that revealed our data had a 95% power. This evaluation demonstrated that our present sample size would have to increase to 88 subjects (44 per group) in order to obtain sufficient power to detect a significant difference if our sample means remained the same **(Figure 17)**.

Figure 15.

A.

B.
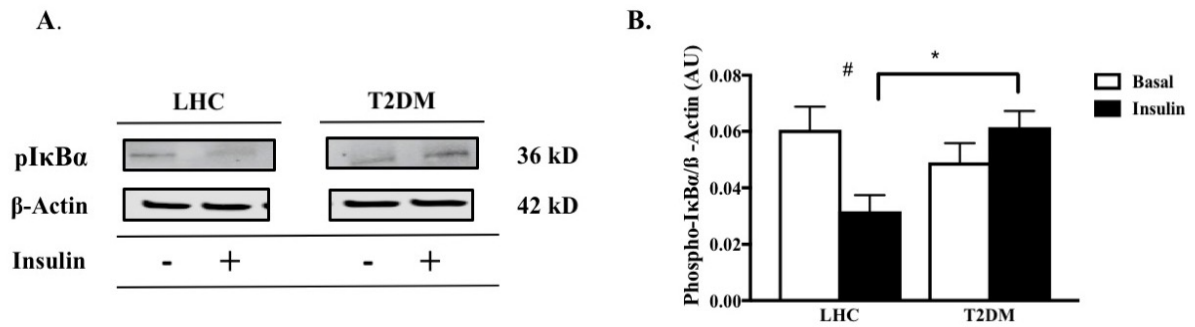
Figure 15. Hyperinsulinemic-euglycemic clamp comparison of IκBα phosphorylation protein expression between lean healthy controls and individuals with type 2 diabetes. (A) Representative Western blot image of phospho-IκBα. (B) phospho-IκBα protein expression in skeletal muscle of LHC and T2DM during basal and insulin-stimulated states of the hyperinsulinemic-euglycemic clamp. LHC, (n=8), T2DM, (n = 4). * indicates a significant effect of group, P < 0.05. # indicates a significant effect of condition (Basal vs. Insulin), P < 0.05. Signal relative intensity was normalized to ß-Actin and results represent the means ± SE for each group. P < 0.05 was considered significant, and data are presented as mean ± SEM.

Figure 16.

A.

B.
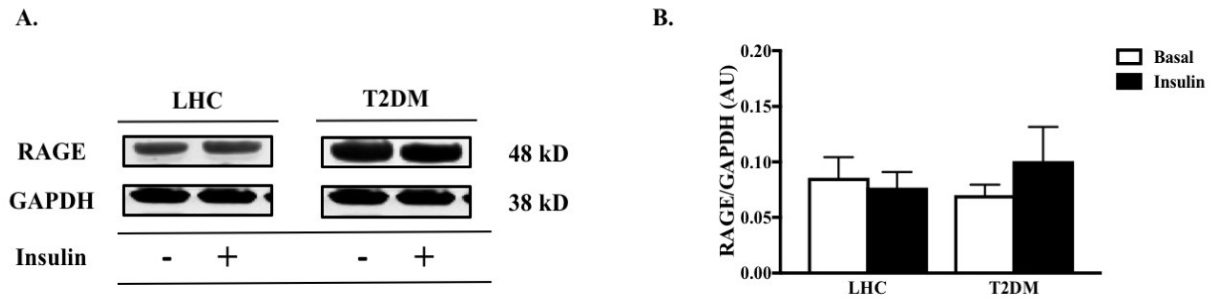
Figure 1. Hyperinsulinemic-euglycemic clamp comparison of RAGE protein expression between lean healthy controls and individuals with type 2 diabetes. (A) Representative Western blot image of RAGE. (B) RAGE protein expression in skeletal muscle of LHC and T2DM during basal and insulin-stimulated states of the hyperinsulinemic-euglycemic clamp. LHC, (n = 8); T2DM, (n = 4). Insulin stimulation in either group did not influence RAGE protein concentration. Signal relative intensity was normalized to GAPDH and results represent the means ± SE for each group. P < 0.05 was considered significant, and data are presented as mean ± SEM.

Figure 17.

A.

B.
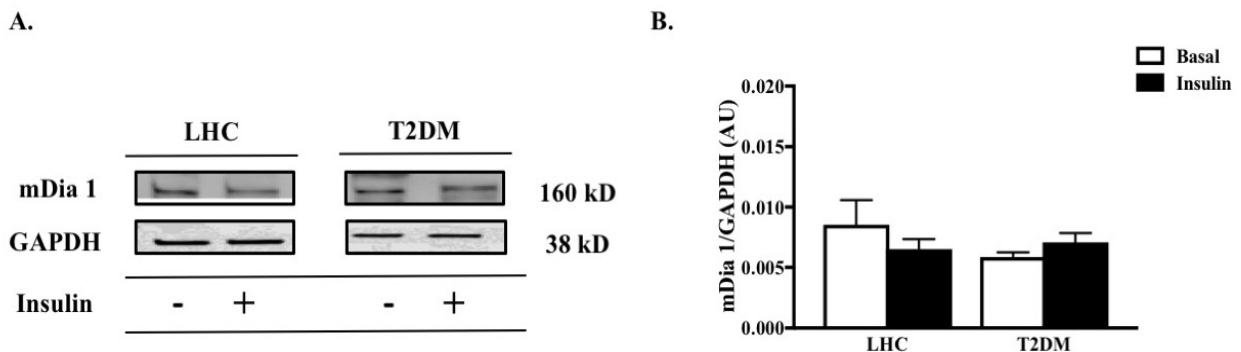
Figure 17. Hyperinsulinemic-euglycemic clamp comparison of mDia 1 protein expression between lean healthy controls and individuals with type 2 diabetes. (A) Representative Western blot image of mDia 1. (B) mDia 1 protein expression in skeletal muscle of LHC and T2DM during basal and insulin-stimulated states of the hyperinsulinemic-euglycemic clamp. LHC, (n = 8); T2DM, (n =4). Signal relative intensity was normalized to GAPDH and results represent the means ± SE for each group. P < 0.05 was considered significant, and data are presented as mean ± SEM.

To further investigate the role of diabetes presence and experimental hyperinsulinemia on the

RAGE/Nox 2 axis, we next measured total and phosphorylated-Src kinase. Individuals with T2DM

exhibited 42% higher total Src kinase protein concentrations than LHC counterparts at baseline ($P =$

0.008**; Figure 18).** Prolonged hyperinsulinemia did elicit a non-significant increase Src, among the LHC

group (LHC, basial to insulin **Δ** 66%, $P = 0.981$). The T2DM group also showed an insignificant

increase in total Src expression ($P = 0.100$).

Active (phosphorylated) Src kinase analysis revealed that LHC subjects exhibited 43% higher pSrc

concentrations at baseline than individuals with T2DM ($P < 0.001$; **Figure 19**).

Figure 18.

A.

B.
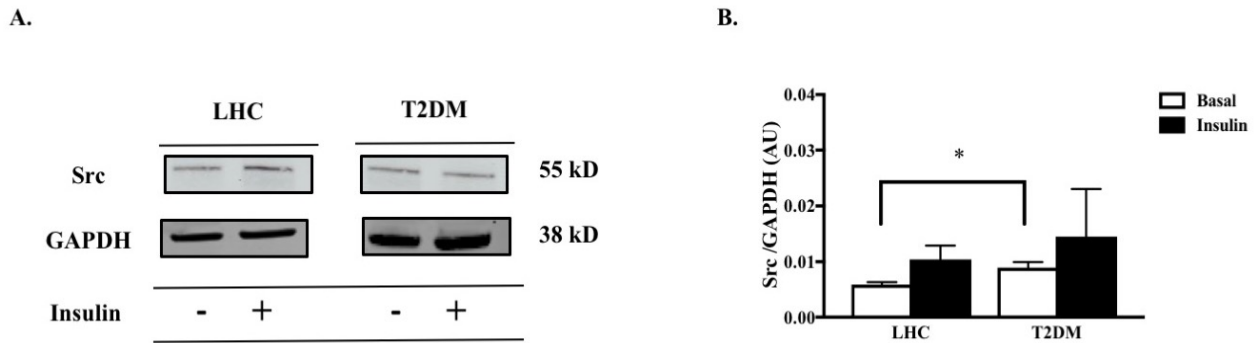
Figure 18. Hyperinsulinemic-euglycemic clamp comparison of Src protein expression between lean healthy controls and individuals with type 2 diabetes. (A) Representative Western blot image of Src. (B) Src protein expression in skeletal muscle of LHC and T2DM during basal and insulin-stimulated states of the hyperinsulinemic-euglycemic clamp. LHC, (n = 8); T2DM, (n = 4). * indicates a significant effect of group, P < 0.05. Signal relative intensity was normalized to GAPDH and results represent the means ± SE for each group. P < 0.05 was considered significant, and data are presented as mean ± SEM.

Figure 19.

A.

B.
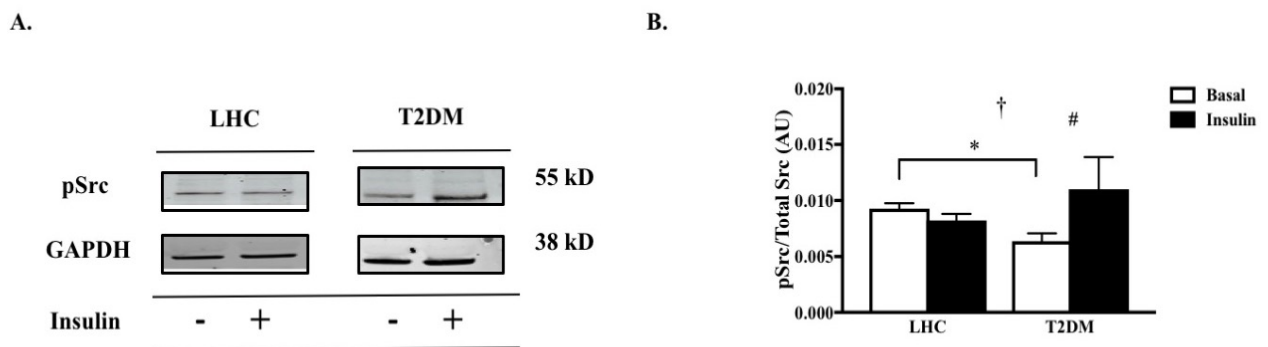
Figure 19. Hyperinsulinemic-euglycemic clamp comparison of pSrc protein expression between lean healthy controls and individuals with type 2 diabetes. (A) Representative Western blot image of pSrc. (B) pSrc protein expression in skeletal muscle of LHC and T2DM during basal and insulin-stimulated states of the hyperinsulinemic-euglycemic clamp. LHC, (n = 8); T2DM, (n = 4). Insulin stimulation significantly influenced pSrc protein concentration in individuals with type 2

diabetes, but not lean healthy controls. * indicates a significant effect of group, P < 0.05. # indicates a significant effect of condition (Basal vs. Insulin), P < 0.05. † indicates a significant interaction. Signal relative intensity was normalized to GAPDH and results represent the means ± SE for each group. P < 0.05 was considered significant, and data are presented as mean ± SEM.

Following insulin stimulation, the LHC group reduces pSrc expression by 11% ($P = 0.362$)

While the T2DM group showed an Δ 83% increase in pSrc expression in the insulin -stimulated condition ($P = 0.013$).

Basal pSrc protein expression was found to be inversely correlated with body fat percentage in all participating subjects ($R = -0.724$, $P = 0.007$), (**Figure 20A)**. Likewise, basal pSrc also inversely correlated with insulin-stimulated glucose disposal rate **(GDR)** in all participating subjects ($R = -0.678$, $P = 0.017$), (**Figure 20B)**.

Figure 20.
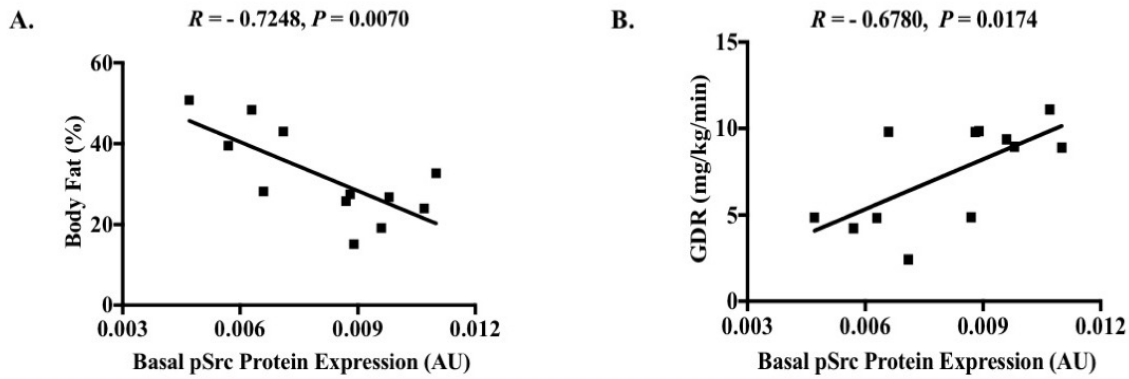
Figure 20. pSrc Protein Correlations. Correlation between basal pSrc protein expression and body fat percentage in the all study subjects (A), (n = 12). Correlation between basal pSrc protein expression and GDR in all study subjects (B), (n = 12).

In order to determine if NADPH oxidase complex constitutes were present and augmentable by hyperinsulinemic conditions, Rac 1, phosphorylated Rac 1, p47^{phox} and membrane bound Nox 2 were probed for in skeletal muscle. **Figure 21.** demonstrates the band intensities for Rac1 in LHC and T2DM. At baseline, T2DM exhibited a 71 % higher Rac1 than LHC ($P = 0.040$). While 120 minutes of insulin infusion had no effect in LHC individuals, the T2DM group showed significantly increased Rac 1 (basial to insulin Δ 24%, $P = 0.030$). Our in vivo work further shows the basal Rac 1 protein levels were moderately correlated with mean arterial pressures **(MAP)** ($R = 0.613, P = 0.044$).

Figure 21.
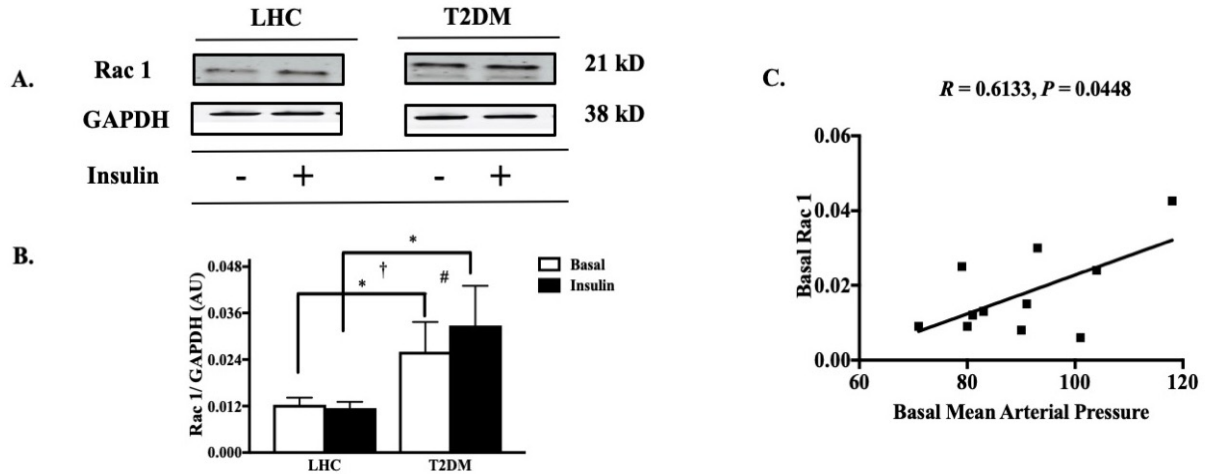
Figure 21. Hyperinsulinemic-euglycemic clamp comparison of Rac 1 protein expression between lean healthy controls and individuals with type 2 diabetes. (A) Representative Western blot image of Rac 1. (B) Rac 1 protein expression in skeletal muscle of LHC and T2DM during basal and insulin-stimulated states of the hyperinsulinemic-euglycemic clamp. LHC, (n = 8); T2DM, (n = 4). * indicates a significant effect of group, P < 0.05. # indicates a significant effect of condition (Basal vs. Insulin), P < 0.05. † indicates a significant interaction. Signal relative intensity was normalized to GAPDH and results represent the means ± SE for each group. P < 0.05 was considered significant, and data are presented as mean ± SEM.

pRac 1 protein expression was similar between both groups at baseline (LHC 0. 0097 ± 0.0004 vs. 0.007 ± 0.0016). Insulin stimulation suppressed pRac 1 expression in LHC but induced a non-significant increase in individuals with T2DM (basal to insulin Δ 225%, *P* = 0.983). Further, activated phospho-Rac 1 showed a modest negative correlation MAP (R = 0.6133, P = 0.0448). **(Figure 22).**

Figure 22.
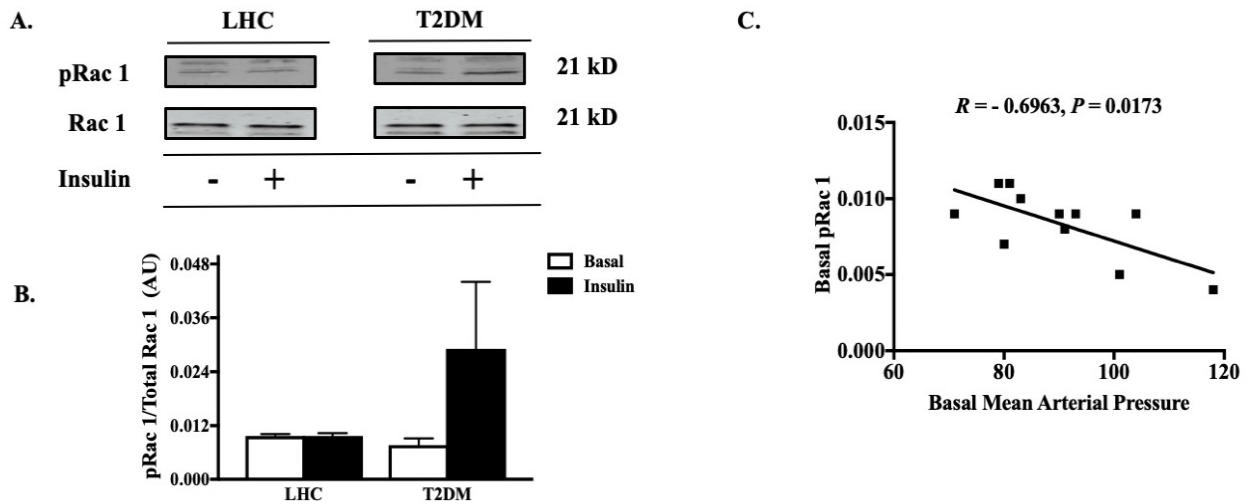
Figure 22. Hyperinsulinemic-euglycemic clamp comparison of pRac 1 protein expression between lean healthy controls and individuals with type 2 diabetes. (A) Representative Western blot image of pRac 1. (B) pRac 1 protein expression in skeletal muscle of LHC and T2DM during basal and insulin-stimulated states of the hyperinsulinemic-euglycemic clamp. LHC, (n = 8); T2DM, (n = 4). Signal relative intensity was normalized to total Rac 1 and results represent the means ± SE for each group. P < 0.05 was considered significant, and data are presented as mean ± SEM.

In the LHC group, insulin-infusion had no effect on skeletal muscle p47[phox] levels (basal 0.0009 ± 0.0004 vs. insulin 0.0010 ± 0.0007). In T2DM subjects, insulin provoked a large, yet non-significant increase p47[phox] protein expression (basal to insulin Δ 95%, $P = 0.082$), (**Figure 23**).

Figure 23.

A.

B.
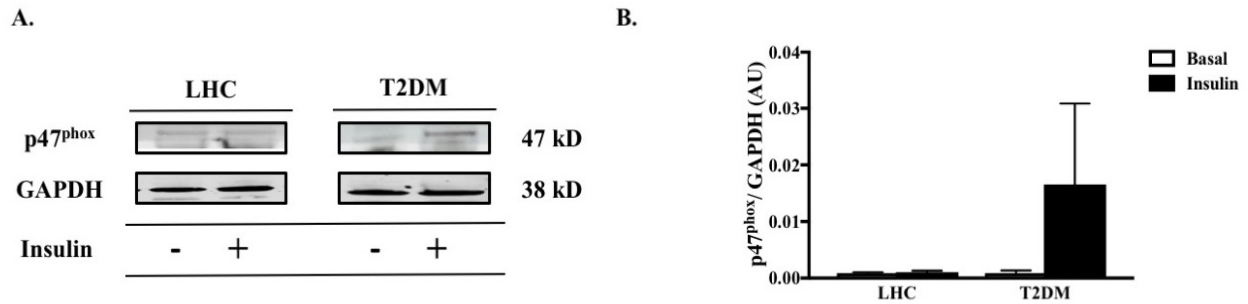
Figure 23. Hyperinsulinemic-euglycemic clamp comparison of p47^{phox} protein expression between lean healthy controls and individuals with type 2 diabetes. (A) Representative Western blot image of p47phox. (B) p47phox protein expression in skeletal muscle of LHC and T2DM during basal and insulin-stimulated states of the hyperinsulinemic-euglycemic clamp. LHC, (n = 8); T2DM, (n = 4). Signal relative intensity was normalized to total GAPDH and results represent the means ± SE for each group. P < 0.05 was considered significant, and data are presented as mean ± SEM.

Total skeletal muscle Nox 2 protein levels proved to be the most abundant protein measured in the within RAGE/Nox 2 axis. Nox 2 remained persistent and unaffected by 120 minute of insulin infusion in both groups (LHC basal 0.4175 ± 0.0228, LHC post clamp 0.4099) vs. (T2DM basal 0.4396 ± 0.0709, T2DM post clamp 0.4988 ± 0.0842) (**Figure 24B**). Additionally, basal Nox 2 protein expression was found to be inversely correlated with fat free mass in all participating subjects ($R = -0.5818$, $P = 0.047$), (**Figure 24C**).

The null result obtained from this experiment was important to the overall interpretation of the results. Since other studies indicated that T2DM subjects expressed greater Nox 2 protein concentrations than LCH we were surprised by our negative findings. Therefore, we carried out a post hoc power analysis to determine if whether our experimental design had enough power to detect a significant between our two populations. Since increased Nox 2 levels has been shown to increase inflammation and oxidative stress *in vivo* and *in vitro studies*, we wanted

to investigate Nox 2 in available muscle tissue. In a subset of LHC (n=8) and T2DM (n=4), total Nox 2 protein expression were not different between groups at baseline (*p*>0.05). Given our limited sample size, we performed a post-hoc power calculation (continuous endpoint, two independent samples) with α=0.05 that revealed our data had a 95% power. To inform us about potential future studies we performed a sample size calculation (continuous endpoint, two independent samples) where α=0.05 and ß=0.2 which revealed 385 subjects (179 per group) would be sufficient to detect a significant difference if our sample means remained the same.

Figure 24.
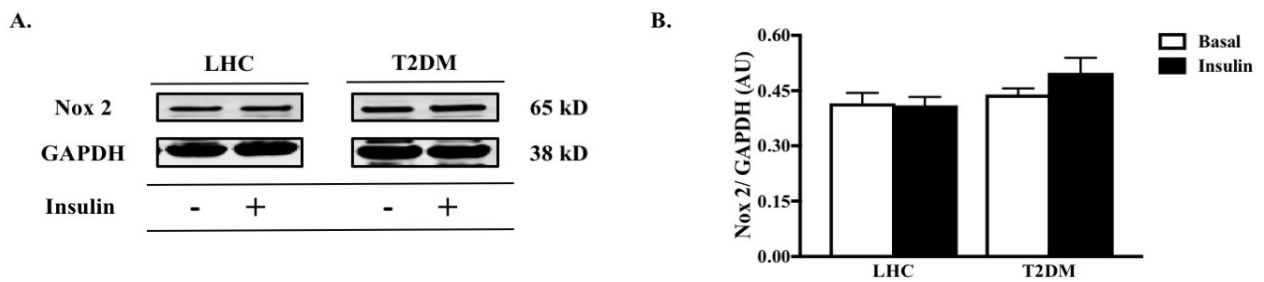
Figure 24. Hyperinsulinemic-euglycemic clamp comparison of Nox 2 protein expression between lean healthy controls and individuals with type 2 diabetes. (A) Representative Western blot image of Nox 2. (B) Nox 2 protein expression in skeletal muscle of LHC and T2DM during basal and insulin-stimulated states of the hyperinsulinemic-euglycemic clamp. LHC, (n = 8); T2DM, (n = 4). Signal relative intensity was normalized to total GAPDH and results represent the means ± SE for each group. P < 0.05 was considered significant, and data are presented as mean ± SEM.

Results Pertaining to Specific Aim 2:

It has been demonstrated in non-skeletal muscle tissues that glycated albumin **(GLY-ALB)** induces the activation and assembly of NADPH oxidase [330, 593]. However, the mechanisms responsible for this signaling cascade are not well understood, nor have they been explored in human skeletal muscle. We believe that RAGE-mediated NADPH oxidase activation is facilitated primarily by Src kinase. Therefore, in an effort to better understand these mechanisms, we conducted the following cell culture experiments to determine if GLY-ALB-induced, RAGE mediated Src phosphorylation occurs in HSkMCs.

Dose Response Effects of Acute (2 hour) Glycated Albumin on RAGE/Nox 2 axis HSkMCs

Summary:

To recreate an environment similar to the T2DM condition with respect to circulating AGEs, HSkMCs were stimulated with AGEs in dose and time increments. Additionally, we utilized these experiments to probe for other potential RAGE/Nox 2 axis mediators consisting of p47^{phox}, Ras-related G-proteins Rac1 and phosphorylated Rac 1. These targets have been reported as significant factors in NADPH oxidase assembly in other tissues, but no data exists on the involvement of Rac 1, pRac 1 and p47^{phox} in skeletal muscle.

GLY-ALB Treatment Has no Effect on RAGE & mDia 1 Protein Expression

We first set out to verify that RAGE was present in culture cells and examine if its protein expression was modulated by GLY-ALB stimulation. No significant differences were observed in RAGE protein expression between the control and experimental groups when stimulated with 100 or 200 μg/mL of ALB, or GLY-ALB. Interestingly, at the 400 μg/mL, GLY-ALB treated cells exhibited 1.9-fold decline

in expression compared to ALB treated cells (400 µg/mL ALB 0.0751 ± 0.1401 vs. 400 µg/mL GLY-ALB 0.0390 ± 0.1200 $P = 0.0080$). Further, a significant within-group change was identified in GLY-ALB treated cells between 100 and 400 µg/mL concentrations. Again, stimulating cells with 400 µg/mL of GLY-ALB resulted in a 2-fold reduction on RAGE expression (100 µg/mL GLY-ALB 0.0733 ± 0.0040 vs. 400 µg/mL GLY-ALB 0.03921 ± 0.1204, $P = 0.0320$), (**Figure 25**). This result may suggest that elevated concentrations of GLY-ALB induce cytotoxicity in HSkMCs.

Having successfully identified mDia 1 protein expression in our in vivo samples, we next wanted to verify the presences of mDia 1 in an experimental model and determine if GLY-ALB stimulation modified its protein expression in a dose dependent manner. mDia 1 has previously been identified in several animal studies as well as various skeletal muscle cell lines, but an in-depth review of the literature revels that mDia 1 has not been explored in HSkMCs lines [594-596]. **Figure 27** reveals that mDia 1 is present in HSkMCs, however GLY-ALB stimulation has a null effect on its protein expression.

Figure 25.

A.

B.
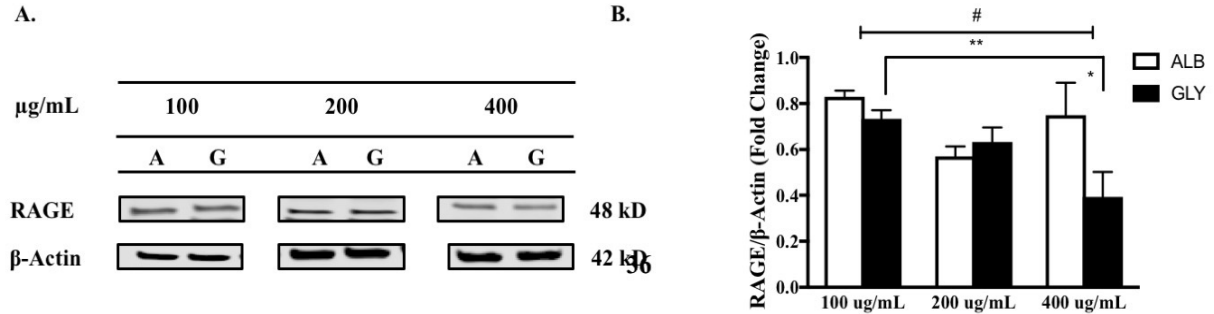
Figure 25. Dose Effects of Glycated Albumin on RAGE in HSkMCs (2 hour).
HSkMCs were stimulated with 100, 200 and 400 µg/mL of native (n = 3) or glycated albumin (n = 3) for 2 hours. 10 µg of protein was loaded for western blot analysis of (A) RAGE. (B) Representative images of RAGE protein expression. * indicates a significance effect of groups, $P < 0.05$. # indicates significance effect of dose, $P < 0.05$. ## denotes significance effect within groups. β-Actin was used as a loading control and values are represented as mean $\pm$ SEM.

Figure 26.

A.

B.
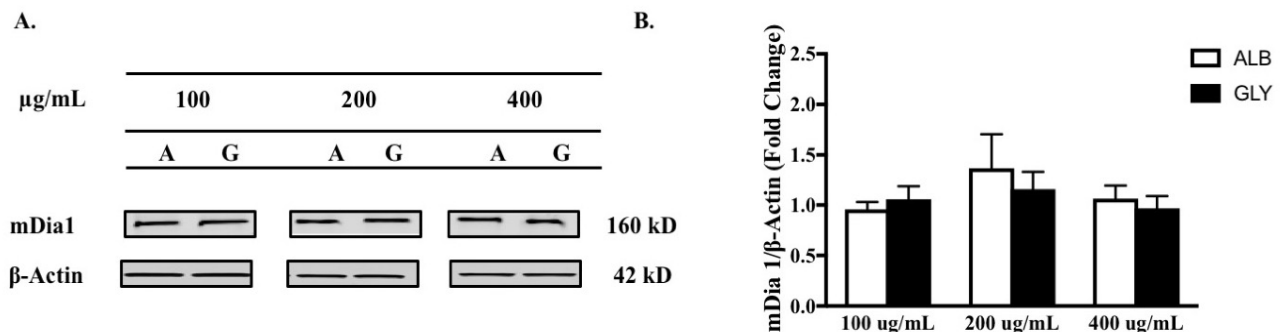
Figure 26. - Dose Effects of Glycated Albumin on mDia1 in HSkMCs (2 hour).
HSkMCs were stimulated with 100, 200 and 400 µg/mL of native (n = 3) or glycated albumin (n = 3) for 2 hours. 10 µg of protein was loaded for western blot analysis of (A) mDia1. (B) Representative images of mDia1. β-Actin was used as a loading control and values are represented as mean $\pm$ SEM.

GLY-ALB Treatment Augments pSrc and Reduces Total Src protein Expression in A Dose Dependent Manner

The non-receptor tyrosine kinase, Src, regulates and maintains a vast array of cellular activities under basal conditions, while constitutively active or unregulated of Src activation is involved in pathogenic signaling. While Src's role in ROS production remains unclear, we hypothesized that Src becomes activated via RAGE signaling and this event propagates the RAGE message to downstream targets, resulting in NADPH oxidase assembly and subsequent ROS production.

pSrc expression was significantly enhanced by GLY-ALB stimulation at 100 and 200 µg/mL increments. At 100 µg/mL GLY-ALB treated cells demonstrated a 1.6-fold increase in proteins expression compared to control cells (100 µg/mL GLY-ALB 0.6001 $\pm$ 0.1200. vs. 100 µg/mL GLY-ALB 0.9703 $\pm$ 0.0302, P =0.001) (**Figure 27**). Likewise, doubling the dose to 200 µg/mL of GLY-ALB also resulted in 1.7-fold increase in pSrc expression (100 µg/mL GLY-ALB 0.7007 $\pm$ 0.0601 vs. 100 µg/mL GLY-ALB 1.2001 $\pm$ 0.120, P = 0.0040). At the maximum dose, GLY-ALB treated cells were significantly reduced compared to other treatment groups. Thus, 400 µg/mL of GLY-ALB proves to be a cytotoxic dose that significantly reduces pSrc expression in HSkMCs.

Total Src kinase expression demonstrated no changes between control and experimental cells at 100 or 200 µg/mL doses. Surprisingly, HSkMCs treated in 400 µg/mL of GLY-ALB almost completely deleted Src kinase expression. These changes in Src levels induced significant within changes among the treatment group (**Figure 28**). Currently, mechanisms of action for AGE-induced Src deletion is unidentified, nor reported. This irregularity will require further investigation.

Figure 27.
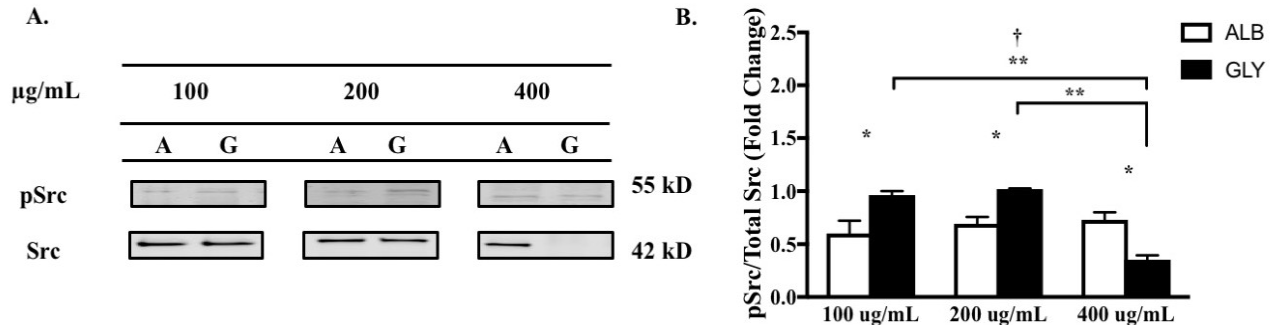
Figure 27. Dose Effects of Glycated Albumin on pSrc in HSkMCs (2 hour).
HSkMCs were stimulated with 100, 200 and 400 µg/mL of native (n = 3) or glycated albumin (n = 3) for 2 hours. 10 µg of protein was loaded for western blot analysis of (A) pSrc. (B) Representative images of pSrc. * indicates a significance effect of groups, P < 0.05. † indicates a significant interaction and ** denotes significance effect within groups. Total Src was used as a loading control and values are represented as mean + SEM.

Figure 28.
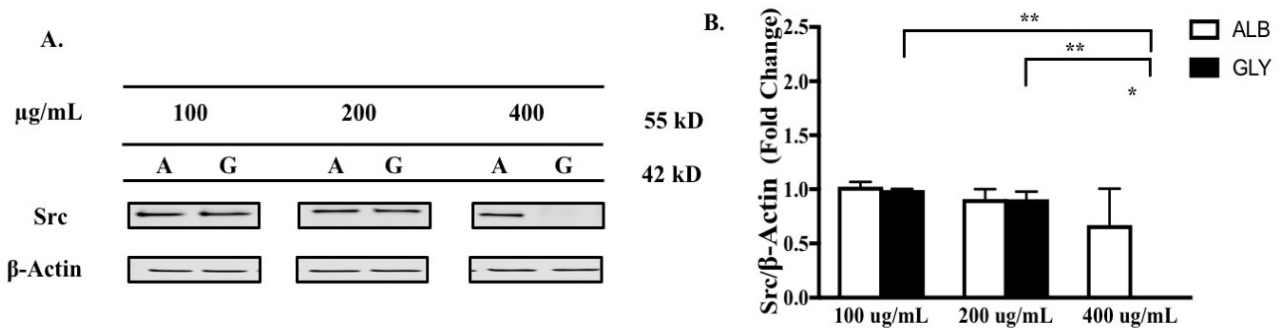
Figure 28. Dose Effects of Glycated Albumin on Src in HSkMCs (2 hour).

HSkMCs were stimulated with 100, 200 and 400 µg/mL of native (n = 3) or glycated albumin (n = 3) for 2 hours. 10 µg of protein was loaded for western blot analysis of (A) Src. (B) Representative images of Src * indicates a significance effect of groups, $P < 0.05$. † indicates a significant interaction and ** denotes significance effect within groups. β-Actin was used as a loading control and values are represented as mean + SEM.

Rage/Nox 2 Axis signaling intermediates, p47^{phox}, Rac 1 and pRac 1 protein expression Are Unaffected by GLY-ALB Treatment

While the assembly of phagocytic NADPH oxidase requires the phosphorylation of multiple serine residues on p47^{phox}, the role of Src- medicated tyrosine phosphorylation of p47^{phox} and consequent NADPH oxidase assembly is uncertain in HSkMCs. It has been determined in previous studies that Nox 2 assembly is provoked by the binding of the cytosolic subunit p47phox, which transitions from the cytoplasm to the cell membrane once phosphorylated. Given our experimental model, we then hypothesized that active -Src may stimulate the phosphorylation of p47^{phox}. Therefore, we next examined if GLY-ALB impacted p47^{phox} protein expression in a dose dependent manner. This experiment concluded in a null effect, as Skeletal muscle p47^{phox} expression was unchanged by GLY-ALB treatment by dose increments **(Figure 29).**

Figure 29
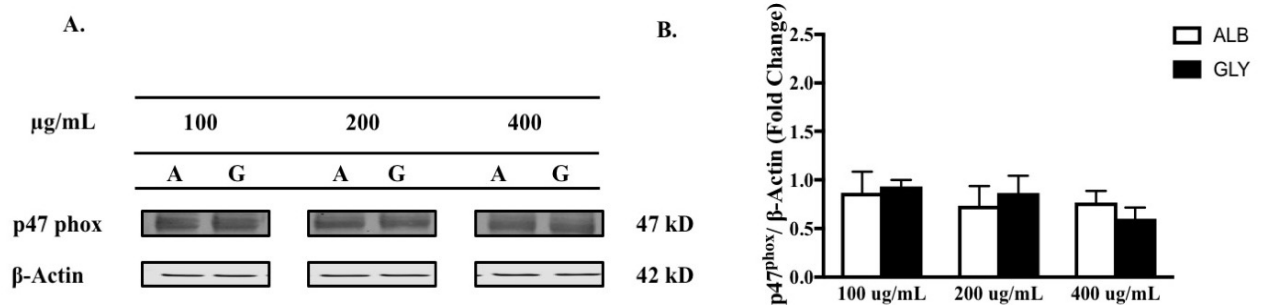
Figure 29. Dose Effects of Glycated Albumin on p47^{phox} in HSkMCs (2 hour).
HSkMCs were stimulated with 100, 200 and 400 µg/mL of native (n = 3) or glycated albumin (n = 3) for 2 hours. 10 µg of protein was loaded for western blot analysis of (A) p47^{phox}. (B) Representative images of p47^{phox}. β-Actin was used as a loading control and values are represented as mean $\pm$ SEM.

Next, we wanted to evaluate both total and active-Rac1 protein expression to establish if increasing doses of GLU-ALB augment Rac 1 protein expression in HSkMCs. In diverse tissues, Rho-like small GTPases Rac1 is linked to NADPH oxidase assembly and activation. Since our assessment of p47phox produced a null effect, we considered the possibility that Rac 1 may be an alternative NADPH oxidase activator. Rac 1 phosphorylation 1 is part of signaling cascades that are reported to be as a critical step in NADPH oxidase assembly. Therefore, we first measured pRac 1 protein expression in a dose-dependent manner. No dose-dependent modifications were identified in pRac 1 protein expression between control and treatments cells **(Figure 30)**. This data also indicates that Rac 1 is activated during GLY-ALB stimulation at dose increments, although no significant findings were identified between control and

treatment groups. However, when investigating total Rac protein expression, a 51% decrease was

identified within the GLY-ALB group from 100 to 400 µg/mL increments (100 µg/mL GLY-ALB

0.9500 + 0.1410 vs. 400 µg/mL GLY-ALB 0.4440 + 0.3512, P = 0.0502) **(Figure 32)**. In line with our

previous findings, declining levels of Rac protein expression may be a consequence of cell toxicity

mediated by high doses of GLY-ALB.

Figure 30.
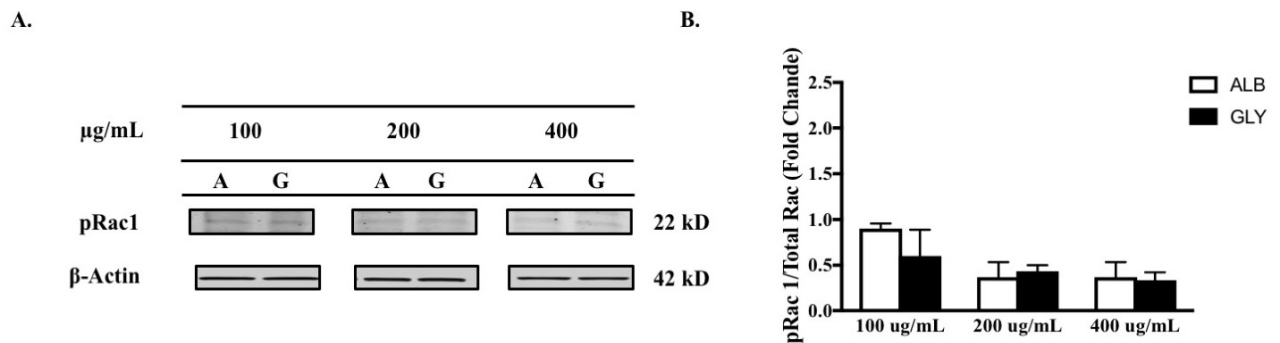
Figure 30. Dose Effects of Glycated Albumin on pRac 1 in HSkMCs (2 hour).
HSkMCs were stimulated with 100, 200 and 400 µg/mL of native (n = 3) or glycated albumin (n = 3) for
2 hours. 10 µg of protein was loaded for western blot analysis of (A) Rac 1. (B) Representative images
of Rac 1. β-Actin was used as a loading control and values are represented as mean + SEM.

Figure 31.

A.

μg/mL   100   200   400
         A   G   A   G   A   G

Rac 1   21 kD

β-Actin   42 kD

B.
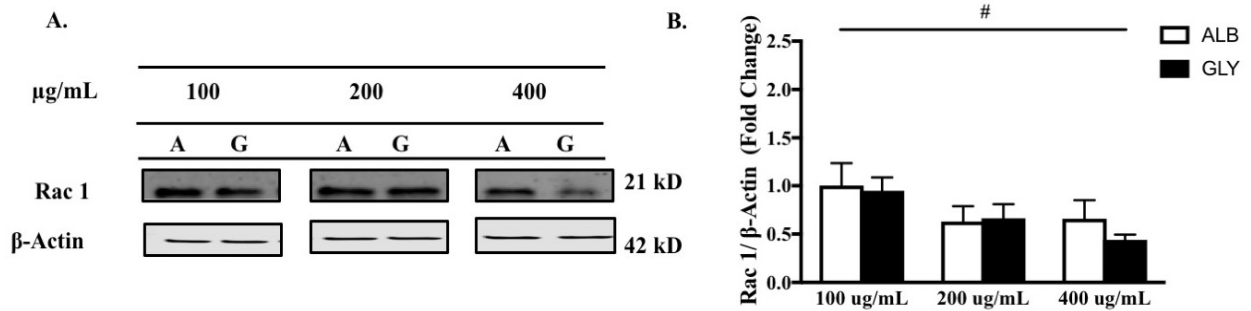
Figure 31. Dose Effects of Glycated Albumin on Rac 1 in HSkMCs (2 hour).
HSkMCs were stimulated with 100, 200 and 400 μg/mL of native (n = 3) or glycated albumin (n = 3) for 2 hours. 10 μg of protein was loaded for western blot analysis of (A) Rac 1. (B) Representative images of Rac 1. # indicates significance effect of dose, $P < 0.05$ β-Actin was used as a loading control and values are represented as mean + SEM.

GLY-ALB Treatment Has No Effect on NADPH oxidase subunit, Nox 2 protein expression

Nox2 is identified as a prominent source of O_2^- generation in diverse cell types and it has emerged as an influential source of ROS generation in mitogenic signaling. Our in *vivo*, and preliminary work showed that Nox 2 was abundant and the principal Nox subunit in skeletal muscle. Our next experiment was designed to establish that Nox 2 was expressed in HSkMCs and to assess if various concertation of GLY-ALB modulated Nox 2 protein expression. Contrary to our original hypothesis, no significant changes were detected Nox 2 protein expression GLY-ALB (**Figure 32).**

Figure 32.

A.

B.
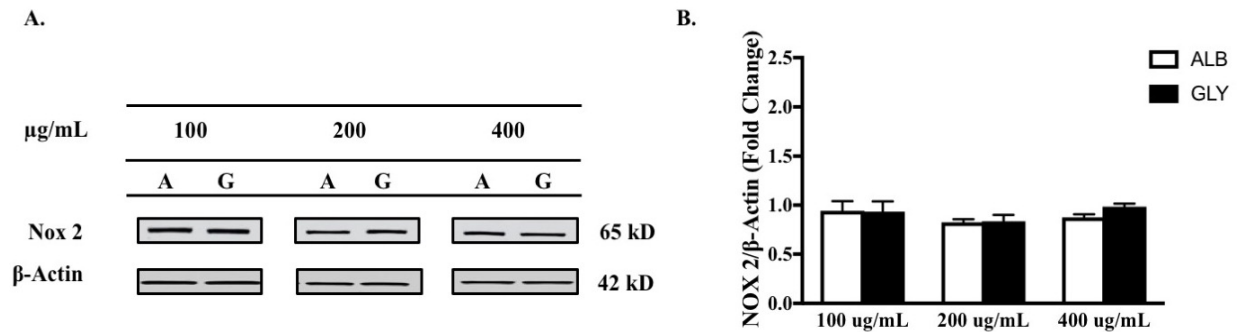
Figure 32. Dose Effects of Glycated Albumin on Nox 2 in HSkMCs (2 hour).
HSkMCs were stimulated with 100, 200 and 400 μg/mL of native (n = 3) or glycated albumin (n = 3) for 2 hours. 10 μg of protein was loaded for western blot analysis of (A) Nox 2. (B) Representative images of Nox 2. β-Actin was used as a loading control and values are represented as mean ± SEM

Effect of GLY-ALB treatment on RAGE/NADPH Oxidase Axis signaling Intermediate protein-to-protein Associations

We intended to further validate our hypothesis by performing immunoprecipitation experiments to demonstrate physical association between signaling axis intermediates. Importantly, despite no change in protein abundance in our previous set of experiences, we did identify several critical associations. RAGE has been identified as a receptor that is vacant of intrinsic tyrosine kinase activity. Thus, we hypothesized the possibility that Src kinase, a non-tyrosine kinase, may become stimulated by RAGE-ligand interaction and aid in propagating RAGE-induced downstream signaling. We further postulated that mDia 1, and p47^{phox} associate with active Src, assembling an intracellular axis that may activate Nox 2 assembly and subsequent ROS production. To test these ideas, we employed our previously

confirmed experimental model (see above) and stimulated HSkMCs with 100 μg/ml of GLY-ALB for 2 hours.

To begin, 30 and 50 μg of cell lysate was used to IP for mDia 1. Following the initial IP experiments, we next wanted to immunoblot the purified precipitates to establish that mDi1 was present at these concentrations of protein **(Figure 33A)**. Having successfully detected mDia 1 in HSkMCs, we next set out to establish if RAGE and mDia 1 were associated upon 100 μg/ml of serum depleted GLY-ALB for 2 hours. RAGE and mDia 1 were associated when using both 30 or 50 μg of cell lysate. RAGE precipitates were then analyzed by immunoblotting with a monoclonal mDia 1 antibody. Our initial experiments were unsuccessful, and no bands were detectable at anticipated molecular weight. These null findings resulted in further optimization efforts. We conducted two more trials increasing cell lysate concentrations to 60, 80, 100, and 150 μg, respectively. Results confirmed that 100 and 150 μg of cell lysate promoted successful expression of mDia 1 at 160 kD **(Figure 33B)**.

Having established that mDia 1 was associated with RAGE under GLY-ALB stimulation, we next set out to determine if pSrc associated with mDia 1 under GLY-ALB treatment. We next tested the hypotheses that RAGE-ligand interaction provokes mDia 1 and pSrc association. We conducted a series of cell lysate titrations once more to ensure the detection of pSrc under experimental conditions. 30, 60, 90 and 120 μg of cell lysate were immunoprecipitated with mDia 1 monoclonal antibody. mDia 1 precipitates were then examined by immunoblotting with a monoclonal pSrc antibody at autophosphorylation site, Tyr 416. While the lower lysate concentrations resulted in null findings, the use of 120 μg of cell lysate indicated that pSrc and mDia 1 were associate after 120 minutes of GLY-ALB stimulation **(Figure 33C).**

Lastly, reports indicate that the initiation of NADPH oxidase assembly requires extensive serine phosphorylation of regulatory subunit, p47^{phox}. While numerous reports pinpoint serine-379 as the molecular switch in p47^{phox} activation, the role of tyrosine phosphorylation on p47^{phox} is far less understood and requires further investigation. Since Src kinase specifically targets tyrosine residues, we set out to establish if RAGE- induced Src activation can result in phosphorylation of p47^{phox} tyrosine residues. To begin, 30 and 40 μg of cell lysate was used to IP for p47^{phox} using a monoclonal antibody. Following the preliminary IP experiments, we then immunoblot the purified p47^{phox} precipitates with a monoclonal antibody that recognizes phosphotyrosine containing proteins. Tyrosine phosphorylation of p47^{phox} was undetectable and requires further invitation **(Figure 33D).**

Figure 33.
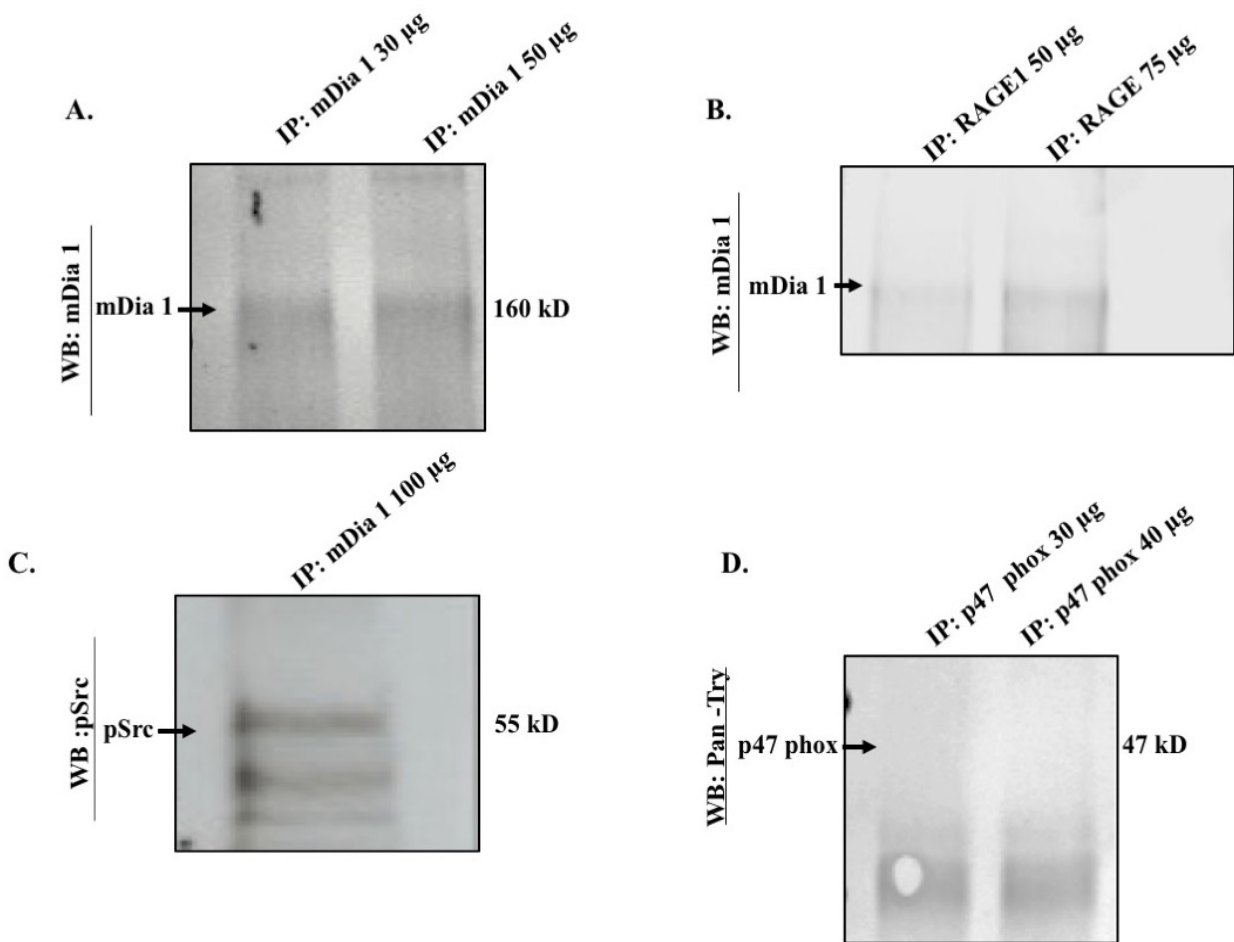
Figure 33. Immunoprecipitation experiments.
Immunoprecipitation was used to determine protein interactions within the proposed RAGE/Nox 2 Axis. HSkMCs were stimulated with 100 µg/mL of glycated albumin for 120 minutes. mDia1, RAGE & p47phox were immunoprecipitated from HSkMCs. Immunoprecipitated products were then subjected to Western blot analysis. (A) To determine if mDia 1 was expressed on HSkMCs, a preliminary experiment was conducted to IP for mDia 1 and Western blot analysis of mDia 1. (B) To determine if RAGE and mDia 1 were associated during glycated albumin stimulation we conducted an IP for RAGE and Western blot analysis of mDia 1. (C) To determine if mDia 1 and pSrc associate during glycated albumin stimulation we conducted an IP for mDia 1 and Western blot analysis pSrc. (D) To determine if glycated albumin treatment activated p47phox via tyrosine phosphorylation, we conducted an IP for p47phox and Western blot analysis using a Pan –tyrosine antibody.

Time course Effects of Chronic (4 & 8 hour) GLY-ALB treatment Augments Key RAGE/NADPH Oxidase Axis Proteins HSkMCs.

Summary:

Given we observed null effects in signaling intermediate protein expression with dose-dependent Gly-ALB treatment conditions, we next sought to examine a longer time course of treatment that likely better represents chronic AGE stimulation in vivo. These series of experiments employed 100 µg/mL treatment as dose-responses did not provide any additional effect of greater stimulus from above experiments and the potential cytotoxic effect of high age dose. Further, literature values of AGE treatment in cell culture are typically 100 ug/mL. HSkMCs were stimulated with 100 µg/mL of native or glycated albumin for 4 and 8 hours. 10 µg of protein was loaded for western blot analysis.

Chronic GLY-ABL Stimulation Augments Membrane Associated Proteins RAGE and mDia 1.

We first probed for membrane associated proteins RAGE and mDia 1. At baseline measurements, RAGE protein levels were similar between control and experimental HSkMCs. After 4 hours of GLY-ALB stimulation, cells treated with GLY-ALB exhibited 1.5-fold higher RAGE expression, compared to control cells that were incubated in native albumin (ALB 1.1101 ± 0.0250 vs. GLY- ALB 1.7320 ± 0.0641, $P = 0.002$) (**Figure 34**). RAGE augmentation was no longer evident at 8 hours of AGEs stimulation, as not significant changes were established. Consistent with the observations identified in RAGE the previous experiment, mDia 1 protein expression also exhibited a 1.79-fold increase in protein expression compared to control cells (ALB 1.1031 ± 0.0190 vs. GLY- ALB 1.9722 ± 0.172, $P = 0.001$) (**Figure 35).** These results may suggest that GLY-ALB provokes a parallel transcriptional mechanism that upregulates RAGE and mDia 1 protein over the course of 4-hours.

Figure 34.
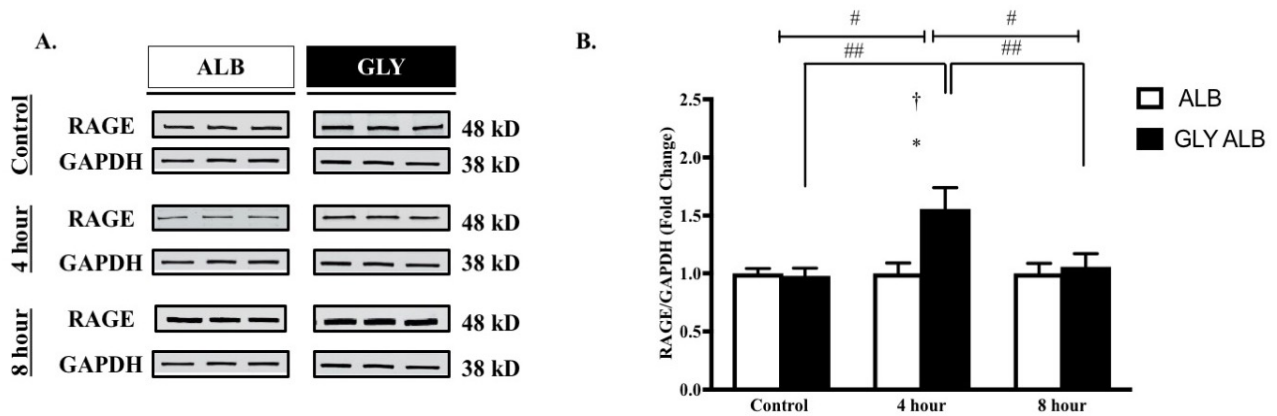
Figure 34. Time Dependent Effects of Chronic Glycated Albumin Stimulation on RAGE Expression. Time effects of native and glycated albumin on RAGE protein expression. HSkMCs were stimulated with 100 µg/mL of native (n = 3) or glycated albumin (n = 3) for control, 4 and 8 hours. (A) 10 µg of protein was loaded for western blot analysis of RAGE. (B) Representative images of independent experiments. * indicates significance effect of group, $P < 0.05$. # indicates significance effect of time, $P < 0.05$. † indicates a significant interaction and ## denotes significance effect within group. GAPDH was used as a loading control and values are represented as mean $\pm$ SEM.

Figure 35.
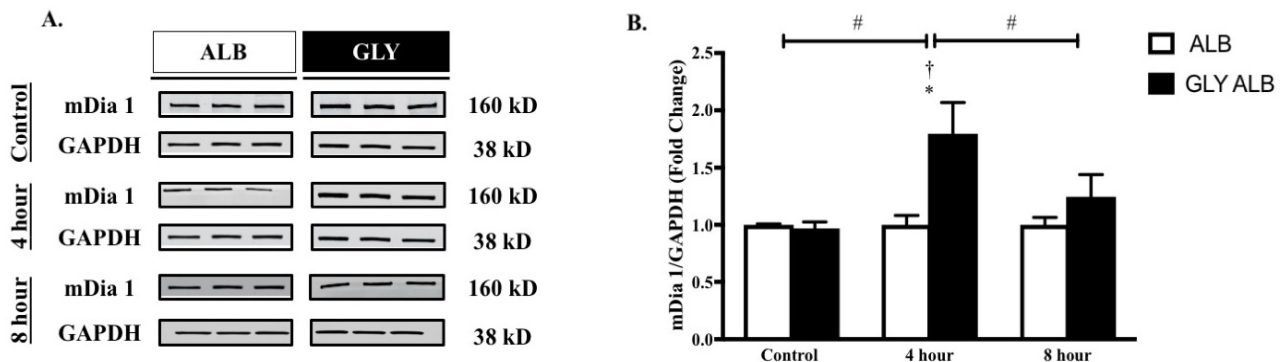
Figure 35. Time Dependent Effects of Chronic Glycated Albumin Stimulation on mDia 1 Expression. Time effects of native and glycated albumin on mDia 1 protein expression. HSkMCs were stimulated with 100 µg/mL of native (n = 3) or glycated albumin (n = 3) for control, 4 and 8 hours. (A) 10 µg of protein was loaded for western blot analysis of mDia 1. (B) Representative images of

independent experiments. * indicates significance effect of group, P < 0.05. # indicates significance effect of time, P < 0.05. † indicates a significant interaction and ## denotes significance effect within group. GAPDH was used as a loading control and values are represented as mean + SEM.

Chronic GLY-ABL Stimulation Induces Alterations in Total Src & Phosphorylated Src.

Figure 36 demonstrates that pSrc was significantly increased by RAGE ligand GLY- ALB at both 4 and 8-hour time points. Immunoblot results demonstrate that 4 hours of GLY-ALB stimulation significantly increased pSrc 1.37-fold increased form control cells (ALB 0.8870 $\pm$ 0.0491 vs. GLY- ALB 1.2030 $\pm$ 0.2311, $P = 0.053$). Likewise, 8 hours of GLY-ALB stimulation also induced a 1.44-fold increase in Src phosphorylation compared to control cells treated with ALB (ALB 1.0074 $\pm$ 0.0690 vs. GLY- ALB 1.4501 $\pm$ 0.0047, $P = 0.016$). Interestingly, increase in pSrc activation may have been driven by decreased total Src expression. Total Src kinase showed no significant alterations in expression between control and treatment groups. However, this data shows significant oscillation in Src protein levels. After 4 hours of GLY-ALB stimulation, Src protein expression showed a 2.5-fold decline compared to baseline samples (0 hr. GLY-ALB 1.0523 $\pm$ 0.1110 vs. 4 hr. GLY-ALB 0.4142 $\pm$ 0.0360, $P = 0.019$). Interestingly, after 8 hours of GLY-AGE stimulation, total Src protein increased nearly 4-fold from the 4-hour samples (4 hr. GLY-ALB 0.4147 $\pm$ 0.0364 vs. 8 hr. GLY-ALB 1.6301 $\pm$ 0.3121, $P < 0.001$) (**Figure 37**).

Figure 36.
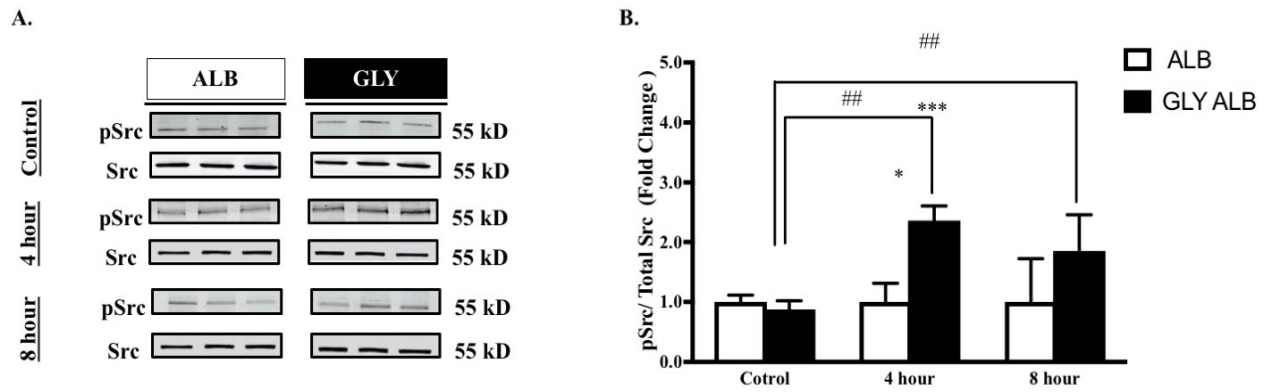
Figure 36. Time Dependent Effects of Chronic Glycated Albumin Stimulation on pSrc phosphorylation Expression. Time effects of native and glycated albumin on pSrc protein expression. HSkMCs were stimulated with 100 µg/mL of native (n = 3) or glycated albumin (n = 3) for control, 4 and 8 hours. (A) 10 µg of protein was loaded for western blot analysis of pSrc. (B) Representative images of independent experiments. * indicates significance effect of group, $P < 0.05$. # indicates significance effect of time, $P < 0.05$. ## denotes significance effect within group. Total Src was used as a loading control for pSrc quantification and values are represented as mean $\pm$ SEM.

Figure 37.
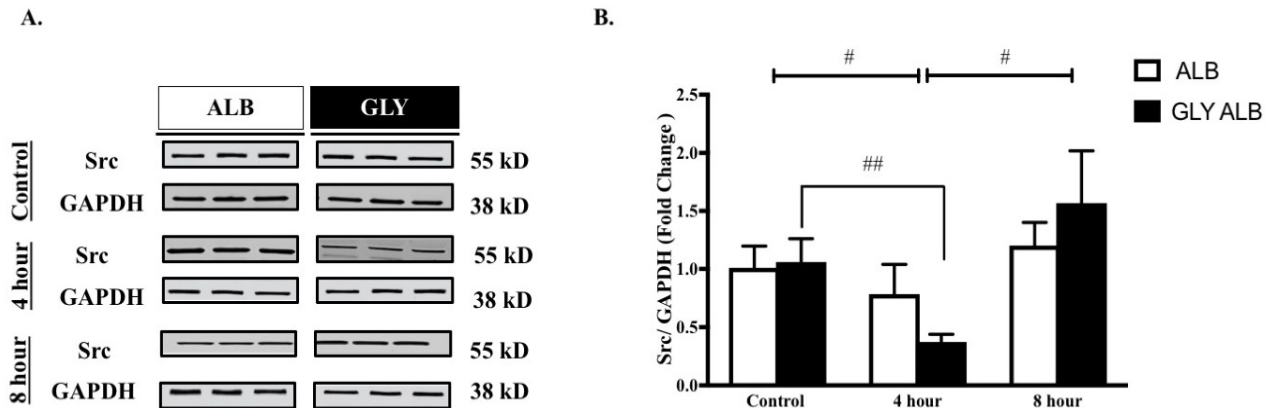
Figure 37. Time Dependent Effects of Chronic Glycated Albumin Stimulation on Src Expression. Time effects of native and glycated albumin on Src protein expression. HSkMCs were stimulated with 100 μg/mL of native (n = 3) or glycated albumin (n = 3) for control, 4 and 8 hours. (A) 10 μg of protein was loaded for western blot analysis of Src. (B) Representative images of independent experiments. # indicates significance effect of time, P < 0.05. ## denotes significance effect within group. GAPDH was used as a loading control and values are represented as mean + SEM.

Chronic GLY-ABL Stimulation Augments ROS Producing Protein Nox 2

Nox 2 is a critical marker for NADPH oxidase expression. At 4 hours of GLY-ALB stimulation, enhanced Nox 2 expression was observed in the experiment cell culture, but not in control cells. GLY-ALB treated cells displayed a significant 1.4-fold increase in protein expression when compared to the 4-hour control group (4 hr. ALB 1.1402 $\pm$ 0.0990 vs. 4 hr. GLY- ALB 1.5530 $\pm$ 0.134, P = 0.021) (**Figure 38**).

Figure 38.
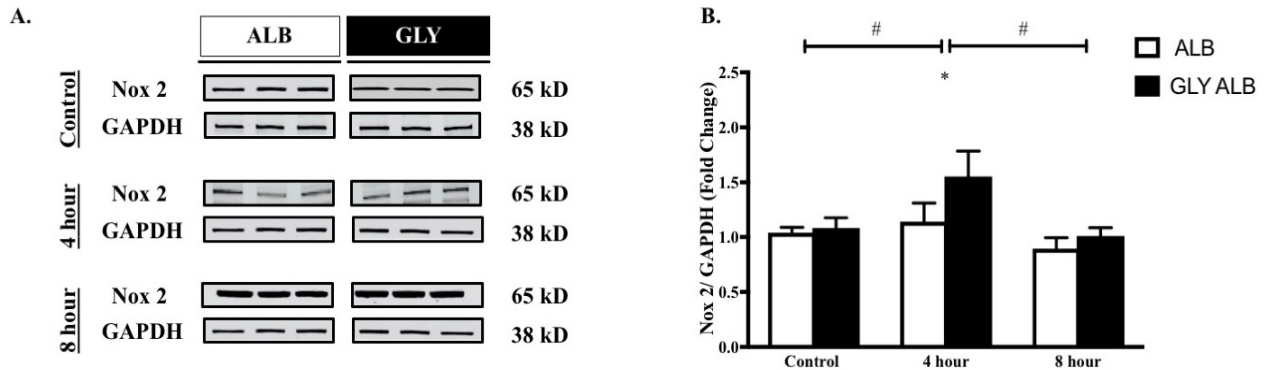
Figure 38. Time Dependent Effects of Chronic Glycated Albumin Stimulation on Nox 2 Expression. Time effects of native and glycated albumin on Nox 2 protein expression. HSkMCs were stimulated with 100 µg/mL of native (n = 3) or glycated albumin (n = 3) for control, 4 and 8 hours. (A) 10 µg of protein was loaded for western blot analysis of Nox 2. (B) Representative images of independent experiments. * indicates significance effect of group, $P < 0.05$. # indicates significance effect of time, $P < 0.05$. GAPDH was used as a loading control and values are represented as mean + SEM.

Results Pertaining to Specific Aim 3:

Experiments designed for specific aim 3 were executed to (1) determine if NRROS was present in human skeletal muscle and HSkMCs, (2) identify and characterize NRROS protein distinctions that may exist between lean healthy control and diabetic human skeletal muscle under basal and insulin stimulated conditions, (3) elucidate how AGEs stimulation impacts NRROS expression in HSkMCs in the presence of diabetes.

Summary:

 First, we were interested in identifying and characterizing NRROS between LHC and T2DM subjects. Further, if NRROS was present in human skeletal muscle, we wanted to establish if hyperinsulinemic conditions impacted NRROS protein expression. Interestingly, NRROS expression in LHC was very lowly expressed under basal metabolic conditions. Following, 120 minutes of hyperinsulinism, NRROS protein expression levels were unaltered (LHC basal $0.0039 + 0.0013$, LHC post clamp $0.0033 + 0.00$, $P = 0.923$). Conversely, individuals with T2DM exhibited robust levels on NRROS protein expression under basal conditions compared to lean healthy counterparts (LHC basal 0.0039 ± 0.0013 vs. T2DM basal 0.1255 ± 0.0453, $P = 0.029$). Upon concluding the clamp procedure, T2DM NRROS levels were also significantly different than LHC, suggesting that hyperinsulinemia (LHC post clamp $0.0033 + 0.0009$ vs. T2DM post clamp 0.0976 ± 0.0346, $P = 0.026$). in T2DM group, insulin infusion induced a 29% decrease in NRROS expression, which was determined nonsignificant statically, $P = 0.2130$. Since increased NRROS has been shown to alleviate ROS production and oxidative stress *in-vitro*, we wanted to investigate NRROS protein expression modifications in available muscle tissue. In a subset of LHC (n=8), and T2DM (n=4), total NRROS protein expression were not different between groups at baseline ($p>0.05$). Given our limited sample size, we performed a post-hoc power calculation (continuous endpoint, two independent samples) with $\alpha=0.05$ that revealed our data only had a 95% power. To inform us about potential future studies we performed a sample size calculation (continuous endpoint, two independent samples) where $\alpha=0.05$ and $\text{ß}=0.2$ which revealed 16 subjects (8 per group) would be sufficient to detect a significant difference if our sample means remained the same. Further, we ran an ANCOVA to indicated if any significant main effect for chronological age associated with insulin-stimulated NRROS protein expression, $F(4.917)$ $(P = 0.05)$, confirming that mean differences between

the LHC and T2DM groups associated with insulin-stimulated NORRS expression may be associated

with differences in chronological age. (**Figure 39**).

Figure 39.
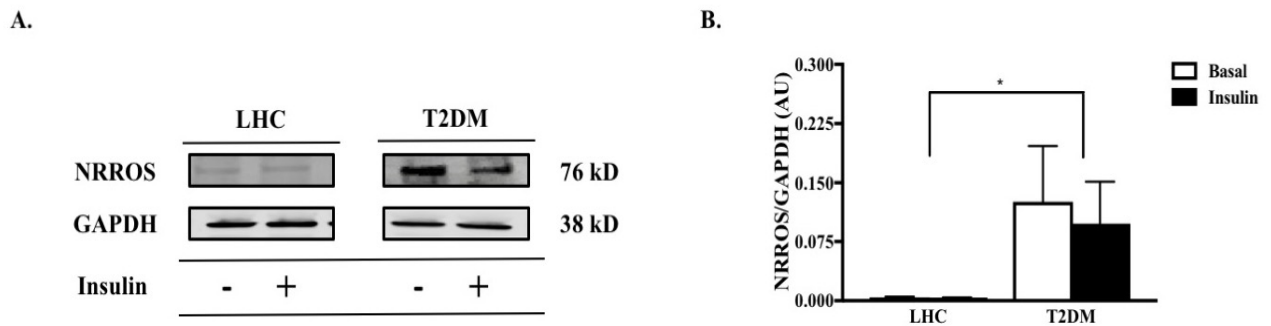
Figure 39. Hyperinsulinemic-euglycemic clamp comparison of NRROS protein expression between lean healthy controls and individuals with type 2 diabetes. (A) Representative Western blot image of NRROS. (B) NRROS protein expression in skeletal muscle of LHC and T2DM during basal and insulin-stimulated states of the hyperinsulinemic-euglycemic clamp. LHC, (n = 8); T2DM, (n = 4). * indicates a significant effect of group, $P < 0.05$. Signal relative intensity was normalized to total Rac 1 and results represent the means ± SE for each group. $P < 0.05$ was considered significant, and data are presented as mean ± SEM.

GLY-ALB Treatment Has No Effect on NADPH oxidase Inhibitor, NRROS

We next set out to verify that NRROS was present in culture cells and examine if its protein expression was modulated by GLY-ALB stimulation. HSkMCs were stimulated with GLY-ALB in dose increments 100, 200 and 400 µg/mL of native albumin or GLY-ALB for two-hours, (**Figure 40).**

Figure 40.
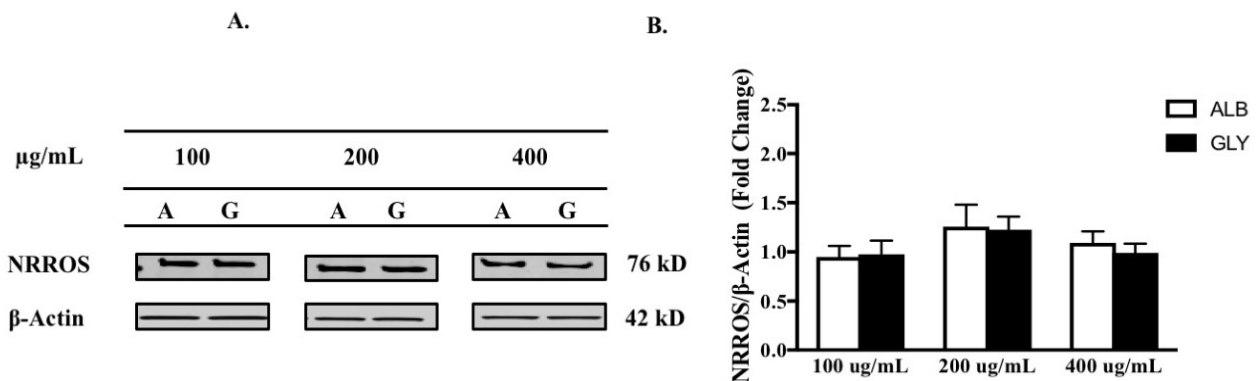
Figure 40. Dose Response Curve of Glycated Albumin on NRROS Glycated Albumin on NRROS in HSkMCs (2 hour). HSkMCs were stimulated with 100, 200 and 400 µg/mL of native (n = 3) or glycated albumin (n = 3) for 2 hours. 10 µg of protein was loaded for western blot analysis of (A) NRROS. (B) Representative images of NRROS. β-Actin was used as a loading control and values are represented as mean ± SEM.

Chronic GLY-ABL Stimulation Has No Effect on NADPH oxidase Inhibitor, NRROS, In HSkMCs

 As previously described, HSkMCs were stimulated with 100 µg/mL of native or glycated albumin for 4 and 8 hours. 10 µg of protein was loaded for Western blot analysis using an anti-NRROS monoclonal; antibody. Our initial observations verified NRROS protein is robustly expressed in HSkMCs. Further, GLY-ALB stimulation had no impact on NRROS levels across time. Moreover, no oscillations in NRROS protein levels were detected between cells treated with GLY-ABL or native albumin at any time point (**Figure 41**).

Figure 41.
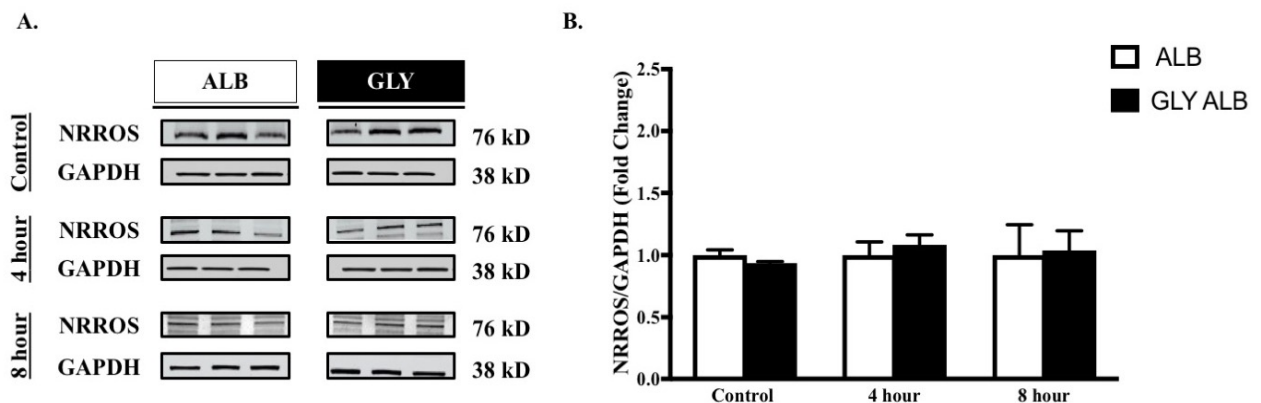
**Figure 41. Time Dependent Effects of Chronic Glycated Albumin Stimulation on NRROS Expression.** Time effects of native and glycated albumin on NRROS protein expression. HSkMCs were stimulated with 100 µg/mL of native (n=3) or glycated albumin (n=3) for 0, 4 and 8 hours. (A) 10 µg of protein was loaded for western blot analysis of NRROS. (B) Representative images of independent

experiments. A two-way ANOVA analysis was conducted, and significant effects were determined using a Bonferroni adjustment for multiple comparisons. * indicates significance effect of group, $P < 0.05$. # indicates significance effect of time, $P < 0.05$. † indicates a significant interaction and ## denotes significance effect within group. GAPDH was used as a loading control and values are represents as mean + SEM.

Section III. C. Discussion

The concept of RAGE-mediated ROS production in a diabetic phenotype has gained much attention over the past decade. However, the mechanism underlining active RAGE induced ROS production is complex and unique among various tissue types. Further, Nox 2 is reported to be implicated in ROS production in response to AGE stimulation, but these associations remain unexplored in human skeletal muscle. In the present study, we accept the null hypothesis, which indicates that active RAGE does not initiate the assembly of NADPH oxidase assembly through Src kinase recruitment. Although we did identify that active RAGE does recruit mDia1 and initiate Src kinase phosphorylation, we unsuccessfully identify the recruitment of further downstream mediators that may induce NADPH assembly and consequential ROS production. An alternative hypothesis may be that Src kinase does play a role in NADPH oxidase assembly, but it may induce activation through NADPH oxidase subunit p60, or it indirectly activates p47pnox through an adapter protein that we may not have considered in these experiments.

Conversely, we did demonstrate that in human skeletal muscle hyperinsulinemia may represent a mechanism that upregulates the protein expression of signal mediators comprising of the RAGE/Nox 2 axis. This event may play a critical role in priming human skeletal muscle with the necessary machinery to provoke chronic inflammation, and Nox 2 mediated oxidative stress. Independent of hyperinsulinemia, this work also demonstrates that ligand-bound RAGE further provokes the

upregulation of the RAGE/Nox 2 axis signal mediators. Taken together, these deleterious metabolic adaptations represent two following events that occur over the course of the natural history of T2DM. Taken together, the sequence of adverse metabolic modification that occurs over the course of the natural history of T2DM may collectively contribute to the significant disruption of redox balance and initiate proinflammatory pathways in insulin-resistant human skeletal muscle.

Additionally, this work provided us with novel data, showing for the first time in skeletal muscle, that non-tyrosine Src kinase undergoes significant phosphorylation in the presence of ligand-bound RAGE and hyperinsulinemia. Furthermore, we are the first group to identify and characterizes- nonphagocytic NRROS in human skeletal tissue where NRROS was significantly higher in insulin-resistant tissue than lean, healthy counterparts. These findings are relevant because the mechanisms responsible for RAGE-induced NADPH oxidase assembly are still mostly unknown. Our work highlights the pSrc and NRROS overly expressed in the diabetic milieu; therefore, these proteins may highlight important signaling abnormalities to consider for future therapeutic strategies.

Importantly, both in vivo and in vitro experiments induced an increase in the RAGE/Nox 2 axis. Hence, in a pathological setting, hyperinsulinemia and ligand-bound RAGE are both mechanisms that may regulate the transcriptional and translational machinery associated with RAGE/Nox 2 axis proteins. Although we did not measure mRNA levels in these experiments, and we recognize it as a major limitation of these studies, we can speculate that the increases in RAGE/Nox 2 proteins are mediated via a network of ROS and inflammatory signals.

The data obtained from the hyperinsulinemic -euglycemic clamp work showed that only the T2DM group exhibited modified protein expression of the RAGE/Nox 2 axis. This response to insulin was also coupled with an increase in pIκBα protein expression, inferring that hyperinsulinemia might stimulate pIκBα phosphorylation and NF-κB translocation to the nucleus. Conversely, the LHC group exhibited a global reduction in RAGE/Nox 2 axis proteins, including pIκBα levels under hyperglycemic conditions. Although the data obtained during these experiments were not statistically significant, they strongly indicate a diverging trend between healthy and diabetic phenotypes [597-600]. Importantly, both age in years and the onset of obesity may introduce confounding factors to this research that negatively impact the interpretation of our work, as both are strongly associated with the elevated exposure to circulating AGEs as well as enhanced RAGE and Nox 2 protein expression. Although these experiments could conceivably be conducted across the spectrum of chronological age groups and various degrees of metabolic derangement, our work is limited to the LHC controls composed of a mean age of (26.3 ± 1) and T2DM counterparts consisting of a mean age of (59 ± 6). We recognize that our LHC group is significantly younger than the T2DM population, and such widespread age discrepancies could impact out measurable outcomes associated with the portion mediators that make up the RAGE/Nox 2 axis. In reference to the pathogenesis and progression of obesity, this work was intentionally designed to measure how divergence form a healthy metabolism may upregulate the ligands and mediates associated with the RAGE/Nox 2 axis. Thus, since our subjects were not age-matched, we used the ANCOVA to only control for potential confounding variables associated with age in years. This analysis reveals that only insulin-stimulated NRROS expression showed and significant association with chronical age.

As evidence indicates, insulin differentially stimulates the metabolic and mitogenic signaling branches in skeletal muscle [601-603] In insulin-resistant tissue, defects in single transduction along the metabolic

branch ultimately downgrade GLUT4 translocation and reduce systemic insulin-mediated glucose disposal. The compensatory hyperinsulinemia that accompanies these adverse modifications continues to mediate signaling through the MAP kinase branch, and among various tissues, this series of events have been implicated in increasing NF-κB activity and other inflammatory signals. Therefore, we speculate that clinically induced -hyperinsulinemia is overstimulation of the MAP kinase pathway and provoking changes in gene expression through NF-κB activation.

To support this hypothesis, a study conducted by Cusi et al. revealed that obese, insulin-resistant individuals with T2DM demonstrated marked downregulation of the metabolic arm of insulin signaling while maintaining regular MAP kinase pathway stimulation [604]. Although Cusi and associates did not measure NF-κB, others indicate that stimulation of the mitogenic pathway augments NF-κB expression and activity [605, 606]. Furthermore, Madonna et al. reported similar findings when investigating the impact of insulin on NF-κB activation in HUVAC cells. This group reported that pathophysiological concentrations of insulin resulted in a significant increase in IκBα phosphorylation and NF-κB translocation to the nucleus [607]. In another study, Bertrand et al. demonstrated that wild-type mammalian cells stimulated with insulin resulted in NF-κB activation in a concentration-dependent manner. They further argue that insulin-induced NF-κB activation is mediated directly through the insulin receptor. To confirm their hypothesis, this group conducted the same experiments with a modified cell line expressing defective insulin receptors [608].

Alternatively, the upregulation of RAGE/Nox 2 axis proteins might be a compensatory response that leads to the accumulation of insulin signaling intermediates in diabetic skeletal muscle. Many of the proteins we investigated also play an influential role in insulin-mediated glucose uptake. For example,

Src activation has been implicated in several insulin-dependent signaling responsibilities, where it is reported to regulate the phosphorylation PKC in skeletal muscle [30].Others examining Src investigated insulin-mediated Src activation have proposed that insulin signaling act upon Src's activation loop, which rapidly induces the Src phosphorylation [609].Once active, pSrc promotes tyrosine phosphorylation of the insulin receptor, PKC activation and IRS docking [610-612]. However, In the development of T2DM, pSrc action is reduced, resulting in post-receptor insulin resistance and impaired glucose disposal [613]

To strengthen the notion that insulin mediators may become overexpressed in insulin-resistant skeletal muscle, we found that pSrc correlated with several indices of metabolic health that impact whole-body glucose disposal. We first identified that pSrc negatively correlated with body fat percentage, suggesting one consequence of developing obesity is lower pSrc protein expression under basal conditions. The development of obesity has commonly been identified as the initial insult associated with the progression of insulin resistance and glucose dysregulation. This correlation may support the notion that the onset of obesity induces an intracellular reduction in pSrc protein expression, and jointly these physiological modifications may contribute to mild insulin resistance early in the natural history of T2DM. To further support the role of pSrc in glucose disposal, we also identified that pSrc protein expression correlated positively with Glucose Disposal Rate (GDR) measured during the clamp procedure. This data implies that individuals with greater concentrations of pSrc prior to insulin signaling may be more responsive to insulin-mediated glucose uptake, as opposed to those subjects who have lower pSrc expression. Lastly, pSrc protein expression also correlated with RAGE proteins expression, while evaluating the RAGE delta values between balsa and insulin-stimulated conditions, we observed that pSrc delta values correlated positively with RAGE expression. Indeed, we hypothesized

that RAGE mediates its signal though pSrc, so this correlation provides encouraging insight into the probable relationship between these two components of RAGE/Nox 2 axis.

Likewise, the cytoskeleton-regulating GTPase Rac1 plays a crucial role in insulin-mediated glucose disposal. In murine skeletal muscle, Rac 1 knockout experiments repress Akt phosphorylation and subsequent GLUT4 translocation [614-616]. With the development of diabetes, Rac 1 protein expression becomes augmented, as demonstrated by Gumustekin et al. who show that Wistar rats were experiencing hyperinsulinemia overexpress Rac 1 protein in hepatocytes [617]. Together, this evidence indicates that Rac1 is not only central for insulin-dependent GLUT4 translocation in skeletal muscle but in diabetic phenotypes, both basal and insulin-mediated Rac levels may become intensified.

Moreover, NADPH subunits, Nox 2 & p47phox, also mediate glucose disposal and transport in skeletal muscle. In a study conducted by Espinosa et al., insulin signaling prompted the activation and mobilization of p47phox [618]. This event was associated with ROS levels that were also generated during insulin signaling, indicating that NADPH oxidase was assembled and active. Additionally, experiments conducted in Nox 2 deficient mice revealed that wild-type rodents had significantly lower plasma glucose levels than Nox 2 knockout counterparts [382]. Taken together these studies confirm that Nox 2 and p47phox both mediate glucose disposal in skeletal muscle.

 Ligand-bound RAGE stimulation also increased the RAGE/Nox 2 axis, resulting in significant increases in RAGE, mDia 1, pSrc, and Nox 2 protein expression. This data suggests that active RAGE also plays a role in regulating the gene expression of proteins in the RAGE/Nox 2 axis. While the mechanisms responsible for the augmentation of these mediators remain elusive, we can speculate ligand bound

RAGE may regulate gene transcription through ROS and inflammatory mediation. Others have shown that RAGE induced ROS can trigger the activation of various transcription factors and stimulate NF-κB. To support this postulation, Clynes et al. showed that RAGE ligand accumulation and receptor engagement resulted in a significant increase in RAGE mRNA, protein expression and inflammatory cytokines, illustrating the active RAGE regulates its gene and protein expression [10].Likewise, RAGE activation has also been shown to increase the production of both ROS and TNFα, which have been identified as a potent inducer of Nox 2 expression [619-621]. Unfortunately, research focusing on the pathological role mDia 1 biology in skeletal muscle has been minimal over the past decade. mDia1 is now recognized as a vital protein in RAGE propagation. Work conducted by Yan et. al. shows that mDia1 knockdown models impact regulate RAGE protein, yet research highlighting the effect of RAGE activation on mDia1 protein expression has not yet been conducted [280]. Thus, shows that RAGE activation may control mDia1 gene expression, which further new insight into the relationship of between RAGE and mDia 1 in skeletal muscle.

Contrary to our findings, it has also been shown that circulating AGEs are elevated in individuals with T2DM, which has been implicated in augmentations RAGE expression within various tissues [149, 622]. We examined serum CML, an abundant AGE, and potent RAGE ligand, levels in both LHC and T2DM groups at baseline and insulin-stimulated timepoints. To our surprise, we observed no significant differences between groups at either time point. One reason we may not have identified significant findings between these two groups could be due to the limited sample size in our T2DM group (we were underpowered). An alternative explanation for this discrepancy may be that we concentrated our attention solely CML. Although CML is considered the most prevalent of AGEs, it represents only one

variation of various AGEs. Conceivably, if we were to measure an array of circulating AGEs, our data would produce different results.

Despite the CML data, we elected to create an AGE model of diabetes in cell culture. based upon work previously conducted by Zhang et. al., [361]. We designed a series of experiments to evaluate if the RAGE/Nox 2 axis was adversely regulated by AGEs. Our results show that AGE-mediated RAGE activation resulted in altered Src kinase protein expression over time and in dose-dependent manner. Furthermore, HSkMCs treated with GLY-ALB provoked the upregulation of RAGE and other critical proteins within the RAGE/Nox 2 axis, including mDia1, pSrc, and Nox 2. Conversely, control cells did not exhibit changes in RAGE/Nox 2 protein expression, these observations suggest that ligand bound RAGE propagates its message through Src activation. Additionally, Active RAGE may also regulate transcription and translational machinery of crucial axis mediators in parallel. We believe that this response shows as dependency among these proteins. Our IP results further support this these relationships, as it depicts that RAGE, mDia 1 and pSrc associate when stimulated with AGEs. Finally, we show that in HSkMCs, mDia1 is required for RAGE-medicated Src-phosphorylation.

It is important to note that non-tyrosine Src kinase is an intercellular network hub, as Src has been identified in activating a complex web of cellular signaling pathways [623]. Contrary to our initial hypothesis, we did not observe the Src-mediated tyrosine phosphorylation of p47^{phox} in cultured cells. Whether these results were due to experimental error or a poor pan-tyrosine antibody selection requires further evaluation. However, little is known concerning tyrosine phosphorylation of p47^{phox}, activation of NADPH oxidase assembly, and ROS generation in skeletal muscle. Others looking tyrosine-induced p47^{phox} activation had reported that p47^{phox} is activated by pSrc, but the data fails to disclose which

tyrosine residue it occurs upon. In HPAECs, cells exposed to hyperoxia exhibited robust tyrosine

phosphorylation of p47hox, which was stimulated by active Src [414]. This signaling event was also

accompanied by signing increases in ROS production. Although p47^{phox} is a necessary element required

for NADPH oxidase assembly in various tissues, its precise mechanism in skeletal muscle is largely

unknown. We believe that Src-induced p47^{phox} activation may still represent attractive targets for

investigation, but perhaps we need to consider the possibility that these two proteins are linked by a

tyrosine dependent adapter protein that is receptive to active pSrc. Other Nox isoforms (Nox 1 and 3)

depend on Src meditated activation of **Tks5 (tyrosine kinase substrates with 5 SH3 domains)** proteins

to mediate Src propagation to p47phox phosphorylation [624].

 Lastly, NRROS is identified as a protein that negative that stifles ROS generation through degradation

of Nox 2. In this study, we investigate the role of NORRS through the lens of hyperinsulinemia and

ligand-bound RAGE signaling. For the first time in human skeletal muscle, we observed that NRROS

protein expression is significantly upregulated in the diabetic phenotype. Interestingly, the T2DM group

revealed that NRROS was to only protein within the RAGE/Nox 2 axis to reduce expression under

insulin stimulation. Conversely, the LHC group showed no changes in NRROS between basal and

insulin-stimulated conditions. A search of literature shows that only 7 published paper currently exist

surrounding NRROS biology. Thus, we can only speculate why insulin stimulation rescued NRROS

protein expression in diabetic skeletal muscles. It has been reported that NRROS targets Nox to facilitate

ROS restraint. Once NRROS these two proteins associate, they inter the **endoplasmic-reticulum-

associated protein degradation pathway (ERAD)** and undergo degradation[34]. We believe that

hyperinsulinemia may be stimulating both agonist (NRROS) and antagonist (Nox 2) simultaneously in

diabetic skeletal muscle, and as a result, we observed NRROS protein reduction because it has

dimerized with Nox 2 and initiated the duration process via the ERAD pathway. Figueiredo et, al. demonstrated that Nox 2 gene expression is upregulated in insulin-resistant skeletal muscle [382]. Indeed, in Nox 2 gene expression in stimulated by insulin signaling, that could explain why there is such a robust difference in NRROS protein expression between LHC and T2DM groups. NRROS may be overly expressed to suppress Nox 2 expression and NADPH mediated ROS procuring

Limitations & Future Directions (Recommendations for Future Research

This work provided our team with both novel and innovating data which suggest the possibility that RAGE/Nox 2 axis not only exists in human skeletal muscle but also becomes excitable by AGE/RAGE interaction and hyperinsulinemia autonomously of one another. However, these results should be interpreted with our study limitations in mind. To begin, the in vivo work used an inadequate sample size for the T2DM group (n=4). However, despite this shortcoming, the 2-way repeated measures ANOVA is a valid statistical test and bestows confidence in the results. Still, though these subject numbers may not meet the statistical assumptions of a 2-way ANOVA, our data was normally distributed. Future studies employing larger, adequately matched cohorts would be prudent before strict conclusions are made on RAGE/Nox 2 axis biology in the context of T2DM.

Regrettably, this work was conducted without validating our antibodies. Protein-specific antibodies are one of the most frequently used research tools for immunoblotting, immunofluorescent and immunoprecipitation-based experiments. Due to the nature of these collected experiments, it would be of great benefit to validate each of the nine antibodies to improve the diagnostic procedures and assure accurate and replicable data. Since this work is clinical in nature, it is even more imperative that we approach this work with absolute certainty that we are detecting the proteins that we are examining or to

avoid poor science and accurate interpretations. Thus, the quality of our interpretation in these experiments is only an accurate as the antibodies that were used to develop our conclusion and prove out hypotheses. In the future, it is essential to validate that the antibodies selected are detecting the amino acid sequence that whey were designed for. It would also be beneficial to limit error in protein detection by selecting only monoclonal antibodies. By selecting monoclonal antibodies, we could reduce the probability of cross-reactive and assure that the proper antigen/antibody complex is being formed.

Further, the extent of our in vivo evaluations was limited to Western blot analysis. Since this is a novel investigation in human skeletal muscle, support in project conception and validation methods surrounding our targets of interest in scientific literature was limited, specifically in skeletal muscle. Therefore, our optimization and validation processes were long standing. If more time and resources were available, we would have also included mRNA analysis for each target, conducted immunoprecipitation tests to determine protein-to-protein associations under insulin stimulation, and finally, we would utilize histological evaluations to detect where these targets exist before and after insult stimulation. Lastly, were also limited by tissue availability in human subjects. While optimizing out IP procedures, some experiment required up to 100ug or greater of tissue. These costly employments of precious samples are not sustainable.

As is common in other tissues, human skeletal muscle carries an elaborate network of microvasculature that branches out from arteries into miniature vessels. In skeletal muscle specifically, a group of capillary networks runs alongside muscle fibers, providing the muscle fibers with oxygen and nutrients while also aiding in metabolites and waste removal [625]. Several studies indicate that endothelial cells also carry

NADPH oxidase subunit Nox 2 [626, 627]. Although this particular study did not concentrations vascular density in our samples, we cannot ignore that human skeletal muscle contains endothelial cells that have also been reported to express Nox 2 protein. These findings would suggest that our biopsy samples may not be a heterogeneous tissue sample, as we were unable to differentiate the Nox 2 protein expression between muscle and capillaries [628]. To address this concern, we utilized HSkMCs in culture to determine if Nox 2 was present in skeletal muscle isolated from endothelial vascular beds. Our findings show that independent of endothelial, NADPH Oxidase subunit Nox 2 protein expression is also robustly expressed in human skeletal muscle, without the influence of endothelial based Nox 2 expression commonly associated with skeletal muscle microvasculature.

The in-vitro work conducted by our team was merely a modest look into RAGE/Nox 2 axis. While our initial intentions were to characterize these targets in HSkMCs and determine the role of Src kinase as a critical mediator in RAGE-mediated ROS production, many more facets of this proposed pathway could be explored to provide greater clarity concerning the nature of this project. To begin, RAGE protein expression exhibited fluctuation in several of our cell culture experiments. Whether this activity was the result of RAGE shredding, downregulation of RAGE mRNA production or a combination of both is currently unknown. Thus, in future work, measuring both RAGE mRNA, MMP activity and sRAGE would provide ample support critically evaluate the nature of RAGE in this pathway.

Concerning mDai1, little is known about its role in skeletal muscle. As previously mentioned, mDia1 regulation is reported to be dependent on Rho GTPase effectors, but few reports have implicated Rac 1 - medicated mDia1 activation directly in disease processes. Therefore, our work in mDia1 biology in skeletal muscle was exploratory. A more considerable effort to define the nature of mDia1 in a tissue-

specific manner would then be advantageous. To accomplish this in future work, we would conduct IP experiments between mDia1, Rac 1 and pRac 1 to surmise how Rho GTPase effectors are governing formin activity in a RAGE dependent manner. Immunofluorescent work would also be useful, as we could determine the nature of mDia1 translocation action upon stimulation. Several reports indicate the active mDia1 freely mobilizes throughout the cytosol through use of actin skeleton [629-631]. Rather than measuring total mDia1 content, in the future, we will utilize more specific methodologies to understand mDia1 activity and associations preferences under RAGE signaling.

Another limitation of this work was not looking further into Src dynamics subsequent to our preliminary experiments. Src exhibited unique behavior in out cell culture work that wanted more critical consideration. As the data indicates, Src kinase was increasing phosphorylation activists while also declining in total Src content. It would have been in our best interest to evaluate Src mRNA throughout these experiments to determine if gene expression was downregulated or Src was undergoing truncation. In the future, and assessment of mRNA in combination with the use of N-terminal specific antibodies for total Src detections would better aid us in better understanding the nature of Src in this context. In the current work, we used C - terminal antibody to detect specifically Tyr 416 (active Src) and Try 519) inactive Src). In addition to these specific antibodies, a third, N-terminal specify antibody may be necessary so that we could cross-reference Src measurements at different time points. Lastly, Src truncation is reported to be medicated though calpains. It would, therefore, be advantageous to measure this calcium-dependent protease under our experimental conditions n the future, as they may also play a role in RAGE/Nox 2 axis pathway.

The most significant limitation to this study is likely the absence of any REDOX data. To begin, no measures of ROS production were performed in cell culture or in vivo experiments. To genuinely discern the nature of RAGE -medicated ROS production, an array of measurements should have been conducted in parallel to our cell treatments. To begin, we should have employed a method that involved detecting oxidizable fluorescent dyes, such as 2′-7′-dichlorofluorescein (DCF) and dihydroethidium. Since DHE specifically measures superoxide anions, this would have provided us with greater insight into Nox 2-mediated ROS production. Whereas DCF would have provided us more critical insight into H2O2 formation, as this methodology measures a wider range of ROS, but is particularly useful at detecting H2O2. In addition to detecting ROS formation in real-time, we also failed to obtain any biomarkers of ROS mediated cell damage such as markers of lipid peroxidation through isoprostanes or thiobarbituric acid reactive substances (TBARS), post-translational protein modification indicators such as S-glutathionylation or 8-hydroxy 2 deoxyguanosine to detect ROS medicated DNA damage. Regrettably, we utilized protein expression as a surrogate indicator of NADPH oxidase activation. While we did obtain compelling data to support RAGE-mediated NADPH oxidase activation, future work will involve a more detailed assessment of ROS production, biomarkers of ROS medicated cell damage and analysis of antioxidant expression throughout all experiments. This endeavor would also be pending on greater access to funds and time. In the future, will employee an activity assay to determine Nox 2 mediated ROS production. Importantly, these methods require specific instrumentation to properly assess ROS being generated in real time

In addition to the redox specific measurements, a more thoughtful and critical effort will be made in obtaining inflammatory measurement across all cell culture work. Oxidative stress and inflammatory biomarkers appear to be promising diagnostic tools in individuals with T2DM. While most of our energies

were dedicated to characterizing the proposed pathway, we did not obtain crucial NF-KB data, nor other key inflammatory markers such as IL-1, IL-6, IL-18, high-sensitivity C-reactive protein. Excessive ROS production not only induces severe inflammation, but it can also be said that the severity of inflammation can likewise trigger ROS generation. These harmful stimuli operate in tandem with one another, yet in how they contribute to activating and driving RAGE/Nox 2 axis in skeletal muscle is undefined. Hence a more inflammatory centered series of experiments superimposed with redox particulars would adequately fortify out protein expression work before you.

Lastly, another critical limitation this work failed to explorer was siRNA mediated knocked-down experiments employed to determine downstream signaling from active RAGE. Specifically, siRNA-mediated Src knock-down trials alone would have provided this work with the necessary evidence to convincingly determine if RAGE -induced Src activation mediates NADPH oxidase assembly and subsequent ROS production. Src-specific knocked-down models have been proven by other groups investigating the role of Src kinase in ROS production. Likewise, conducting knock-down experiments for other axis mediators would provide this work additional clarity centering around signaling propagation downstream of active RAGE. Future work would be designed with these limitations in mind. One of the most perplexing aspects surrounding this body of work is the continuity in which these mediators or recruited and upregulated. Indeed, the proteins that we have targeted for detection are sensitive to the RAGE message. However, their sequence of activation and preferential association still remains poorly understood, specifically in the context of human skeletal muscle. A series of knock-down experiments would assuredly shed light on these puzzle pieces.

CHAPTER VI. CONCLUSION

This study provides important links between hyperinsulinemia, RAGE/Nox 2 axis and skeletal muscle metabolic wellness. Using a clinical-translational approach we demonstrated 120 minutes of insulin infusion resulted in the upregulation of the proposed axis targets in the skeletal muscle of individuals with insulin resistance and T2DM compared to a lean, healthy reference group. Since the clamp procedure fundamentally replicates compensatory hyperinsulinemia, a preliminary stage in the natural history of types diabetes, we can postulate that this phase in the pathogenesis of T2DM may prime skeletal muscle for aberrant ROS production by upregulating the key components of RAGE/Nox 2 axis.

In addition to our *in vivo* work, we further elucidated skeletal muscle specific mechanisms effected by RAGE signaling through *in vitro* trials. If hyperinsulinemia does in fact upregulate axis mediators, thereby readying the cellular milieu with excessive ROS producing machinery, then we must consider the physiological alterations that will occur once beta cells begin to fail and insulin levels subsequently decline. Beta cell failure results in a decrease of both insulin content and action. This regression consequently generates persistently elevated glucose levels, presenting a pro-pathogenic environment for elevated glucose concentrations to forms covalent adducts with the plasma proteins. These events may augment endogenous formation of AGEs while synchronously increasing AGE/RAGE interface probability.

Ligand bound RAGE is implicated in various pathological consequences and disrupting metabolic regulation of numerous proteins. Our cell culture work demonstrated that AGE-mediated RAGE activation induced a transient intensification in axis target protein expression. More importantly perhaps, Src kinase demonstrated an acute sensitivity to RAGE signaling suggesting that phospho-Src may be a novel RAGE-

associated mediator involved in RAGE signaling in human skeletal muscle. Although, these association require more in-depth investigations Src kinase may represent a potential therapeutic target to dampen RAGE signaling and ROS production.

To conclude, this work represents a critical platform to understanding how the pathogenies of diabetes intensifies over the course of the natural history of T2DM through two independent but intersecting pathways. First, 120 minutes of hyperinsulinemia augmented the protein expression of key mediators identified in RAGE/Nox 2 axis. These modifications occurred in individuals that were metabolic compromised, as the lean healthy reference group uniformly demonstrate a decline in axis target protein expression. Next, we showed that independent of hyperinsulinemia, AGE-mediated RAGE activation further induced the upregulation of axis targets, especially Src kinase, which we believe is a key component accountable for RAGE/NADPH oxidase crosstalk and subsequent ROS generation. Although, hyperinsulinemia may be a compensatory response provoked to safeguard whole body glucose metabolism and prevent the development of hyperglycemia in insulin-resistant individuals, the heavy price paid is the adverse upregution of RAGE/NADPH oxidase proteins. These augmented mechanisms deleteriously furnish skeletal muscle with the appropriate machinery to generate chronic inflammation and irregular ROS production that will become intensely stimulated following the decline in beta cell function and action, resulting in greater AGE formation and RAGE interaction.

APPLICATIONS

The elucidation of molecular mechanisms related to skeletal muscle insulin resistance, ROS generation, and inflammation is imperative to understand both the etiology and pathology of T2DM. Given the damaging effects of hyperglycemia, superimposed with AGE mediated RAGE activation, and the prime importance skeletal muscle plays on whole-body glucose metabolism, therapeutic interventions targeting skeletal muscle insulin sensitivity have been a premier area of T2DM research. Studies centering around hyperinsulinemia and RAGE signaling show that a decline in these pathway's messages can improve whole-body glucose metabolism, diminishes aberrant ROS generation and extinguish chronic inflammation. The results of our investigations provide strong proof of concept that RAGE/Nox 2 axis is dysregulated in by hyperinsulinemia and AGE stimulation, specifically in an insulin-resistant model. It is also important to note that both pathways, independent of each other, increased RAGE expression, thereby equipping skeletal muscle with machine to intensify RAGE-medicate cellulate injury. Thus, T2DM skeletal muscle and therapeutic interventions targeted at these axis mediators may prove to be an effective part of a comprehensive treatment plan for T2DM.

CHAPTER VIII. PERSPECTIVE

This body of explorative work collectively represents a novel platform by which the previously indistinct mechanisms responsibly for RAGE-mediated ROS production have been unveiled and characterized for the first time in human skeletal muscle. Further, we believe the succession of in vivo work, followed by our in vitro experiments, provide us with an innovative viewpoint as to how hyperinsulinemia may upregulate critical mediators that substantiate the foundation of a RAGE/ Nox 2 axis at a critical point in the natural history of T2DM.

One of the initial pathological insults to transpire within the natural history of diabetes is moderate insulin resistance among various metabolic tissues. With a diminished response to insulin signaling, beta cells intensify insulin production and delivery into the circulation to dispute the continued high blood glucose levels. In insulin-defiant tissues, compensatory hyperinsulinemia provokes a threshold concentration of insulin that drives glucose into cells while maintaining whole-body glucose metabolism.

Clinically induced hyperinsulinemia by way of the hyperinsulinemic-euglycemic clamp fundamentally replicates compensatory hyperinsulinemia action provoked during the early stages of insulin resistance. Following these in vivo experiments, we observed that T2DM skeletal muscle increased the protein expression of axis targets, thereby priming the muscle with added proinflammatory and prooxidative machinery. These events could then further exacerbate the T2DM condition as RAGE, and other intermediates demonstrated an unfavorable response to insulin. Whether or not the degree of diabetes experience by our T2DM population is a critical factor in the extent of axis target upregulation remains to be determined. However, the collective response to insulin infusion by our T2DM subjects exhibited an increase axis protein, while or lean, healthy reference group unitedly lowered axis protein expression.

Following our clinical assessments, the series of in vitro work demonstrated how circulating AGE production might become augmented following the decline of compensatory hyperinsulinism, thereby producing a more agreeable milieu for AGE/RAGE binding potential. As presented in our cell culture work, GLY-ALB stimulated cells provoked a transient rise in axis proteins, suggesting that these mediators are sensitive to RAGE signaling. While most targets returned to baseline levels throughout our experiments, for the first time, we reveal that RAGE activation, independent of hyperinsulinemia, increases the protein expression of intracellular mediator we believe are involved in RAGE-mediated ROS generation.

Perhaps the most compelling findings that this body of work revels is the manner in which Src & pSrc behave under hyperinsulinemia and AGE stimulation. Little is known about Src content and action in human skeletal muscle. We believe are one of the few groups to investigate this protein under our experiment circumstances. whether or not the deterioration of total Src content under AGE stimulation is a protective or deleterious response requires more research. Notwithstanding, Src and active Src play indispensable roles in numerous physiological activities, thus its decline or truncation is certain to have intracellular and perhaps systemic consequences. Src kinase offers a unique target to further investigate its role in a T2DM phenotype.

For the first time, we have outlined the potential existence of a pathway whose key mediators are markedly increased by hyperinsulinemia in T2DM skeletal muscle. Future investigations are warranted to determine the therapeutic potential of normalizing RAGE/Nox 2 axis in the prevention and treatment of insulin resistance and T2DM. The next logical progression of RAGE/Nox 2 axis research in T2DM skeletal

muscle should involve more diverse methodology to investigate whether silencing these mediators may play a protective role in reducing ROS and inflammatory markers associated with the T2DM condition. If these meditators are associated and increase expression in a pathological context, then they provide not only skeletal muscle researchers with a new collection of therapeutic targets assist reducing the injury induced by RAGE signaling, subsequent inflammation, and connections ROS production. Stifling these converging pathways would then improve global glucose tolerance, chronic inflammation and improve the quality of life in individuals living with T2DM.

We have presented novel insight into RAGE metabolism in the context of ROS production, inflammation, and T2DM. Skeletal muscle axis protein expression is markedly reduced in lean healthy individuals. However, individuals spanning across the natural progression to T2DM demonstrate susceptibility to upregulation of RAGE/Nox 2 axis modification when in the presence of hyperinsulinemia. further, we have identified novel dysregulation of RAGE/Nox 2 axis mediators with AGE stimulation that may underlie the increase in ROS production, inflammation and cell injury.This work provides us with the fundamental steps in identifying a novel skeletal muscle-specific mechanism to combat RAGE signaling.

The bulk of current literature has demonstrated fragmentary evidence associated with RAGE biology as it pertains to ROS production in skeletal muscle. While most studies provide evidence that active RAGE induces ROS generation in skeletal muscle, mechanisms centering around the propagation of this signal have not been completely identified. Given the development and complications of T2DM are secondary to skeletal muscle insulin resistance, understanding the role of RAGE/Nox 2 axis in this context will significantly advance the field.

Herein, we provide a significant expansion of the effects of RAGE signaling in highly metabolic skeletal muscle tissue. This work provides a necessary transition from the obscurely described cross-talk between RAGE and NADPH oxidase, and resolutely exposes plausible mediators that may propagate the RAGE message. While more work is needed to further elucidate this pathway, we have provided innovative players that may be accountable for the deterioration in skeletal muscle health and accelerator of the natural history of T2DM.

GRANTS

LITERATURE CITED

1.   DeMarco, V.G., A.R. Aroor, and J.R. Sowers, *The pathophysiology of hypertension in patients with obesity.* Nat Rev Endocrinol, 2014. **10**(6): p. 364-76.

2.   Brownlee, M., *The pathobiology of diabetic complications: a unifying mechanism.* Diabetes, 2005. **54**(6): p. 1615-25.

3.   Defronzo, R.A., *Banting Lecture. From the triumvirate to the ominous octet: a new paradigm for the treatment of type 2 diabetes mellitus.* Diabetes, 2009. **58**(4): p. 773-95.

4.   DeFronzo, R.A. and D. Tripathy, *Skeletal muscle insulin resistance is the primary defect in type 2 diabetes.* Diabetes Care, 2009. **32 Suppl 2**: p. S157-63.

5.   de Carvalho Vidigal, F., et al., *The role of hyperglycemia in the induction of oxidative stress and inflammatory process.* Nutr Hosp, 2012. **27**(5): p. 1391-8.

6.   Fiorentino, T.V., et al., *Hyperglycemia-induced oxidative stress and its role in diabetes mellitus related cardiovascular diseases.* Curr Pharm Des, 2013. **19**(32): p. 5695-703.

7.   Keane, K.N., et al., *Molecular Events Linking Oxidative Stress and Inflammation to Insulin Resistance and beta-Cell Dysfunction.* Oxid Med Cell Longev, 2015. **2015**: p. 181643.

8.   Bierhaus, A., et al., *Diabetes-associated sustained activation of the transcription factor nuclear factor-kappaB.* Diabetes, 2001. **50**(12): p. 2792-808.

9.   Cai, W., et al., *Oral advanced glycation endproducts (AGEs) promote insulin resistance and diabetes by depleting the antioxidant defenses AGE receptor-1 and sirtuin 1.* Proc Natl Acad Sci U S A, 2012. **109**(39): p. 15888-93.

10.   Ramasamy, R., S.F. Yan, and A.M. Schmidt, *Receptor for AGE (RAGE): signaling mechanisms in the pathogenesis of diabetes and its complications.* Ann N Y Acad Sci, 2011. **1243**: p. 88-102.

11.   Donato, R., *RAGE: a single receptor for several ligands and different cellular responses: the case of certain S100 proteins.* Curr Mol Med, 2007. **7**(8): p. 711-24.

12.   Li, Y., et al., *RAGE/NF-kappaB pathway mediates lipopolysaccharide-induced inflammation in alveolar type I epithelial cells isolated from neonate rats.* Inflammation, 2014. **37**(5): p. 1623-9.

13.   Johar, R., et al., *Role of Reactive Oxygen Species in Estrogen Dependant Breast Cancer Complication.* Anticancer Agents Med Chem, 2015. **16**(2): p. 190-9.

14.   Wautier, M.P., et al., *Activation of NADPH oxidase by AGE links oxidant stress to altered gene expression via RAGE.* Am J Physiol Endocrinol Metab, 2001. **280**(5): p. E685-94.

15.   Denu, J.M. and K.G. Tanner, *Specific and reversible inactivation of protein tyrosine phosphatases by hydrogen peroxide: evidence for a sulfenic acid intermediate and implications for redox regulation.* Biochemistry, 1998. **37**(16): p. 5633-42.

16.   Li, N., et al., *NADPH oxidase NOX2 defines a new antagonistic role for reactive oxygen species and cAMP/PKA in the regulation of insulin secretion.* Diabetes, 2012. **61**(11): p. 2842-50.

17.   Ushio-Fukai, M. and Y. Nakamura, *Reactive oxygen species and angiogenesis: NADPH oxidase as target for cancer therapy.* Cancer Lett, 2008. **266**(1): p. 37-52.

18.   Chakraborti, S. and T. Chakraborti, *Oxidant-mediated activation of mitogen-activated protein kinases and nuclear transcription factors in the cardiovascular system: a brief overview.* Cell Signal, 1998. **10**(10): p. 675-83.

19.   Chang, H.Y., et al., *Activation of apoptosis signal-regulating kinase 1 (ASK1) by the adapter protein Daxx.* Science, 1998. **281**(5384): p. 1860-3.

20.   Taniguchi, K., et al., *Inhibition of Src kinase blocks high glucose-induced EGFR transactivation and collagen synthesis in mesangial cells and prevents diabetic nephropathy in mice.* Diabetes, 2013. **62**(11): p. 3874-86.

21.   Levinson, N.M., et al., *A Src-like inactive conformation in the abl tyrosine kinase domain.* PLoS Biol, 2006. **4**(5): p. e144.

22.   Reinehr, R., et al., *Involvement of NADPH oxidase isoforms and Src family kinases in CD95-dependent hepatocyte apoptosis.* J Biol Chem, 2005. **280**(29): p. 27179-94.

23.   Reddy, M.A., et al., *Key role of Src kinase in S100B-induced activation of the receptor for advanced glycation end products in vascular smooth muscle cells.* J Biol Chem, 2006. **281**(19): p. 13685-93.

24. Sangle, G.V., et al., *Involvement of RAGE, NADPH oxidase, and Ras/Raf-1 pathway in glycated LDL-induced expression of heat shock factor-1 and plasminogen activator inhibitor-1 in vascular endothelial cells.* Endocrinology, 2010. **151**(9): p. 4455-66.

25. Kim, J.M., et al., *Kaempferol modulates pro-inflammatory NF-kappaB activation by suppressing advanced glycation endproducts-induced NADPH oxidase.* Age (Dordr), 2010. **32**(2): p. 197-208.

26. Hudson, B.I., et al., *Interaction of the RAGE cytoplasmic domain with diaphanous-1 is required for ligand-stimulated cellular migration through activation of Rac1 and Cdc42.* J Biol Chem, 2008. **283**(49): p. 34457-68.

27. Meng, W., et al., *DIP (mDia interacting protein) is a key molecule regulating Rho and Rac in a Src-dependent manner.* Embo j, 2004. **23**(4): p. 760-71.

28. Satoh, S. and T. Tominaga, *mDia-interacting protein acts downstream of Rho-mDia and modifies Src activation and stress fiber formation.* J Biol Chem, 2001. **276**(42): p. 39290-4.

29. Wang, H., et al., *Caveolin-1 phosphorylation regulates vascular endothelial insulin uptake and is impaired by insulin resistance in rats.* Diabetologia, 2015. **58**(6): p. 1344-53.

30. Rosenzweig, T., et al., *Src tyrosine kinase regulates insulin-induced activation of protein kinase C (PKC) delta in skeletal muscle.* Cell Signal, 2004. **16**(11): p. 1299-308.

31. Dysken, M.W., et al., *Effect of vitamin E and memantine on functional decline in Alzheimer disease: the TEAM-AD VA cooperative randomized trial.* Jama, 2014. **311**(1): p. 33-44.

32. Semba, R.D., et al., *Resveratrol levels and all-cause mortality in older community-dwelling adults.* JAMA Intern Med, 2014. **174**(7): p. 1077-84.

33. Albanes, D., et al., *Alpha-Tocopherol and beta-carotene supplements and lung cancer incidence in the alpha-tocopherol, beta-carotene cancer prevention study: effects of base-line characteristics and study compliance.* J Natl Cancer Inst, 1996. **88**(21): p. 1560-70.

34. Noubade, R., et al., *NRROS negatively regulates reactive oxygen species during host defence and autoimmunity.* Nature, 2014. **509**(7499): p. 235-9.

35.   Liu, J., et al., *Identification and characterization of a unique leucine-rich repeat protein (LRRC33) that inhibits Toll-like receptor-mediated NF-kappaB activation.* Biochem Biophys Res Commun, 2013. **434**(1): p. 28-34.

36.   Ibrahim, Z.A., et al., *RAGE and TLRs: relatives, friends or neighbours?* Mol Immunol, 2013. **56**(4): p. 739-44.

37.   Lee, J.W., N.H. Kim, and A. Milanesi, *Thyroid Hormone Signaling in Muscle Development, Repair and Metabolism.* J Endocrinol Diabetes Obes, 2014. **2**(3): p. 1046.

38.   Mahmoud, A.M., et al., *Skeletal Muscle Vascular Function: A Counterbalance of Insulin Action.* Microcirculation, 2015. **22**(5): p. 327-47.

39.   Mahmoud, A.M., et al., *Hyperinsulinemia augments endothelin-1 protein expression and impairs vasodilation of human skeletal muscle arterioles.* Physiol Rep, 2016. **4**(16).

40.   Mahmoud, A.M., et al., *Nox2 contributes to hyperinsulinemia-induced redox imbalance and impaired vascular function.* Redox Biol, 2017. **13**: p. 288-300.

41.   Cusick, M., et al., *Associations of mortality and diabetes complications in patients with type 1 and type 2 diabetes: early treatment diabetic retinopathy study report no. 27.* Diabetes Care, 2005. **28**(3): p. 617-25.

42.   Ginter, E. and V. Simko, *Type 2 diabetes mellitus, pandemic in 21st century.* Adv Exp Med Biol, 2012. **771**: p. 42-50.

43.   Ginter, E. and V. Simko, *Global prevalence and future of diabetes mellitus.* Adv Exp Med Biol, 2012. **771**: p. 35-41.

44.   Conway, B.N., et al., *The obesity epidemic and rising diabetes incidence in a low-income racially diverse southern US cohort.* PLoS One, 2018. **13**(1): p. e0190993.

45.   Weiss, R., et al., *Prediabetes in obese youth: a syndrome of impaired glucose tolerance, severe insulin resistance, and altered myocellular and abdominal fat partitioning.* Lancet, 2003. **362**(9388): p. 951-7.

46.   Abdul-Ghani, M.A., M. Matsuda, and R.A. DeFronzo, *Strong association between insulin resistance in liver and skeletal muscle in non-diabetic subjects.* Diabet Med, 2008. **25**(11): p. 1289-94.

47.   Boucher, J., A. Kleinridders, and C.R. Kahn, *Insulin receptor signaling in normal and insulin-resistant states.* Cold Spring Harb Perspect Biol, 2014. **6**(1).

48.   Porksen, N., et al., *Pulsatile insulin secretion: detection, regulation, and role in diabetes.* Diabetes, 2002. **51 Suppl 1**: p. S245-54.

49.   Martin, B.C., et al., *Role of glucose and insulin resistance in development of type 2 diabetes mellitus: results of a 25-year follow-up study.* Lancet, 1992. **340**(8825): p. 925-9.

50.   Monzillo, L.U., et al., *Effect of lifestyle modification on adipokine levels in obese subjects with insulin resistance.* Obes Res, 2003. **11**(9): p. 1048-54.

51.   Rowe, J.W., et al., *Characterization of the insulin resistance of aging.* J Clin Invest, 1983. **71**(6): p. 1581-7.

52.   Kelley, D.E., et al., *Skeletal muscle fatty acid metabolism in association with insulin resistance, obesity, and weight loss.* Am J Physiol, 1999. **277**(6 Pt 1): p. E1130-41.

53.   Iwahashi, H., et al., *Insulin-secretion capacity in normal glucose tolerance, impaired glucose tolerance, and diabetes in obese and non-obese Japanese patients.* J Diabetes Investig, 2012. **3**(3): p. 271-5.

54.   Abdul-Ghani, M.A., et al., *Insulin secretion and action in subjects with impaired fasting glucose and impaired glucose tolerance: results from the Veterans Administration Genetic Epidemiology Study.* Diabetes, 2006. **55**(5): p. 1430-5.

55.   Lillioja, S., et al., *Impaired glucose tolerance as a disorder of insulin action. Longitudinal and cross-sectional studies in Pima Indians.* N Engl J Med, 1988. **318**(19): p. 1217-25.

56.   Hansen, T., *Type 2 diabetes mellitus--a multifactorial disease.* Ann Univ Mariae Curie Sklodowska Med, 2002. **57**(1): p. 544-9.

57.   Prentki, M. and C.J. Nolan, *Islet beta cell failure in type 2 diabetes.* J Clin Invest, 2006. **116**(7): p. 1802-12.

58.   Porte, D., Jr. and S.E. Kahn, *beta-cell dysfunction and failure in type 2 diabetes: potential mechanisms.* Diabetes, 2001. **50 Suppl 1**: p. S160-3.

59.   Gungor, N. and S. Arslanian, *Progressive beta cell failure in type 2 diabetes mellitus of youth.* J Pediatr, 2004. **144**(5): p. 656-9.

60.   Stolk, R.P., et al., *Diabetes mellitus, impaired glucose tolerance, and hyperinsulinemia in an elderly population. The Rotterdam Study.* Am J Epidemiol, 1997. **145**(1): p. 24-32.

61.   de Pablos-Velasco, P.L., et al., *Prevalence and determinants of diabetes mellitus and glucose intolerance in a Canarian Caucasian population - comparison of the 1997 ADA and the 1985 WHO criteria. The Guia Study.* Diabet Med, 2001. **18**(3): p. 235-41.

62.   Festa, A., et al., *Beta-cell dysfunction in subjects with impaired glucose tolerance and early type 2 diabetes: comparison of surrogate markers with first-phase insulin secretion from an intravenous glucose tolerance test.* Diabetes, 2008. **57**(6): p. 1638-44.

63.   Poitout, V. and R.P. Robertson, *Minireview: Secondary beta-cell failure in type 2 diabetes--a convergence of glucotoxicity and lipotoxicity.* Endocrinology, 2002. **143**(2): p. 339-42.

64.   Kaiser, N., G. Leibowitz, and R. Nesher, *Glucotoxicity and beta-cell failure in type 2 diabetes mellitus.* J Pediatr Endocrinol Metab, 2003. **16**(1): p. 5-22.

65.   Porte, D., Jr. and S.E. Kahn, *The key role of islet dysfunction in type II diabetes mellitus.* Clin Invest Med, 1995. **18**(4): p. 247-54.

66.   Alejandro, E.U., et al., *Natural history of beta-cell adaptation and failure in type 2 diabetes.* Mol Aspects Med, 2015. **42**: p. 19-41.

67.   Godoy-Matos, A.F., *The role of glucagon on type 2 diabetes at a glance.* Diabetol Metab Syndr, 2014. **6**(1): p. 91.

68.   Leclercq, I.A., et al., *Insulin resistance in hepatocytes and sinusoidal liver cells: mechanisms and consequences.* J Hepatol, 2007. **47**(1): p. 142-56.

69.   Titchenell, P.M., et al., *Direct Hepatocyte Insulin Signaling Is Required for Lipogenesis but Is Dispensable for the Suppression of Glucose Production.* Cell Metab, 2016. **23**(6): p. 1154-1166.

70.   Roden, M., *Hepatic glucose production and insulin resistance.* Wien Med Wochenschr, 2008. **158**(19-20): p. 558-61.

71.   Boden, G., *Gluconeogenesis and glycogenolysis in health and diabetes.* J Investig Med, 2004. **52**(6): p. 375-8.

72.   Ferrannini, E. and L.C. Groop, *Hepatic glucose production in insulin-resistant states.* Diabetes Metab Rev, 1989. **5**(8): p. 711-26.

73.   Felig, P., *Interaction of insulin and amino acid metabolism in the regulation of gluconeogenesis.* Isr J Med Sci, 1972. **8**(3): p. 262-70.

74.   Boden, G., X. Chen, and T.P. Stein, *Gluconeogenesis in moderately and severely hyperglycemic patients with type 2 diabetes mellitus.* Am J Physiol Endocrinol Metab, 2001. **280**(1): p. E23-30.

75.   Gastaldelli, A., et al., *Effect of physiological hyperinsulinemia on gluconeogenesis in nondiabetic subjects and in type 2 diabetic patients.* Diabetes, 2001. **50**(8): p. 1807-12.

76.   Wajngot, A., et al., *Quantitative contributions of gluconeogenesis to glucose production during fasting in type 2 diabetes mellitus.* Metabolism, 2001. **50**(1): p. 47-52.

77.   Gastaldelli, A., et al., *Separate contribution of diabetes, total fat mass, and fat topography to glucose production, gluconeogenesis, and glycogenolysis.* J Clin Endocrinol Metab, 2004. **89**(8): p. 3914-21.

78.   Meyer, C., et al., *Role of human liver, kidney, and skeletal muscle in postprandial glucose homeostasis.* Am J Physiol Endocrinol Metab, 2002. **282**(2): p. E419-27.

79.   DeFronzo, R.A., et al., *Effects of insulin on peripheral and splanchnic glucose metabolism in noninsulin-dependent (type II) diabetes mellitus.* J Clin Invest, 1985. **76**(1): p. 149-55.

80.   Mitrakou, A., et al., *Role of reduced suppression of glucose production and diminished early insulin release in impaired glucose tolerance.* N Engl J Med, 1992. **326**(1): p. 22-9.

81.   Ramnanan, C.J., et al., *Molecular characterization of insulin-mediated suppression of hepatic glucose production in vivo.* Diabetes, 2010. **59**(6): p. 1302-11.

82.   Vander Kooi, B.T., et al., *The three insulin response sequences in the glucose-6-phosphatase catalytic subunit gene promoter are functionally distinct.* J Biol Chem, 2003. **278**(14): p. 11782-93.

83.   Chakravarty, K., et al., *Factors that control the tissue-specific transcription of the gene for phosphoenolpyruvate carboxykinase-C.* Crit Rev Biochem Mol Biol, 2005. **40**(3): p. 129-54.

84.   Burgess, S.C., et al., *Cytosolic phosphoenolpyruvate carboxykinase does not solely control the rate of hepatic gluconeogenesis in the intact mouse liver.* Cell Metab, 2007. **5**(4): p. 313-20.

85.   Stark, R., et al., *A role for mitochondrial phosphoenolpyruvate carboxykinase (PEPCK-M) in the regulation of hepatic gluconeogenesis.* J Biol Chem, 2014. **289**(11): p. 7257-63.

86.   Quinn, P.G. and D. Yeagley, *Insulin regulation of PEPCK gene expression: a model for rapid and reversible modulation.* Curr Drug Targets Immune Endocr Metabol Disord, 2005. **5**(4): p. 423-37.

87.   Sharabi, K., et al., *Molecular pathophysiology of hepatic glucose production.* Mol Aspects Med, 2015. **46**: p. 21-33.

88.   Adkins, A., et al., *Higher insulin concentrations are required to suppress gluconeogenesis than glycogenolysis in nondiabetic humans.* Diabetes, 2003. **52**(9): p. 2213-20.

89.   Oakes, N.D., et al., *Mechanisms of liver and muscle insulin resistance induced by chronic high-fat feeding.* Diabetes, 1997. **46**(11): p. 1768-74.

90.   Basu, R., et al., *Pathogenesis of prediabetes: role of the liver in isolated fasting hyperglycemia and combined fasting and postprandial hyperglycemia.* J Clin Endocrinol Metab, 2013. **98**(3): p. E409-17.

91.   Bock, G., et al., *Pathogenesis of pre-diabetes: mechanisms of fasting and postprandial hyperglycemia in people with impaired fasting glucose and/or impaired glucose tolerance.* Diabetes, 2006. **55**(12): p. 3536-49.

92.   Heilbronn, L.K., et al., *Glucose tolerance and skeletal muscle gene expression in response to alternate day fasting.* Obes Res, 2005. **13**(3): p. 574-81.

93.   Koranyi, L.I., et al., *Level of skeletal muscle glucose transporter protein correlates with insulin-stimulated whole body glucose disposal in man.* Diabetologia, 1991. **34**(10): p. 763-5.

94.   DeFronzo, R.A., et al., *The effect of insulin on the disposal of intravenous glucose. Results from indirect calorimetry and hepatic and femoral venous catheterization.* Diabetes, 1981. **30**(12): p. 1000-7.

95.   Edelman, S.V., et al., *Kinetics of insulin-mediated and non-insulin-mediated glucose uptake in humans.* Diabetes, 1990. **39**(8): p. 955-64.

96.   Ojuka, E.O. and V. Goyaram, *Mechanisms in exercise-induced increase in glucose disposal in skeletal muscle.* Med Sport Sci, 2014. **60**: p. 71-81.

97.   Kelley, D.E., M. Mokan, and L.J. Mandarino, *Intracellular defects in glucose metabolism in obese patients with NIDDM.* Diabetes, 1992. **41**(6): p. 698-706.

98.   Chung, J.W., et al., *Contribution of obesity to defects of intracellular glucose metabolism in NIDDM.* Diabetes Care, 1995. **18**(5): p. 666-73.

99.   Martins, A.R., et al., *Mechanisms underlying skeletal muscle insulin resistance induced by fatty acids: importance of the mitochondrial function.* Lipids Health Dis, 2012. **11**: p. 30.

100.   Shepherd, P.R. and B.B. Kahn, *Glucose transporters and insulin action--implications for insulin resistance and diabetes mellitus.* N Engl J Med, 1999. **341**(4): p. 248-57.

101.   DeFronzo, R.A., *Pathogenesis of type 2 diabetes mellitus.* Med Clin North Am, 2004. **88**(4): p. 787-835, ix.

102.   Kohanski, R.A., *Insulin receptor autophosphorylation. I. Autophosphorylation kinetics of the native receptor and its cytoplasmic kinase domain.* Biochemistry, 1993. **32**(22): p. 5766-72.

103.   Lee, J. and P.F. Pilch, *The insulin receptor: structure, function, and signaling.* Am J Physiol, 1994. **266**(2 Pt 1): p. C319-34.

104.   Ottensmeyer, F.P., et al., *Mechanism of transmembrane signaling: insulin binding and the insulin receptor.* Biochemistry, 2000. **39**(40): p. 12103-12.

105.   Backer, J.M., et al., *Phosphatidylinositol 3'-kinase is activated by association with IRS-1 during insulin stimulation.* Embo j, 1992. **11**(9): p. 3469-79.

106.   Myers, M.G., Jr., et al., *IRS-1 activates phosphatidylinositol 3'-kinase by associating with src homology 2 domains of p85.* Proc Natl Acad Sci U S A, 1992. **89**(21): p. 10350-4.

107.   Mora, A., et al., *PDK1, the master regulator of AGC kinase signal transduction.* Semin Cell Dev Biol, 2004. **15**(2): p. 161-70.

108.   Hermida, M.A., J. Dinesh Kumar, and N.R. Leslie, *GSK3 and its interactions with the PI3K/AKT/mTOR signalling network.* Adv Biol Regul, 2017. **65**: p. 5-15.

109.   Yoon, M.S., *The Role of Mammalian Target of Rapamycin (mTOR) in Insulin Signaling.* Nutrients, 2017. **9**(11).

110.   Brunet, A., et al., *Akt promotes cell survival by phosphorylating and inhibiting a Forkhead transcription factor.* Cell, 1999. **96**(6): p. 857-68.

111.   Alvim, R.O., et al., *General aspects of muscle glucose uptake.* An Acad Bras Cienc, 2015. **87**(1): p. 351-68.

112.   Kahn, C.R., D.M. Neville, Jr., and J. Roth, *Insulin-receptor interaction in the obese-hyperglycemic mouse. A model of insulin resistance.* J Biol Chem, 1973. **248**(1): p. 244-50.

113.   Livingston, J.N., P. Cuatrecasa, and D.H. Lockwood, *Insulin insensitivity of large fat cells.* Science, 1972. **177**(4049): p. 626-8.

114.   Kono, T. and F.W. Barham, *The relationship between the insulin-binding capacity of fat cells and the cellular response to insulin. Studies with intact and trypsin-treated fat cells.* J Biol Chem, 1971. **246**(20): p. 6210-6.

115.   Amatruda, J.M., J.N. Livingston, and D.H. Lockwood, *Insulin receptor: role in the resistance of human obesity to insulin.* Science, 1975. **188**(4185): p. 264-6.

116.   Olefsky, J.M., et al., *Insulin resistance in non-insulin dependent (type II) and insulin dependent (type I) diabetes mellitus.* Adv Exp Med Biol, 1985. **189**: p. 176-205.

117.   Nolan, J.J., et al., *Mechanisms of the kinetic defect in insulin action in obesity and NIDDM.* Diabetes, 1997. **46**(6): p. 994-1000.

118. Olefsky, J.M. and G.M. Reaven, *Insulin binding in diabetes. Relationships with plasma insulin levels and insulin sensitivity.* Diabetes, 1977. **26**(7): p. 680-8.

119. Copps, K.D. and M.F. White, *Regulation of insulin sensitivity by serine/threonine phosphorylation of insulin receptor substrate proteins IRS1 and IRS2.* Diabetologia, 2012. **55**(10): p. 2565-2582.

120. Hancer, N.J., et al., *Insulin and metabolic stress stimulate multisite serine/threonine phosphorylation of insulin receptor substrate 1 and inhibit tyrosine phosphorylation.* J Biol Chem, 2014. **289**(18): p. 12467-84.

121. Pederson, T.M., D.L. Kramer, and C.M. Rondinone, *Serine/threonine phosphorylation of IRS-1 triggers its degradation: possible regulation by tyrosine phosphorylation.* Diabetes, 2001. **50**(1): p. 24-31.

122. Paz, K., et al., *A molecular basis for insulin resistance. Elevated serine/threonine phosphorylation of IRS-1 and IRS-2 inhibits their binding to the juxtamembrane region of the insulin receptor and impairs their ability to undergo insulin-induced tyrosine phosphorylation.* J Biol Chem, 1997. **272**(47): p. 29911-8.

123. Kim, Y.B., et al., *Normal insulin-dependent activation of Akt/protein kinase B, with diminished activation of phosphoinositide 3-kinase, in muscle in type 2 diabetes.* J Clin Invest, 1999. **104**(6): p. 733-41.

124. Wymann, M.P. and L. Pirola, *Structure and function of phosphoinositide 3-kinases.* Biochim Biophys Acta, 1998. **1436**(1-2): p. 127-50.

125. Shepherd, P.R., D.J. Withers, and K. Siddle, *Phosphoinositide 3-kinase: the key switch mechanism in insulin signalling.* Biochem J, 1998. **333 (Pt 3)**: p. 471-90.

126. Ramjaun, A.R. and J. Downward, *Ras and phosphoinositide 3-kinase: partners in development and tumorigenesis.* Cell Cycle, 2007. **6**(23): p. 2902-5.

127. Goodyear, L.J., et al., *Insulin receptor phosphorylation, insulin receptor substrate-1 phosphorylation, and phosphatidylinositol 3-kinase activity are decreased in intact skeletal muscle strips from obese subjects.* J Clin Invest, 1995. **95**(5): p. 2195-204.

128. Knight, Z.A., et al., *A pharmacological map of the PI3-K family defines a role for p110alpha in insulin signaling.* Cell, 2006. **125**(4): p. 733-47.

129.   Schiaffino, S. and C. Mammucari, *Regulation of skeletal muscle growth by the IGF1-Akt/PKB pathway: insights from genetic models.* Skelet Muscle, 2011. **1**(1): p. 4.

130.   Whiteman, E.L., H. Cho, and M.J. Birnbaum, *Role of Akt/protein kinase B in metabolism.* Trends Endocrinol Metab, 2002. **13**(10): p. 444-51.

131.   Fayard, E., et al., *Protein kinase B/Akt at a glance.* J Cell Sci, 2005. **118**(Pt 24): p. 5675-8.

132.   Stephens, L., et al., *Protein kinase B kinases that mediate phosphatidylinositol 3,4,5-trisphosphate-dependent activation of protein kinase B.* Science, 1998. **279**(5351): p. 710-4.

133.   Cleasby, M.E., et al., *Functional studies of Akt isoform specificity in skeletal muscle in vivo; maintained insulin sensitivity despite reduced insulin receptor substrate-1 expression.* Mol Endocrinol, 2007. **21**(1): p. 215-28.

134.   Cozzone, D., et al., *Isoform-specific defects of insulin stimulation of Akt/protein kinase B (PKB) in skeletal muscle cells from type 2 diabetic patients.* Diabetologia, 2008. **51**(3): p. 512-21.

135.   Krook, A., et al., *Insulin-stimulated Akt kinase activity is reduced in skeletal muscle from NIDDM subjects.* Diabetes, 1998. **47**(8): p. 1281-6.

136.   Brozinick, J.T., Jr., B.R. Roberts, and G.L. Dohm, *Defective signaling through Akt-2 and -3 but not Akt-1 in insulin-resistant human skeletal muscle: potential role in insulin resistance.* Diabetes, 2003. **52**(4): p. 935-41.

137.   Brosius, F.C., 3rd, et al., *Insulin-responsive glucose transporter expression in renal microvessels and glomeruli.* Kidney Int, 1992. **42**(5): p. 1086-92.

138.   Rothman, D.L., R.G. Shulman, and G.I. Shulman, *31P nuclear magnetic resonance measurements of muscle glucose-6-phosphate. Evidence for reduced insulin-dependent muscle glucose transport or phosphorylation activity in non-insulin-dependent diabetes mellitus.* J Clin Invest, 1992. **89**(4): p. 1069-75.

139.   Pedersen, O., et al., *Evidence against altered expression of GLUT1 or GLUT4 in skeletal muscle of patients with obesity or NIDDM.* Diabetes, 1990. **39**(7): p. 865-70.

140.   Ciaraldi, T.P., et al., *Role of glucose transport in the postreceptor defect of non-insulin-dependent diabetes mellitus.* Diabetes, 1982. **31**(11): p. 1016-22.

141. Garvey, W.T., et al., *Evidence for defects in the trafficking and translocation of GLUT4 glucose transporters in skeletal muscle as a cause of human insulin resistance.* J Clin Invest, 1998. **101**(11): p. 2377-86.

142. Ryder, J.W., et al., *Use of a novel impermeable biotinylated photolabeling reagent to assess insulin- and hypoxia-stimulated cell surface GLUT4 content in skeletal muscle from type 2 diabetic patients.* Diabetes, 2000. **49**(4): p. 647-54.

143. Schalkwijk, C.G. and T. Miyata, *Early- and advanced non-enzymatic glycation in diabetic vascular complications: the search for therapeutics.* Amino Acids, 2012. **42**(4): p. 1193-204.

144. Ansari, N.A. and D. Dash, *Amadori glycated proteins: role in production of autoantibodies in diabetes mellitus and effect of inhibitors on non-enzymatic glycation.* Aging Dis, 2013. **4**(1): p. 50-6.

145. Xue, J., et al., *Advanced glycation end product recognition by the receptor for AGEs.* Structure, 2011. **19**(5): p. 722-32.

146. Song, F. and A.M. Schmidt, *Glycation and insulin resistance: novel mechanisms and unique targets?* Arterioscler Thromb Vasc Biol, 2012. **32**(8): p. 1760-5.

147. Gillery, P., *[Advanced glycation end products (AGEs), free radicals and diabetes].* J Soc Biol, 2001. **195**(4): p. 387-90.

148. Vlassara, H. and J. Uribarri, *Advanced glycation end products (AGE) and diabetes: cause, effect, or both?* Curr Diab Rep, 2014. **14**(1): p. 453.

149. Singh, V.P., et al., *Advanced glycation end products and diabetic complications.* Korean J Physiol Pharmacol, 2014. **18**(1): p. 1-14.

150. Chang, C.C., et al., *Hyperglycemia and advanced glycation end products (AGEs) suppress the differentiation of 3T3-L1 preadipocytes.* Oncotarget, 2017. **8**(33): p. 55039-55050.

151. Rodino-Janeiro, B.K., et al., *Glycated albumin, a precursor of advanced glycation end-products, up-regulates NADPH oxidase and enhances oxidative stress in human endothelial cells: molecular correlate of diabetic vasculopathy.* Diabetes Metab Res Rev, 2010. **26**(7): p. 550-8.

152. Awasthi, S., K. Sankaranarayanan, and N.T. Saraswathi, *Advanced glycation end products induce differential structural modifications and fibrillation of albumin.* Spectrochim Acta A Mol Biomol Spectrosc, 2016. **163**: p. 60-7.

153. Kyle, R.A. and P.R. Greipp, *3. The laboratory investigation of monoclonal gammopathies.* Mayo Clin Proc, 1978. **53**(11): p. 719-39.

154. Yoon, H.J., et al., *Glycated Albumin Levels in Patients with Type 2 Diabetes Increase Relative to HbA1c with Time.* Biomed Res Int, 2015. **2015**: p. 576306.

155. Kratz, F., *Albumin as a drug carrier: design of prodrugs, drug conjugates and nanoparticles.* J Control Release, 2008. **132**(3): p. 171-83.

156. Valencia, J.V., et al., *Binding of receptor for advanced glycation end products (RAGE) ligands is not sufficient to induce inflammatory signals: lack of activity of endotoxin-free albumin-derived advanced glycation end products.* Diabetologia, 2004. **47**(5): p. 844-52.

157. Song, Y.M., et al., *Glycated albumin causes pancreatic beta-cells dysfunction through autophagy dysfunction.* Endocrinology, 2013. **154**(8): p. 2626-39.

158. Cassese, A., et al., *In skeletal muscle advanced glycation end products (AGEs) inhibit insulin action and induce the formation of multimolecular complexes including the receptor for AGEs.* J Biol Chem, 2008. **283**(52): p. 36088-99.

159. Zurlo, F., et al., *Skeletal muscle metabolism is a major determinant of resting energy expenditure.* J Clin Invest, 1990. **86**(5): p. 1423-7.

160. Lemon, P.W. and J.P. Mullin, *Effect of initial muscle glycogen levels on protein catabolism during exercise.* J Appl Physiol Respir Environ Exerc Physiol, 1980. **48**(4): p. 624-9.

161. Bottinelli, R. and C. Reggiani, *Human skeletal muscle fibres: molecular and functional diversity.* Prog Biophys Mol Biol, 2000. **73**(2-4): p. 195-262.

162. Kelley, D.E., *Skeletal muscle fat oxidation: timing and flexibility are everything.* J Clin Invest, 2005. **115**(7): p. 1699-702.

163. Baldwin, K.M., et al., *Respiratory capacity of white, red, and intermediate muscle: adaptive response to exercise.* Am J Physiol, 1972. **222**(2): p. 373-8.

164. Narkar, V.A., et al., *AMPK and PPARdelta agonists are exercise mimetics.* Cell, 2008. **134**(3): p. 405-15.

165. Muoio, D.M., *Metabolic inflexibility: when mitochondrial indecision leads to metabolic gridlock.* Cell, 2014. **159**(6): p. 1253-62.

166. Chen, D.L., et al., *Phenotypic Characterization of Insulin-Resistant and Insulin-Sensitive Obesity.* J Clin Endocrinol Metab, 2015. **100**(11): p. 4082-91.

167. Brehm, A., et al., *Increased lipid availability impairs insulin-stimulated ATP synthesis in human skeletal muscle.* Diabetes, 2006. **55**(1): p. 136-40.

168. Shaw, C.S., D.A. Jones, and A.J. Wagenmakers, *Network distribution of mitochondria and lipid droplets in human muscle fibres.* Histochem Cell Biol, 2008. **129**(1): p. 65-72.

169. Powell, D.J., et al., *Intracellular ceramide synthesis and protein kinase Czeta activation play an essential role in palmitate-induced insulin resistance in rat L6 skeletal muscle cells.* Biochem J, 2004. **382**(Pt 2): p. 619-29.

170. Adams, S.H., *Emerging perspectives on essential amino acid metabolism in obesity and the insulin-resistant state.* Adv Nutr, 2011. **2**(6): p. 445-56.

171. Cooney, G.J., et al., *Muscle long-chain acyl CoA esters and insulin resistance.* Ann N Y Acad Sci, 2002. **967**: p. 196-207.

172. Itani, S.I., et al., *Lipid-induced insulin resistance in human muscle is associated with changes in diacylglycerol, protein kinase C, and IkappaB-alpha.* Diabetes, 2002. **51**(7): p. 2005-11.

173. Katzmarzyk, P.T., I. Janssen, and C.I. Ardern, *Physical inactivity, excess adiposity and premature mortality.* Obes Rev, 2003. **4**(4): p. 257-90.

174. Hilton, T.N., et al., *Excessive adipose tissue infiltration in skeletal muscle in individuals with obesity, diabetes mellitus, and peripheral neuropathy: association with performance and function.* Phys Ther, 2008. **88**(11): p. 1336-44.

175. Turcotte, L.P. and J.S. Fisher, *Skeletal muscle insulin resistance: roles of fatty acid metabolism and exercise.* Phys Ther, 2008. **88**(11): p. 1279-96.

176. Zhang, L., et al., *Role of fatty acid uptake and fatty acid beta-oxidation in mediating insulin resistance in heart and skeletal muscle.* Biochim Biophys Acta, 2010. **1801**(1): p. 1-22.

177. Straczkowski, M., et al., *Increased skeletal muscle ceramide level in men at risk of developing type 2 diabetes.* Diabetologia, 2007. **50**(11): p. 2366-73.

178. Bruce, C.R., et al., *Endurance training in obese humans improves glucose tolerance and mitochondrial fatty acid oxidation and alters muscle lipid content.* Am J Physiol Endocrinol Metab, 2006. **291**(1): p. E99-e107.

179. Ellis, B.A., et al., *Long-chain acyl-CoA esters as indicators of lipid metabolism and insulin sensitivity in rat and human muscle.* Am J Physiol Endocrinol Metab, 2000. **279**(3): p. E554-60.

180. Barma, P., et al., *Lipid induced overexpression of NF-kappaB in skeletal muscle cells is linked to insulin resistance.* Biochim Biophys Acta, 2009. **1792**(3): p. 190-200.

181. Santamaria-Kisiel, L., A.C. Rintala-Dempsey, and G.S. Shaw, *Calcium-dependent and -independent interactions of the S100 protein family.* Biochem J, 2006. **396**(2): p. 201-14.

182. Ostendorp, T., et al., *Structural and functional insights into RAGE activation by multimeric S100B.* Embo j, 2007. **26**(16): p. 3868-78.

183. Xie, J., et al., *Hexameric calgranulin C (S100A12) binds to the receptor for advanced glycated end products (RAGE) using symmetric hydrophobic target-binding patches.* J Biol Chem, 2007. **282**(6): p. 4218-31.

184. Mitrakou, A., et al., *Contribution of abnormal muscle and liver glucose metabolism to postprandial hyperglycemia in NIDDM.* Diabetes, 1990. **39**(11): p. 1381-90.

185. Huebschmann, A.G., et al., *Diabetes and advanced glycoxidation end products.* Diabetes Care, 2006. **29**(6): p. 1420-32.

186. Dyer, D.G., et al., *Formation of pentosidine during nonenzymatic browning of proteins by glucose. Identification of glucose and other carbohydrates as possible precursors of pentosidine in vivo.* J Biol Chem, 1991. **266**(18): p. 11654-60.

187. Yerneni, K.K., et al., *Hyperglycemia-induced activation of nuclear transcription factor kappaB in vascular smooth muscle cells.* Diabetes, 1999. **48**(4): p. 855-64.

188. Nishikawa, T., et al., *Normalizing mitochondrial superoxide production blocks three pathways of hyperglycaemic damage.* Nature, 2000. **404**(6779): p. 787-90.

189. Ulrich, P. and A. Cerami, *Protein glycation, diabetes, and aging.* Recent Prog Horm Res, 2001. **56**: p. 1-21.

190. Chellan, P. and R.H. Nagaraj, *Early glycation products produce pentosidine cross-links on native proteins. novel mechanism of pentosidine formation and propagation of glycation.* J Biol Chem, 2001. **276**(6): p. 3895-903.

191. Stitt, A., et al., *The AGE inhibitor pyridoxamine inhibits development of retinopathy in experimental diabetes.* Diabetes, 2002. **51**(9): p. 2826-32.

192. Glomb, M.A. and V.M. Monnier, *Mechanism of protein modification by glyoxal and glycolaldehyde, reactive intermediates of the Maillard reaction.* J Biol Chem, 1995. **270**(17): p. 10017-26.

193. Thornalley, P.J. and H.S. Minhas, *Rapid hydrolysis and slow alpha,beta-dicarbonyl cleavage of an agent proposed to cleave glucose-derived protein cross-links.* Biochem Pharmacol, 1999. **57**(3): p. 303-7.

194. El-Bassossy, H.M., N. Dsokey, and A. Fahmy, *Characterization of vascular complications in experimental model of fructose-induced metabolic syndrome.* Toxicol Mech Methods, 2014. **24**(8): p. 536-43.

195. Yang, D.H., et al., *Increased levels of circulating advanced glycation end-products in menopausal women with osteoporosis.* Int J Med Sci, 2014. **11**(5): p. 453-60.

196. Basta, G., A.M. Schmidt, and R. De Caterina, *Advanced glycation end products and vascular inflammation: implications for accelerated atherosclerosis in diabetes.* Cardiovasc Res, 2004. **63**(4): p. 582-92.

197. Monnier, V.M., et al., *The mechanism of collagen cross-linking in diabetes: a puzzle nearing resolution.* Diabetes, 1996. **45 Suppl 3**: p. S67-72.

198. Ott, C., et al., *Role of advanced glycation end products in cellular signaling.* Redox Biol, 2014. **2**: p. 411-29.

199. Toth, C., J. Martinez, and D.W. Zochodne, *RAGE, diabetes, and the nervous system.* Curr Mol Med, 2007. **7**(8): p. 766-76.

200. Twigg, S.M., et al., *Advanced glycosylation end products up-regulate connective tissue growth factor (insulin-like growth factor-binding protein-related protein 2) in human fibroblasts: a potential mechanism for expansion of extracellular matrix in diabetes mellitus.* Endocrinology, 2001. **142**(5): p. 1760-9.

201. Stirban, A., T. Gawlowski, and M. Roden, *Vascular effects of advanced glycation endproducts: Clinical effects and molecular mechanisms.* Mol Metab, 2014. **3**(2): p. 94-108.

202. Prasad, K. and M. Mishra, *AGE-RAGE Stress, Stressors, and Antistressors in Health and Disease.* Int J Angiol, 2018. **27**(1): p. 1-12.

203. Goldberg, T., et al., *Advanced glycoxidation end products in commonly consumed foods.* J Am Diet Assoc, 2004. **104**(8): p. 1287-91.

204. Uribarri, J., et al., *Dietary glycotoxins correlate with circulating advanced glycation end product levels in renal failure patients.* Am J Kidney Dis, 2003. **42**(3): p. 532-8.

205. O'Brien, J. and P.A. Morrissey, *Nutritional and toxicological aspects of the Maillard browning reaction in foods.* Crit Rev Food Sci Nutr, 1989. **28**(3): p. 211-48.

206. Kellow, N.J. and G.S. Savige, *Dietary advanced glycation end-product restriction for the attenuation of insulin resistance, oxidative stress and endothelial dysfunction: a systematic review.* Eur J Clin Nutr, 2013. **67**(3): p. 239-48.

207. Sonoda, N. and T. Inoguchi, *[Role of oxidative stress in pathogenesis of diabetic complications].* Nihon Rinsho, 2012. **70 Suppl 5**: p. 231-5.

208. Paul, R.G. and A.J. Bailey, *The effect of advanced glycation end-product formation upon cell-matrix interactions.* Int J Biochem Cell Biol, 1999. **31**(6): p. 653-60.

209. Ross, R., *The pathogenesis of atherosclerosis: a perspective for the 1990s.* Nature, 1993. **362**(6423): p. 801-9.

210. Cai, W., et al., *Oral glycotoxins determine the effects of calorie restriction on oxidant stress, age-related diseases, and lifespan.* Am J Pathol, 2008. **173**(2): p. 327-36.

211. Koschinsky, T., et al., *Orally absorbed reactive glycation products (glycotoxins): an environmental risk factor in diabetic nephropathy.* Proc Natl Acad Sci U S A, 1997. **94**(12): p. 6474-9.

212. Uribarri, J., et al., *Dietary advanced glycation end products and their role in health and disease.* Adv Nutr, 2015. **6**(4): p. 461-73.

213. Brownlee, M., *Biochemistry and molecular cell biology of diabetic complications.* Nature, 2001. **414**(6865): p. 813-20.

214. Miyata, T., et al., *Renal catabolism of advanced glycation end products: the fate of pentosidine.* Kidney Int, 1998. **53**(2): p. 416-22.

215. Rabbani, N. and P.J. Thornalley, *Advanced glycation end products in the pathogenesis of chronic kidney disease.* Kidney Int, 2018. **93**(4): p. 803-813.

216. Hyogo, H. and S. Yamagishi, *Advanced glycation end products (AGEs) and their involvement in liver disease.* Curr Pharm Des, 2008. **14**(10): p. 969-72.

217. DeGroot, J., et al., *Accumulation of advanced glycation endproducts reduces chondrocyte-mediated extracellular matrix turnover in human articular cartilage.* Osteoarthritis Cartilage, 2001. **9**(8): p. 720-6.

218. Verzijl, N., et al., *Effect of collagen turnover on the accumulation of advanced glycation end products.* J Biol Chem, 2000. **275**(50): p. 39027-31.

219. Thornalley, P.J., et al., *Quantitative screening of advanced glycation endproducts in cellular and extracellular proteins by tandem mass spectrometry.* Biochem J, 2003. **375**(Pt 3): p. 581-92.

220. McCance, D.R., et al., *Maillard reaction products and their relation to complications in insulin-dependent diabetes mellitus.* J Clin Invest, 1993. **91**(6): p. 2470-8.

221. Ono, Y., et al., *Increased serum levels of advanced glycation end-products and diabetic complications.* Diabetes Res Clin Pract, 1998. **41**(2): p. 131-7.

222. Vlassara, H., M. Brownlee, and A. Cerami, *Nonenzymatic glycosylation: role in the pathogenesis of diabetic complications.* Clin Chem, 1986. **32**(10 Suppl): p. B37-41.

223. Vlassara, H., L. Moldawer, and B. Chan, *Macrophage/monocyte receptor for nonenzymatically glycosylated protein is upregulated by cachectin/tumor necrosis factor.* J Clin Invest, 1989. **84**(6): p. 1813-20.

224. Vlassara, H., et al., *Role of oxidants/inflammation in declining renal function in chronic kidney disease and normal aging.* Kidney Int Suppl, 2009(114): p. S3-11.

225. van Boekel, M.A., *Formation of flavour compounds in the Maillard reaction.* Biotechnol Adv, 2006. **24**(2): p. 230-3.

226. Yamada, Y., et al., *The expression of advanced glycation endproduct receptors in rpe cells associated with basal deposits in human maculas.* Exp Eye Res, 2006. **82**(5): p. 840-8.

227. Yang, Z., et al., *Two novel rat liver membrane proteins that bind advanced glycosylation endproducts: relationship to macrophage receptor for glucose-modified proteins.* J Exp Med, 1991. **174**(3): p. 515-24.

228. Cai, W., et al., *Advanced glycation end product (AGE) receptor 1 suppresses cell oxidant stress and activation signaling via EGF receptor.* Proc Natl Acad Sci U S A, 2006. **103**(37): p. 13801-6.

229. Villegas-Rodriguez, M.E., et al., *The AGE-RAGE Axis and Its Relationship to Markers of Cardiovascular Disease in Newly Diagnosed Diabetic Patients.* PLoS One, 2016. **11**(7): p. e0159175.

230. Iacobini, C., et al., *Galectin-3/AGE-receptor 3 knockout mice show accelerated AGE-induced glomerular injury: evidence for a protective role of galectin-3 as an AGE receptor.* Faseb j, 2004. **18**(14): p. 1773-5.

231. Uribarri, J., et al., *Restriction of advanced glycation end products improves insulin resistance in human type 2 diabetes: potential role of AGER1 and SIRT1.* Diabetes Care, 2011. **34**(7): p. 1610-6.

232. He, C.J., et al., *Differential expression of renal AGE-receptor genes in NOD mice: possible role in nonobese diabetic renal disease.* Kidney Int, 2000. **58**(5): p. 1931-40.

233. Skolnik, E.Y., et al., *Human and rat mesangial cell receptors for glucose-modified proteins: potential role in kidney tissue remodelling and diabetic nephropathy.* J Exp Med, 1991. **174**(4): p. 931-9.

234.   Torreggiani, M., et al., *Advanced glycation end product receptor-1 transgenic mice are resistant to inflammation, oxidative stress, and post-injury intimal hyperplasia.* Am J Pathol, 2009. **175**(4): p. 1722-32.

235.   Lu, C., et al., *Advanced glycation endproduct (AGE) receptor 1 is a negative regulator of the inflammatory response to AGE in mesangial cells.* Proc Natl Acad Sci U S A, 2004. **101**(32): p. 11767-72.

236.   Mosquera, J.A., *[Role of the receptor for advanced glycation end products (RAGE) in inflammation].* Invest Clin, 2010. **51**(2): p. 257-68.

237.   Xiong, F., et al., *Receptor for advanced glycation end products (RAGE) prevents endothelial cell membrane resealing and regulates F-actin remodeling in a beta-catenin-dependent manner.* J Biol Chem, 2011. **286**(40): p. 35061-70.

238.   Brett, J., et al., *Survey of the distribution of a newly characterized receptor for advanced glycation end products in tissues.* Am J Pathol, 1993. **143**(6): p. 1699-712.

239.   Ahmed, B., et al., *Diabetes mellitus, hypothalamic hypoestrogenemia, and coronary artery disease in premenopausal women (from the National Heart, Lung, and Blood Institute sponsored WISE study).* Am J Cardiol, 2008. **102**(2): p. 150-4.

240.   Chuah, Y.K., et al., *Receptor for advanced glycation end products and its involvement in inflammatory diseases.* Int J Inflam, 2013. **2013**: p. 403460.

241.   Fadini, G.P., et al., *Circulating endothelial progenitor cells are reduced in peripheral vascular complications of type 2 diabetes mellitus.* J Am Coll Cardiol, 2005. **45**(9): p. 1449-57.

242.   Guo, Z.J., et al., *Advanced oxidation protein products activate vascular endothelial cells via a RAGE-mediated signaling pathway.* Antioxid Redox Signal, 2008. **10**(10): p. 1699-712.

243.   Schmidt, A.M., et al., *Regulation of human mononuclear phagocyte migration by cell surface-binding proteins for advanced glycation end products.* J Clin Invest, 1993. **91**(5): p. 2155-68.

244.   Lee, E.J. and J.H. Park, *Receptor for Advanced Glycation Endproducts (RAGE), Its Ligands, and Soluble RAGE: Potential Biomarkers for Diagnosis and Therapeutic Targets for Human Renal Diseases.* Genomics Inform, 2013. **11**(4): p. 224-9.

245. Sourris, K.C., et al., *Can Targeting the Incretin Pathway Dampen RAGE-Mediated Events in Diabetic Nephropathy?* Curr Drug Targets, 2016. **17**(11): p. 1252-64.

246. Suzuki, D., et al., *Relationship between the expression of advanced glycation end-products (AGE) and the receptor for AGE (RAGE) mRNA in diabetic nephropathy.* Intern Med, 2006. **45**(7): p. 435-41.

247. Tanji, N., et al., *Expression of advanced glycation end products and their cellular receptor RAGE in diabetic nephropathy and nondiabetic renal disease.* J Am Soc Nephrol, 2000. **11**(9): p. 1656-66.

248. Chen, Y.S., et al., *Serum levels of soluble receptor for advanced glycation end products and of S100 proteins are associated with inflammatory, autoantibody, and classical risk markers of joint and vascular damage in rheumatoid arthritis.* Arthritis Res Ther, 2009. **11**(2): p. R39.

249. Heo, Y.J., et al., *The expression of the receptor for advanced glycation end-products (RAGE) in RA-FLS is induced by IL-17 via Act-1.* Arthritis Res Ther, 2011. **13**(4): p. R113.

250. Pullerits, R., et al., *High mobility group box chromosomal protein 1, a DNA binding cytokine, induces arthritis.* Arthritis Rheum, 2003. **48**(6): p. 1693-700.

251. Foell, D., et al., *Expression of the pro-inflammatory protein S100A12 (EN-RAGE) in rheumatoid and psoriatic arthritis.* Rheumatology (Oxford), 2003. **42**(11): p. 1383-9.

252. Wu, S.Y. and K. Watabe, *The roles of microglia/macrophages in tumor progression of brain cancer and metastatic disease.* Front Biosci (Landmark Ed), 2017. **22**: p. 1805-1829.

253. Khorramdelazad, H., et al., *S100A12 and RAGE expression in human bladder transitional cell carcinoma: a role for the ligand/RAGE axis in tumor progression?* Asian Pac J Cancer Prev, 2015. **16**(7): p. 2725-9.

254. Nasser, M.W., et al., *RAGE mediates S100A7-induced breast cancer growth and metastasis by modulating the tumor microenvironment.* Cancer Res, 2015. **75**(6): p. 974-85.

255. Yamagishi, S. and T. Matsui, *Role of receptor for advanced glycation end products (RAGE) in liver disease.* Eur J Med Res, 2015. **20**: p. 15.

256. Pinkas, A. and M. Aschner, *AGEs/RAGE-Related Neurodegeneration: daf-16 as a Mediator, Insulin as an Ameliorant, and C. elegans as an Expedient Research Model.* Chem Res Toxicol, 2017. **30**(1): p. 38-42.

257. Salahuddin, P., G. Rabbani, and R.H. Khan, *The role of advanced glycation end products in various types of neurodegenerative disease: a therapeutic approach.* Cell Mol Biol Lett, 2014. **19**(3): p. 407-37.

258. Byun, K., et al., *Advanced glycation end-products produced systemically and by macrophages: A common contributor to inflammation and degenerative diseases.* Pharmacol Ther, 2017. **177**: p. 44-55.

259. Li, J. and A.M. Schmidt, *Characterization and functional analysis of the promoter of RAGE, the receptor for advanced glycation end products.* J Biol Chem, 1997. **272**(26): p. 16498-506.

260. Hancock, D.B., et al., *Meta-analyses of genome-wide association studies identify multiple loci associated with pulmonary function.* Nat Genet, 2010. **42**(1): p. 45-52.

261. Repapi, E., et al., *Genome-wide association study identifies five loci associated with lung function.* Nat Genet, 2010. **42**(1): p. 36-44.

262. Yan, S.F., R. Ramasamy, and A.M. Schmidt, *Receptor for AGE (RAGE) and its ligands-cast into leading roles in diabetes and the inflammatory response.* J Mol Med (Berl), 2009. **87**(3): p. 235-47.

263. Chen, Q., et al., *The role of high mobility group box 1 (HMGB1) in the pathogenesis of kidney diseases.* Acta Pharm Sin B, 2016. **6**(3): p. 183-8.

264. Leclerc, E., et al., *Binding of S100 proteins to RAGE: an update.* Biochim Biophys Acta, 2009. **1793**(6): p. 993-1007.

265. Schmidt, A.M., et al., *The multiligand receptor RAGE as a progression factor amplifying immune and inflammatory responses.* J Clin Invest, 2001. **108**(7): p. 949-55.

266. Yoon, Y.W., et al., *Pathobiological role of advanced glycation endproducts via mitogen-activated protein kinase dependent pathway in the diabetic vasculopathy.* Exp Mol Med, 2008. **40**(4): p. 398-406.

267.   Shang, L., et al., *RAGE modulates hypoxia/reoxygenation injury in adult murine cardiomyocytes via JNK and GSK-3beta signaling pathways.* PLoS One, 2010. **5**(4): p. e10092.

268.   Tobon-Velasco, J.C., E. Cuevas, and M.A. Torres-Ramos, *Receptor for AGEs (RAGE) as mediator of NF-kB pathway activation in neuroinflammation and oxidative stress.* CNS Neurol Disord Drug Targets, 2014. **13**(9): p. 1615-26.

269.   Macaione, V., et al., *RAGE-NF-kappaB pathway activation in response to oxidative stress in facioscapulohumeral muscular dystrophy.* Acta Neurol Scand, 2007. **115**(2): p. 115-21.

270.   Monici, M.C., et al., *Activation of nuclear factor-kappaB in inflammatory myopathies and Duchenne muscular dystrophy.* Neurology, 2003. **60**(6): p. 993-7.

271.   Neumann, A., et al., *High molecular weight hyaluronic acid inhibits advanced glycation endproduct-induced NF-kappaB activation and cytokine expression.* FEBS Lett, 1999. **453**(3): p. 283-7.

272.   Tanaka, N., et al., *The receptor for advanced glycation end products is induced by the glycation products themselves and tumor necrosis factor-alpha through nuclear factor-kappa B, and by 17beta-estradiol through Sp-1 in human vascular endothelial cells.* J Biol Chem, 2000. **275**(33): p. 25781-90.

273.   He, H.Q., et al., *Advanced glycation endproducts regulate smooth muscle cells calcification in cultured HSMCs.* Int J Clin Exp Pathol, 2015. **8**(10): p. 12260-7.

274.   Clayton, K.A., A.A. Van Enoo, and T. Ikezu, *Alzheimer's Disease: The Role of Microglia in Brain Homeostasis and Proteopathy.* Front Neurosci, 2017. **11**: p. 680.

275.   Schmidt, A.M., et al., *Activation of receptor for advanced glycation end products: a mechanism for chronic vascular dysfunction in diabetic vasculopathy and atherosclerosis.* Circ Res, 1999. **84**(5): p. 489-97.

276.   Huttunen, H.J., C. Fages, and H. Rauvala, *Receptor for advanced glycation end products (RAGE)-mediated neurite outgrowth and activation of NF-kappaB require the cytoplasmic domain of the receptor but different downstream signaling pathways.* J Biol Chem, 1999. **274**(28): p. 19919-24.

277.   de la Maza, M.P., et al., *Weight increase is associated with skeletal muscle immunostaining for advanced glycation end products, receptor for advanced glycation end products, and oxidation injury.* Rejuvenation Res, 2008. **11**(6): p. 1041-8.

278.   *Receptor for advanced glycation end products (RAGEs) and experimental diabetic neuropathy. Diabetes 2008;57:1002-1017. DOI: 10.2337/db07-0339.* Diabetes, 2014. **63**(5): p. 1817.

279.   Lue, L.F., et al., *Receptor for advanced glycation end products: its role in Alzheimer's disease and other neurological diseases.* Future Neurol, 2009. **4**(2): p. 167-177.

280.   Yan, S.F., R. Ramasamy, and A.M. Schmidt, *The RAGE axis: a fundamental mechanism signaling danger to the vulnerable vasculature.* Circ Res, 2010. **106**(5): p. 842-53.

281.   Han, S.H., Y.H. Kim, and I. Mook-Jung, *RAGE: the beneficial and deleterious effects by diverse mechanisms of actions.* Mol Cells, 2011. **31**(2): p. 91-7.

282.   Aftab, M.F., et al., *A bis-Schiff base of isatin improves methylglyoxal mediated insulin resistance in skeletal muscle cells.* Arch Pharm Res, 2015.

283.   Chiu, C.Y., et al., *Advanced glycation end-products induce skeletal muscle atrophy and dysfunction in diabetic mice via a RAGE-mediated, AMPK-down-regulated, Akt pathway.* J Pathol, 2016. **238**(3): p. 470-82.

284.   Muth, I.E., et al., *HMGB1 and RAGE in skeletal muscle inflammation: Implications for protein accumulation in inclusion body myositis.* Exp Neurol, 2015. **271**: p. 189-97.

285.   Son, M., et al., *Age dependent accumulation patterns of advanced glycation end product receptor (RAGE) ligands and binding intensities between RAGE and its ligands differ in the liver, kidney, and skeletal muscle.* Immun Ageing, 2017. **14**: p. 12.

286.   Serrao, P.R., et al., *Expression of receptors of advanced glycation end product (RAGE) and types I, III and IV collagen in the vastus lateralis muscle of men in early stages of knee osteoarthritis.* Connect Tissue Res, 2014. **55**(5-6): p. 331-8.

287.   Riuzzi, F., et al., *S100B engages RAGE or bFGF/FGFR1 in myoblasts depending on its own concentration and myoblast density. Implications for muscle regeneration.* PLoS One, 2012. **7**(1): p. e28700.

288.   Sorci, G., et al., *S100B protein in tissue development, repair and regeneration.* World J Biol Chem, 2013. **4**(1): p. 1-12.

289.   Tafani, M., et al., *Hypoxia-increased RAGE and P2X7R expression regulates tumor cell invasion through phosphorylation of Erk1/2 and Akt and nuclear translocation of NF-{kappa}B.* Carcinogenesis, 2011. **32**(8): p. 1167-75.

290.   Kim, T.N., et al., *The association of low muscle mass with soluble receptor for advanced glycation end products (sRAGE): The Korean Sarcopenic Obesity Study (KSOS).* Diabetes Metab Res Rev, 2018. **34**(3).

291.   Miranda, E.R., et al., *Circulating soluble RAGE isoforms are attenuated in obese, impaired-glucose-tolerant individuals and are associated with the development of type 2 diabetes.* Am J Physiol Endocrinol Metab, 2017. **313**(6): p. E631-e640.

292.   Larkin, D.J., et al., *Inflammatory markers associated with osteoarthritis after destabilization surgery in young mice with and without Receptor for Advanced Glycation End-products (RAGE).* Front Physiol, 2013. **4**: p. 121.

293.   Mattiello-Sverzut, A.C., et al., *Morphological adaptation of muscle collagen and receptor of advanced glycation end product (RAGE) in osteoarthritis patients with 12 weeks of resistance training: influence of anti-inflammatory or glucosamine treatment.* Rheumatol Int, 2013. **33**(9): p. 2215-24.

294.   Basta, G., et al., *Elevated soluble receptor for advanced glycation end product levels in patients with acute coronary syndrome and positive cardiac troponin I.* Coron Artery Dis, 2011. **22**(8): p. 590-4.

295.   Falcone, C., et al., *Plasma levels of soluble receptor for advanced glycation end products and coronary atherosclerosis: possible correlation with clinical presentation.* Dis Markers, 2013. **35**(3): p. 135-40.

296.   Jensen, L.J., A. Flyvbjerg, and M. Bjerre, *Soluble Receptor for Advanced Glycation End Product: A Biomarker for Acute Coronary Syndrome.* Biomed Res Int, 2015. **2015**: p. 815942.

297.   Sakaguchi, M., et al., *Signal Diversity of Receptor for Advanced Glycation End Products.* Acta Med Okayama, 2017. **71**(6): p. 459-465.

298.   Dulyaninova, N.G., et al., *S100A4 regulates macrophage invasion by distinct myosin-dependent and myosin-independent mechanisms.* Mol Biol Cell, 2018. **29**(5): p. 632-642.

299. Gebhardt, C., et al., *RAGE signaling sustains inflammation and promotes tumor development.* J Exp Med, 2008. **205**(2): p. 275-85.

300. Tubaro, C., et al., *S100B protein in myoblasts modulates myogenic differentiation via NF-kappaB-dependent inhibition of MyoD expression.* J Cell Physiol, 2010. **223**(1): p. 270-82.

301. Volpe, C.M.O., et al., *Cellular death, reactive oxygen species (ROS) and diabetic complications.* Cell Death Dis, 2018. **9**(2): p. 119.

302. Yan, S.D., et al., *Enhanced cellular oxidant stress by the interaction of advanced glycation end products with their receptors/binding proteins.* J Biol Chem, 1994. **269**(13): p. 9889-97.

303. Thomas, M.C., et al., *Interactions between renin angiotensin system and advanced glycation in the kidney.* J Am Soc Nephrol, 2005. **16**(10): p. 2976-84.

304. Feng, J.X., et al., *Restricted intake of dietary advanced glycation end products retards renal progression in the remnant kidney model.* Kidney Int, 2007. **71**(9): p. 901-11.

305. Schmidt, A.M., et al., *RAGE: a novel cellular receptor for advanced glycation end products.* Diabetes, 1996. **45 Suppl 3**: p. S77-80.

306. Xu, L., et al., *Inhibition of autophagy increased AGE/ROS-mediated apoptosis in mesangial cells.* Cell Death Dis, 2016. **7**(11): p. e2445.

307. Sivitz, W.I. and M.A. Yorek, *Mitochondrial dysfunction in diabetes: from molecular mechanisms to functional significance and therapeutic opportunities.* Antioxid Redox Signal, 2010. **12**(4): p. 537-77.

308. Chen, Y.H., et al., *AGE/RAGE-Induced EMP Release via the NOX-Derived ROS Pathway.* J Diabetes Res, 2018. **2018**: p. 6823058.

309. Powers, S.K., et al., *Reactive oxygen species: impact on skeletal muscle.* Compr Physiol, 2011. **1**(2): p. 941-69.

310. Powers, S.K. and M.J. Jackson, *Exercise-induced oxidative stress: cellular mechanisms and impact on muscle force production.* Physiol Rev, 2008. **88**(4): p. 1243-76.

311.	Reid, M.B., *Nitric oxide, reactive oxygen species, and skeletal muscle contraction.* Med Sci Sports Exerc, 2001. **33**(3): p. 371-6.

312.	Smith, M.A. and M.B. Reid, *Redox modulation of contractile function in respiratory and limb skeletal muscle.* Respir Physiol Neurobiol, 2006. **151**(2-3): p. 229-41.

313.	Ferreira, L.F. and O. Laitano, *Regulation of NADPH oxidases in skeletal muscle.* Free Radic Biol Med, 2016. **98**: p. 18-28.

314.	Cunha, T.F., et al., *Exercise training decreases NADPH oxidase activity and restores skeletal muscle mass in heart failure rats.* J Appl Physiol (1985), 2017. **122**(4): p. 817-827.

315.	Shadel, G.S. and T.L. Horvath, *Mitochondrial ROS signaling in organismal homeostasis.* Cell, 2015. **163**(3): p. 560-9.

316.	Cortassa, S., et al., *A mitochondrial oscillator dependent on reactive oxygen species.* Biophys J, 2004. **87**(3): p. 2060-73.

317.	Hoffmann, S., et al., *Reactive oxygen species derived from the mitochondrial respiratory chain are not responsible for the basal levels of oxidative base modifications observed in nuclear DNA of Mammalian cells.* Free Radic Biol Med, 2004. **36**(6): p. 765-73.

318.	Jastroch, M., et al., *Mitochondrial proton and electron leaks.* Essays Biochem, 2010. **47**: p. 53-67.

319.	Fisher-Wellman, K.H. and P.D. Neufer, *Linking mitochondrial bioenergetics to insulin resistance via redox biology.* Trends Endocrinol Metab, 2012. **23**(3): p. 142-53.

320.	St-Pierre, J., et al., *Topology of superoxide production from different sites in the mitochondrial electron transport chain.* J Biol Chem, 2002. **277**(47): p. 44784-90.

321.	Poljsak, B., D. Suput, and I. Milisav, *Achieving the balance between ROS and antioxidants: when to use the synthetic antioxidants.* Oxid Med Cell Longev, 2013. **2013**: p. 956792.

322.	Rani, V., et al., *Oxidative stress and metabolic disorders: Pathogenesis and therapeutic strategies.* Life Sci, 2016. **148**: p. 183-93.

323.   Newsholme, P., et al., *Molecular mechanisms of ROS production and oxidative stress in diabetes.* Biochem J, 2016. **473**(24): p. 4527-4550.

324.   Coughlan, M.T., et al., *RAGE-induced cytosolic ROS promote mitochondrial superoxide generation in diabetes.* J Am Soc Nephrol, 2009. **20**(4): p. 742-52.

325.   Marchi, S., et al., *Mitochondria-ros crosstalk in the control of cell death and aging.* J Signal Transduct, 2012. **2012**: p. 329635.

326.   Suzuki, Y., et al., *Galectin-3 but not galectin-1 induces mast cell death by oxidative stress and mitochondrial permeability transition.* Biochim Biophys Acta, 2008. **1783**(5): p. 924-34.

327.   Yamagishi, S., et al., *Role of advanced glycation end products (AGEs) and oxidative stress in vascular complications in diabetes.* Biochim Biophys Acta, 2012. **1820**(5): p. 663-71.

328.   Koulis, C., et al., *Linking RAGE and Nox in diabetic micro- and macrovascular complications.* Diabetes Metab, 2015. **41**(4): p. 272-81.

329.   Thallas-Bonke, V., et al., *Inhibition of NADPH oxidase prevents advanced glycation end product-mediated damage in diabetic nephropathy through a protein kinase C-alpha-dependent pathway.* Diabetes, 2008. **57**(2): p. 460-9.

330.   Zhang, M., et al., *Glycated proteins stimulate reactive oxygen species production in cardiac myocytes: involvement of Nox2 (gp91phox)-containing NADPH oxidase.* Circulation, 2006. **113**(9): p. 1235-43.

331.   Metz, T.O., et al., *Pyridoxamine, an inhibitor of advanced glycation and lipoxidation reactions: a novel therapy for treatment of diabetic complications.* Arch Biochem Biophys, 2003. **419**(1): p. 41-9.

332.   Takeuchi, M., et al., *Immunological detection of a novel advanced glycation end-product.* Mol Med, 2001. **7**(11): p. 783-91.

333.   Monnier, V.M., R.R. Kohn, and A. Cerami, *Accelerated age-related browning of human collagen in diabetes mellitus.* Proc Natl Acad Sci U S A, 1984. **81**(2): p. 583-7.

334.   Kierdorf, K. and G. Fritz, *RAGE regulation and signaling in inflammation and beyond.* J Leukoc Biol, 2013. **94**(1): p. 55-68.

335. Bongarzone, S., et al., *Targeting the Receptor for Advanced Glycation Endproducts (RAGE): A Medicinal Chemistry Perspective.* J Med Chem, 2017. **60**(17): p. 7213-7232.

336. Rai, V., et al., *Signal transduction in receptor for advanced glycation end products (RAGE): solution structure of C-terminal rage (ctRAGE) and its binding to mDia1.* J Biol Chem, 2012. **287**(7): p. 5133-44.

337. Kuhn, S. and M. Geyer, *Formins as effector proteins of Rho GTPases.* Small GTPases, 2014. **5**: p. e29513.

338. Young, K.G. and J.W. Copeland, *Formins in cell signaling.* Biochim Biophys Acta, 2010. **1803**(2): p. 183-90.

339. Wallar, B.J. and A.S. Alberts, *The formins: active scaffolds that remodel the cytoskeleton.* Trends Cell Biol, 2003. **13**(8): p. 435-46.

340. Watanabe, N., et al., *p140mDia, a mammalian homolog of Drosophila diaphanous, is a target protein for Rho small GTPase and is a ligand for profilin.* Embo j, 1997. **16**(11): p. 3044-56.

341. Wasserman, S., *FH proteins as cytoskeletal organizers.* Trends Cell Biol, 1998. **8**(3): p. 111-5.

342. Toure, F., et al., *Formin mDia1 mediates vascular remodeling via integration of oxidative and signal transduction pathways.* Circ Res, 2012. **110**(10): p. 1279-93.

343. Chojnacka, K. and D.D. Mruk, *The Src non-receptor tyrosine kinase paradigm: New insights into mammalian Sertoli cell biology.* Mol Cell Endocrinol, 2015. **415**: p. 133-42.

344. Ishizawar, R. and S.J. Parsons, *c-Src and cooperating partners in human cancer.* Cancer Cell, 2004. **6**(3): p. 209-14.

345. Abram, C.L. and S.A. Courtneidge, *Src family tyrosine kinases and growth factor signaling.* Exp Cell Res, 2000. **254**(1): p. 1-13.

346. Kawasaki, B.T., Y. Liao, and L. Birnbaumer, *Role of Src in C3 transient receptor potential channel function and evidence for a heterogeneous makeup of receptor- and store-operated Ca2+ entry channels.* Proc Natl Acad Sci U S A, 2006. **103**(2): p. 335-40.

347. Thomas, S.M. and J.S. Brugge, *Cellular functions regulated by Src family kinases.* Annu Rev Cell Dev Biol, 1997. **13**: p. 513-609.

348. Xu, W., S.C. Harrison, and M.J. Eck, *Three-dimensional structure of the tyrosine kinase c-Src.* Nature, 1997. **385**(6617): p. 595-602.

349. Okada, M. and H. Nakagawa, *A protein tyrosine kinase involved in regulation of pp60c-src function.* J Biol Chem, 1989. **264**(35): p. 20886-93.

350. Senis, Y.A., A. Mazharian, and J. Mori, *Src family kinases: at the forefront of platelet activation.* Blood, 2014. **124**(13): p. 2013-24.

351. Nada, S., et al., *Cloning of a complementary DNA for a protein-tyrosine kinase that specifically phosphorylates a negative regulatory site of p60c-src.* Nature, 1991. **351**(6321): p. 69-72.

352. Joukov, V., et al., *Identification of csk tyrosine phosphorylation sites and a tyrosine residue important for kinase domain structure.* Biochem J, 1997. **322 (Pt 3)**: p. 927-35.

353. Kmiecik, T.E. and D. Shalloway, *Activation and suppression of pp60c-src transforming ability by mutation of its primary sites of tyrosine phosphorylation.* Cell, 1987. **49**(1): p. 65-73.

354. Han, B., et al., *Conversion of mechanical force into biochemical signaling.* J Biol Chem, 2004. **279**(52): p. 54793-801.

355. Shao, X., et al., *Mechanical stimulation induces formin-dependent assembly of a perinuclear actin rim.* Proc Natl Acad Sci U S A, 2015. **112**(20): p. E2595-601.

356. Iba, H., et al., *Rous sarcoma virus variants that carry the cellular src gene instead of the viral src gene cannot transform chicken embryo fibroblasts.* Proc Natl Acad Sci U S A, 1984. **81**(14): p. 4424-8.

357. Johnson, L.N., M.E. Noble, and D.J. Owen, *Active and inactive protein kinases: structural basis for regulation.* Cell, 1996. **85**(2): p. 149-58.

358. Ristow, M., et al., *Antioxidants prevent health-promoting effects of physical exercise in humans.* Proc Natl Acad Sci U S A, 2009. **106**(21): p. 8665-70.

359. Yang, S.J., et al., *Activation of Akt by advanced glycation end products (AGEs): involvement of IGF-1 receptor and caveolin-1*. PLoS One, 2013. **8**(3): p. e58100.

360. Warboys, C.M., H.B. Toh, and P.A. Fraser, *Role of NADPH oxidase in retinal microvascular permeability increase by RAGE activation.* Invest Ophthalmol Vis Sci, 2009. **50**(3): p. 1319-28.

361. Zhang, W., et al., *Role of Src in Vascular Hyperpermeability Induced by Advanced Glycation End Products.* Sci Rep, 2015. **5**: p. 14090.

362. Allen, D.G., et al., *Calcium and the damage pathways in muscular dystrophy.* Can J Physiol Pharmacol, 2010. **88**(2): p. 83-91.

363. Whitehead, N.P., et al., *Skeletal muscle NADPH oxidase is increased and triggers stretch-induced damage in the mdx mouse.* PLoS One, 2010. **5**(12): p. e15354.

364. Pal, R., et al., *Src-dependent impairment of autophagy by oxidative stress in a mouse model of Duchenne muscular dystrophy.* Nat Commun, 2014. **5**: p. 4425.

365. Cai, W., et al., *AGER1 regulates endothelial cell NADPH oxidase-dependent oxidant stress via PKC-delta: implications for vascular disease.* Am J Physiol Cell Physiol, 2010. **298**(3): p. C624-34.

366. Gianni, D., et al., *The involvement of the tyrosine kinase c-Src in the regulation of reactive oxygen species generation mediated by NADPH oxidase-1.* Mol Biol Cell, 2008. **19**(7): p. 2984-94.

367. Brooks, S.V., et al., *Repeated bouts of aerobic exercise lead to reductions in skeletal muscle free radical generation and nuclear factor kappaB activation.* J Physiol, 2008. **586**(16): p. 3979-90.

368. Henriquez-Olguin, C., et al., *Altered ROS production, NF-kappaB activation and interleukin-6 gene expression induced by electrical stimulation in dystrophic mdx skeletal muscle cells.* Biochim Biophys Acta, 2015. **1852**(7): p. 1410-9.

369. Crosswhite, P. and Z. Sun, *Nitric oxide, oxidative stress and inflammation in pulmonary arterial hypertension.* J Hypertens, 2010. **28**(2): p. 201-12.

370. Brown, D.I. and K.K. Griendling, *Regulation of signal transduction by reactive oxygen species in the cardiovascular system.* Circ Res, 2015. **116**(3): p. 531-49.

371. Skonieczna, M., et al., *NADPH Oxidases: Insights into Selected Functions and Mechanisms of Action in Cancer and Stem Cells.* Oxid Med Cell Longev, 2017. **2017**: p. 9420539.

372. El-Benna, J., P.M. Dang, and M.A. Gougerot-Pocidalo, *Role of the NADPH oxidase systems Nox and Duox in host defense and inflammation.* Expert Rev Clin Immunol, 2007. **3**(2): p. 111-5.

373. Sumimoto, H., *Structure, regulation and evolution of Nox-family NADPH oxidases that produce reactive oxygen species.* Febs j, 2008. **275**(13): p. 3249-77.

374. Lassegue, B. and K.K. Griendling, *NADPH oxidases: functions and pathologies in the vasculature.* Arterioscler Thromb Vasc Biol, 2010. **30**(4): p. 653-61.

375. Jiang, F., et al., *Systemic upregulation of NADPH oxidase in diet-induced obesity in rats.* Redox Rep, 2011. **16**(6): p. 223-9.

376. Gill, P.S. and C.S. Wilcox, *NADPH oxidases in the kidney.* Antioxid Redox Signal, 2006. **8**(9-10): p. 1597-607.

377. Liang, S., T. Kisseleva, and D.A. Brenner, *The Role of NADPH Oxidases (NOXs) in Liver Fibrosis and the Activation of Myofibroblasts.* Front Physiol, 2016. **7**: p. 17.

378. Geiszt, M. and T.L. Leto, *The Nox family of NAD(P)H oxidases: host defense and beyond.* J Biol Chem, 2004. **279**(50): p. 51715-8.

379. Hidalgo, C., et al., *A transverse tubule NADPH oxidase activity stimulates calcium release from isolated triads via ryanodine receptor type 1 S -glutathionylation.* J Biol Chem, 2006. **281**(36): p. 26473-82.

380. Hidalgo, C., *Cross talk between Ca2+ and redox signalling cascades in muscle and neurons through the combined activation of ryanodine receptors/Ca2+ release channels.* Philos Trans R Soc Lond B Biol Sci, 2005. **360**(1464): p. 2237-46.

381. Okutsu, M., et al., *Extracellular superoxide dismutase ameliorates skeletal muscle abnormalities, cachexia, and exercise intolerance in mice with congestive heart failure.* Circ Heart Fail, 2014. **7**(3): p. 519-30.

382. Souto Padron de Figueiredo, A., et al., *Nox2 mediates skeletal muscle insulin resistance induced by a high fat diet.* J Biol Chem, 2015. **290**(21): p. 13427-39.

383. Nauseef, W.M., *Assembly of the phagocyte NADPH oxidase.* Histochem Cell Biol, 2004. **122**(4): p. 277-91.

384. Sun, Q.A., et al., *Oxygen-coupled redox regulation of the skeletal muscle ryanodine receptor-Ca2+ release channel by NADPH oxidase 4.* Proc Natl Acad Sci U S A, 2011. **108**(38): p. 16098-103.

385. Groemping, Y., et al., *Molecular basis of phosphorylation-induced activation of the NADPH oxidase.* Cell, 2003. **113**(3): p. 343-55.

386. Sumimoto, H., et al., *Assembly and activation of the phagocyte NADPH oxidase. Specific interaction of the N-terminal Src homology 3 domain of p47phox with p22phox is required for activation of the NADPH oxidase.* J Biol Chem, 1996. **271**(36): p. 22152-8.

387. Groemping, Y. and K. Rittinger, *Activation and assembly of the NADPH oxidase: a structural perspective.* Biochem J, 2005. **386**(Pt 3): p. 401-16.

388. Massenet, C., et al., *Effects of p47phox C terminus phosphorylations on binding interactions with p40phox and p67phox. Structural and functional comparison of p40phox and p67phox SH3 domains.* J Biol Chem, 2005. **280**(14): p. 13752-61.

389. Yuzawa, S., et al., *A molecular mechanism for autoinhibition of the tandem SH3 domains of p47phox, the regulatory subunit of the phagocyte NADPH oxidase.* Genes Cells, 2004. **9**(5): p. 443-56.

390. Vignais, P.V., *The superoxide-generating NADPH oxidase: structural aspects and activation mechanism.* Cell Mol Life Sci, 2002. **59**(9): p. 1428-59.

391. Lapouge, K., et al., *Architecture of the p40-p47-p67phox complex in the resting state of the NADPH oxidase. A central role for p67phox.* J Biol Chem, 2002. **277**(12): p. 10121-8.

392. Kami, K., et al., *Diverse recognition of non-PxxP peptide ligands by the SH3 domains from p67(phox), Grb2 and Pex13p.* Embo j, 2002. **21**(16): p. 4268-76.

393. el Benna, J., L.P. Faust, and B.M. Babior, *The phosphorylation of the respiratory burst oxidase component p47phox during neutrophil activation. Phosphorylation of sites recognized by protein kinase C and by proline-directed kinases.* J Biol Chem, 1994. **269**(38): p. 23431-6.

394. Faust, L.R., et al., *The phosphorylation targets of p47phox, a subunit of the respiratory burst oxidase. Functions of the individual target serines as evaluated by site-directed mutagenesis.* J Clin Invest, 1995. **96**(3): p. 1499-505.

395. Hare, J.M., F. Beigi, and K. Tziomalos, *Nitric oxide and cardiobiology-methods for intact hearts and isolated myocytes.* Methods Enzymol, 2008. **441**: p. 369-92.

396. Riganti, C., et al., *Diphenyleneiodonium inhibits the cell redox metabolism and induces oxidative stress.* J Biol Chem, 2004. **279**(46): p. 47726-31.

397. Lassegue, B., A. San Martin, and K.K. Griendling, *Biochemistry, physiology, and pathophysiology of NADPH oxidases in the cardiovascular system.* Circ Res, 2012. **110**(10): p. 1364-90.

398. Schroder, K., N. Weissmann, and R.P. Brandes, *Organizers and activators: Cytosolic Nox proteins impacting on vascular function.* Free Radic Biol Med, 2017. **109**: p. 22-32.

399. Dorseuil, O., M.T. Quinn, and G.M. Bokoch, *Dissociation of Rac translocation from p47phox/p67phox movements in human neutrophils by tyrosine kinase inhibitors.* J Leukoc Biol, 1995. **58**(1): p. 108-13.

400. Bokoch, G.M., B.P. Bohl, and T.H. Chuang, *Guanine nucleotide exchange regulates membrane translocation of Rac/Rho GTP-binding proteins.* J Biol Chem, 1994. **269**(50): p. 31674-9.

401. El-Benna, J., et al., *p47phox, the phagocyte NADPH oxidase/NOX2 organizer: structure, phosphorylation and implication in diseases.* Exp Mol Med, 2009. **41**(4): p. 217-25.

402. von Lohneysen, K., et al., *Structural insights into Nox4 and Nox2: motifs involved in function and cellular localization.* Mol Cell Biol, 2010. **30**(4): p. 961-75.

403. Lomax, K.J., et al., *Recombinant 47-kilodalton cytosol factor restores NADPH oxidase in chronic granulomatous disease.* Science, 1989. **245**(4916): p. 409-12.

404. de Mendez, I., N. Homayounpour, and T.L. Leto, *Specificity of p47phox SH3 domain interactions in NADPH oxidase assembly and activation.* Mol Cell Biol, 1997. **17**(4): p. 2177-85.

405. Hiroaki, H., et al., *Solution structure of the PX domain, a target of the SH3 domain.* Nat Struct Biol, 2001. **8**(6): p. 526-30.

406. Fuchs, A., M.C. Dagher, and P.V. Vignais, *Mapping the domains of interaction of p40phox with both p47phox and p67phox of the neutrophil oxidase complex using the two-hybrid system.* J Biol Chem, 1995. **270**(11): p. 5695-7.

407. Inanami, O., et al., *Activation of the leukocyte NADPH oxidase by phorbol ester requires the phosphorylation of p47PHOX on serine 303 or 304.* J Biol Chem, 1998. **273**(16): p. 9539-43.

408. Babior, B.M., *Oxidants from phagocytes: agents of defense and destruction.* Blood, 1984. **64**(5): p. 959-66.

409. Babior, B.M., *NADPH oxidase: an update.* Blood, 1999. **93**(5): p. 1464-76.

410. Dang, P.M., et al., *Protein kinase C zeta phosphorylates a subset of selective sites of the NADPH oxidase component p47phox and participates in formyl peptide-mediated neutrophil respiratory burst.* J Immunol, 2001. **166**(2): p. 1206-13.

411. Wei, Y., et al., *Angiotensin II-induced NADPH oxidase activation impairs insulin signaling in skeletal muscle cells.* J Biol Chem, 2006. **281**(46): p. 35137-46.

412. Touyz, R.M., G. Yao, and E.L. Schiffrin, *c-Src induces phosphorylation and translocation of p47phox: role in superoxide generation by angiotensin II in human vascular smooth muscle cells.* Arterioscler Thromb Vasc Biol, 2003. **23**(6): p. 981-7.

413. Yang, H., et al., *Up-regulation of Heme Oxygenase-1 by Korean Red Ginseng Water Extract as a Cytoprotective Effect in Human Endothelial Cells.* J Ginseng Res, 2011. **35**(3): p. 352-9.

414. Chowdhury, A.K., et al., *Src-mediated tyrosine phosphorylation of p47phox in hyperoxia-induced activation of NADPH oxidase and generation of reactive oxygen species in lung endothelial cells.* J Biol Chem, 2005. **280**(21): p. 20700-11.

415. Gupte, S.A., et al., *Peroxide generation by p47phox-Src activation of Nox2 has a key role in protein kinase C-induced arterial smooth muscle contraction.* Am J Physiol Heart Circ Physiol, 2009. **296**(4): p. H1048-57.

416. Wang, Z., et al., *Alveolar macrophages from septic mice promote polymorphonuclear leukocyte transendothelial migration via an endothelial cell Src kinase/NADPH oxidase pathway.* J Immunol, 2008. **181**(12): p. 8735-44.

417.   Karihtala, P. and Y. Soini, *Reactive oxygen species and antioxidant mechanisms in human tissues and their relation to malignancies.* Apmis, 2007. **115**(2): p. 81-103.

418.   Varga, Z.V., et al., *Interplay of oxidative, nitrosative/nitrative stress, inflammation, cell death and autophagy in diabetic cardiomyopathy.* Biochim Biophys Acta, 2015. **1852**(2): p. 232-42.

419.   Hare, J.M. and J.S. Stamler, *NO/redox disequilibrium in the failing heart and cardiovascular system.* J Clin Invest, 2005. **115**(3): p. 509-17.

420.   Allen, J.F., *Redox control of transcription: sensors, response regulators, activators and repressors.* FEBS Lett, 1993. **332**(3): p. 203-7.

421.   Bartosz, G., *Reactive oxygen species: destroyers or messengers?* Biochem Pharmacol, 2009. **77**(8): p. 1303-15.

422.   Lander, H.M., *An essential role for free radicals and derived species in signal transduction.* Faseb j, 1997. **11**(2): p. 118-24.

423.   Loschen, G., et al., *Superoxide radicals as precursors of mitochondrial hydrogen peroxide.* FEBS Lett, 1974. **42**(1): p. 68-72.

424.   Cho, K.J., J.M. Seo, and J.H. Kim, *Bioactive lipoxygenase metabolites stimulation of NADPH oxidases and reactive oxygen species.* Mol Cells, 2011. **32**(1): p. 1-5.

425.   Singh, I., *Biochemistry of peroxisomes in health and disease.* Mol Cell Biochem, 1997. **167**(1-2): p. 1-29.

426.   Loh, K., et al., *Reactive oxygen species enhance insulin sensitivity.* Cell Metab, 2009. **10**(4): p. 260-72.

427.   Monaghan-Benson, E. and K. Burridge, *The regulation of vascular endothelial growth factor-induced microvascular permeability requires Rac and reactive oxygen species.* J Biol Chem, 2009. **284**(38): p. 25602-11.

428.   McCord, J.M., R.S. Roy, and S.W. Schaffer, *Free radicals and myocardial ischemia. The role of xanthine oxidase.* Adv Myocardiol, 1985. **5**: p. 183-9.

429.   Freeman, B.A. and J.D. Crapo, *Biology of disease: free radicals and tissue injury.* Lab Invest, 1982. **47**(5): p. 412-26.

430.   Keller, M.A., G. Piedrafita, and M. Ralser, *The widespread role of non-enzymatic reactions in cellular metabolism.* Curr Opin Biotechnol, 2015. **34**: p. 153-61.

431.   Niki, E., *Free radicals in the 1900's: from in vitro to in vivo.* Free Radic Res, 2000. **33**(6): p. 693-704.

432.   Hamanaka, R.B. and N.S. Chandel, *Mitochondrial reactive oxygen species regulate cellular signaling and dictate biological outcomes.* Trends Biochem Sci, 2010. **35**(9): p. 505-13.

433.   Murphy, M.P., *How mitochondria produce reactive oxygen species.* Biochem J, 2009. **417**(1): p. 1-13.

434.   Maranzana, E., et al., *Mitochondrial respiratory supercomplex association limits production of reactive oxygen species from complex I.* Antioxid Redox Signal, 2013. **19**(13): p. 1469-80.

435.   Turrens, J.F. and A. Boveris, *Generation of superoxide anion by the NADH dehydrogenase of bovine heart mitochondria.* Biochem J, 1980. **191**(2): p. 421-7.

436.   Raha, S., et al., *Superoxides from mitochondrial complex III: the role of manganese superoxide dismutase.* Free Radic Biol Med, 2000. **29**(2): p. 170-80.

437.   Pizzino, G., et al., *Oxidative Stress: Harms and Benefits for Human Health.* Oxid Med Cell Longev, 2017. **2017**: p. 8416763.

438.   Kehrer, J.P. and L.O. Klotz, *Free radicals and related reactive species as mediators of tissue injury and disease: implications for Health.* Crit Rev Toxicol, 2015. **45**(9): p. 765-98.

439.   Hayyan, M., M.A. Hashim, and I.M. AlNashef, *Superoxide Ion: Generation and Chemical Implications.* Chem Rev, 2016. **116**(5): p. 3029-85.

440.   Foyer, C.H., M.H. Wilson, and M.H. Wright, *Redox regulation of cell proliferation: Bioinformatics and redox proteomics approaches to identify redox-sensitive cell cycle regulators.* Free Radic Biol Med, 2018.

441.   Novak, M.L. and T.J. Koh, *Phenotypic transitions of macrophages orchestrate tissue repair.* Am J Pathol, 2013. **183**(5): p. 1352-1363.

442.   Saclier, M., et al., *Monocyte/macrophage interactions with myogenic precursor cells during skeletal muscle regeneration.* Febs j, 2013. **280**(17): p. 4118-30.

443.   Chen, Y., et al., *[Role of NADPH oxidase in oxidative stress injury of human dermal fibroblasts].* Nan Fang Yi Ke Da Xue Xue Bao, 2016. **36**(3): p. 391-5.

444.   Stockwell, B.R., et al., *Ferroptosis: A Regulated Cell Death Nexus Linking Metabolism, Redox Biology, and Disease.* Cell, 2017. **171**(2): p. 273-285.

445.   Rodopulo, A.K., *[Oxidation of tartaric acid in wine in the presence of heavy metal salts (activation of oxygen by iron)].* Izv Akad Nauk SSSR Biol, 1951. **3**: p. 115-28.

446.   Radak, Z., et al., *Muscle soreness-induced reduction in force generation is accompanied by increased nitric oxide content and DNA damage in human skeletal muscle.* Free Radic Biol Med, 1999. **26**(7-8): p. 1059-63.

447.   Pacher, P., J.S. Beckman, and L. Liaudet, *Nitric oxide and peroxynitrite in health and disease.* Physiol Rev, 2007. **87**(1): p. 315-424.

448.   Beckman, J.S., *Oxidative damage and tyrosine nitration from peroxynitrite.* Chem Res Toxicol, 1996. **9**(5): p. 836-44.

449.   Pryor, W.A. and G.L. Squadrito, *The chemistry of peroxynitrite: a product from the reaction of nitric oxide with superoxide.* Am J Physiol, 1995. **268**(5 Pt 1): p. L699-722.

450.   Radak, Z., et al., *Exercise, oxidative stress and hormesis.* Ageing Res Rev, 2008. **7**(1): p. 34-42.

451.   Pattwell, D.M., et al., *Release of reactive oxygen and nitrogen species from contracting skeletal muscle cells.* Free Radic Biol Med, 2004. **37**(7): p. 1064-72.

452.   Lennicke, C., et al., *Hydrogen peroxide - production, fate and role in redox signaling of tumor cells.* Cell Commun Signal, 2015. **13**: p. 39.

453. Sies, H., *Hydrogen peroxide as a central redox signaling molecule in physiological oxidative stress: Oxidative eustress.* Redox Biol, 2017. **11**: p. 613-619.

454. Rhee, S.G., et al., *Cellular regulation by hydrogen peroxide.* J Am Soc Nephrol, 2003. **14**(8 Suppl 3): p. S211-5.

455. Yang, N.J. and M.J. Hinner, *Getting across the cell membrane: an overview for small molecules, peptides, and proteins.* Methods Mol Biol, 2015. **1266**: p. 29-53.

456. Zamocky, M., et al., *Molecular evolution of hydrogen peroxide degrading enzymes.* Arch Biochem Biophys, 2012. **525**(2): p. 131-44.

457. Okuda, S., et al., *Hydrogen peroxide-mediated neuronal cell death induced by an endogenous neurotoxin, 3-hydroxykynurenine.* Proc Natl Acad Sci U S A, 1996. **93**(22): p. 12553-8.

458. Winterbourn, C.C., *Toxicity of iron and hydrogen peroxide: the Fenton reaction.* Toxicol Lett, 1995. **82-83**: p. 969-74.

459. Fujimura, N., et al., *Effect of free radical scavengers on diaphragmatic contractility in septic peritonitis.* Am J Respir Crit Care Med, 2000. **162**(6): p. 2159-65.

460. Deng, Y. and Z.A. Almsherqi, *Evolution of cubic membranes as antioxidant defence system.* Interface Focus, 2015. **5**(4): p. 20150012.

461. Lubrano, V. and S. Balzan, *Enzymatic antioxidant system in vascular inflammation and coronary artery disease.* World J Exp Med, 2015. **5**(4): p. 218-24.

462. Halliwell, B., *Reactive species and antioxidants. Redox biology is a fundamental theme of aerobic life.* Plant Physiol, 2006. **141**(2): p. 312-22.

463. Halliwell, B., *How to characterize an antioxidant: an update.* Biochem Soc Symp, 1995. **61**: p. 73-101.

464. Zhan, C.D., et al., *Superoxide dismutase, catalase and glutathione peroxidase in the spontaneously hypertensive rat kidney: effect of antioxidant-rich diet.* J Hypertens, 2004. **22**(10): p. 2025-33.

465. Fukai, T. and M. Ushio-Fukai, *Superoxide dismutases: role in redox signaling, vascular function, and diseases.* Antioxid Redox Signal, 2011. **15**(6): p. 1583-606.

466. Kurutas, E.B., *The importance of antioxidants which play the role in cellular response against oxidative/nitrosative stress: current state.* Nutr J, 2016. **15**(1): p. 71.

467. Goldsteins, G., et al., *Deleterious role of superoxide dismutase in the mitochondrial intermembrane space.* J Biol Chem, 2008. **283**(13): p. 8446-52.

468. He, C., et al., *SOD2 and the Mitochondrial UPR: Partners Regulating Cellular Phenotypic Transitions.* Trends Biochem Sci, 2016. **41**(7): p. 568-577.

469. Laurila, J.P., et al., *Extracellular superoxide dismutase is a growth regulatory mediator of tissue injury recovery.* Mol Ther, 2009. **17**(3): p. 448-54.

470. Imlay, J.A., *Cellular defenses against superoxide and hydrogen peroxide.* Annu Rev Biochem, 2008. **77**: p. 755-76.

471. Phaniendra, A., D.B. Jestadi, and L. Periyasamy, *Free radicals: properties, sources, targets, and their implication in various diseases.* Indian J Clin Biochem, 2015. **30**(1): p. 11-26.

472. Noor, R., S. Mittal, and J. Iqbal, *Superoxide dismutase--applications and relevance to human diseases.* Med Sci Monit, 2002. **8**(9): p. Ra210-5.

473. Sies, H., *Role of metabolic H2O2 generation: redox signaling and oxidative stress.* J Biol Chem, 2014. **289**(13): p. 8735-41.

474. Fischbacher, A., C. von Sonntag, and T.C. Schmidt, *Hydroxyl radical yields in the Fenton process under various pH, ligand concentrations and hydrogen peroxide/Fe(II) ratios.* Chemosphere, 2017. **182**: p. 738-744.

475. Williams, J., *THE DECOMPOSITION OF HYDROGEN PEROXIDE BY LIVER CATALASE.* J Gen Physiol, 1928. **11**(4): p. 309-37.

476. Ray, G. and S.A. Husain, *Oxidants, antioxidants and carcinogenesis.* Indian J Exp Biol, 2002. **40**(11): p. 1213-32.

477.   Giordano, C.R., et al., *Catalase therapy corrects oxidative stress-induced pathophysiology in incipient diabetic retinopathy.* Invest Ophthalmol Vis Sci, 2015. **56**(5): p. 3095-102.

478.   Higuchi, M., et al., *Superoxide dismutase and catalase in skeletal muscle: adaptive response to exercise.* J Gerontol, 1985. **40**(3): p. 281-6.

479.   Steinbeck, M.J., et al., *Involvement of hydrogen peroxide in the differentiation of clonal HD-11EM cells into osteoclast-like cells.* J Cell Physiol, 1998. **176**(3): p. 574-87.

480.   Heck, D.E., et al., *Mechanisms of oxidant generation by catalase.* Ann N Y Acad Sci, 2010. **1203**: p. 120-5.

481.   Espinosa-Diez, C., et al., *Antioxidant responses and cellular adjustments to oxidative stress.* Redox Biol, 2015. **6**: p. 183-97.

482.   Escobar, J.A., M.A. Rubio, and E.A. Lissi, *Sod and catalase inactivation by singlet oxygen and peroxyl radicals.* Free Radic Biol Med, 1996. **20**(3): p. 285-90.

483.   Takemoto, K., et al., *Low catalase activity in blood is associated with the diabetes caused by alloxan.* Clin Chim Acta, 2009. **407**(1-2): p. 43-6.

484.   Bloch, K., et al., *Catalase expression in pancreatic alpha cells of diabetic and non-diabetic mice.* Histochem Cell Biol, 2007. **127**(2): p. 227-32.

485.   Miki, A., et al., *Divergent antioxidant capacity of human islet cell subsets: A potential cause of beta-cell vulnerability in diabetes and islet transplantation.* PLoS One, 2018. **13**(5): p. e0196570.

486.   Lubos, E., J. Loscalzo, and D.E. Handy, *Glutathione peroxidase-1 in health and disease: from molecular mechanisms to therapeutic opportunities.* Antioxid Redox Signal, 2011. **15**(7): p. 1957-97.

487.   Rotruck, J.T., et al., *Selenium: biochemical role as a component of glutathione peroxidase.* Science, 1973. **179**(4073): p. 588-90.

488.   Martinez, J.I., R.D. Garcia, and A.M. Galarza, *The kinetic mechanism of glutathione peroxidase from human platelets.* Thromb Res, 1982. **27**(2): p. 197-203.

489. Lu, S.C., *Regulation of glutathione synthesis.* Mol Aspects Med, 2009. **30**(1-2): p. 42-59.

490. Erden Inal, M., A. Akgun, and A. Kahraman, *The effects of exogenous glutathione on reduced glutathione level, glutathione peroxidase and glutathione reductase activities of rats with different ages and gender after whole-body Gamma-irradiation.* J Am Aging Assoc, 2003. **26**(3-4): p. 55-8.

491. Ray, P.D., B.W. Huang, and Y. Tsuji, *Reactive oxygen species (ROS) homeostasis and redox regulation in cellular signaling.* Cell Signal, 2012. **24**(5): p. 981-90.

492. Winterbourn, C.C. and M.B. Hampton, *Thiol chemistry and specificity in redox signaling.* Free Radic Biol Med, 2008. **45**(5): p. 549-61.

493. Finkel, T., *From sulfenylation to sulfhydration: what a thiolate needs to tolerate.* Sci Signal, 2012. **5**(215): p. pe10.

494. Rossi, F. and M. Zatti, *Biochemical aspects of phagocytosis in polymorphonuclear leucocytes. NADH and NADPH oxidation by the granules of resting and phagocytizing cells.* Experientia, 1964. **20**(1): p. 21-3.

495. Klebanoff, S.J., *Myeloperoxidase: contribution to the microbicidal activity of intact leukocytes.* Science, 1970. **169**(3950): p. 1095-7.

496. Furchgott, R.F. and J.V. Zawadzki, *The obligatory role of endothelial cells in the relaxation of arterial smooth muscle by acetylcholine.* Nature, 1980. **288**(5789): p. 373-6.

497. Fridovich, I., *The biology of oxygen radicals.* Science, 1978. **201**(4359): p. 875-80.

498. Harman, D., *The aging process.* Proc Natl Acad Sci U S A, 1981. **78**(11): p. 7124-8.

499. Powers, S.K., et al., *Reactive oxygen species are signalling molecules for skeletal muscle adaptation.* Exp Physiol, 2010. **95**(1): p. 1-9.

500. Reid, M.B., *Invited Review: redox modulation of skeletal muscle contraction: what we know and what we don't.* J Appl Physiol (1985), 2001. **90**(2): p. 724-31.

501. McArdle, A., et al., *Overexpression of HSP70 in mouse skeletal muscle protects against muscle damage and age-related muscle dysfunction.* Faseb j, 2004. **18**(2): p. 355-7.

502. Li, N. and M. Karin, *Is NF-kappaB the sensor of oxidative stress?* Faseb j, 1999. **13**(10): p. 1137-43.

503. Flohe, L., et al., *Redox regulation of NF-kappa B activation.* Free Radic Biol Med, 1997. **22**(6): p. 1115-26.

504. Ghosh, S. and M. Karin, *Missing pieces in the NF-kappaB puzzle.* Cell, 2002. **109 Suppl**: p. S81-96.

505. Klotz, L.O., et al., *Redox regulation of FoxO transcription factors.* Redox Biol, 2015. **6**: p. 51-72.

506. Sundaresan, M., et al., *Requirement for generation of H2O2 for platelet-derived growth factor signal transduction.* Science, 1995. **270**(5234): p. 296-9.

507. Juntilla, M.M., et al., *AKT1 and AKT2 maintain hematopoietic stem cell function by regulating reactive oxygen species.* Blood, 2010. **115**(20): p. 4030-8.

508. Turpaev, K.T., *Reactive oxygen species and regulation of gene expression.* Biochemistry (Mosc), 2002. **67**(3): p. 281-92.

509. Bentzinger, C.F., et al., *Cellular dynamics in the muscle satellite cell niche.* EMBO Rep, 2013. **14**(12): p. 1062-72.

510. Barbieri, E. and P. Sestili, *Reactive oxygen species in skeletal muscle signaling.* J Signal Transduct, 2012. **2012**: p. 982794.

511. Corcoran, A. and T.G. Cotter, *Redox regulation of protein kinases.* Febs j, 2013. **280**(9): p. 1944-65.

512. Lee, S.R., et al., *Reversible inactivation of protein-tyrosine phosphatase 1B in A431 cells stimulated with epidermal growth factor.* J Biol Chem, 1998. **273**(25): p. 15366-72.

513. Meng, T.C., T. Fukada, and N.K. Tonks, *Reversible oxidation and inactivation of protein tyrosine phosphatases in vivo.* Mol Cell, 2002. **9**(2): p. 387-99.

514. Heffetz, D., et al., *The insulinomimetic agents H2O2 and vanadate stimulate protein tyrosine phosphorylation in intact cells.* J Biol Chem, 1990. **265**(5): p. 2896-902.

515. Wray, C.J., et al., *Sepsis upregulates the gene expression of multiple ubiquitin ligases in skeletal muscle.* Int J Biochem Cell Biol, 2003. **35**(5): p. 698-705.

516. Espinosa, A., et al., *Myotube depolarization generates reactive oxygen species through NAD(P)H oxidase; ROS-elicited Ca2+ stimulates ERK, CREB, early genes.* J Cell Physiol, 2006. **209**(2): p. 379-88.

517. Ji, L.L., M.C. Gomez-Cabrera, and J. Vina, *Role of free radicals and antioxidant signaling in skeletal muscle health and pathology.* Infect Disord Drug Targets, 2009. **9**(4): p. 428-44.

518. Bouayed, J. and T. Bohn, *Exogenous antioxidants--Double-edged swords in cellular redox state: Health beneficial effects at physiologic doses versus deleterious effects at high doses.* Oxid Med Cell Longev, 2010. **3**(4): p. 228-37.

519. Le Lay, S., et al., *Oxidative stress and metabolic pathologies: from an adipocentric point of view.* Oxid Med Cell Longev, 2014. **2014**: p. 908539.

520. Sifuentes-Franco, S., et al., *The Role of Oxidative Stress, Mitochondrial Function, and Autophagy in Diabetic Polyneuropathy.* J Diabetes Res, 2017. **2017**: p. 1673081.

521. Gelderman, K.A., et al., *Rheumatoid arthritis: the role of reactive oxygen species in disease development and therapeutic strategies.* Antioxid Redox Signal, 2007. **9**(10): p. 1541-67.

522. Pop-Busui, R., A. Sima, and M. Stevens, *Diabetic neuropathy and oxidative stress.* Diabetes Metab Res Rev, 2006. **22**(4): p. 257-73.

523. Miranda-Diaz, A.G., et al., *Oxidative Stress in Diabetic Nephropathy with Early Chronic Kidney Disease.* J Diabetes Res, 2016. **2016**: p. 7047238.

524. Tibaut, M. and D. Petrovic, *Oxidative Stress Genes, Antioxidants and Coronary Artery Disease in Type 2 Diabetes Mellitus.* Cardiovasc Hematol Agents Med Chem, 2016. **14**(1): p. 23-38.

525. Standl, E., O. Schnell, and A. Ceriello, *Postprandial hyperglycemia and glycemic variability: should we care?* Diabetes Care, 2011. **34 Suppl 2**: p. S120-7.

526. Da Ros, R., R. Assaloni, and A. Ceriello, *Antioxidant therapy in diabetic complications: what is new?* Curr Vasc Pharmacol, 2004. **2**(4): p. 335-41.

527. Russell, A.P., et al., *Lipid peroxidation in skeletal muscle of obese as compared to endurance-trained humans: a case of good vs. bad lipids?* FEBS Lett, 2003. **551**(1-3): p. 104-6.

528. Jancic, S.A. and B.Z. Stosic, *Cadmium effects on the thyroid gland.* Vitam Horm, 2014. **94**: p. 391-425.

529. Njie-Mbye, Y.F., et al., *Lipid peroxidation: pathophysiological and pharmacological implications in the eye.* Front Physiol, 2013. **4**: p. 366.

530. Ingram, K.H., et al., *Skeletal muscle lipid peroxidation and insulin resistance in humans.* J Clin Endocrinol Metab, 2012. **97**(7): p. E1182-6.

531. Berlett, B.S. and E.R. Stadtman, *Protein oxidation in aging, disease, and oxidative stress.* J Biol Chem, 1997. **272**(33): p. 20313-6.

532. Chakravarti, B. and D.N. Chakravarti, *Oxidative modification of proteins: age-related changes.* Gerontology, 2007. **53**(3): p. 128-39.

533. Levine, R.L. and E.R. Stadtman, *Oxidative modification of proteins during aging.* Exp Gerontol, 2001. **36**(9): p. 1495-502.

534. Cadet, J. and J.R. Wagner, *DNA base damage by reactive oxygen species, oxidizing agents, and UV radiation.* Cold Spring Harb Perspect Biol, 2013. **5**(2).

535. Cadet, J. and J.R. Wagner, *Oxidatively generated base damage to cellular DNA by hydroxyl radical and one-electron oxidants: similarities and differences.* Arch Biochem Biophys, 2014. **557**: p. 47-54.

536. Blaak, E.E., *Metabolic fluxes in skeletal muscle in relation to obesity and insulin resistance.* Best Pract Res Clin Endocrinol Metab, 2005. **19**(3): p. 391-403.

537. Katsuki, A., et al., *Increased oxidative stress is associated with serum levels of triglyceride, insulin resistance, and hyperinsulinemia in Japanese metabolically obese, normal-weight men.* Diabetes Care, 2004. **27**(2): p. 631-2.

538.   Golovchenko, I., et al., *Hyperinsulinemia enhances transcriptional activity of nuclear factor-kappaB induced by angiotensin II, hyperglycemia, and advanced glycosylation end products in vascular smooth muscle cells.* Circ Res, 2000. **87**(9): p. 746-52.

539.   Kyselova, P., et al., *Hyperinsulinemia and oxidative stress.* Physiol Res, 2002. **51**(6): p. 591-5.

540.   Giugliano, D., A. Ceriello, and G. Paolisso, *Diabetes mellitus, hypertension, and cardiovascular disease: which role for oxidative stress?* Metabolism, 1995. **44**(3): p. 363-8.

541.   Habib, M.P., F.D. Dickerson, and A.D. Mooradian, *Effect of diabetes, insulin, and glucose load on lipid peroxidation in the rat.* Metabolism, 1994. **43**(11): p. 1442-5.

542.   Krieger-Brauer, H.I. and H. Kather, *Human fat cells possess a plasma membrane-bound H2O2-generating system that is activated by insulin via a mechanism bypassing the receptor kinase.* J Clin Invest, 1992. **89**(3): p. 1006-13.

543.   Facchini, F.S., et al., *Hyperinsulinemia: the missing link among oxidative stress and age-related diseases?* Free Radic Biol Med, 2000. **29**(12): p. 1302-6.

544.   Wind, S., et al., *Oxidative stress and endothelial dysfunction in aortas of aged spontaneously hypertensive rats by NOX1/2 is reversed by NADPH oxidase inhibition.* Hypertension, 2010. **56**(3): p. 490-7.

545.   Nourooz-Zadeh, J., et al., *Relationships between plasma measures of oxidative stress and metabolic control in NIDDM.* Diabetologia, 1997. **40**(6): p. 647-53.

546.   Nourooz-Zadeh, J., et al., *Elevated levels of authentic plasma hydroperoxides in NIDDM.* Diabetes, 1995. **44**(9): p. 1054-8.

547.   Facchini, F.S., et al., *Relation between insulin resistance and plasma concentrations of lipid hydroperoxides, carotenoids, and tocopherols.* Am J Clin Nutr, 2000. **72**(3): p. 776-9.

548.   Hemmingsen, B., et al., *Diet, physical activity or both for prevention or delay of type 2 diabetes mellitus and its associated complications in people at increased risk of developing type 2 diabetes mellitus.* Cochrane Database Syst Rev, 2017. **12**: p. Cd003054.

549.   Mayer-Davis, E.J., et al., *Incidence Trends of Type 1 and Type 2 Diabetes among Youths, 2002-2012.* N Engl J Med, 2017. **376**(15): p. 1419-1429.

550.   Tikellis, C., et al., *Cardiac inflammation associated with a Western diet is mediated via activation of RAGE by AGEs.* Am J Physiol Endocrinol Metab, 2008. **295**(2): p. E323-30.

551.   Aronson, D. and E.J. Rayfield, *How hyperglycemia promotes atherosclerosis: molecular mechanisms.* Cardiovasc Diabetol, 2002. **1**: p. 1.

552.   Koff, E., J. Rierdan, and M.L. Stubbs, *Conceptions and misconceptions of the menstrual cycle.* Women Health, 1990. **16**(3-4): p. 119-36.

553.   Barata, D.S., et al., *The effect of the menstrual cycle on glucose control in women with type 1 diabetes evaluated using a continuous glucose monitoring system.* Diabetes Care, 2013. **36**(5): p. e70.

554.   Mumford, S.L., et al., *Variations in lipid levels according to menstrual cycle phase: clinical implications.* Clin Lipidol, 2011. **6**(2): p. 225-234.

555.   Abraham, S., et al., *Menstruation, menstrual protection and menstrual cycle problems. The knowledge, attitudes and practices of young Australian women.* Med J Aust, 1985. **142**(4): p. 247-51.

556.   Ginther, O.J., et al., *Follicular-phase concentrations of progesterone, estradiol-17beta, LH, FSH, and a PGF2alpha metabolite and daily clustering of prolactin pulses, based on hourly blood sampling and hourly detection of ovulation in heifers.* Theriogenology, 2013. **79**(6): p. 918-28.

557.   Kesner, J.S., V. Padmanabhan, and E.M. Convey, *Estradiol induces and progesterone inhibits the preovulatory surges of luteinizing hormone and follicle-stimulating hormone in heifers.* Biol Reprod, 1982. **26**(4): p. 571-8.

558.   Solomon, T.P., et al., *A low-glycemic index diet combined with exercise reduces insulin resistance, postprandial hyperinsulinemia, and glucose-dependent insulinotropic polypeptide responses in obese, prediabetic humans.* Am J Clin Nutr, 2010. **92**(6): p. 1359-68.

559.   Pisprasert, V., et al., *Limitations in the use of indices using glucose and insulin levels to predict insulin sensitivity: impact of race and gender and superiority of the indices derived from oral glucose tolerance test in African Americans.* Diabetes Care, 2013. **36**(4): p. 845-53.

560.   Williamson, D.L., et al., *Aberrant REDD1-mTORC1 responses to insulin in skeletal muscle from Type 2 diabetics.* Am J Physiol Regul Integr Comp Physiol, 2015. **309**(8): p. R855-63.

561. Bierhaus, A., et al., *Methylglyoxal modification of Nav1.8 facilitates nociceptive neuron firing and causes hyperalgesia in diabetic neuropathy.* Nat Med, 2012. **18**(6): p. 926-33.

562. Harris, J.A. and F.G. Benedict, *A Biometric Study of Human Basal Metabolism.* Proc Natl Acad Sci U S A, 1918. **4**(12): p. 370-3.

563. Frankenfield, D.C., E.R. Muth, and W.A. Rowe, *The Harris-Benedict studies of human basal metabolism: history and limitations.* J Am Diet Assoc, 1998. **98**(4): p. 439-45.

564. Trappe, T.A., et al., *Local anesthetic effects on gene transcription in human skeletal muscle biopsies.* Muscle Nerve, 2013. **48**(4): p. 591-3.

565. Haus, J.M., et al., *Collagen, cross-linking, and advanced glycation end products in aging human skeletal muscle.* J Appl Physiol (1985), 2007. **103**(6): p. 2068-76.

566. Bergstrom, J., *Percutaneous needle biopsy of skeletal muscle in physiological and clinical research.* Scand J Clin Lab Invest, 1975. **35**(7): p. 609-16.

567. Miyata, T., et al., *Angiotensin II receptor antagonists and angiotensin-converting enzyme inhibitors lower in vitro the formation of advanced glycation end products: biochemical mechanisms.* J Am Soc Nephrol, 2002. **13**(10): p. 2478-87.

568. Forbes, J.M., et al., *Modulation of soluble receptor for advanced glycation end products by angiotensin-converting enzyme-1 inhibition in diabetic nephropathy.* J Am Soc Nephrol, 2005. **16**(8): p. 2363-72.

569. Nakamura, K., et al., *Telmisartan inhibits expression of a receptor for advanced glycation end products (RAGE) in angiotensin-II-exposed endothelial cells and decreases serum levels of soluble RAGE in patients with essential hypertension.* Microvasc Res, 2005. **70**(3): p. 137-41.

570. Wake, H., et al., *Histamine inhibits advanced glycation end products-induced adhesion molecule expression on human monocytes.* J Pharmacol Exp Ther, 2009. **330**(3): p. 826-33.

571. Wang, Z., et al., *Anti-Hypertensive Medication Use, Soluble Receptor for Glycation End Products and Risk of Pancreatic Cancer in the Women's Health Initiative Study.* J Clin Med, 2018. **7**(8).

572. Izuhara, Y., et al., *Renoprotective properties of angiotensin receptor blockers beyond blood pressure lowering.* J Am Soc Nephrol, 2005. **16**(12): p. 3631-41.

573. Ferhani, N., et al., *Expression of high-mobility group box 1 and of receptor for advanced glycation end products in chronic obstructive pulmonary disease.* Am J Respir Crit Care Med, 2010. **181**(9): p. 917-27.

574. Iwamoto, H., et al., *Soluble receptor for advanced glycation end-products and progression of airway disease.* BMC Pulm Med, 2014. **14**: p. 68.

575. Nakamura, T., et al., *Calcium channel blocker inhibition of AGE and RAGE axis limits renal injury in nondiabetic patients with stage I or II chronic kidney disease.* Clin Cardiol, 2011. **34**(6): p. 372-7.

576. Matsui, T., et al., *Nifedipine, a calcium-channel blocker, inhibits advanced glycation end-product-induced expression of monocyte chemoattractant protein-1 in human cultured mesangial cells.* J Int Med Res, 2007. **35**(1): p. 107-12.

577. Matsui, T., et al., *Dipeptidyl peptidase-4 deficiency protects against experimental diabetic nephropathy partly by blocking the advanced glycation end products-receptor axis.* Lab Invest, 2015. **95**(5): p. 525-33.

578. Nakashima, S., et al., *Linagliptin blocks renal damage in type 1 diabetic rats by suppressing advanced glycation end products-receptor axis.* Horm Metab Res, 2014. **46**(10): p. 717-21.

579. Saftig, P. and K. Reiss, *The "A Disintegrin And Metalloproteases" ADAM10 and ADAM17: novel drug targets with therapeutic potential?* Eur J Cell Biol, 2011. **90**(6-7): p. 527-35.

580. Lam, J.K., et al., *Effect of insulin on the soluble receptor for advanced glycation end products (RAGE).* Diabet Med, 2013. **30**(6): p. 702-9.

581. Raucci, A., et al., *A soluble form of the receptor for advanced glycation endproducts (RAGE) is produced by proteolytic cleavage of the membrane-bound form by the sheddase a disintegrin and metalloprotease 10 (ADAM10).* Faseb j, 2008. **22**(10): p. 3716-27.

582. Riboulet-Chavey, A., et al., *Methylglyoxal impairs the insulin signaling pathways independently of the formation of intracellular reactive oxygen species.* Diabetes, 2006. **55**(5): p. 1289-99.

583. Schalkwijk, C.G., O. Brouwers, and C.D. Stehouwer, *Modulation of insulin action by advanced glycation endproducts: a new player in the field.* Horm Metab Res, 2008. **40**(9): p. 614-9.

584.   Zhou, Z., et al., *Metformin Inhibits Advanced Glycation End Products-Induced Inflammatory Response in Murine Macrophages Partly through AMPK Activation and RAGE/NFkappaB Pathway Suppression.* J Diabetes Res, 2016. **2016**: p. 4847812.

585.   Ouslimani, N., et al., *Metformin reduces endothelial cell expression of both the receptor for advanced glycation end products and lectin-like oxidized receptor 1.* Metabolism, 2007. **56**(3): p. 308-13.

586.   Beisswenger, P. and D. Ruggiero-Lopez, *Metformin inhibition of glycation processes.* Diabetes Metab, 2003. **29**(4 Pt 2): p. 6s95-103.

587.   Quade-Lyssy, P., et al., *Statins stimulate the production of a soluble form of the receptor for advanced glycation end products.* J Lipid Res, 2013. **54**(11): p. 3052-61.

588.   Ishibashi, Y., et al., *Pravastatin inhibits advanced glycation end products (AGEs)-induced proximal tubular cell apoptosis and injury by reducing receptor for AGEs (RAGE) level.* Metabolism, 2012. **61**(8): p. 1067-72.

589.   Haus, J.M., et al., *Plasma ceramides are elevated in obese subjects with type 2 diabetes and correlate with the severity of insulin resistance.* Diabetes, 2009. **58**(2): p. 337-43.

590.   Haus, J.M., et al., *Decreased visfatin after exercise training correlates with improved glucose tolerance.* Med Sci Sports Exerc, 2009. **41**(6): p. 1255-60.

591.   DeFronzo, R.A., J.D. Tobin, and R. Andres, *Glucose clamp technique: a method for quantifying insulin secretion and resistance.* Am J Physiol, 1979. **237**(3): p. E214-23.

592.   Solomon, T.P., et al., *Randomized trial on the effects of a 7-d low-glycemic diet and exercise intervention on insulin resistance in older obese humans.* Am J Clin Nutr, 2009. **90**(5): p. 1222-9.

593.   Li, Y. and S. Wang, *Glycated albumin activates NADPH oxidase in rat mesangial cells through up-regulation of p47phox.* Biochem Biophys Res Commun, 2010. **397**(1): p. 5-11.

594.   Maiti, S., et al., *Structure and activity of full-length formin mDia1.* Cytoskeleton (Hoboken), 2012. **69**(6): p. 393-405.

595.   Wallace, M.A., et al., *Overexpression of Striated Muscle Activator of Rho Signaling (STARS) Increases C2C12 Skeletal Muscle Cell Differentiation.* Front Physiol, 2016. **7**: p. 7.

596. Chun, K.H., et al., *Regulation of glucose transport by ROCK1 differs from that of ROCK2 and is controlled by actin polymerization.* Endocrinology, 2012. **153**(4): p. 1649-62.

597. Senatus, L.M. and A.M. Schmidt, *The AGE-RAGE Axis: Implications for Age-Associated Arterial Diseases.* Front Genet, 2017. **8**: p. 187.

598. Yan, S.F., et al., *Receptor for Advanced Glycation Endproducts (RAGE): a formidable force in the pathogenesis of the cardiovascular complications of diabetes & aging.* Curr Mol Med, 2007. **7**(8): p. 699-710.

599. Fan, L.M., et al., *Aging-associated metabolic disorder induces Nox2 activation and oxidative damage of endothelial function.* Free Radic Biol Med, 2017. **108**: p. 940-951.

600. Gkogkolou, P. and M. Bohm, *Advanced glycation end products: Key players in skin aging?* Dermatoendocrinol, 2012. **4**(3): p. 259-70.

601. Draznin, B., *Mechanism of the mitogenic influence of hyperinsulinemia.* Diabetol Metab Syndr, 2011. **3**(1): p. 10.

602. Orellana, R.A., et al., *Insulin signaling in skeletal muscle and liver of neonatal pigs during endotoxemia.* Pediatr Res, 2008. **64**(5): p. 505-10.

603. Poloz, Y. and V. Stambolic, *Obesity and cancer, a case for insulin signaling.* Cell Death Dis, 2015. **6**: p. e2037.

604. Cusi, K., et al., *Insulin resistance differentially affects the PI 3-kinase- and MAP kinase-mediated signaling in human muscle.* J Clin Invest, 2000. **105**(3): p. 311-20.

605. Puri, P.L. and V. Sartorelli, *Regulation of muscle regulatory factors by DNA-binding, interacting proteins, and post-transcriptional modifications.* J Cell Physiol, 2000. **185**(2): p. 155-73.

606. Goalstone, M., et al., *Insulin stimulates the phosphorylation and activity of farnesyltransferase via the Ras-mitogen-activated protein kinase pathway.* Endocrinology, 1997. **138**(12): p. 5119-24.

607. Madonna, R., et al., *The prominent role of p38 mitogen-activated protein kinase in insulin-mediated enhancement of VCAM-1 expression in endothelial cells.* Int J Immunopathol Pharmacol, 2007. **20**(3): p. 539-55.

608.   Bertrand, F., et al., *Insulin activates nuclear factor kappa B in mammalian cells through a Raf-1-mediated pathway.* J Biol Chem, 1995. **270**(41): p. 24435-41.

609.   Meng, Y. and B. Roux, *Locking the active conformation of c-Src kinase through the phosphorylation of the activation loop.* J Mol Biol, 2014. **426**(2): p. 423-35.

610.   Lee, S., et al., *Protein kinase C-zeta phosphorylates insulin receptor substrate-1, -3, and -4 but not -2: isoform specific determinants of specificity in insulin signaling.* Endocrinology, 2008. **149**(5): p. 2451-8.

611.   Roskoski, R., Jr., *Src kinase regulation by phosphorylation and dephosphorylation.* Biochem Biophys Res Commun, 2005. **331**(1): p. 1-14.

612.   Sun, X.J., et al., *The Fyn tyrosine kinase binds Irs-1 and forms a distinct signaling complex during insulin stimulation.* J Biol Chem, 1996. **271**(18): p. 10583-7.

613.   Sato, H., et al., *Src regulates insulin secretion and glucose metabolism by influencing subcellular localization of glucokinase in pancreatic beta-cells.* J Diabetes Investig, 2016. **7**(2): p. 171-8.

614.   Sylow, L., et al., *Rac1 signaling is required for insulin-stimulated glucose uptake and is dysregulated in insulin-resistant murine and human skeletal muscle.* Diabetes, 2013. **62**(6): p. 1865-75.

615.   Sylow, L., et al., *Akt and Rac1 signaling are jointly required for insulin-stimulated glucose uptake in skeletal muscle and downregulated in insulin resistance.* Cell Signal, 2014. **26**(2): p. 323-31.

616.   Sylow, L., et al., *Rac1 and AMPK Account for the Majority of Muscle Glucose Uptake Stimulated by Ex Vivo Contraction but Not In Vivo Exercise.* Diabetes, 2017. **66**(6): p. 1548-1559.

617.   Gumustekin, M., et al., *The effect of insulin treatment on Rac1 expression in diabetic kidney.* Ren Fail, 2013. **35**(3): p. 396-402.

618.   Espinosa, A., et al., *NADPH oxidase and hydrogen peroxide mediate insulin-induced calcium increase in skeletal muscle cells.* J Biol Chem, 2009. **284**(4): p. 2568-75.

619.   Mukherjee, T.K., S. Mukhopadhyay, and J.R. Hoidal, *The role of reactive oxygen species in TNFalpha-dependent expression of the receptor for advanced glycation end products in human umbilical vein endothelial cells.* Biochim Biophys Acta, 2005. **1744**(2): p. 213-23.

620. Gauss, K.A., et al., *Role of NF-kappaB in transcriptional regulation of the phagocyte NADPH oxidase by tumor necrosis factor-alpha.* J Leukoc Biol, 2007. **82**(3): p. 729-41.

621. Chen, X., et al., *Role of Reactive Oxygen Species in Tumor Necrosis Factor-alpha Induced Endothelial Dysfunction.* Curr Hypertens Rev, 2008. **4**(4): p. 245-255.

622. Schmidt, A.M., *2016 ATVB Plenary Lecture: Receptor for Advanced Glycation Endproducts and Implications for the Pathogenesis an Treatment of Cardiometabolic Disorders: Spotlight on the Macrophage.* Arterioscler Thromb Vasc Biol, 2017. **37**(4): p. 613-621.

623. Lowell, C.A., *Src-family and Syk kinases in activating and inhibitory pathways in innate immune cells: signaling cross talk.* Cold Spring Harb Perspect Biol, 2011. **3**(3).

624. Gianni, D., et al., *Novel p47(phox)-related organizers regulate localized NADPH oxidase 1 (Nox1) activity.* Sci Signal, 2009. **2**(88): p. ra54.

625. Latroche, C., et al., *Skeletal Muscle Microvasculature: A Highly Dynamic Lifeline.* Physiology (Bethesda), 2015. **30**(6): p. 417-27.

626. Tarafdar, A. and G. Pula, *The Role of NADPH Oxidases and Oxidative Stress in Neurodegenerative Disorders.* Int J Mol Sci, 2018. **19**(12).

627. Bedard, K. and K.H. Krause, *The NOX family of ROS-generating NADPH oxidases: physiology and pathophysiology.* Physiol Rev, 2007. **87**(1): p. 245-313.

628. Petry, A., et al., *NOX2 and NOX4 mediate proliferative response in endothelial cells.* Antioxid Redox Signal, 2006. **8**(9-10): p. 1473-84.

629. Jegou, A., M.F. Carlier, and G. Romet-Lemonne, *Formin mDia1 senses and generates mechanical forces on actin filaments.* Nat Commun, 2013. **4**: p. 1883.

630. Mizuno, H., et al., *Rotational movement of the formin mDia1 along the double helical strand of an actin filament.* Science, 2011. **331**(6013): p. 80-3.

631. Mizuno, H. and N. Watanabe, *mDia1 and formins: screw cap of the actin filament.* Biophysics (Nagoya-shi), 2012. **8**: p. 95-102.

APPENDICES

APPENDIX A: Metabolic Equations

Equation 1 (HOMA-IR)

Homeostatic model assessment for insulin resistance (HOMA-IR)

HOMA-IR = (fasting plasma glucose (mg/dl) x fasting insulin level (μU/ml))/405. (302)

Equation 2 (MATSUDA INDEX)

Index of insulin sensitivity derived from an oral glucose tolerance test developed by Matsuda et al.

Matsuda index = 10,000/square root of [(fasting plasma glucose (mg/dl) x fasting insulin level (μU/ml))

x (average glucose during OGTT x average insulin during OGTT)]. (303)

Equation 3 (M/I: insulin sensitivity)

The M value is described as the average rate of glucose infusion between the period of 80–120 minutes

from the start of the insulin infusion. The M/I ratio is the ratio of glucose infusion (M) value to the

average plasma insulin concentration during the same period

Equation 4 (Harris-Benedict)

Men: $66.47 + (13.75 \times W) + (5 \times H) - (6.75 \times A)$

Women: $665.1 + (9.563 \times W) + (1.85 \times H) - (4.676 \times A)$

W = weight in kilograms, H = height in centimeters, and A= age in years:

APPENDIX B: **Methods Protocols**

Maintaining Cell Culture Line – Thawing, Sub culturing and Freezing

Prior to all cell culture work, decontaminate all surfaces, equipment and containers with 70% EtOH

solution. Use aseptic technique for all procedures.

Thawing Human Skeletal Muscle Cells/Initiating Cell Culture Process

1. Prepare 5-6 mLs or 1ml/5cm^2 growth medium (SkBM) supplemented with growth factors (SkGM) in

    T25 flask and place in incubator (37°C, 5% CO2) to warm ~30 minutes PRIOR to obtaining cells from

    LN2.

2. Remove a cryovial of HSKMC from LN2 and QUICKLY transfer to cell culture room.

a. Relieve pressure of the vial – within cell culture hood, twist cap a quarter turn to release

    pressure and immediately retighten.

b. Place cryovial into water bath (37°C) for 2 minutes. DO NOT submerge the cap in the

    water and DO NOT incubate for longer than 2 minutes.

3. Resuspend cells in cryovial (with ~1 mL growth medium)

4. Dispense cells into previously prepared culture flask. Rock flask gently to evenly distribute cells.

5. Incubate (37°C, 5% CO2) for 24 hours to allow for cell attachment before replacing medium.

6. @80+% confluence, subculture all cells from T25 to T75

Sub culturing Human Skeletal Muscle Cells

Recommended seeding density for SkMC culture is 3,500 cells/cm^2 (Lonza)

1. When cells are ~80% confluent, prepare all solutions and flasks necessary for subculture.

2. Remove medium from cell culture and wash cells in D-PBS to remove elements that may inhibit trypsin function (calcium, etc).

3. Detach cells from flask.

a. Cover cells with ~2mL trypsin (TrypLE). Be sure the entire surface of the flask is covered with trypsin.

b. Incubate in 37°C, 5% CO_2 for 2-6 minutes, viewing under the microscope intermittently, until ~90% of cells are rounded up.

c. Tap side of flask moderately to vigorously to release the cells that remain attached to the flask surface.

d. If cells do not detach, continue trypsin incubation for 30 more seconds, view, and tap again. Repeat as necessary until >95% of cells have detached into suspension.

4. Transfer the detached cells suspended in trypsin to sterile 15 mL falcon tube.

a. Rinse flask with D-PBS to collect leftover cells and add this to 15mL falcon tube.

5. Deactivate trypsin

a. Add an equal volume of basal medium to 15 mL falcon tube. This prevents the trypsin from potentially harming cells.

6. View 'empty' flask under microscope, <5% of cells should be remaining.

7. Centrifuge harvested cells in 15 mL falcon tube at 220xg for 5 minutes to pellet the cells.

8. Decant the supernatant and resuspend the cells in 2-3 mL of growth medium (record this volume).

9. Determine cell count/density using a hemocytometer and Trypan Blue.

a. Refer to 'Determining Cell Density and Viability' protocol

10. desired volume of cells into respective vessels

a. Transfer desired volume of cells into a new T-75 flask (or experimental vessel) with growth factor supplemented medium already warmed and present.

b. Prepare a new T75 flask for continuous cell line propagation.

c. If cell density permits, prepare an additional T-75 flask to be grown to confluence and returned to LN2 for future cell culture experiments.

11. Change the growth medium the day after seeding and every other day thereafter. As the cells become more confluent, increase the volume of medium as follows:

> ➤ Under 25% confluence then feed cells 1 ml per 5 cm2
>
> ➤ 25-45% confluence then feed cells 1.5 ml per 5 cm2
>
> ➤ Over 45% confluence then feed cells 2 ml per 5 cm2

Freezing

Human Skeletal Muscle Cells/Replenishing Cell Supply

1. When cells are ~80% confluent, prepare solutions and flasks necessary for freezing cells.

2. Wash cells in D-PBS to remove elements of the basal medium that may inhibit trypsin function (calcium, etc)

3. Detach cells from flask.

a. Cover cells with ~2mL trypsin (TrypLE). Be sure the entire surface of the flask is covered with trypsin. Incubate in 37°C, 5% CO2 for 2-6 minutes, viewing under the microscope intermittently, until ~90% of cells are rounded up.

b. Tap side of flask moderately to vigorously to release the cells that remain attached to the flask surface.

c. If cells do not detach, continue trypsin incubation for 30 more seconds, view, and tap again. Repeat as necessary until >95% of cells have detached into suspension.

4. Transfer the detached cells suspended in trypsin to sterile 15 mL falcon tube.

a. Rinse flask with D-PBS to collect leftover cells and add this to 15mL falcon tube.

5. Deactivate trypsin.

a. Add an equal volume of basal medium to 15 mL falcon tube. This prevents the trypsin from potentially harming cells.

6. View 'empty' flask under microscope, <5% of cells should be remaining.

7. Centrifuge harvested cells in 15 mL falcon tube at 220xg for 5 minutes to pellet the cells.

8. Decant the supernatant and resuspend the cells in 1 mL volumes of freezing medium depending on the density of cells. (~1/2 a confluent T75 per vial)

9. Place ~1mL aliquots of cell suspension into a labeled cryovial (passage x+1) and place into "Mr. Frosty" container in -80°C freezer for 24 hours.

10. Transfer cryovial from "Mr. Frosty" into LN2 within the designated and labeled box.

Working with Myotubes – Differentiating and Harvesting

Prior to all cell culture work, decontaminate all surfaces, equipment and containers with 70% EtOH solution. Use aseptic technique for all procedures.

Differentiating Human Skeletal Muscle Cells/Formation of Myotubes

Differentiation must occur in experimental vessel. Myotubes cannot be transferred to new vessels after differentiation.

1. Culture myoblasts under standard culturing conditions in SkBM until culture has achieved ~95+% confluence.

2. Remove SkBM and replace with an equal volume of differentiation medium (DMEM-F12 supplemented with 2% horse serum).

3. Continue to culture the cells in the differentiation medium (replacing every other day) for ~3 to 5 days, or until myotubes are observed throughout the culture.

a. Observe multinucleated (more than 3 nuclei) myotubes.

4. If the myotubes are to be used in assays that require an extended period in culture, following

   differentiation, replace differentiation medium with SkBM. For best performance, myotube cultures are

   best used by 2 weeks post differentiation.

Harvesting Human Skeletal Muscle Cells

1. Perform desired experimental procedures and incubations.

2. Remove medium (collect this if your target of interest may be released in the medium).

3. Rinse cells with D-PBS

4. Add 100uL of Lysis Buffer (supplemented with Protease/Phosphatase Inhibitors)

5. *Optional: If harvesting entire plate/flask for homogenization, place into -20°C for <5 minutes. This

   helps to prime the cells for removal from treatment vessel.*

6. Using a cell scraper, scrape cells from top to bottom. Be sure to scrape close to the edges of the well. It

   helps to tip the vessel at ~45 degrees, so that the cells are scraped into the homogenization buffer that

   collects at the bottom of the well.

7. Rotate plate 90° and repeat scraping process. Repeat until entire well surface has been scraped

   appropriately.

8. Collect cells suspended in the homogenization buffer into 1.5 mL Eppendorf tube.

9. Vortex cell suspension.

10. Rock on ice for 30 minutes to ensure cell lysis and homogenization.

Experimental Procedures in Human Myotubes

Determining Cell Density and Viability

Trypan Blue will not penetrate cells with an intact cell membrane. Dead cells will appear filled with the blue die. Viable cells will be outlined but have a clear interior.

1. Combine 15 uL of cell suspension with 15 uL Trypan blue in Eppendorf tube.

2. Inject 15 uL of the cell/Trypan mix into the hemocytometer and view under microscope.

3. Count viable cells to obtain an average # of cells in a 4x4 block. Ie. count total cells in all 4 corner boxes and divide by 4. This is your "cell count." See image.

Corner boxes are 4x4 squares - outlined in RED.
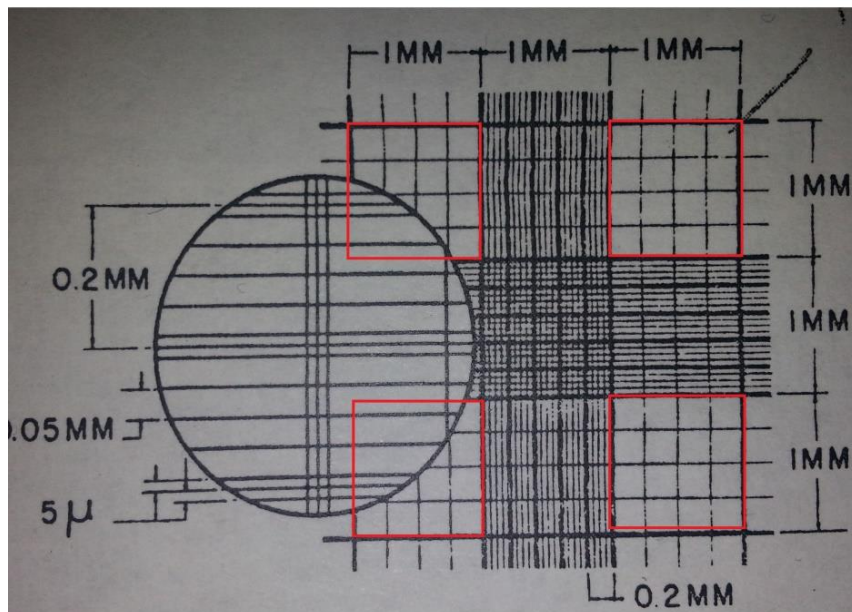
4. **Determine percent viability:**

o Count dead cells.

o Add viable and dead cell totals together.

o Viability = #Viable Cells/#Total Cells x100%

• **Determine cell density:**

o Multiply cell count by 10,000 (volume factor converting to cells/mL)

o Multiply by dilution factor of 2 (1:1, cell suspension:Trypan Blue)

i. Use this value to determine volume of cell suspension to load per vessel.

c. Multiply by total volume of cell suspension stock to determine total cells

i. Use this value to determine # of possible experiments.

Medium Preparations

Warming Aliquots of Growth/Differentiation Medium

It is optimal to avoid warming and cooling the full supply of cell culture medium whenever possible. To achieve this, aliquot only the required amount of medium (into a 15 or 50 mL Falcon tube) under sterile conditions. Return stock medium to 4° storage and incubate aliquot as necessary. Supplementing Growth Factors (SkGM) to Growth Medium (SkBM)

Growth factors (stored in -20°C) come in multi-vial kits contained in sealed plastic bags.

1.Thaw all components from a single kit (bag) on ice.

2. In the hood, add all thawed components to a new 500 mL container of SkBM. 3. Fill out the Growth Factor Checklist included with the SkGM kit.

1. Be sure to include date

2. Place Growth Factor Checklist (peel off sticker) onto SkBM container.

3. Fill out the Growth Factor Checklist included with the SkGM kit.

a. Be sure to include date

b. Place Growth Factor Checklist (peel off sticker) onto SkBM container.

4. Return the now GF-supplemented SkBM to 4° storage.

Preparing Differentiation Medium (DMEM-F12 supplemented with 2% horse serum)
1. Thaw horse serum (stored in -20°C) on ice.

2. In cell culture hood, aliquot ONLY the amount of DMEM F12 needed for your experiments into 50 mL falcon tubes. DO NOT add horse serum to DMEM stock – adding horse serum will reduce the shelf life to ~

30 days.

3. In cell culture hood, add horse serum to DMEM aliquot to a final concentration of 2% (v/v) horse serum. Ie. 49 mL DMEM + 1 mL horse serum.
4. Return the now horse serum-supplemented DMEM to 4° storage.
   Preparing Freezing Medium

1. Combine the following ingredients into a 15 mL falcon tube.

2. Store leftover freezing medium solution in -20°C

   ✓ 10% (v/v) DMSO

Cell Culture Images
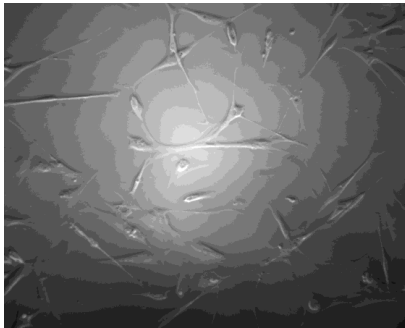
(1) Myoblasts after 24-hour seeding in 6-well plate (seeded @3,500 cells/cm^2 or 40,000 cells per well) at ~30% confluence.
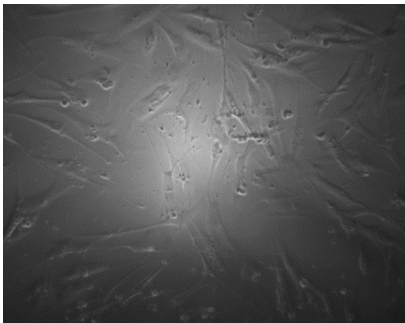
(2) Myoblasts grown to ~65% confluence prior to differentiation.
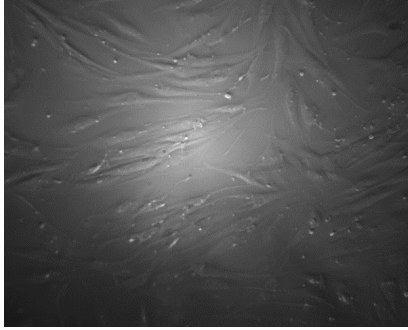
(3) Partially differentiated myotubes 2 days after differentiation medium.
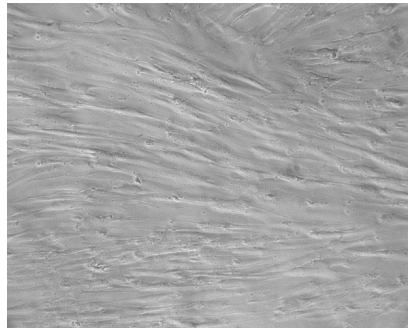
(4) Fully differentiated myotubes.

Product List

Product	Supplier	Cat. No.	Description
SkBM	Lonza	CC-3161	Basal Medium for Skeletal Muscle Cells
SkGM SingleQuots	Lonza	CC-4139	Growth Factors for SkBM
DMEM:F12	Lonza	BE04-687F/U1	Differentiation Medium
Horse Serum	Gibco	16050-130	Horse Serum
D-PBS	Gibco	14190-144	Wash buffer for cell culture

TrypLE	Gibco	12563-029	For cell transfer/ subculture
T-75 Flask	CytoOne	CC7682-4875	Polystyrene, Sterile
6-Well Plate	CytoOne	CC7682-7506	Flat Bottom
Trypan Blue (0.4%)	Lonza	17-942E	Cell Staining
Cell Lysis Buffer (10x)	Cell Signaling	9803S	Homogenization
10 mL Sterile Pipettes	USA Scientific	1071-0810	Cell Culture Supply
1 mL Sterile Pipettes	USA Scientific	1070-1210	Cell Culture Supply

IMMUNOPRECIPITATION/ WESTERN BLOTTING PROTOCOL

IMMUNOPRECIPITATION

1. **ALIQUOTTING DYNABEADS PROTEIN G**

A. Remove vial of Dynabeads protein G (Thermo Fischer Cat # 10003D) from 4ºC and resuspend the beads by gentle aspiration until the beads are distributed uniformly through the suspension.

B. Place 50uL of beads into a twist cap vial **WITH O-RING**. This is to ensure that none of the solution can escape during the inversion steps

C. Place tube on Dynamag and remove the supernatant. MOVE TO STEP 2

2. GENERATING DYNABEAD-ANTIBODY COMPLEX

A. In a separate vial, make a working solution for the antibody that you will use to pull down your protein of interest. Use technical support and the data sheet for your antibody of interest to figure out what you will need.

B. In order to prepare working solution, place your desired volume of antibody into 200uL of PBS w/ 0.02% Tween. You can make a large stock of this diluted solution to use for all of the vials that you will use for the experiment.

C. Place working solution of antibody (200uL PBS-T and antibody volume) into vial containing the beads from step 1 and aspirate until the beads are fully resuspended into the solution.

D. Place on rotator and incubate for 10-30 min. at room temperature. Ensure that the bead-antibody solution inverts on every rotation to ensure maximal interaction between the antibody and protein G. **Use table 1** to determine the affinity that protein G has to your antibody as the incubation time may need to be increased if the binding affinity is low.

E. Once the incubation has completed, place the bead-antibody suspension on the Dynamag and remove the supernatant

F. Wash the beads with 200uL of PBS-T by gentle aspiration.

G. Place the beads back on the magnet and remove the wash solution and proceed to step 4.

3. GENERATING DYNABEAD-ANTIBODY-ANTIGEN COMPLEX

A. Now that the beads have formed a complex with the antibody, your sample containing your protein of interest can now be added.

B. The total amount of protein needed will depend on your protein target which will need to be optimized. In the lab, we have already been successful with **50-200ug** of total protein, so this could be used a starting point for your optimization trials.

C. Add the desired amount of total protein to your beads and bring to a volume of 200uL with PBS to ensure that there is enough volume for suspension to completely invert during rotation.

D. The total amount of time required to pull down the optimal amount of your protein interest will vary. Thermo Fischer recommends 10 min. with rotation at room temperature, but if this is not sufficient, this time can be increased as far as overnight incubation with rotation at 4ºC.

E. Following the incubation, place the tube on the dynamag and remove the supernatant containing your sample. DO NOT DISCARD, as this sample can be reprobed for other protein targets.

F. Wash the beads 3 times with 1x PBS as done previously in **2F**. On the final wash, you may notice that some of the beads have demagnetized and are no longer able to join the pellet. This is a normal part of the process and does not mean that anything is wrong with the beads. Another reason why normalizing to the pulled down protein is crucial to ensure accuracy of the results.

G. Following the last wash, resuspend the beads in 100uL of 1x PBS and place into an Eppendorf tube with a pop cap (NOT TWIST CAP).

H. Place tube on magnet and remove supernatant.

4. DENATURATION STEP

A. Resuspend the beads in 20 uL of 1x sample buffer which contains **1:1, Blue Buffer (95% Laemmli Buffer, 5% BME): DIH20**. DIH2O can be replaced with 1x lysis buffer to increase the elution capability of the sample buffer.

B. Heat the bead slurry containing the antibody-antigen complex at 70ºC for 10 minutes.

C. Following this step, place the bead slurry on the magnet and remove the supernatant. The supernatant can either be loaded directly on the gel or can be placed in another vial to be saved for future analysis.

OPTIMIZATION NOTES

A. Whenever resuspending the beads in solution, ALWAYS use gentle aspiration to avoid excessive physical force from disrupting the complex formation. However, during the denaturation step, because everything in the solution will be analyzed, it is acceptable to resuspend the beads in sample buffer by vortexing. This also prevents sample loss as this particular suspension has a high affinity for the pipette tips during aspiration.

B. If nonspecific binding and high background is a problem,
        -Add a non-ionic detergent (Tween-20 or Triton X-100) to the washing buffer,   in concentrations between 0.01-0.1%

        -If the beads are blocked before precipitation, add identical blocker to the washing buffer

        -Increase the number of washing steps

        -Prolong the washing steps

        -Decrease incubation time (beads and sample)

        -Try the indirect IP method (**SEE PROTOCOL BELOW**)

-Decrease the antibody concentration

-A pre-clearing step may be performed to remove molecules that nonspecifically   bind   to the Protein G or the beads themselves

INDIRECT IP PROTOCOL

Binding antibody with target protein:

-Add 10-500 µg cell lysate plus the recommended amount of antibody. The amount of protein and antibody depends on the relative abundance of the target and the affinity of the antibody for the target. A pilot experiment where a fixed amount of protein is precipitated by increasing amounts of antibody is recommended.

-Incubate the sample with the antibody for 1 hour to overnight at 4°C, under agitation.
Total volume should be sufficient to allow mixing by agitation, preferably end-over-end mixing.

Prepared Dynabeads:

-Completely resuspend Dynabeads by pipetting

-Transfer 50 µl (1.5 mg) Dynabeads to a tube.

-Place the tube on the magnet to separate the beads from the solution and remove the supernatant.

-Remove the tube from the magnet.

-Place the tube on the magnet to separate the beads from the solution and remove the supernatant.

Immunoprecipitate Target Antigen:

-Add your sample containing the antigen-antibody complexes to the washed Dynabeads (typically 100–1000 µL) and gently pipette to resuspend the Dynabeads.

-Mix beads end-over-end or with agitation for 4 hours at 4°C.

-Place the tube on the magnet. Transfer the supernatant to a clean tube for further analysis, if desired.

-Wash the Dynabeads-Ab-Ag complex 3 times using 200 µL Washing Buffer for each wash. Separate on the magnet between each wash, remove supernatant and resuspend by gentle pipetting.

-Resuspend the Dynabeads-Ab-Ag complex in 100 µL Washing Buffer and transfer the bead suspension to a clean tube. This is recommended to avoid co-elution of proteins bound to the tube wall.

Elute the Antigen:

-Place the tube on the magnet and remove the supernatant.

-Add 20 µl sample buffer Gently pipette to resuspend the Dynabeads-Ab-Ag complex.

-Heat for 10 min at 70°C

-Place the tube on the magnet and load the supernatant/sample onto the gel.

WESTERN BLOTTING PROTOCOL

GEL RUN

A. Load sample into individual well. Avoid contact with the well walls or floor and avoid emitting any bubbles into the loaded sample as you approach the second stop while dispensing your sample into the well. Place the pipette tip as close to the top of the sample level while dispensing to avoid "splashing"

B. The gel that can be used varies depending on your protein of interest as this alters the amount of separation that will occur in different areas of the gel.

Taken from Abcam's western blotting guide

Protein size	Gel acrylamide percentage
4–40 kDa	20%
12–45 kDa	15%
10–70 kDa	12.5%
15–100 kDa	10%
25–200 kDa	8%

If probing for proteins that have a large disparity in molecular weight, then a graded gel such as (4-20%) could be used in order to maximize separation at both high and low molecular weights.

C. Run the gel at a voltage and time that is optimized for your protein of interest. However, if "band smiling" is an issue then you should reduce the voltage and run for longer at a lower voltage so that the sample runs uniformly down the gel.

GEL→MEMBRANE TRANSFER

D. Following the run, remove the gel from the cassette and wash both sides of the gel with transfer buffer to remove SDS that could lead to excessive background on the membrane. Alternatively, you can incubate the gel in transfer buffer for the same time as the membrane and other components.

E. Pre-incubate all components of the transfer sandwich (filter paper, sponges, and membrane

Nitrocellulose→ incubate in ice cold transfer buffer for 10 minutes.

PVDF→ incubate for 2 minutes in methanol to activate, followed by 5-10   minutes in ice cold transfer buffer

ALL other components can be incubated in transfer buffer for 10 minutes.

F. Prepare the transfer sandwich as displayed below
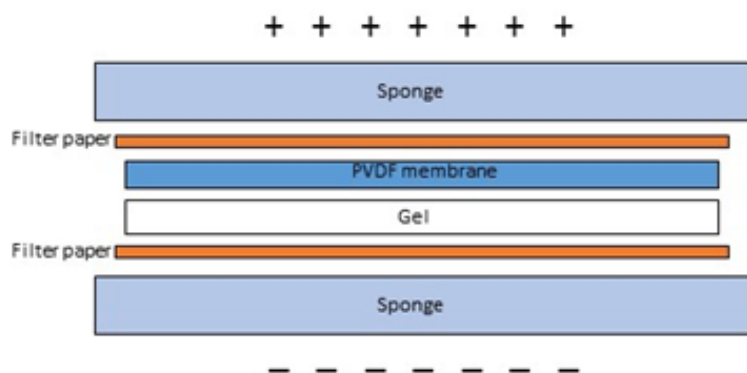
*For our BioRad setup, the **cathode will be the red side** and the **anode will be the black side**. Proteins will transfer from anode to cathode

BioRad recommends for a typical transfer of 100V for 1hr for tank blotting. However, the voltage and time can be modified depending on your protein of interest. Also, methanol and SDS can be reduced or added, respectively, to increase transfer of high molecular weight proteins. More information on that is displayed below

Large proteins (>100 kD)

Large proteins will tend to precipitate in the gel, hindering transfer. Adding   SDS to a final concentration of 0.1% in the transfer buffer will discourage this.

Methanol tends to remove SDS from proteins, so reducing the methanol percentage to 10% or less will also guard against precipitation. Lowering the methanol percentage in the transfer buffer also promotes swelling of the gel, allowing large proteins to transfer more easily.

Methanol is only necessary if using nitrocellulose. If using PVDF, methanol can be removed from the transfer buffer altogether, and is only needed to activate the PVDF before assembling the gel/membrane sandwich.

<u>Small proteins (<100 kD)</u>

All proteins are hindered from binding to membranes by SDS but small proteins more so than large proteins. If your protein of interest is small, omit SDS from transfer buffer.

Keep the methanol concentration at 20%

G. Following the transfer, disassemble the transfer sandwich and submerge the membrane 3x in DI H20

H. **PVDF**- Dry membrane and reactivate by incubating with methanol for 5 minutes followed by 1xTBS for 5 minutes prior to blocking **Nitrocellulose**- Dry membrane (optional) and can then be immediately placed in blocking buffer.

MEMBRANE BLOCKING AND PRIMARY INCUBATION

I. Both PVDF and nitrocellulose can be blocked using Licor Odyssey Blocking Buffer (OBB) for 1 hr.

J. Following blocking step, incubate your membrane with your antibody solution. The concentration will vary depending on your protein of interest and manufacturer. However, for housekeeper proteins (GADPH and B-Actin) 1: 5,000 has been shown to be effective. Prepare your antibody solution in the same blocking buffer that you used during the blocking step. Additionally, Tween 20 can be added at varying concentrations (0.1-0.2%) to remove nonspecific binding. DO NOT ADD SDS TO THE PRIMARY ANTIBODY INCUBATION. Also, it is important to prepare enough solution volume to submerge your membrane fully. A typical primary antibody recipe could look like this:

    1:1,000 Primary antibody- 5uL
    0.1% Tween 20- 5uL
    5mL OBB

K. Incubation times should be optimized for your protein of interest, but overnight incubation at 4ºC with rocking seems to work for most protein targets. Housekeeping protein probes can be reduced to 1 hr.

L. Following the primary incubation, membranes should be washed extensively with 1x TBS supplemented with 0.1% Tween 20. A typical wash protocol would be 3x5min. TBST, however, this can be modified depending on the level of nonspecific binding.

SECONDARY INCUBATION

M. For the LiCor Odyssey imaging system, it is recommended that you use a secondary antibody concentration of 1: 5,000-1: 25,000. For most protein targets, 1: 20,000 has been shown to be effective and minimizes excessive background. For both PVDF and Nitrocellulose, Tween 20 should be added (0.1-0.2%) to the antibody cocktail to reduce excessive background. For PVDF specifically, SDS can be added (0.01%-0.02%) to further reduce background. A typical secondary antibody solution could look like this:

    1:20,000 Mouse Anti-Rabbit 800- 0.5uL
    0.1% Tween 20- 10uL
    0.01% of 10%SDS (PVDF)- 10uL
    10mL OBB

Incubate the membrane for 1 hr. at room temperature <u>while protecting from light</u>

N. Wash the membrane extensively with TBS-T, similar to step L. However, this should always be followed by a wash with 1xTBS to remove tween from your membrane that could interfere with the imaging of your proteins.

O. Keep the membrane in 1xTBS to keep wet and Image the membrane using the LiCor Odyssey system

P. Following imaging, place the membrane back into 1xTBS. If you plan on stripping the membrane, it is imperative that the membrane remain wet.

STRIPPING PROTOCOL

Note: This protocol has been optimized for western blot analysis of total cell lysate and needs to be further optimized if using immunoprecipitated samples

A. Heat an aliquot of 0.2M NaOH to 37ºC

B. Place enough volume on the membrane in order to fully submerge in solution.

C. Incubate for 30min. with rocking

D. Wash the membrane in 1xTBS for 5min. prior to scanning to removing stripping solution

E. Following the scan, re-block membrane in OBB for 1 hr. prior to incubating with primary antibody

Table 1. Binding strength of Protein A and G to different species of Igs and their subclasses

Table 1

Ig origin	Affinity for Protein A	Affinity for Protein G
Human IgG1,2,4	+++	+++
Human IgD	-	-
Human IgA, E, M	+	-

Human IgG3	+	+++
Mouse IgG1	+	+++
Mouse IgG2, 2b, 3	+++	+++
Mouse IgM	+	+
Rat IgG1	+	+
Rat IgG2a	-	+++
Rat IgG2b	-	+
Rat IgG2c	+++	+
Bovine IgG1	+	+++
Bovine IgG2	+++	+++
Chicken IgY	-	-
Dog IgG	+++	+
Goat IgG1	+	+++
Goat IgG2	+++	+++
Guinea Pig IgG	+++	+
Hamster	+	NA
Horse IgG	+	+++
Monkey IgG	+++	+++
Porcine IgG	+++	+++
Rabbit IgG	+++	+++
Sheep IgG1	+	+++
Sheep IgG2	+++	+++

PROCEDURES FOR IMMUNOFLUORESCENTS AND THE DETERMINATION OF RAGE IN FROZEN HUMAN SKELETAL MUSCLE

Table 2

Supplies Needed	Company	Cat No.
Dry Ice	RRC	N/A
Clear Nail Enamel	RRC	N/A
Disposable Microtome Blades; Stainless Steel	VWR	00498-336
Plastic Tray/Paper Towels/ Tinfoil	Lab supply	N/A
Eppendorf microtubes	Sigma	Z606340-1000EA
Disposable Pasteur Pipets	Fisher	1367821A
OCT Compound for Cryostat Sectioning	Ted Pella	27050
PAP Pen	EMS	71310
Microscope Glass Slides (white)	Fisher	413051
Cover slips	Fisher	4-13521
Acetone	Fisher	A18-1
Formaldehyde	Fisher	F81-11
Albumen (Bovine)	Amresco	015725g
Whole Goat Serum	Jackson Research	005000003
Primary Antibody Mouse Monoclonal IgG	Santa Cruz	sc-2078
Antibody Goat anti-mouse IgG TR	Santa Cruz sc-2078	sc-2054
DAPI antifade solution	Millipore	S7113
PBS 10x/pH 7.2	Gibco	00941

Sample Handling:

- Basal/Insulin Histology samples are located in the -80° freezer
- Samples to be transferred between labs or waiting sectioning should be stored on dry ice or in the cryostat chamber and never allowed to thaw. Thawing will affect ability to obtain cross-sectional; cuts, tissue quality and staining.

Cryostat:

- Turn on Cryostat machine by holding down the "key" button on interface for 5 seconds – this will "unlock" the machine and allow you to adjust the chamber temperature and cut size for tissue

- Cryostat machine should be set for -30° and tissue samples are to be transferred from dry ice immediately into the Cryostat chamber
- Place the Micotome blade on the sectioning platform and fasten blade with the table lever
- Affix muscle sample to the sectioning adapter with OTC compound – allow compound to freeze until the compound is a white color
- Cut 10μ sections and affix sample to the glass slide by gently pressing the side to the cut (4 max per slide)
- Allow slides containing newly cut samples to dry at room temperature for 60 minutes

Fixation:

- Immerse dried slides in 100% acetone for 10 min. Acetone should be chilled at -20° before beginning the fixation process
- After fixation, slides should air dry at room temperature for 10 minutes, allowing all residual acetone to evaporate
- Apply PAP pen to dried glass slides and encapsulate each tissue section with a circular marking. Assure the tissue sample is directly in the center of the circle, and allow enough space on all sides of the sample to work without disturbing the tissue

Washing Step #1:

- Rehydrate tissue sections with 3 x 5washes of 1X PBS (make sure you provide enough PBS to completely cover the tissue samples)
- Avoiding contact with tissues samples, carefully remove PBS with a Pipetman
- Wash 3 times X 5 min using PBB (0.5%BSA/1X PBS).

Blocking:

- With a Kimwipe, remove excess moisture from the bottom of the slides and around the sample site
- Place slides in a plastic tray lined with moist paper towels
- Each sample should be blocked with 2% BSA.
- PBS + 2% BSA = 2g Albumin per 100mL 1X PBS
- Alternatively, blocking can also be conducted with 20% serum in PBS+0.5% BSA (PBB)
- Current secondary is goat anti-mouse, therefore we use goat serum to block
- Gently drop 70-100 μl blocking buffer over the section, completely covering the section in solution
- Block for 60 minutes at room temperature and cover plastic tray with tinfoil

Wash Step #2:

- 3 washes X 5min with PBB

Primary antibody:

Santa Cruz – Mouse monoclonal IgG (RAGE antibody)
- Dilute to the desired concentration (1:50)
- Gently drop 70-100 µl antibody solution over the section, completely covering the section in solution.
- Incubate for overnight. This long incubation time requires placing a piece of wet paper towel in your slide box with your samples to minimize evaporation of your primary antibody solution. Overnight incubations should be conducted at 4°

Wash Step #3:

- 3 washes X 5min with PBB

Secondary antibody – This step need to be performed in the dark

Santa Cruz Goat Anti-Mouse IgG TR

- With a Kimwipe, remove excess moisture from the bottom of the slides and around the sample site Minimize all light exposure to the secondary antibody- Apply antibody in a dark room.
- Dilute to the desired concentration (1:100) in PBB and vortex gently
- Gently drop 70-100 µl antibody solution over the section, completely covering the section in solution.
- Incubate at room temperature for 60 minutes (made in PBB, vortex)
- Once applied, cover the slides with foil to further reduce exposure to light
- After incubation, carefully remove secondary solution with a pipetman – place the pipet tip in an area away from the sample and extract solution slowly
- Allow slide to air dry at room temp for an additional 5 minutes

Wash Step #4:

- In the dark, wash sections with (PBS 1X) 3 times X 5 min each

DAPI Step: This step need to be performed in the dark

Millipore DAPI Antifade Solution

- With a Kimwipe, remove excess moisture from the bottom of the slides and around the sample site
- In the dark, Add DAPI stain 30 seconds to stain the nuclei
- Adhere cover glass over your sample in the dark.
- Seal the cover slip to the slide with clear nail polish. Make sure no bubbles are trapped beneath the coverslip.
- Wrap the slide in foil and take it to the microscope

Microscopy/ Image Capture:

- Turn on computer and allow all drivers to be mapped before powering the fluorescents tower and camera module.
- Once you have confirmed the all drivers have been mapped, power the Nikon fluorescents tower and camera module. Make sure the camera module is on "camera 1"
- Open imaging software
- Activate the "live" icon – this will allow the microscope to interact with the computer screen
- Select a filter
    - #1 for DAPI (DAPI)
    - #2 for FITC (GREEN)
    - #4 for Texas Red (TR)
- Once a filter is select on the microscope, the same filter must be selected on the computer screen
- Select either DAPI /FITC or /TR filters on the imagining interface – these are located in the toolbar at the top of the screen
- Align slides under the microspore so the tissue sample is clearly present on the computer monitor
- Adjust quality of sample by fine tuning the image with the focus dials
- Adjust image quality before capturing the final image - this can be performed by selecting "file"/"image enhancement." This will present you with an option to adjust shutter speed in seconds, or millisecond. For DAPI – shutter speeds between 100 – 300 milliseconds are currently being used- For FITC, 1-3 seconds is currently being used.
- To capture a desired image – press the capture button – this will captures the image and present a new window of the image in a PDF format
- Save captured image to folder

Comments:

Higher exposure time in the microscope is not recommended. The higher the exposure the more autofluorescence that will be captured.

3-15- 14 – Primary 1:50 & Secondary 1:100

Brian K. Blackburn

Translational Scientist
M.S. CSCS. Ph.D.

110 N.Lima St. Unit E, Sierra Madre, CA, 91024   Cell (847) 508 1170   bblack20@uic.edu

Summary

Accomplished and steadfast translational scientist with training in biomedical science, exercise physiology and metabolism. My academic and clinical education centers on macronutrient metabolism and skeletal muscle physiology. Specifically, I investigate the role of glucose and lipid metabolism with the development of obesity, diabetes, and redox disequilibrium.

Experience

Founder & Exercise Physiologist , Peak Fire Speed, Agility & Power Systems, CA 2017 - Present
Perform detailed evaluations of athletes spanning the athletic continuum. Assess mobility flexibility, physical performance measurements, mental performance test and a comprehensive bio-mechanical analysis performance. Following the initial assessment, customized training programs are designed integrating muscular physiology, evidence-based nutrition, and biomedical science to produce elite, sports specific athletes of all ages.

Graduate Research Assistant , University of Illinois; Chicago, IL 2011 - Present
Translational scientist specializing in metabolism and bioenergetics. Assisted in skeletal muscle biopsy procedures in both healthy and pathogenic populations to investigate the molecular mechanism responsible for alterations in metabolic flexibility, glucose tolerance, glucose disposal in human skeletal muscle. Utilized biochemical and molecular analysis to establish novel metabolic pathways associated with free radical production in in human subjects.
Advisor: Dr. Jacob M. Haus, Ph.D.

Graduate Teaching Assistant, University of Illinois; Chicago, IL   2011 - Present
Designed and implement bioenergetic, exercise physiology and exercise prescription lessons in the Department of Kinesiology and Nutrition. Directed university level courses centering around VO_2 /Maximal oxygen consumption protocols, lactic acid kinetics, skeletal muscle metabolism and fiber selectivity in the UIC exercise science laboratory.
Additional duties included instructing students on data collection, computation, and interpretation skills to design more favorable outcomes in exercise prescription and performance.
Advisor: Dr. Tracy Baynard, Ph.D.

Adjunct Faculty, Department of Human Health & Biological Sciences, College of Lake County, Grayslake, IL 2008 - 2012
Courses taught include Sport and Exercise Physiology, Sports Nutrition, Theory and Practice of Fitness, Strength & Conditioning.

Chicago Blackhawks Testing Training Camps for Pre & Post Season Assessment, College of Lake County, Grayslake, IL 2009 - 2012
Assisted in physical fitness assessments. Physical perforce testing included strength, agility, flexibility speed, power and oxidative capacity on pre & post season Chicago Blackhawks athletes.

Founder & Exercise Physiologist, Wrecking Ball Performance Center: Grayslake, IL 2005 - Present
Train, condition and instruct professional combative athletes in Mixed Martial Arts, Boxing & Muay Thai. Design and implement comprehensive strength and conditioning programs

Literature Instructor, Carl Sandburg Middle School, Mundelein, IL 2005-2010
Design and implement lesson plans, conduct ongoing classroom assessment, and implement continuous improvement planning. Created content to enhance critical thinking capacities, higher order thinking skills, involving reading, writing, and grammar

Cross Curriculum Instructor, North Chicago High School, North Chicago, IL 2003-2005
Delivered instruction in literature and Science. Design and implement lesson plans, conduct ongoing classroom assessment, and implement continuous improvement planning. Facilitated a learning environment dedicated to developing critical, scientific inquiry aptitudes ,acquisitive, organizational, creative, manipulative, and communicative skills in inflammatory/oxidative injury and assessment.

Strength and Conditioning Consultant, North Chicago High School, North Chicago: IL 2005 - 2007
Worked to enhance athletes' strength, speed, explosiveness and agility during preseason training. Designed injury prevention drills and educated students in sports nutrition and dietary habits to achieve elite performance.

Chef, Wolfgang Puck's Spago's, Chicago, IL 2001 - 2003
Provided customized, private and event chef services. Catering services to clients desiring healthier food choices

_____

Education
The University of Illinois at Chicago, Chicago, IL - **Ph.D.** Dept. Kinesiology and Nutrition,
Thesis - The Natural History of Type 2 Diabetes Modifies Receptor for Advanced Glycation End Products and induces NADPH Oxidase Signaling in Human Skeletal Muscle

California University*,* California, PA - **M.S.** Exercise Sciences, Health & Wellness
Thesis - Long-Term Effects of Weight Cycling in Combative Athletes and Implications on Human Performance

DePaul University, Chicago, IL - **B.A.** Education with concentration in literature and composition

Culinary Institute of America, Poughkeepsie, NY - **A.A.** Culinary studies & French cooking methodology

---

Skills
Education & Lecturing: Over a decade of professional work focusing on education, training, curriculum development, and coaching in primary, secondary, and tertiary education sectors

Translational Science and Research: Experience using a clinical-translational research approach involving: human subjects, cell culture, and enzymatic activity studies

Clinical Procedures: Hyperinsulinemic-euglycemic clamp, aerobic exercise training & maximal effort testing, Parvo metabolic cart, skeletal muscle biopsy & tissue processing, nutrition counseling & diet analysis, IRB/recruitment/subject screening , research design

Cell Culture: Human skeletal muscle (HSkMCs) and Human umbilical vein endothelial cells (HUVEC) lines, experimental design & method development

Wet Lab Procedures: Western blotting, LI-COR Infrared imaging , Immunoprecipitation, enzyme-linked immunosorbent assay (ELISA), enzymatic activity assays, method design and development, histology.

Lectures	2017, " Exercise and Beta Cell Function in Diseased and Healthy Populations" Presented at the CF-155 Performance Center, Chicago, IL

2016, " The Natural History of Type 2 Diabetes Modifies RAGE End products induced NADPH Oxidase Signaling in Human Skeletal Muscle" Presented at the Department of Applied Health Sciences Cells to Community lecture series, University of Illinois at Chicago, Chicago, IL

2015, " Maximal Oxidative Capacity During Exercise Is Associated with Skeletal Muscle Fuel Selection and Dynamic Changes in Mitochondrial Protein Acetylation " Presented at the Dept. of Endocrinology, UIC College of Medicine, Chicago, IL

2014, "Hyperinsulinaemia Disrupts Vascular Homeostasis, Enhances Oxidative Stress and Impairs Flow Induced Dilation of Human Skeletal Muscle Arterioles" Presented at UIC Diabetes Day, Chicago, IL

2013, "Acute Aerobic Exercise Increase Plasma Soluble Receptor of Advanced Glycation End Products (AGEs) in Insulin Resistant Adults" Presented at American College of Sports Medicine poster session, Indianapolis, IN

2013, "Acute Aerobic Exercise Increase Plasma Soluble Receptor of Advanced Glycation End products (AGEs) in Insulin Resistant Adults" Presented at American Diabetes Association poster session, Chicago, IL

2011, "Complete Conditioning for Combative Athletes" Midwest Strength and Conditioning Conference, McHenry County College, Crystal Lake, IL

Achievements Collaborated with, and assisted, my Ph.D. advisor (Dr. Jacob Haus Ph.D.) with grant proposal composition, which subsequently, earned our lab the prestigious RO1 Award by the National Institute of Health (NIH), 2016/2017

Finalist for Sigma Xi grant award upon submitting an abstract for "Incretin, Feed-Forward Signaling and DPP-4 Inhibition in Diabetes", 2014

Proposed and developed curriculum for a Sport and Exercise Nutrition course at the College of Lake County. The program earned a 3 credit state-approved 200-level approval, 2013

Proposed and developed curriculum for an Introduction to Mixed Martial Arts and Combative Athletics course at the College of Lake County. The program earned a 2 credit state-approved 200-level approval, 2013

Memberships	Society for Redox Biology and Medicine	American Sport and Fitness Association
	National Academy of Sports Medicine	National Wellness Institute
	American College of Sports Medicine	American Diabetes Association
	Illinois Teaching Association	Illinois Boxing & MMA Association

Publications

Mey JT, Blackburn BK, Miranda ER, Chaves AB, Bonini M, Haus JM. Skeletal Muscle Dicarobnyl Stress and Glyoxalase System Regulation in Type II Diabetes. Am J Physiol Regul.

Miranda ER, Mey Jt, Blackburn BK, Haus JM, Quinn L. Circulating Soluble RAGE Isoforms are Attenuated in Obese, Impaired Glucose Tolerant Individuals and are Associated with the Development of Type 2 Diabetes. Aug 2017AJP Endocrinology and Metabolism

Williamson DL, Dungan CM, Mahmoud AM, Mey JT, Blackburn BK, Haus JM. Aberrant REDD1-mTORC1 responses to insulin in skeletal muscle from type 2 diabetics. Am J Physiol Regul Integr Comp Physiol. 2015 Aug 12. doi: 10.1152/ajpregu.00285.2015. [Epub ahead of print] PMID: 26269521

Mahmoud AM, Szczurek MR, Blackburn BK, Mey JT, Chen Z, Robinson AT, Bian JT, Unterman TG, Minshall RD, Brown MD, Kirwan JP, Phillips SA, Haus JM. Hyperinsulinemia Augments Endothelin-1 Release and Impairs Vasodilation of Human Skeletal Muscle Arterioles. Physiol Rep. 2016 Aug;4(16). pii:e12895. Epub 2016 Aug 22

Mahmoud AM, Ali M, Miranda ER, Mey JT, Blackburn BK, Haus JM, Phillips SA Hyperinsulinemia-induced Oxidative Stress and Endothelial Nitric Oxide Synthase Uncoupling Involves NADPH Oxidase in Microvascular Endothelium. Arteriosclerosis, Thrombosis, and Vascular Biology. ATVB/2016/308989. In Review

Abstracts	Jacob T. Mey, Brian K. Blackburn, Thomas P. J. Solomon, Ciaran E. Fealy, Steven K. Malin, John P. Kirwan, Jacob M. Haus. Diminished Glyoxalase I Activity in Skeleta Muscle of Obese Individuals is Associated with Determinants of Metabolic Health – American Diabetes Association, Chicago 2013 - accepted as poster (Presenting Author)
	Abeer M. Mahmoud, Brian K. Blackburn, Karia Coleman, Jacob T. Mey, Vikram S. Somal, Thomas P. J. Solomon, Ciaran E. Fealy, Steven K. Malin, John P. Kirwan, Jacob M. Haus. Aerobic Exercise Induces RAGE Shedding via ADAM10 in Human Skeletal Muscle - 13th Biennial Advances in Skeletal Muscle Biology in Health and Diseases Conference, Gainesville, FL 2014
	Jacob M. Haus, Vikram S. Somal, Sarah S. Farabi, Jacob T. Mey, Brian K. Blackburn, Karia Coleman, Laurie Quinn. Acute Aerobic Exercise Increases Plasma Soluble Receptor of Advanced Glycation End Products (sRAGE) in Obese Insulin Resistant Adults – American Diabetes Association, Boston, MA 2015
	Erin Bohne, Brian K. Blackburn, Jacob T. Mey, Jacob M. Haus. Bone Insulin Resistance: Potential Link To Fragility in Type 2 Diabetes

---

Committees	Nutritional Reformation Committee, Mudelein District 75 - Lead instructor for development of D75 healthy lunch program
	Technology & Education Integration Committee, Mudelein District 75
	Health and Wellness Advisory Committee, College of Lake County, Grayslake, Illinois
	Personal Training Advisory Committee, College of Lake County, Grayslake, Illinois
	Massage Therapy Advisory Committee, College of Lake County, Grayslake, Illinois
	Literacy Committee, Mudelein District 75

Certifications	Certified K-12 Teacher, Illinois State Teaching
	Certified Specialist in Speed and Explosion for Sports and Competition, National Association of Speed and Explosion

Certified Wellness Practitioner (CWP), National Wellness Institute (NWI), Stevens Point, Wisconsin

First Aid, Cardio-Pulmonary Resuscitation (CPR), and Automated External Defibrillation (AED), American Red Cross

References

Dr. Jacob Haus, (Ph.D. Advisor) Department of Kinesiology & Nutrition, University of Michigan

Dr. Marcello Bonini, Department of Medicine, Pharmacology and Pathology, University of Illinois

Dr. Michael Brown, Department of Kinesiology & Nutrition, University of Illinois

Dr. Shane Phillips, Department Head of Physical Therapy , University of Illinois

Dr. Jacob Mey, Department of Metabolism, Cleveland Clinic

Dr. Austin Robinson, Department of Biomedical Research, University of Delaware